

THE ENTANGLEMENT AND MEASUREMENT OF
NON-ABELIAN ANYONS
AS AN APPROACH TO QUANTUM COMPUTATION

B.J. Overbosch

THE ENTANGLEMENT AND MEASUREMENT OF
NON-ABELIAN ANYONS
AS AN APPROACH TO QUANTUM COMPUTATION

Bas Jorn Overbosch

'Doctoraal-scriptie'
Supervisor: Prof. dr. ir. F.A. Bais

Institute for Theoretical Physics
University of Amsterdam
Valckenierstraat 65
1018 XE Amsterdam, the Netherlands

September 2000

Abstract

We investigate the proposal of Kitaev and Preskill to use non-abelian anyons for quantum computation. Non-abelian anyons are two-dimensional particles with a topological interaction. The internal states of non-abelian anyons are intrinsically decoherence free, and may thus serve as fault-tolerant qubits. We base the description of non-abelian anyons mathematically on a quantum group: the quantum double $D(H)$ of a finite group H , as described by a discrete gauge theory. The central topic of this thesis consists of the analysis of various double slit interference experiments, in particular the double slit experiments named ‘one-to-one’ and ‘many-to-one’. These experiments can be used to perform a quantum measurement on the internal states of non-abelian anyons. The result of a measurement is a projection on an eigenspace of some operator. This projection is a statistical average; we supply an extensive proof for this result.

Through various examples with $H = S_3$ we find evidence that there is a $D(H)$ -symmetry, acting through a global transformations, that leaves the outcomes of experiments invariant. Furthermore, we describe an ordering process, that orders a setup with many non-abelian anyons into piles that are made of identical non-abelian anyons with identical internal states. This ordering especially works for non-abelian anyons that were pair-created from the vacuum; these highly entangled vacuumstates can in some well defined sense be described by unentangled states.

The group S_3 does not yield a universal set, as needed for quantum computation. As we have not considered other larger finite groups explicitly, we do not know if there exists a group H that may generate a universal set, but this may very well be the case, perhaps for the group A_5 as suggested by Preskill. Our description of measurements and ordering of vacuumstates lays a firm basis for the quest for a universal set implemented through non-abelian anyons. We conclude with a speculative discussion about the pursuit of this quest: one should not stick to a description in terms of internal states of non-abelian anyons, but rather use a description in terms of the underlying representation-theory instead.

CONTENTS

1	Introduction	4
1.1	Quantum Computation (QC)	4
1.1.1	The promise of quantum computation	4
1.1.2	QC basics	5
1.1.3	Universal sets	5
1.1.4	The enemy named ‘decoherence’	8
1.1.5	Discrete Gauge Theories: decoherence free	8
1.2	Three problems with Discrete Gauge Theories	8
1.2.1	The physical implementation of this theoretical model	9
1.2.2	$H = A_5$: huge group	9
1.2.3	Quantum measurements	9
1.3	Outline	9
2	Topologically interacting particles and interference (in 2D)	12
2.1	Free particles in two dimensions	12
2.2	The ideal double slit experiment	13
2.3	The non-ideal case	14
2.4	Abelian anyons	17
2.5	The Aharonov-Bohm effect	18
2.6	Non-abelian anyons	21
2.7	The non-abelian, or entangled, double slit experiment	24
2.8	Summary	27
3	Two double slit experiments with non-abelian anyons	29
3.1	The one-to-one experiment, where the out-state is the next in-state	29
3.1.1	What is ‘one-to-one’ and what is its interference pattern	30
3.1.2	The one-to-one experiment in more detail	31
3.1.3	The resulting state is locked in an eigenspace of the monodromy operator	33
3.1.4	An example	33
3.2	The many-to-one experiment: probe one particle with many identical other particles	36
3.2.1	Description of the experiment	36
3.2.2	Final states	38
3.2.3	Every initial state will end up on a final state in some U eigenspace	41
3.2.4	Eigenvalues of the U -matrix	44
3.2.5	Relaxing the constraint $\mathcal{R} = \mathcal{R}^{-1}$	45
3.3	Summary	45
4	Discrete gauge theories	47
4.1	Spontaneously broken discrete gauge theories	47
4.1.1	Yang-Mills Higgs action	48

4.1.2	Classifying vortex solutions: fluxes	48
4.1.3	Other particles: charges and dyons	50
4.2	Quantum double $D(H)$	51
4.2.1	Algebras	51
4.2.2	Irreps of algebras	53
4.2.3	Coalgebras, bialgebras	55
4.2.4	Quasitriangular bialgebras	57
4.2.5	Exchange operators \mathcal{R}	58
4.2.6	Truncated braid group representations	59
4.2.7	Hopf algebras	59
5	An example: manipulation with $D(S_3)$	61
5.1	Preliminaries for experiments with $D(S_3)$	61
5.2	Special $ 13\rangle$ flux state as a starting point of a sequence of experiments	63
5.3	Arbitrary $ 12\rangle$ state as a starting point of the same sequence	67
5.4	Global $D(S_3)$ transformations explain similarity	70
5.5	A similar ordering with the flux $ 123\rangle$	72
5.6	Identifying unentangled basis-states by relabeling	72
6	Qubits, gates and measurements with $D(H)$	75
6.1	Fluxless pairs as measurable qubits	75
6.2	The <i>Not</i> -gate	76
6.3	Creating combinations of $ 0\rangle$ and $ 1\rangle$ in the relabeled basis	77
6.4	Example of a suggestive mistake	78
6.5	Constructing compatible qubits, gates and measurements is non-trivial	79
6.6	Does $D(H)$ become universal for some H ?	80
7	Do vacuumstates exhibit the whole structure of $D(H)$?	81
7.1	Vacuumstates have a unital density-matrix	82
7.2	Fusion of, or \mathcal{R}^2 on two vacuumstates yields all channels	85
7.3	Projection E_λ commutes with group-action, but not always with action of $D(H)$	86
7.4	All channels are possible if only one particle is a vacuumstate	87
7.5	Relabeling leaves unital density-matrices invariant	88
7.6	Ordering process for particles pulled from the vacuum	89
7.7	Representation-theory instead of description with states	92
8	Conclusions	94
8.1	The generic many-to-one experiment	94
8.2	Scattering versus double slit experiments	97
8.3	Summary	98
	Acknowledgements	102
A	Proof of projection (locking) for double slit experiments	103
A.1	Solving the problem for two eigenvalues	103
A.1.1	Translating the problem from physics to mathematics	103
A.1.2	A new probability distribution: $P_n(z)$	106
A.1.3	Scaling of $P_n^A(z)$ and $P_n^B(z)$ with n yields solution	107
A.2	Examples and more for the case of two eigenvalues	110
A.3	The case for arbitrary many eigenvalues extends easily from that of two eigenvalues	117
A.3.1	Three eigenvalues	117
A.3.2	M eigenvalues	119

B	The spectrum of $D(H)$, with $H = S_3$ as an example	120
B.1	The group S_3 , irreps of $D(S_3)$	120
B.2	Character matrices for $D(H)$ irreps, spin	121
B.3	S -matrix, fusion rules and \mathcal{R}^2 -eigenvalues	123
B.4	An alternative $D(H)$ character-table	126
C	Braid Group B_n	128
D	Graphical notation for the U-matrix	130
	Bibliography	132

CHAPTER 1

INTRODUCTION

The motivation for writing this thesis is to explore the basic features of a rather new and speculative field of research denoted as quantum computation, where the basic hope is to revolutionize computer science. Central in this development is the idea to directly exploit the quantum properties of matter on the fundamental level in order to vastly increase our computational power.

Our work will in particular be concerned with the theoretical possibility to use non-abelian anyons to build a quantum computer. In this chapter, we mainly give a brief introduction to quantum computation, concluding with an outline of the contents of the other chapters.

1.1 Quantum Computation (QC)

We briefly summarize the main features and basic ingredients of quantum computation. We have restricted ourselves to those aspects which are related to our own research. There exist more extensive reviews, Preskill [1], [2–4], to which we refer the interested reader.

1.1.1 The promise of quantum computation

Quantum computation as an area of physics (or science in general) has been known for quite some time. Ever since the development of quantum mechanics the idea of manipulating (and entangling) quantum systems existed. But only recently it has actually caught serious attention and has become a field of rapidly growing interest. A major impetus was the work of Shor [5, 6] who derived an algorithm with which prime-factorization could be performed on a quantum computer faster than on any conventional computer with a conventional algorithm. Since then the exploration (or ‘colonization’) of this new, rather unfamiliar, area (‘territory’) of physics, computer science and mathematics, has accelerated.

A challenge indeed it is. Though progress has been made, both experimentally and theoretically, more research is needed, because as of today it is still unknown and even doubtful whether there ever will be a quantum computer which can demonstrate its miracles. But, even if the answer will be negative, then the lessons we have learned about quantum states and their manipulation have been worth the effort.

And mind you, the quantum world can deceive us easily; making us think that (non-classical) tricks can be done, while in the end this turns out to be impossible. We may recall the Einstein-Podolsky-Rosen problem of entangled particles at first sight suggested the possibility of faster-than-light-transmission: yet another ‘would-be’ possibility that turned out impossible. So we

should be aware, that doing quantum information manipulation ‘almost’, is not good enough. Handwaving arguments and partial calculations will not do. Only a complete (!) calculation will. Or, one’s precious eigenvalues may well average out to zero, or one’s faster-than-light information is purely random, or

1.1.2 QC basics

A quantum computer consists of N *qubits* (qubit = ‘quantum bit’). A single qubit is a state $|\psi\rangle$ in a two dimensional Hilbert space¹. Using the standard basis $\{|0\rangle, |1\rangle\}$ then every qubit-state is a complex, normalized superposition of these two basis-vectors:

$$|\psi\rangle = \alpha|0\rangle + \beta|1\rangle \quad |\alpha|^2 + |\beta|^2 = 1 \quad (1.1)$$

The value of a qubit can be measured, but this measurement projects the state onto one of the basis-vectors. So when measuring the value of $|\psi\rangle$ from (1.1), with probability $|\alpha|^2$ ($|\beta|^2$) the state $|0\rangle$ ($|1\rangle$) is the result of the measurement². A state may be changed to another through a unitary transformation, or in other words a $U(2)$ transformation (because the dimension is two).

The quantum state of the N qubits is the tensor product of the single qubits. This is a 2^N -dimensional Hilbert space with standard basis $|0\rangle \otimes |0\rangle \otimes \dots \otimes |0\rangle, |000\dots\rangle, \dots, |1111\dots 1\rangle$. This state may also be manipulated by unitary transformations, but these are now elements from the group $U(2^N)$. Different single qubits can become *entangled* after such a transformations. An entangled state is a state which cannot be factorised in a tensor product of single qubit states.

The unitary transformations are performed by applying a *gate*. Every gate is a fixed unitary $U(2^m)$ transformation that works on m (arbitrarily chosen by us) qubits and is also called m -qubit-gate.

To do quantum computation, one should be able to perform the whole range of $U(2^N)$ transformations, or at least a dense subset, so that every transformation in $U(2^N)$ can be approximated with arbitrary precision. Although $U(2^N)$ is a continuous group, such a dense subset can be generated by a finite number of gates, as we will show shortly. Such a set is called a *universal set*. One needs a universal set to perform quantum computation.

1.1.3 Universal sets

There are many ways to construct a universal set. We will work out some particular examples below.

The set of all 1-qubit-gates is not universal. If we have a set of gates which generate $U(2)$, i.e. all unitary transformations on one qubit, we could not make $U(2^N)$, so this is not a universal set. This is so, because $U(2) \otimes U(2) \dots \otimes U(2) \neq U(2^N)$. To see this in another way: with 1-qubit-gates one can not create entanglement between qubits, which $U(2^N)$ ($N \geq 2$) can.

In matrix-language all 1-qubit-gates are of the form:

$$U \in U(2) : U = \begin{pmatrix} a & b \\ c & d \end{pmatrix} \quad (1.2)$$

¹A qubit can be thought of as the spinor describing a spin- $\frac{1}{2}$ -particle. That spinor is also a state in a two-dimensional Hilbert space.

²To continue with spin- $\frac{1}{2}$ -particles, the eigenstates of the spin in the z -direction σ_z can serve as the standard basis. Measurements on this standard basis are then measurements of σ_z , the z -component of the spin. For spins, a measurement along another axis is also possible, for instance σ_x . For generic qubits this need not be the case.

with a, b, c, d arbitrary, but obeying unitarity conditions. In the space of two qubits these look like (remember, basis is now: $\{|00\rangle, |01\rangle, |10\rangle, |11\rangle\}$):

$$U \in U(4) : \quad \mathbb{1} \otimes U = \begin{pmatrix} a & b & 0 & 0 \\ c & d & 0 & 0 \\ 0 & 0 & a & b \\ 0 & 0 & c & d \end{pmatrix} \quad U \otimes \mathbb{1} = \begin{pmatrix} a & 0 & b & 0 \\ 0 & a & 0 & b \\ c & 0 & d & 0 \\ 0 & c & 0 & d \end{pmatrix} \quad (1.3)$$

But with only these matrices one can never get (by multiplying them) a $U(4)$ transformation like:

$$W = \begin{pmatrix} 1 & 0 & 0 & 0 \\ 0 & 1 & 0 & 0 \\ 0 & 0 & a & b \\ 0 & 0 & c & d \end{pmatrix} \quad (1.4)$$

In other words, one can only generate a $U(2) \otimes U(2)$ subgroup of $U(4)$, and the operators that generate entanglement belong therefore to the coset $U(4)/U(2) \times U(2)$.

All 1-qubit-gates and $CNot$ are universal. Let us add now to the previous set of 1-qubit-gates just one particular 2-qubit-gate, which can entangle two qubits and makes the total set universal. An example of such a 2-qubit-gate is the '*controlled not*' or just $CNot$.

	In		Out		
	qb 1	qb 2	qb 1	qb 2	
$CNot :$	$ 0\rangle$	$ 0\rangle$	$ 0\rangle$	$ 0\rangle$	
	$ 0\rangle$	$ 1\rangle$	$ 0\rangle$	$ 1\rangle$	
	$ 1\rangle$	$ 0\rangle$	$ 1\rangle$	$ 1\rangle$	
	$ 1\rangle$	$ 1\rangle$	$ 1\rangle$	$ 0\rangle$	(1.5)

As a unitary 4×4 matrix it corresponds to:

$$CNot = \begin{pmatrix} 1 & 0 & 0 & 0 \\ 0 & 1 & 0 & 0 \\ 0 & 0 & 0 & 1 \\ 0 & 0 & 1 & 0 \end{pmatrix} \quad (1.6)$$

Now, by applying multiple 1-qubit-gates (the U 's) and $CNot$ -gates it is possible to form a gate like W from (1.4), which one can for instance prove with a straightforward calculation that uses conjugation properties of $SU(2)$ -matrices. Another, nice, proof is given in Barenco et al. [7].

Gates of the form of W of (1.4) (with $a, b, c, d \in \mathbb{C}$ and obeying unitarity) do form a universal set, see Barenco et al. [7] for further references in which this is proven.

All 1-qubit-gates can be approximated by a finite set of gates. We also need to generate all 1-qubit-gates with a finite set. This is possible in a few ways. To understand one of these ways, think of $SU(2)$ instead of $U(2)$ which are the same up to an overall (unimportant) phase factor. And think of $SU(2)$ as the group of rotations. Every rotation can be approximated by applying two specific rotations with different rotation-axes and with *irrational* rotation-angles (meaning $n\theta_i \neq 2m\pi \forall n, m \in \mathbb{Z}$, or in other words $\frac{\theta_i}{2\pi} \in \mathbb{R} \setminus \mathbb{Q}$). Two specific 'irrational' 1-qubit-gates can thus generate all 1-qubit-gates. However, there are also other universal sets which do not require such an irrational rotation.

Finite 1-qubit-rotations which generate irrational rotations. It is possible to choose two rotations R_i of finite order, i.e. $\exists n : (R_i)^n = \mathbb{1}$, such that the product of these two rotations to be an irrational rotation. If another suitable irrational rotation can be constructed in such a

way, with two additional finite rotations R'_i , all 1-qubit-gates can be generated. The collection of gates $\{R_i, R'_i\}$ generates an infinite subgroup of $U(2)$. If a gate like $CNot$ is furthermore added, the total set becomes universal.

Gates of finite order which generate a finite group; with the addition of measurements this set is universal. An even smaller set can be universal when we take the measurement process into account. If the gates are all of finite order and they generate a finite group (i.e. a finite subgroup of $U(2^N)$), then by measuring some qubits and applying some other gates based on the outcome of the measurement, the resulting transformation (of the qubits which have not been measured) can be an irrational rotation; see Preskill [8, p. 17,18] for an explicit example, which also uses a 3-qubit-gate called ‘toffoli-gate’.

So, when the outcomes of measurements (and proper actions on these outcomes) are considered, an even ‘smaller’ set of gates can be universal. In fact there might be other possible measurements than just a standard-basis measurement. In spin-language: apart from measuring the spin along the z-axis, it might also be possible to measure it along the x-axis. This difference could render a set universal. Perhaps even other measurements, of two spins combined for example, might be possible.

We come to the following definition. A **universal set**, needed to perform quantum computation, in other words a **quantum computer**, is a collection consisting of:

- a finite set of n_i -qubit-gates, where each n_i -qubit-gate is one specific operation working on n_i qubits. This set of gates generates a, possibly finite, subset of $U(2^N)$.
- a finite set of m_j -qubit-measurements, where each measurement measures an eigenvalue of some hermitian operator on m_j qubits, and thereby projects the m_j qubit state in the corresponding eigen-subspace.
- a (infinite or at least large) source of qubits with a specified initial state.

and these combined can generate any $U(2^N)$ -transformation on any initial N -qubit-state.

Usually, only the *set of gates* is considered when talking about universal sets. But the possible measurements form a crucial element in the discussion as well and therefore should also be kept in mind, as should the initial qubit states.

There is not yet a complete classification of which collection is or is not a universal set. For some it is known that they are universal, others are known to be not universal, but given a collection it is not a trivial job to decide whether it is universal or not. To classify a set, one can try to figure out if the set can generate another set that is known to be universal.

Another classification within the ‘group’ of universal sets is possible. Some universal sets may need many more gates and measurements to obtain a specific transformation than other universal sets. So one could compare two universal sets and conclude which one of the two is faster than the other (or which one can do it with polynomially many gates and which one cannot). But also such a classification – to our knowledge – does not yet exist.

This is basically all we are going to say about universal sets, in fact there are other problems that are more pressing when trying to do quantum computation.

1.1.4 The enemy named ‘decoherence’

Unfortunately, the gates and measurements are not the only things that can change the quantum state. The environment usually also interacts with the quantum-state causing the quantum-state to change, to ‘decohere’. This is especially known to be able to destroy entanglement. This decoherence phenomenon is quite dramatic as it is generally held responsible for the emergence of classical physics from the quantum perspective. But if it is known what error might have occurred in the quantum state, one can at least try to correct it.

A diverse arsenal has been developed to battle decoherence. Single qubits can be encoded into multiple qubits. If an error occurs in one of these qubits (usually the environment interacts locally, thereby disturbing one qubit at a time) the error can be detected and corrected (reversed) without destroying or changing the original encoded quantum superposition. One’s system becomes ‘fault-tolerant’ in the sense that if small or local errors do occur, these are corrected for before they can accumulate and become large errors, which would influence the final result. Also, in some specific models, subspaces of the N -qubit Hilbert space have been discovered which were actually decoherence free: when all the local errors are corrected for, quantum computation can be performed in these (usually) global subspaces.

It is in this hardware-oriented regime of battling decoherence, that a lot of work has been done (perhaps even most of it) in the field of quantum computation, both experimentally and theoretically. Almost all experimental setups use electro-magnetic devices to control, manipulate and measure qubits, and the environment is full of electro-magnetic noise. But suppose one could do quantum computation in completely different surroundings, without any decohering noise

1.1.5 Discrete Gauge Theories: decoherence free

Kitaev [9] and Preskill [10] suggested to use *non-abelian anyons* for quantum computation. Such anyons emerge for example from *discrete gauge theories*, as discussed extensively in Propp and Bais [11]. A discrete gauge theory is a gauge theory spontaneously broken down to a (non)abelian finite (discrete) group. These anyons are particles in two dimensions with topological interactions. These interactions only depend on the topology of the multiparticle configuration space which in two dimensions is not simply connected. These interactions can lead to all kinds of entanglements which depend on what type of particles are moved around each other. The important fact is that the entanglement can only be changed by moving particles around each other and so can not be destroyed by local (other) interactions with the noisy environment: there is no decoherence.

So the quantum states, i.e. the internal states of these particles, do not decohere. Also gates can be constructed by using the topological interaction (pulling pairs through other pairs for instance). If the interaction is rich enough to be able to perform several different gates then a universal set is possible. Thus, this intrinsically decoherence-free theory equipped with a universal set, looks like a very powerful candidate to become a real working quantum computer. The description of the for quantum computation relevant features of the discrete gauge theories is given in terms of a so called *quantum double group*.

1.2 Three problems with Discrete Gauge Theories

For various reasons, however, it is questionable whether a quantum computer based on non-abelian anyons, can ever be realized, which implies that for the moment it only serves as physical ‘model’ for a quantum computer.

1.2.1 The physical implementation of this theoretical model

It is fair to point out that non-abelian anyons up to now have never been seen. The discrete gauge theories are in that sense just an abstract theoretical model with no obvious link to reality. Indications of non-abelian statistics have appeared in quantum-Hall experiments and Kitaev [9] suggested a spin-lattice as a possible realization. One may also think of certain types of defects. Non-abelian anyons suited for quantum computation are thus not complete fiction but surely far away from actual usage.

1.2.2 $H = A_5$: huge group

Another problem is to make the interactions rich enough to be universal. In discrete gauge theories, the particle contents and their interactions are based upon a finite non-abelian group. To be universal this group, H , needs to be large enough. Kitaev [9] found the symmetric group S_5 (which has order 120) to be universal, Preskill [10] could do it with only half of it: the alternating group A_5 (of order 60). This is still a very large group; the corresponding spin-lattice-model needs to have a 60 dimensional spin on each lattice site. So although non-abelian anyons may exist, it will be extremely hard to also form a universal set and do quantum computation.

1.2.3 Quantum measurements

But there is a far more interesting question. If the environment cannot interact with the quantum states, it is questionable if we, as (thought)experimenters, can manipulate and measure the quantum states.

The influence of the topological interactions of non-abelian anyons becomes visible in interference experiments. Quantum interference experiments (like the double slit experiment) with non-abelian anyons are *non-trivial* extensions to ordinary interference experiments and to those based on the Aharonov-Bohm-effect. In the non-abelian case one has to thoroughly deal with the residual entanglement of the particles. This has to our knowledge never been examined to the bone, and this is where the emphasis of the present work has been, and where we have obtained a number of interesting new results.

We will indeed work out these quantum interference experiments and determine what can be measured of the quantum states (and what cannot).

1.3 Outline

It is our aim to critically analyze the very interesting proposal of Kitaev and Preskill (and possibly confirm) that non-abelian anyons, as rather abstract entities as introduced by Bais and De Wild Propitius, can be used for quantum computation. But, as pointed out in section 1.1.3, only when the possible gates, measurements and initial states are known, the question of universality of the set (of gates, measurements and initial states) can be considered. We will reach the point of this question, but we will not supply an (the) answer to it: we will describe double slit interference experiments and describe a process to order non-abelian anyons that were pair-created from the vacuum; these double slit experiments combined with this ordered collection of non-abelian anyons allows to identify measurements and initial states; but this is where this thesis ends, we will not investigate different groups H for universality.

Some aspects of the subject of quantum computation are treated in chapter 1.

Chapter 2 will introduce the idea of topologically interacting particles (i.e. non-abelian anyons) and its consequences for a double slit interference experiment. The non-abelian double slit experiment can be used to actually measure something from the quantum system. There are however in the non-abelian case many more possibilities to set up such experiments than in the abelian (Aharonov-Bohm) case. Two different measurement schemes, called ‘one-to-one’ and ‘many-to-one’, are described in chapter 3. A large part of the proof involved can be found in appendix A.

The discrete gauge theories are described (reviewed) in chapter 4, including an extensive introduction to the quantum double group $D(H)$. From this theory both the non-abelian anyons and their topological interactions emerge naturally. Possible gates follow from this interaction. (Fusion of particles, which also might be a tool for quantum computation, is also described.)

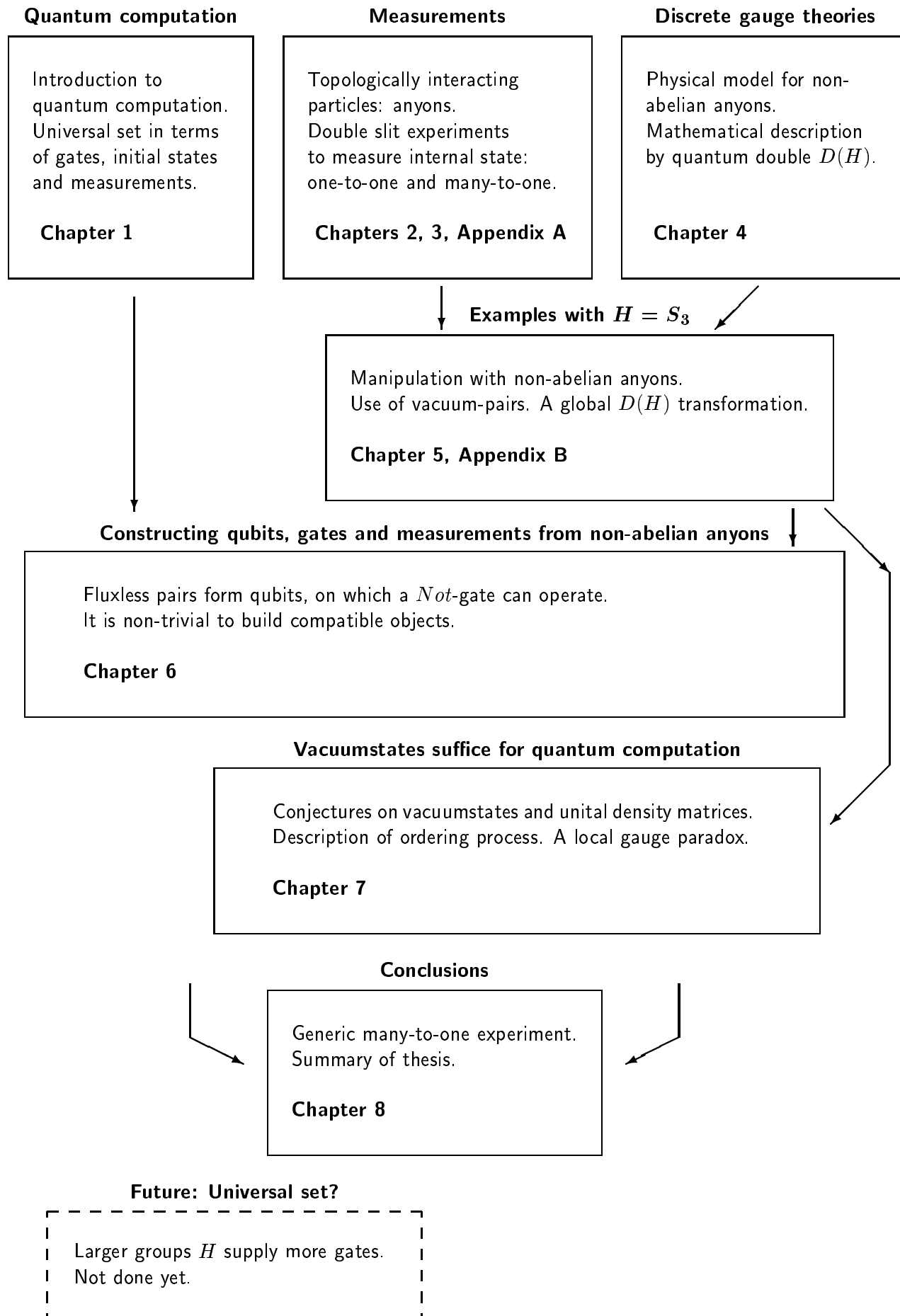
We work out various examples with $H = S_3$ in chapter 5, through which we combine the results of chapters 3 and 4. These examples will not only demonstrate the one-to-one and many-to-one experiments, but will also indicate (1) the presence of some sort of global $D(H)$ symmetry and (2) the possibility that non-abelian anyons that were created from the vacuum are sufficient enough to use for quantum computation. Details concerning $D(S_3)$ are covered in appendix B.

In chapter 6, we will add the ingredients of quantum computation from chapter 1 to the examples with S_3 ; we will construct objects that serve as qubits, gates and measurements. We briefly consider such a, non-trivial, construction, for general $D(H)$; it is imperative that all objects are compatible with each-other.

We take a closer, yet also speculative, look at vacuumstates in chapter 7. Vacuumstates, and their unital density matrices, yield no restrictions on quantum double actions; at least the examples with $D(S_3)$ show such a behavior; unfortunately we have not been able to prove most of the claims we make to show this for general $DH()$. Additionally, we describe an ordering process, through which the highly entangled vacuumstates are mapped on a system of which the state is completely unentangled, and where truly identical particles are neatly ordered on piles. However, this ordering process creates a paradox with respect to local gauge theories, that we will try to explain.

We conclude this thesis with chapter 8. There, we will describe the generic many-to-one double slit experiment as an extension to the description of chapter 3, that is based on the examples with S_3 . We will briefly discuss why we chose for the double slit experiment instead of a scattering experiment. Last, but not least, we will summarize this thesis.

The outline of this thesis is schematically displayed on the next page.



CHAPTER 2

TOPOLOGICALLY INTERACTING PARTICLES AND INTERFERENCE (IN 2D)

In this chapter we will provide the framework for the analysis of double slit experiments with non-abelian anyons, which are possibly entangled two-dimensional particles. In section 2.1 we will describe free particles and in sections 2.2 and 2.3 we will recall the ordinary double slit experiment. Abelian anyons, which are particles with a simple topological interaction, are introduced in section 2.4. In section 2.5 we consider the double slit experiment involving abelian anyons, which reduces to the Aharonov-Bohm case. We continue in section 2.6 with a discussion of non-abelian anyons, which have a richer topological interaction. Preliminary steps for the double slit experiment with non-abelian steps are made in section 2.7. Section 2.8 will summarize this chapter. The problem of actual non-abelian double slit experiments will be taken up for further analysis in chapter 3.

The properties of a topologically interacting theory are simply postulated or stated in this chapter. These properties, such as non-abelian braiding for example, will be derived in chapter 4 where they emerge from the discrete gauge theories.

As mentioned before, an entirely different matter is whether nature admits a physical implementation that exhibits the properties of the theory (as described in this chapter or as in discrete gauge theories). This question will not be considered here. Therefore, one should keep in mind that all experiments that are ‘conducted’ in this thesis are actually ‘thought’ experiments, based on assumptions. Though not yet having a realistic analogue, they do pose a fascinating challenge to both theorists and experimentalists.

2.1 Free particles in two dimensions

Before we begin with interference experiments, let us say something about ‘where’ in physics things will take place (just to assure that there will be no 3+1 dimensional or gravity-involving formulas). Well, we start with nothing more than the quantum mechanics of free particles in two dimensions.

Everything about free quantum mechanical particles and their wave-particle-behaviour (like interference in the double slit experiment) can be found in standard textbooks dealing with quantum mechanics, like Bransden and Joachain [12], Gasiorowicz [13] etcetera.

We then have a two dimensional plane with quantum mechanical particles in it, over which the (three dimensional) experimenter has total control. Thereby we mean that the particles’ wave

function obeys the, non-relativistic, Schrödinger equation in two dimensions for a free particle (which is the wave equation in 2D). Furthermore the experimenter can move the particles in whatever way he likes and can measure its momentum and position. But these measurements are subjected to the Heisenberg uncertainty relation and project out an eigenstate (so momentum and position can not be measured simultaneously with exact precision, and measuring the momentum projects a momentum eigen-state and likewise for the position).

There can be different and identical particles. We assume that different particles have different mass and the experimenter can measure this mass to distinguish particles that are not identical.

What we have so far looks a lot like a three dimensional experimenter playing a game of billiards (which is a two dimensional game). To make clear that these particles are of a quantum mechanical nature we also consider an interference experiment in which the particle-wave-behaviour is observable. This is Young's double slit experiment.

2.2 The ideal double slit experiment

As a warming-up exercise we start with an ideal double slit experiment (even for a thought experiment it is ideal), where the interference pattern can be analytically calculated. For a non-ideal double slit this is not the case, but we will not be needing such an explicit calculation, as will become apparent in the following sections.

In the double slit experiment a particle is directed at an impenetrable wall with two slits, close to each other, in it. Far behind the (wall with the) two slits the particle is again observed at an angle θ . The probability of observing the particle at a specific angle θ can only be understood by the wave-behaviour of the particle, because that is the only way to explain the observed interference pattern (found when repeating this experiment for many particles and making a plot of the angular distribution).

If the incoming particle from the left can be described by a plane wave and the two slits are perfectly identical and ideally infinitesimal small so that circular waves are formed at these two points, then we can calculate this interference pattern easily and exactly.

Let us perform this calculation. Far away from the two slits the amplitude of the two circular waves is proportional to (with k the wave number of the incoming plane wave):

$$\frac{e^{ikr}}{\sqrt{r}} \quad (2.1)$$

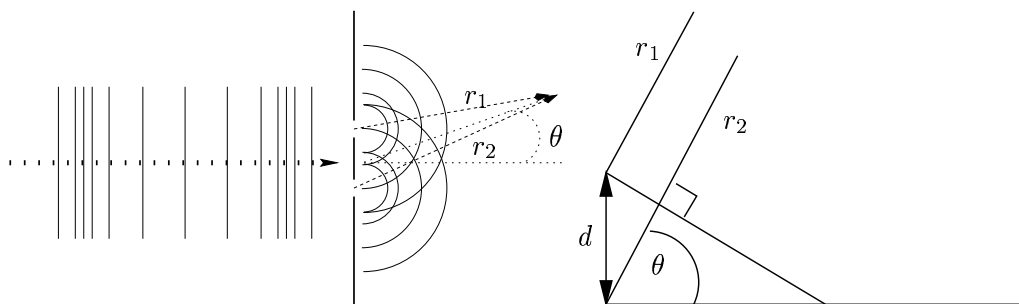


Figure 2.1: The ideal double slit with incoming plane wave and two outgoing circular waves (l). Double slit geometry (r).

There is no need for Bessel functions (which are solutions of the time-independent wave equation) at large distances from the origin; at large distances Bessel functions behave like (2.1). Also, if the distance r is much bigger than the distance d between the two slits then the difference in path-length is:

$$r_2 - r_1 \approx d \sin(\theta) \quad (2.2)$$

The quantum mechanical state $|\psi\rangle$ (the amplitude of the wave) becomes proportional to the sum of two terms. Each term is the contribution from one of the slits:

$$|\psi\rangle = \frac{e^{ikr_1}}{\sqrt{2r_1}} + \frac{e^{ikr_2}}{\sqrt{2r_2}} \quad (2.3)$$

The probability $f(\theta, r)$ to observe the particle at coordinates (θ, r) , is equal to the absolute value squared of the amplitude:

$$\begin{aligned} f(\theta, r) &= ||\psi||^2 = \left| \frac{e^{ikr_1}}{\sqrt{2r_1}} + \frac{e^{ikr_2}}{\sqrt{2r_2}} \right|^2 \\ &= \frac{1}{2r} + \frac{1}{2r} + \frac{e^{ik(r_1-r_2)}}{2r} + \frac{e^{-ik(r_1-r_2)}}{2r} \\ &\approx \frac{1}{r}(1 + \cos(kd \sin(\theta))) \\ &= \frac{2 \cos^2\left(\frac{kd}{2} \sin(\theta)\right)}{r} \end{aligned} \quad (2.4)$$

Which is graphically represented in fig. 2.2.

2.3 The non-ideal case

But, in general, an interference pattern will not look like fig 2.2. This is because in the (general) non-ideal case:

- the incoming particle's wave function is not a plane wave, but some wave packet.
- the two slits are not completely identical.
- the slits are not infinitesimally small, so that the description with circular waves becomes invalid.

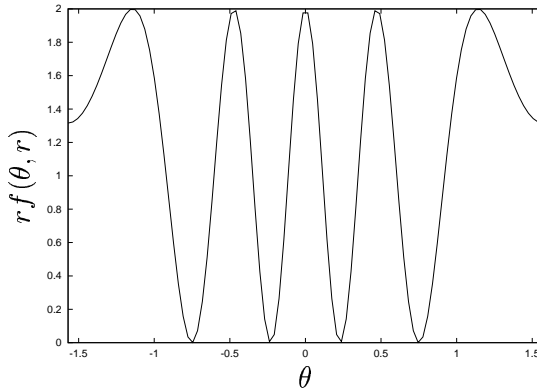


Figure 2.2: Interference pattern in the ideal case. $\lambda = \frac{2\pi}{k} = 2.2d$, so there are two maxima at both sides of $\theta = 0$.

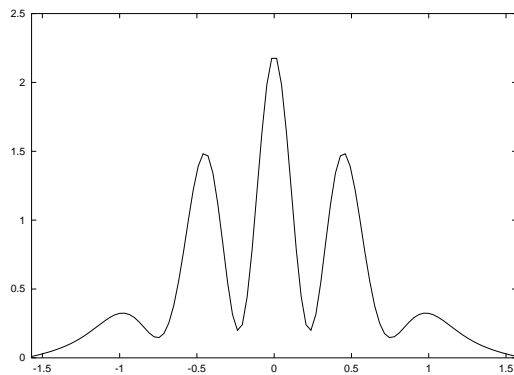


Figure 2.3: A sketch of a more realistic (than in fig 2.2) interference pattern.

Nevertheless, observed interference patterns (with photons or electron for example) look like fig. 2.3, which resembles the ideal case rather good.

So also for the general non-ideal case, we assume we can split the wave function into two parts: one that goes through the upper slit and one that goes through the lower:

$$|\psi\rangle \rightarrow |\psi_{\text{above}}\rangle + |\psi_{\text{below}}\rangle \quad (2.5)$$

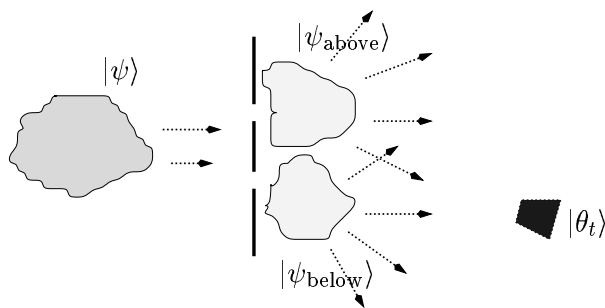


Figure 2.4: The non-ideal double slit

We can expand these two parts (see fig 2.4) in an orthonormal basis $\{|\theta_t\rangle\}$ (indicating the angle θ at a fixed radius r , so it probably is a direction or momentum eigenbasis; a position-eigenbasis is also possible):

$$\begin{aligned} |\psi_{\text{above}}\rangle &= \sum_t c_{\text{above}}^t |\theta_t\rangle & |\psi_{\text{below}}\rangle &= \sum_t c_{\text{below}}^t |\theta_t\rangle \\ c_{\text{above}}^t, c_{\text{below}}^t &\in \mathbb{C} & \langle \theta_{t'} | \theta_t \rangle &= \delta_{t't} \end{aligned} \quad (2.6)$$

Where t (which has nothing to do with time) can be continuous (which the momentum-spectrum is) or discrete (because the number of particle-detectors is probably finite).

The coefficients c_{above}^t and c_{below}^t are *completely determined* by the specific geometry of the double slit setup, and vary with the angle chosen. In other words, c_{above}^t and c_{below}^t are fixed functions of θ_t .

The probability $f(\theta)$ for the particle to be observed behind the double slit, at an angle θ_t , then becomes:

$$f(\theta_t) = |c_{\text{above}}^t + c_{\text{below}}^t|^2$$

$$= |c_{\text{above}}^t|^2 + |c_{\text{below}}^t|^2 + 2\text{Re}(c_{\text{above}}^{t*}c_{\text{below}}^t) \quad (2.7)$$

The functions c_{above}^t and c_{below}^t are normalized such that:

$$\begin{aligned} 1 &= \sum_t f(\theta_t) \\ &= \sum_t |c_{\text{above}}^t|^2 + |c_{\text{below}}^t|^2 + 2\text{Re}(c_{\text{above}}^{t*}c_{\text{below}}^t) \end{aligned} \quad (2.8)$$

indicating that with probability one the particle is found at some angle.

Furthermore at the moment the particle went through the two slits, say at time t_0 , the two parts $|\psi_{\text{above}}\rangle$ and $|\psi_{\text{below}}\rangle$ were at definite different positions in space:

$$\langle\psi_{\text{above}}|\psi_{\text{below}}\rangle = 0 \quad \text{at time } t_0 \quad (2.9)$$

But after that moment t_0 , all time evolution has been unitary (or explicitly: e^{iHt} , where H is the Hamiltonian of this free theory) meaning that (2.9) still holds for later times, implying that:

$$1 = \sum_t |c_{\text{above}}^t|^2 + |c_{\text{below}}^t|^2 \quad (2.10)$$

$$0 = \sum_t c_{\text{above}}^{t*}c_{\text{below}}^t \quad (2.11)$$

For a non-ideal double slit experiment the probability $f(\theta_t)$ is then a sum of three terms:

- $|c_{\text{above}}^t|^2 \geq 0 \forall \theta_t$: the individual contribution from the upper-slit.
- $|c_{\text{below}}^t|^2 \geq 0 \forall \theta_t$: contribution from the lower-slit.
- $2\text{Re}(c_{\text{above}}^{t*}c_{\text{below}}^t)$: an interference term that averages out to zero when summed over all θ_t .

In the case of the ideal double slit interference experiment of the previous section, we can make the following explicit identifications for c_{above}^t and c_{below}^t , at fixed r :

$$\begin{aligned} c_{\text{above}}^t &\longleftrightarrow \frac{e^{ikr_1}}{\sqrt{2r_1}} & r_1 &\approx r + \frac{1}{2}d \sin(\theta^t) \\ c_{\text{below}}^t &\longleftrightarrow \frac{e^{ikr_2}}{\sqrt{2r_2}} & r_2 &\approx r - \frac{1}{2}d \sin(\theta^t) \\ |c_{\text{above}}^t|^2 &\longleftrightarrow \frac{1}{2r} \\ |c_{\text{below}}^t|^2 &\longleftrightarrow \frac{1}{2r} \\ 2\text{Re}(c_{\text{above}}^{t*}c_{\text{below}}^t) &\longleftrightarrow \cos(kd \sin(\theta^t)) \end{aligned}$$

Now we turn to the evolution of the state $|\psi\rangle$. Let E_{θ_t} be the projection operator projecting out the $|\theta_t\rangle$ state, then the particle's wave function during the whole measurement process (passing the two slits, being detected at θ_t , thereby projected at the θ_t -eigenstate) evolves like:

$$|\psi\rangle \rightarrow |\psi'\rangle = |\psi_{\text{above}}\rangle + |\psi_{\text{below}}\rangle \rightarrow |\psi''\rangle = \frac{E_{\theta_t}|\psi'\rangle}{\sqrt{\langle\psi'|E_{\theta_t}|\psi'\rangle}} \quad (2.12)$$

We can then also write $f(\theta_t)$ from (2.7) as:

$$f(\theta_t) = \langle \psi' | E_{\theta_t} | \psi' \rangle \quad (2.13)$$

If one repeats this experiment with many particles (say N) then the observed number N_t of particles at an angle θ_t approaches the probability distribution (2.7):

$$\lim_{N \rightarrow \infty} \frac{N_t}{N} = f(\theta_t) \quad \sum_t N_t = N \quad (2.14)$$

In other words: the observed interference pattern *is* the probability distribution $f(\theta)$. And when talking about the ordinary double slit we use both these two terms to indicate the same thing, because they are the same. However, we emphasize already at this point that when we study non-abelian (entangled) double slit experiments, this identification of the interference pattern with the probability distribution $f(\theta)$ for the single particle does no longer hold necessarily.

This concludes the section about free particles. We are now able to handle a non-ideal double slit: without knowing the exact geometry we know what the probability density distribution $f(\theta_t)$ is, (2.7), and that it is build up from two individual slit terms and an interference term. We know how the state $|\psi\rangle$ changes during the measurement process, when split in $|\psi_{\text{above}}\rangle$ and $|\psi_{\text{below}}\rangle$ and projected with E_{θ_t} , (2.12). We have to be careful when using the terms ‘probability distribution’ $f(\theta_t)$ and ‘interference pattern’ $\lim_{N \rightarrow \infty} \frac{N_t}{N}$, because sometimes they mean the same, sometimes not.

We are now ready to endow the free particles with an interaction, where we select a very special one, denoted as a topological interaction. The difference with the free theory can only be seen in an interference experiment, because as we will show, only the interference term $2\text{Re}(c_{\text{above}}^{t*} c_{\text{below}}^t)$ will change.

2.4 Abelian anyons

The topological interaction of abelian anyons manifests itself in extra phase factors. The difference between abelian anyons and free particles is small, at least compared to the non-abelian anyons which we will describe later. Perhaps most important now, is the introduction of the exchange operators \mathcal{R} and \mathcal{R}^{-1} and the difference between these two.

The two-dimensional particles are now no longer free, because they interact. For we let the wave-function of the free particle $|\psi\rangle$ change in such a way that it gets multiplied by a phase factor F when the particle moves through the plane. This phase factor depends on the taken path of the particle and all the other particles (P_2, \dots, P_N) . So if particle P_1 moves from x_1 to x_2 along a path Γ then:

$$|\psi, x_1\rangle \rightarrow e^{iF(\Gamma, P_2, \dots, P_N)} |\psi, x_2\rangle$$

This is an interaction because P_1 can ‘feel’ the presence of P_2 in its wave-function.

In general, different paths yield different phase factors. But in the case of a topological interaction, there are a lot of different paths that give the same factor. In fact, the phase factor depends only on the topological class the path belongs to.

The physical effect of topological interactions can be efficiently described in terms of the *monodromy* operators. Indicate the monodromy operation, which moves two particles counterclockwise around each other, by \mathcal{R}^2 :

$$\mathcal{R}^2 |P_1, P_2\rangle = e^{i\lambda(P_1, P_2)} |P_1, P_2\rangle \quad (2.15)$$

Moving two particles P_1 and P_2 around each other depends only the types of particle P_1 and P_2 .

As the notation suggests, there is also the counterclockwise exchange or braid operation \mathcal{R} (with of course $\mathcal{R}^2 = (\mathcal{R})^2$) of which the operation is well defined in the case of two identical particles:

$$\mathcal{R}|P_{1(a)}, P_{1(b)}\rangle = e^{i\lambda(P_1, P_1)/2}|P_{1(b)}, P_{1(a)}\rangle \quad (2.16)$$

Particles with this exchanging property have been called ‘anyons’, as a generalization of bosons and fermions for which $\lambda/2 = 0$, $\lambda/2 = \pi$ respectively (the state of two fermions picks up a minus sign when the two are interchanged; nothing happens in the bosonic case).

The clockwise exchange and monodromy are the inverses of \mathcal{R} and \mathcal{R}^2 :¹

$$\mathcal{R}_{\text{clockwise}} = \mathcal{R}^{-1} \quad \mathcal{R}\mathcal{R}^{-1} = \mathcal{R}^{-1}\mathcal{R} = \mathbb{1} \quad (2.17)$$

These operators are linear and also unitary:

$$\mathcal{R}^\dagger\mathcal{R} = \mathcal{R}\mathcal{R}^\dagger = \mathbb{1} \quad (\mathcal{R}^\dagger = \mathcal{R}^{-1}) \quad (2.18)$$

We will use these three operators, the exchangers \mathcal{R} and \mathcal{R}^{-1} and the monodromy \mathcal{R}^2 frequently in everything that will follow. See also fig. 2.5.

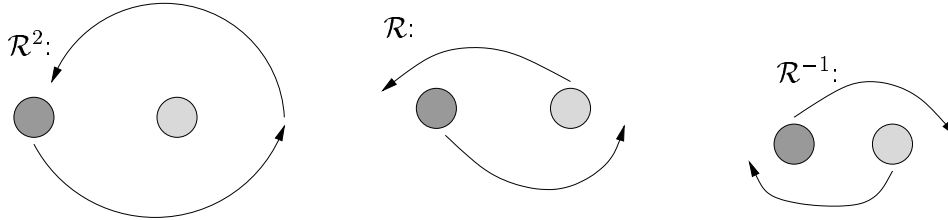


Figure 2.5: Very important operations: monodromy, counterclockwise and clockwise exchange.

Exchanges of multiple particles commute with each other (because phase factors commute); so moving particle 1 around 2 and then particle 2 around 3 is equal to first 2-3 and then 1-2:

$$\mathcal{R}_{12}^2\mathcal{R}_{23}^2 = \mathcal{R}_{23}^2\mathcal{R}_{12}^2 \quad (2.19)$$

This is also the reason to call this ‘abelian braid statistics’. ‘Braid statistics’ because exchanging two particles is not merely a permutation of the two but involves the exchange-direction; ‘abelian’ because different exchanges commute with each other.

We now turn to a double slit experiment with these abelian anyons. Only then the difference with the free theory becomes visible, because of the additional phase factors, which ‘shift’ the interference pattern.

2.5 The Aharonov-Bohm effect

We will again, as in the case of the free theory, first consider the probability $f(\theta_t)$ to find a particle at an angle θ_t , then the evolution of the state during the measurement process and finally what the interference pattern looks like.

¹So \mathcal{R} and \mathcal{R}^{-1} have opposite phase factors. We just choose one of them to be $+\lambda$ and the other $-\lambda$, one clockwise the other counterclockwise, just like we give electrons a negative charge and positrons a positive one: physics will not depend on this choice.

The Aharonov-Bohm effect is the description of the famous phenomena of ‘shifting’ interference patterns when a magnetic flux is put behind the two slits and electrons serve as the incident particles. Although the original paper, Aharonov and Bohm [14], was about a scattering experiment, Feynman, Leighton, and Sands [15] showed the ‘effect’ also with the double slit and since then all quantum mechanics’ textbooks, like Bransden and Joachain [12], illustrate the Aharonov-Bohm effect by means of the double slit experiment. Usually one talks in the context of the $U(1)$ electro-magnetic gauge symmetry, but it works equally well here, since simple phase factors can be considered as elements of $U(1)$.

So, in addition to the double slit, we also position a particle, which we will call A , behind and in between the slits, and then perform the experiment by directing particle B at the two slits. But now, when the two split parts of the wave function, $|\psi_{\text{above}}\rangle$ and $|\psi_{\text{below}}\rangle$ come together again to interfere with each other they have not picked up the same phase factor (also illustrated in fig. 2.6):

$$\begin{aligned} |\psi_B\rangle|A\rangle &\rightarrow |\psi'_B\rangle|A\rangle = |\psi_{\text{above}B}\rangle|A\rangle + |\psi_{\text{below}B}\rangle|A\rangle \\ |\psi'_B\rangle|A\rangle &\rightarrow |A\rangle|\psi''_B\rangle = e^{i\lambda_{\text{above}}}|A\rangle|\psi_{\text{above}B}\rangle + e^{i\lambda_{\text{below}}}|A\rangle|\psi_{\text{below}B}\rangle \end{aligned} \quad (2.20)$$

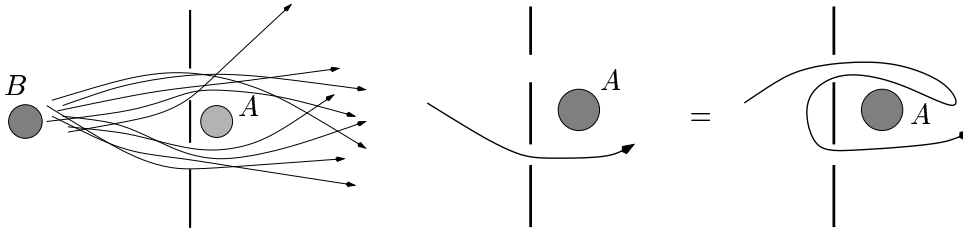


Figure 2.6: The Aharonov-Bohm effect: different paths pick up different phases; But the phase difference is the phase picked up by a closed path around A .

Using again the expansion of $|\psi_{\text{above}}\rangle$ and $|\psi_{\text{below}}\rangle$ of (2.6), we can compute the probability $f(\theta_t)$ of finding particle B at an angle θ_t :

$$|A\rangle|\psi''_B\rangle = \sum_t e^{i\lambda_{\text{above}}} c_{\text{above}}^t |A\rangle|\theta_{tB}\rangle + e^{i\lambda_{\text{below}}} c_{\text{below}}^t |A\rangle|\theta_{tB}\rangle \quad (2.21)$$

$$\begin{aligned} f(\theta_t) &= |e^{i\lambda_{\text{above}}} c_{\text{above}}^t + e^{i\lambda_{\text{below}}} c_{\text{below}}^t|^2 \\ &= |c_{\text{above}}^t|^2 + |c_{\text{below}}^t|^2 + 2\text{Re}(e^{-i(\lambda_{\text{above}} - \lambda_{\text{below}})} c_{\text{above}}^{t*} c_{\text{below}}^t) \end{aligned} \quad (2.22)$$

This resembles the $f(\theta)$ from (2.7) very much: only the interference term has changed, by an extra factor of a phase difference. And we know what the phase difference is (see fig. 2.6):

$$e^{-i(\lambda_{\text{above}} - \lambda_{\text{below}})} = e^{i\lambda(A,B)} \quad \mathcal{R}^2|A\rangle|B\rangle = e^{i\lambda(A,B)}|A\rangle|B\rangle \quad (2.23)$$

It is now convenient to write \mathcal{R} , \mathcal{R}^{-1} and \mathcal{R}^2 explicitly in our equations. Therefore (see also fig. 2.7) we rewrite (2.22) with:

$$|A\rangle|\psi''_B\rangle = \mathcal{R}^{-1}|\psi_{\text{above}B}\rangle|A\rangle + \mathcal{R}|\psi_{\text{below}B}\rangle|A\rangle \quad (2.24)$$

$$E_{\theta_t}|A\rangle|\psi''_B\rangle = c_{\text{above}}^t \mathcal{R}^{-1}|\theta_{tB}\rangle|A\rangle + c_{\text{below}}^t \mathcal{R}|\theta_{tB}\rangle|A\rangle \quad (2.25)$$

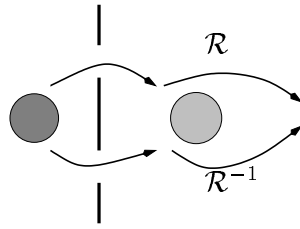


Figure 2.7: The upper part (wave function going through the upper slit) experiences a counterclockwise exchange, \mathcal{R} , and the lower part a clockwise exchange, \mathcal{R}^{-1}

to:

$$f(\theta_t) = \langle \psi_B'' | \langle A | E_{\theta_t} | A \rangle | \psi_B'' \rangle \quad (2.26)$$

$$= |c_{\text{above}}^t|^2 + |c_{\text{below}}^t|^2 + 2\text{Re} \left(c_{\text{above}}^{t*} c_{\text{below}}^t e^{i\lambda(A,B)} \right) \quad (2.27)$$

$$e^{i\lambda(A,B)} = \langle A | \langle \theta_{tB} | \mathcal{R}^2 | \theta_{tB} \rangle | A \rangle = \langle A | \langle B | \mathcal{R}^2 | B \rangle | A \rangle \quad (2.28)$$

where E_{θ_t} is the projection operator projecting on $|\theta_t\rangle$.

In the Aharonov-Bohm effect (the electro-magnetic $U(1)$ -gauge case), where an electron is the incident particle B and a magnetic flux(tube) takes the place of particle A , the \mathcal{R}^2 expectation value in (2.28) is the extra phase factor the electron would pick up if it went around the magnetic flux. Because this phase factor can be continuously changed by changing the magnetic flux the interference pattern $f(\theta)$ can change continuously, resulting in a shifted² pattern, see for instance Silverman [16, p. 16]. We note that \mathcal{R}^2 denoted as the *monodromy operator* will play an essential role in all discussions to come.

What about state-evolution. After measuring the angle θ_t the state will be projected:

$$|A\rangle |\psi_B''\rangle \rightarrow |A\rangle |\psi_B'''\rangle \quad |A\rangle |\psi_B'''\rangle = \frac{E_{\theta_t} |A\rangle |\psi_B''\rangle}{\sqrt{\langle \psi_B'' | \langle A | E_{\theta_t} | A \rangle | \psi_B'' \rangle}} \quad (2.29)$$

Two notational issues, which we already used in the previous equations:

- because \mathcal{R} and \mathcal{R}^{-1} are supposed to be exchange operators we will make this exchange explicit by swapping the two particles in the tensor product after the operation of \mathcal{R} or \mathcal{R}^{-1} :

$$\mathcal{R} : |B\rangle \otimes |A\rangle \rightarrow |\hat{A}\rangle \otimes |\hat{B}\rangle \quad \left(\mathcal{R}^{-1} : |B\rangle \otimes |A\rangle \rightarrow |\tilde{A}\rangle \otimes |\tilde{B}\rangle \right)$$

- the angle-measurement is a local process on B 's state. So in the tensor product, the projection operator E_{θ_t} only projects in B 's state space and behaves as the identity for particle A :

$$E_{\theta_t} : |A\rangle |B\rangle = |A\rangle \otimes |B\rangle \mapsto (\mathbb{1} \otimes E_{\theta_t}) |A\rangle \otimes |B\rangle = |A\rangle (E_{\theta_t} |B\rangle) = |A\rangle |\theta_{tB}\rangle$$

Let us now turn to the interference pattern. An interference pattern, that is a collection $\{N_t\}$, can be obtained in several ways. One could position one particle A behind the two slits and

²To see this 'shift', write the interference term $2\text{Re} \left(c_{\text{above}}^{t*} c_{\text{below}}^t e^{i\lambda(A,B)} \right)$ as $2\text{Re}[a(\theta_t) \exp(ib(\theta_t) + i\lambda)] = 2a(\theta_t) \cos(b(\theta_t) + \lambda)$, where $a(\theta)$, $b(\theta)$ are real functions. So the function $2a(\theta_t)$ is modulated by $\cos(b(\theta_t))$ and this modulation gets shifted by λ .

shoot many B 's at this double slit. One could also have many identical copies of the two particle experiment, where a new particle A , a new B (and perhaps even a new double slit) are used with each next experiment (see fig. 2.8). Nevertheless, these two ways of repeating the experiment and obtaining a set of measured angles $\{\theta_t\}$ are equivalent and both yield the probability distribution $f(\theta_t)$. The interference pattern is the probability distribution, or (as an exact copy of (2.14)):

$$\lim_{N \rightarrow \infty} \frac{N_t}{N} = f(\theta_t) \quad (2.30)$$

But it is important to realize that this is true as a result of a calculation, not by definition. By definition, the probability density distribution is only obtained when repeating the experiment with an ensemble of identically prepared systems.

Since the interference pattern, see (2.27), depends only on the phase factor $e^{i\lambda(A,B)}$ we can define $f_\lambda(\theta_t)$ as the interference pattern for this case (and all other cases with the same λ):

$$f(\theta_t) \equiv f_\lambda(\theta_t) \quad (2.31)$$

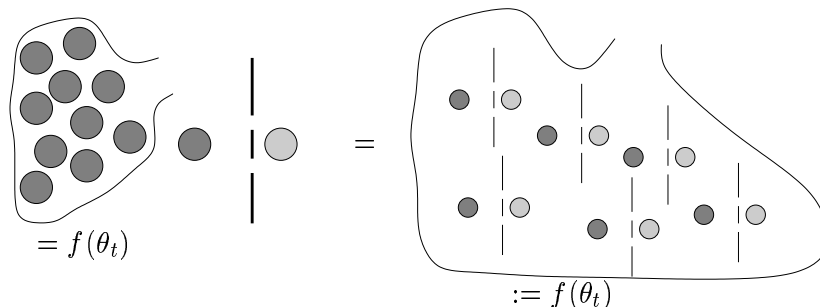


Figure 2.8: Different ways to repeat the experiment; either with a bag of identical particles or with a bag of identical prepared systems. The second one yields the probability distribution $f(\theta_t)$ by definition.

This ends this section about the double slit with abelian anyons. The (abelian) topological interaction changes the interference pattern through a phase factor $e^{i\lambda}$ that depends only on the types of the used particles ($\lambda = \lambda(A, B)$).

We will now consider a more complex topological interaction, which arises if the particles have a higher dimensional internal state space. These internal states can be entangled, and this may have considerable consequences for the double slit experiment.

2.6 Non-abelian anyons

We now consider the case that every particle has a non-trivial internal space, i.e. the one-particle wave function has more components, $|\psi\rangle \in \mathbb{C}^n$. The topological interaction, through the \mathcal{R}^2 operator, will work only on these internal spaces, and is able to entangle two different particles. Next we will consider the problem of how to cope with the, now non-commuting, exchanges. To treat these exchanges consistently turns out to require working with the braid-group B_N instead of the symmetric group (or permutation group) S_n .

So, let's make the interaction between the two-dimensional particles more intricate. We will do it in such a way that the interaction remains topological (in the sense that it only depends on

the number of times particle A winds around particle B) but let it be more than just a phase factor.

This is possible in a system with two particles A and B , endowed with internal degrees of freedom, where we have:

$$|A\rangle = |A_{\text{intern}}\rangle \otimes |A_{\text{extern}}\rangle \quad |B\rangle = |B_{\text{intern}}\rangle \otimes |B_{\text{extern}}\rangle \quad |A_{\text{intern}}\rangle \in V^A, |B_{\text{intern}}\rangle \in V^B$$

The state of the total system is a tensor product of two internal and two external states:

$$|\psi\rangle = |A_{\text{intern}}\rangle \otimes |A_{\text{extern}}\rangle \otimes |B_{\text{intern}}\rangle \otimes |B_{\text{extern}}\rangle$$

An \mathcal{R}^2 operating on these two particles does not change all factors of this two-particle state, because after taking the particles around each other they return to their exact original position in the plane, so \mathcal{R}^2 affects only the internal states:

$$\begin{aligned} |\psi'\rangle = \mathcal{R}^2|\psi\rangle &= |A'_{\text{intern}}\rangle|A_{\text{extern}}\rangle|B'_{\text{intern}}\rangle|B_{\text{extern}}\rangle \\ &= (\mathcal{R}^2 \otimes \mathbb{1} \otimes \mathbb{1}) |A_{\text{intern}}\rangle|B_{\text{intern}}\rangle|A_{\text{extern}}\rangle|B_{\text{extern}}\rangle \\ &= (\mathcal{R}^2|A_{\text{intern}}\rangle|B_{\text{intern}}\rangle) |A_{\text{extern}}\rangle|B_{\text{extern}}\rangle \end{aligned} \quad (2.32)$$

\mathcal{R}^2 is a general³ linear unitary operator operating on the two particles' internal spaces (i.e. $\mathcal{R}^2 \in U(n+m)$ if $\dim V^A = m$ and $\dim V^B = n$), and \mathcal{R}^2 depends furthermore only on the types of particles:

$$\mathcal{R}^2 : V^A \otimes V^B \rightarrow V^A \otimes V^B \quad \mathcal{R}^2 = \mathcal{R}_{AB}^2 \quad (2.33)$$

This means that by acting with \mathcal{R}^2 on A and B , their internal states may become entangled, since \mathcal{R}^2 works on the combined tensor product, and is more than a phase factor, for $\mathcal{R}^2 \neq e^{i\lambda(A,B)}$ (in general, that is). And \mathcal{R}^2 can be different when winding different particles, $\mathcal{R}_{AB}^2 \neq \mathcal{R}_{CD}^2$.

Although phase factors commute with each other (like in the abelian case in the previous section) unitary operators in general do not. So if there are three particles A , B and C then:

$$\mathcal{R}_{AB}^2 \mathcal{R}_{BC}^2 \neq \mathcal{R}_{BC}^2 \mathcal{R}_{AB}^2 \quad (2.34)$$

We can follow the abelian case by introducing the counter- and clockwise exchange operators \mathcal{R} and \mathcal{R}^{-1} . They operate on the internal states, but also swap the particles, which we make explicit by:

$$\mathcal{R}, \mathcal{R}^{-1} : V^A \otimes V^B \rightarrow V^B \otimes V^A \quad \mathcal{R} \neq \mathcal{R}^{-1} = \mathcal{R}^\dagger \quad (2.35)$$

Topologically interacting particles are distinguishable from free particles because of the operation of \mathcal{R} and \mathcal{R}^{-1} . Physical results due to the topological interaction will depend only on these exchange operators, but we will have to keep track of the exchanges ourselves⁴. Especially because of the non-commuting of these exchanges the order of exchanges is important, as are the positions of other particles. This is illustrated in fig. 2.9.

One way to deal with this ordering-problem is by introducing a branchcut or dirac string: attach a string to each particle and keep the other end at some point at spatial infinity and say that an \mathcal{R} or \mathcal{R}^{-1} 'is applied' when a particle crosses another particles' string. See fig. 2.10. Although it involves a choice (namely that of the point at spatial infinity, and what to call \mathcal{R} or \mathcal{R}^{-1}), physics will not depend on this choice.

³In the discrete gauge theories there will be an extra condition satisfied by \mathcal{R}^2 , namely $(\mathcal{R}^2)^m = \mathbb{1}$ for some $m \in \mathbb{Z}$.

⁴We have to do it ourselves, in the sense that we simplified the theory and the interaction by assuming the particles to be almost free, so when two particles exchange we have to apply an \mathcal{R} by hand; because no equation of motion of a free particle will do this for us.

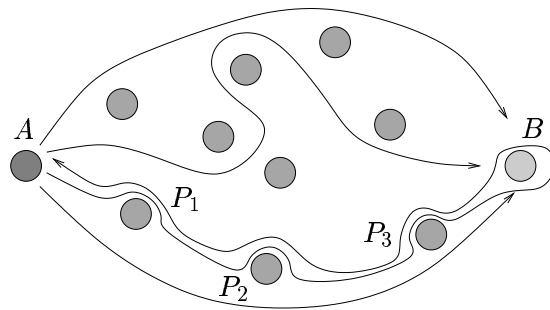


Figure 2.9: How can you exchange A and B when an ‘asteroid field’ of other particles lies between? There are many, topologically different, ways to get from A to B and how can you distinguish between them? In the abelian case this was not a problem because phase factors commute. This is illustrated by a path from A to B with counterclockwise exchanges with P_1 , P_2 and P_3 when A is on its way to B and clockwise exchanges on its way back. These encountered phase factors are opposite and so are all cancelled (except for the \mathcal{R}^2 of A and B). This happens for any path because $e^{i\lambda(\text{path 1})}e^{i\lambda(\text{closed path 2})}e^{i\lambda(\text{path 1 back})} = e^{i\lambda(\text{closed path 2})}$.

We can make life even easier by mapping all particles in the plane on a horizontal line in such a way that all strings run to vertical infinity (this rearrangement can always be done; of course the physical results will never depend on the particular choice one makes to order or label the particles). Then, if we wish to exchange two particles we should exchange them with all particles in between, where ‘between’ now has a well defined meaning. All we have to do further, is to make explicitly clear if an adjacent-particle-pair-exchange is counterclockwise (an \mathcal{R}) or clockwise (\mathcal{R}^{-1}).

All possible exchanges of two arbitrary particles have now become a sequence of neighbour-particle exchanges. To write such a sequence explicitly one can number the positions of the particles and write \mathcal{R}_i for an exchange of the particles at positions i and $i + 1$, in a counterclockwise way. Like in fig. 2.11.

One may show that the successive interchanges form representations of the braid group by their commutation relations:

$$\mathcal{R}_i \mathcal{R}_{i+1} \mathcal{R}_i = \mathcal{R}_{i+1} \mathcal{R}_i \mathcal{R}_{i+1} \quad (2.36)$$

$$\mathcal{R}_i \mathcal{R}_j = \mathcal{R}_j \mathcal{R}_i \quad |j - i| \geq 2 \quad (2.37)$$

These are the celebrated Yang–Baxter relations, which are nothing but the defining relation for generators of the braid group.

This is also why we say that these particles have ‘non-abelian braid statistics’: they form representations of the braid group (therefore ‘braid statistics’) and different braidings do not commute with each other (in general) which makes it a non-abelian group. These particles are also called ‘non-abelian anyons’.

But note that we, as experimenters, cannot directly observe the internal state of a particle nor the entanglement of two particles. As for what we can see, we are still dealing with free particles. Once again we will have to turn to an interference experiment to observe the physical manifestation of the entanglement due to the non-commuting topological features we just described.

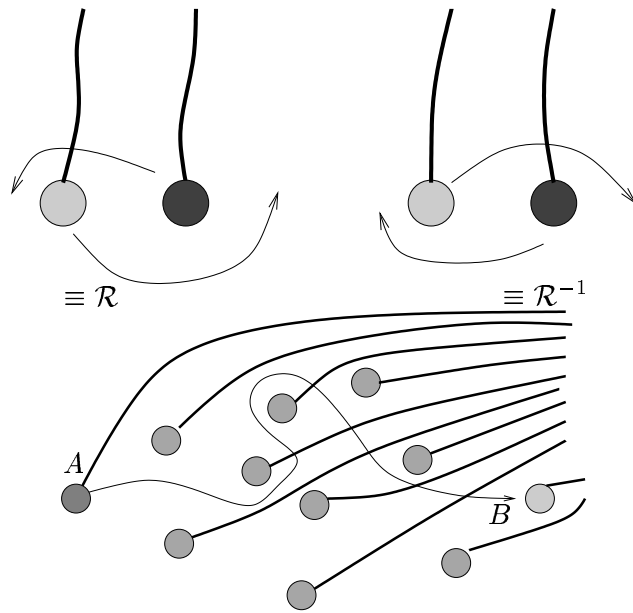


Figure 2.10: Branchcut or dirac string put into practice. If a particle crosses a string the appropriate exchange operator is performed. This solves the problem of which particles to exchange with which when getting from A to B (once the path has been given).

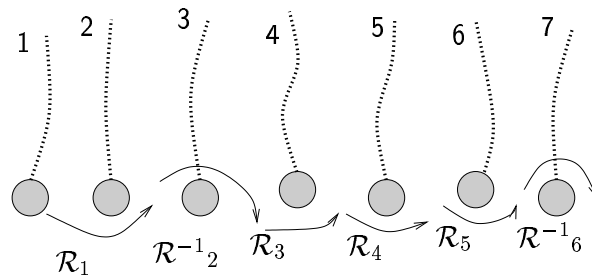


Figure 2.11: Put all the particles on a line and give them (their positions) a number. All exchanges now become combinations of adjacent particle exchanges. \mathcal{R}^{-1}_6 is the clockwise exchange of the two particles currently present at positions 6 and 7.

2.7 The non-abelian, or entangled, double slit experiment

Now we will describe the double slit experiment with the particles that exhibit these non-abelian braid properties. We will follow basically the same steps as in the abelian and free case, although the operation of (for instance) \mathcal{R} does change, of course.

Subsequently we will discuss the probability distribution $f(\theta_t)$, the evolution of the state, most importantly due to the projection E_{θ_t} and finally the interference pattern itself. But here we encounter a problem, because different ways to get an interference pattern give different results. That is due to the entanglement, which changes the initial internal state of the particle behind the two slits. It will only be in chapter 3 that we fully solve this problem.

We start with two particles A and B . A is positioned behind the double slit and B is being directed from the left towards the double slit. The initial state of the system is:

$$|\psi\rangle = |B_{\text{intern}}\rangle|B_{\text{extern}}\rangle|A_{\text{intern}}\rangle|A_{\text{extern}}\rangle$$

Since particle A will not be moved, we can forget about its external state:

$$|A_{\text{extern}}\rangle \rightarrow \dagger$$

When B crosses the two slits its external wave function is split into an upper and lower term, just as in (2.5) and (2.6):

$$|B_{\text{extern}}\rangle \rightarrow |\psi_{\text{above}}\rangle + |\psi_{\text{below}}\rangle \rightarrow |\theta_t\rangle$$

The upper part passes particle A in a clockwise way, the lower part in a counterclockwise fashion, or:

$$|\psi_{\text{above}}\rangle \leftarrow \mathcal{R}^{-1} \quad |\psi_{\text{below}}\rangle \leftarrow \mathcal{R}$$

The new state $|\psi'\rangle$ just before measuring the angle then becomes (see also fig 2.12):

$$|\psi'\rangle = \sum_t [c_{\text{above}}^t \mathcal{R}^{-1} + c_{\text{below}}^t \mathcal{R}] |B_{\text{intern}}\rangle |A_{\text{intern}}\rangle |\theta_t\rangle \quad (2.38)$$

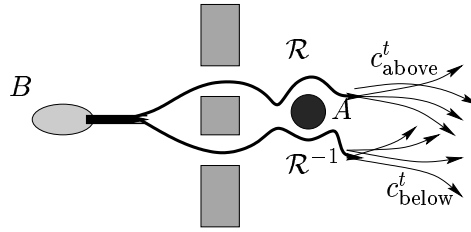


Figure 2.12: A schematic picture of a (non-abelian) double slit experiment.

Because \mathcal{R} and \mathcal{R}^{-1} only work on the internal states we only care about the order in which the internal states appear in the full tensor product. We already stated that the exchange operators explicitly swap the internal states, meaning that:

$$|B_{\text{intern}}\rangle |A_{\text{intern}}\rangle \in V^B \otimes V^A \quad [c_{\text{above}}^t \mathcal{R}^{-1} + c_{\text{below}}^t \mathcal{R}] |B_{\text{intern}}\rangle |A_{\text{intern}}\rangle \in V^A \otimes V^B$$

The probability $f(\theta_t)$ of observing particle B at an angle θ_t now becomes:

$$f(\theta_t) = \langle \psi' | E_{\theta_t} | \psi' \rangle \quad (2.39)$$

$$= |c_{\text{above}}^t|^2 + |c_{\text{below}}^t|^2 + 2\text{Re}(c_{\text{above}}^{t*} c_{\text{below}}^t \langle A_{\text{int}} | \langle B_{\text{int}} | \mathcal{R}^2 | B_{\text{int}} \rangle | A_{\text{int}} \rangle) \quad (2.40)$$

Notice the resemblances and differences of this result with the free (2.7) and abelian (2.27) case.

During this measurement the state $|\psi'\rangle$ is projected on the $|\theta_t\rangle$ eigenstate and thus changes to $|\psi''\rangle$:

$$|\psi''\rangle = \frac{E_{\theta_t} |\psi'\rangle}{\sqrt{\langle \psi' | E_{\theta_t} | \psi' \rangle}} \quad (2.41)$$

$$= \frac{c_{\text{above}}^t \mathcal{R}^{-1} + c_{\text{below}}^t \mathcal{R}}{\sqrt{f(\theta_t)}} |B_{\text{int}}\rangle |A_{\text{int}}\rangle |\theta_t\rangle \quad (2.42)$$

Similar to (2.12) and (2.29) for respectively the free and abelian version of the theory.

Although A is still positioned behind the double slit and B is somewhere at the right of the detecting device, their internal states are in general entangled right now!

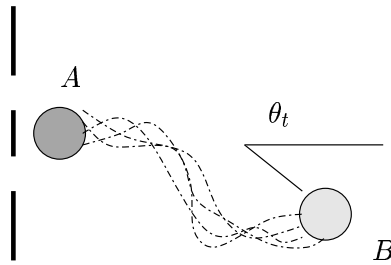


Figure 2.13: A and B are entangled (their internal states) after the observation of B at an angle θ_t .

Now we come to the question of the interference pattern. We mention again that a single observation does not form an interference pattern. For a real visible pattern many observations are needed. Therefore the experiment has to be repeated, but the crucial point is now that this can be done in several ways.

The usual way is to repeat the experiment with a collection of identically prepared systems, so a new A and B are being used with each next experiment. This gives by definition the probability distribution $f(\theta_t)$. In that case we can repeat (2.14):

$$\lim_{N \rightarrow \infty} \frac{N_t}{N} = f(\theta_t) \quad (2.43)$$

And since the eigenvalues of the unitary monodromy operator \mathcal{R}^2 are phases we can write this (or equivalently rewrite (2.40)) as a weighed sum over $f_{\lambda}(\theta_t)$'s from (2.31):

$$f(\theta_t) \equiv \sum_i p_{\lambda_i} f_{\lambda_i}(\theta_t) \quad \sum_i p_{\lambda_i} = 1 \quad (2.44)$$

Where the eigenvalues of \mathcal{R}^2 are the $e^{i\lambda_i}$ and the expectation value for \mathcal{R}^2 is: $\langle \mathcal{R}^2 \rangle = \sum_j p_{\lambda_j} e^{i\lambda_j}$. This result stresses the essential role which the eigenstates and eigenvalues of the \mathcal{R}^2 -matrix play in these types of experiments.

Apart from shifting the probability distribution (as in the abelian case), it has now also become possible to change the amplitude of the interference term. There is even a possibility to lose interference completely now. This happens if $\langle \text{in} | \mathcal{R}^2 | \text{in} \rangle = 0$ (the two-particle internal state changes to another state, orthogonal to the original, after applying \mathcal{R}^2). Then the probability distribution is the sum of probabilities of two single slit experiments and the interference-causing term is lost⁵:

$$\langle \text{in} | \mathcal{R}^2 | \text{in} \rangle = 0 \quad \Rightarrow \quad f(\theta_t) = |c_{\text{above}}^t|^2 + |c_{\text{below}}^t|^2 \quad (2.45)$$

But if we repeat the experiment in a different way, by using the same A behind the two slits every time and using many identically prepared particles B , we will find again a collection of measured angles $\{N'_t\}$ but these do, in general, not yield the same distribution $f(\theta_t)$:

$$\lim_{N' \rightarrow \infty} \frac{N'_t}{N'} = g(\theta_t) \neq f(\theta_t) \quad (2.46)$$

This is so, because the internal state of A changes, as it becomes entangled with all the B 's that already passed the two slits. What this $g(\theta_t)$ will be if it is not $f(\theta_t)$ will be one of the main questions to be answered in this thesis, and is the subject of chapter 3.

Let us now summarize what we have found so far, focussing on the double slit results.

⁵Of course there are also other ways to lose interference, for example (in the conventional way) when probing through which slit the particle went.

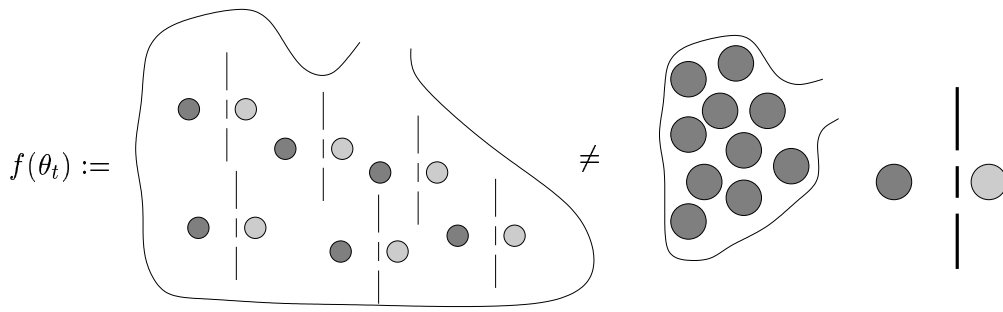


Figure 2.14: In the non-abelian case repeating the experiment with a bag of identical systems is not the same as repeating it with a bag of identical particles, because the state of the particle behind the slit changes (continuously).

2.8 Summary

The three different theories (free, abelian and non-abelian) and their double slit experiment results for the *probability distribution*⁶ are put together in table 2.1.

These results are not new, they're just shown schematically, and written in a suitable notation for what still has to come. These results only consider the probability to find particle B at a certain angle. It does not consider B anymore after it has been detected. In conventional double slit experiments the projectile (photon, electron) is indeed lost after it has been detected. But here, in this setup, this is *not necessarily* the case. Particle B is still part of the total system and is, especially, entangled with A and a position-measurement or other measurement of external degrees of freedom cannot break this entanglement!

Remember that we assumed to have complete control over the particles: we can move them around at will and are allowed to use the same particles in successive experiments if we want to. Perhaps these are optimistic if not crazy assumptions, nevertheless we make them and should continue consistently.

Perhaps we should also note that this chapter has been written with the discrete gauge theories of chapter 4 in mind. The idea of a topological interaction and the entangled double slit can be introduced without the knowledge of such a (more specific) theory. The new elements were the \mathcal{R} -operators satisfying the braid group relations and those were discrete-gauge-theory-inspired.

⁶As already stated, the interference pattern results are postponed till chapter 3.

	probability distribution $f(\theta_t)$	$\mathcal{R}^2 :$ $V^A \otimes V^B \rightarrow V^A \otimes V^B$	$\langle \mathcal{R}^2 \rangle =$ $\langle \text{in} \mathcal{R}^2 \text{in} \rangle$	$f(\theta_t)$ in terms of $f_\lambda(\theta_t)$
Free particles	$ c_{\text{above}}^t ^2 + c_{\text{below}}^t ^2$ $+ 2 \text{Re} (c_{\text{above}}^{t*} c_{\text{below}}^t)$	$\mathbb{1}_A \otimes \mathbb{1}_B$	1	$f_0(\theta_t)$
Abelian interaction	$ c_{\text{above}}^t ^2 + c_{\text{below}}^t ^2$ $+ 2\text{Re} (c_{\text{above}}^{t*} c_{\text{below}}^t e^{i\lambda})$	$e^{i\lambda} \mathbb{1}_A \otimes \mathbb{1}_B$	$e^{i\lambda}$	$f_\lambda(\theta_t)$
Non- abelian interaction	$ c_{\text{above}}^t ^2 + c_{\text{below}}^t ^2$ $+ 2\text{Re} (c_{\text{above}}^{t*} c_{\text{below}}^t \langle \text{in} \mathcal{R}^2 \text{in} \rangle)$	$\mathcal{R}^2 = \sum_j e^{i\lambda_j} E_{\lambda_j}$	$\sum_j p_{\lambda_j} e^{i\lambda_j}$	$\sum_j p_{\lambda_j} f_{\lambda_j}(\theta_t)$
$ \psi\rangle \rightarrow \psi'\rangle = \mathcal{R}^{-1} \psi_{\text{above}}\rangle + \mathcal{R} \psi_{\text{below}}\rangle \rightarrow \psi''\rangle = \frac{E_{\theta_t} \psi'\rangle}{\sqrt{f(\theta_t)}}$ $ \psi_{\text{above}}\rangle = \sum_t c_{\text{above}}^t \theta_t\rangle \quad \psi_{\text{below}}\rangle = \sum_t c_{\text{below}}^t \theta_t\rangle$				

Table 2.1: Schematic results for this chapter. The non-abelian double slit is a generalization of the abelian Aharonov-Bohm effect which is a generalization of the ordinary double slit experiment. E_{λ_j} is the projection operator projecting on the $e^{i\lambda_j}$ eigenspace, $p_{\lambda_j} = \langle \text{in} | E_{\lambda_j} | \text{in} \rangle$ and $\sum_j p_{\lambda_j} = 1$.

CHAPTER 3

TWO DOUBLE SLIT EXPERIMENTS WITH NON-ABELIAN ANYONS

In this chapter we will answer the remaining questions of chapter 2 about the possible interference patterns that may arise in double slit experiments for non-abelian anyons. We will indeed succeed in determining what $g(\theta)$, from (2.46) on page 26, will be: i.e. what we will measure, when we direct many particles at a single particle behind the two slits. We will call this experiment ‘many-to-one’.

But first we will be working out another double slit experiment, one that only requires two particles (not many). Although this experiment, which we will call ‘one-to-one’, yields yet another interference pattern $h(\theta)$, its calculations are easier than for the ‘many-to-one’ case, and it is less technically involved. After treating this ‘one-to-one’ case in section 3.1, which we will solve completely, we will work out the ‘many-to-one’ experiment, which we will solve under certain restrictions (so not yet completely), in section 3.2. As the calculations go along it will also become clear why we need those restrictions. We will summarize our findings in section 3.3, particularly in table 3.1 (p. 46).

We put these two results in a separate chapter, and not in chapter 2 with the other (abelian and free theory) interference experiments, because the results presented here are new, and obtaining them requires more technicalities. A large part of the proof involved has been relegated to appendix A.

Although these kinds of interference experiments have been considered before, in Propitius and Bais [11] and Preskill [10], the role of the remaining entanglement and its drastic effect on the outcomes of the experiments with many successive projectiles, will be treated here thoroughly for the first time.

For both thought experiments, the sequential measurements turn out to lock the system in some specific state; we measure some eigenvalue of an operator on the particles’ internal states, and we thus also project our system onto the measured eigenstate. So, although we can not measure the internal state for a single particle directly (this was one of the important assumptions), we can probe the internal state indirectly through the one-to-one and many-to-one experiments.

3.1 The one-to-one experiment, where the out-state is the next in-state

First we will describe what we mean by the ‘one-to-one’ experiment, and we will already tell what its interference pattern will be, in section 3.1.1. Next, in section 3.1.2, we will work

out the actual problem of projection and eigenvalues. The mathematical part of the proof has been relegated to the appendix. We will then sum up what we have found and give an example to illustrate the process of projection through the successive measurements of angles, in sections 3.1.3 and 3.1.4.

3.1.1 What is ‘one-to-one’ and what is its interference pattern

This experiment requires only two particles: one particle A and one particle B . Both particles are re-used for each consecutive measurement; where we assume that the out-state of a measurement is the in-state for the next.

The total experiment then consists of repeated actions: particle B is directed at the double slit, measured at an angle θ^1 , brought back to its original position, directed again at the slits, measured at $\theta^2 \dots$, as depicted in fig. 3.1. Particle A remains in its position, behind the double slit, during the experiment. With every next (angular) measurement, the two particles A and B (can) become more and more entangled.

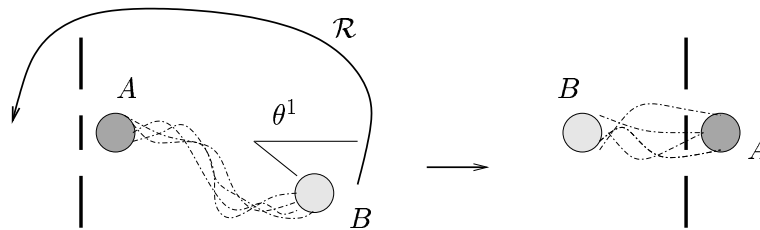


Figure 3.1: Repeat the experiment with the same two particles after bringing back B to its original position, which is done by performing an additional \mathcal{R} -operation.

Having repeated these steps N times, one can (again) define the ‘observed’ interference pattern:

$$h(\theta_t) := \lim_{N \rightarrow \infty} \frac{N_t}{N} \tag{3.1}$$

Where (again) N_t is the number of times particle B has been measured at the angle θ_t .

In this setup, there are two questions one would like to answer:

1. What will be this $h(\theta_t)$ which we will find after N measurements, in the limit $N \rightarrow \infty$?
2. What can we say about the two-particle internal state, given that we found a specific $h(\theta_t)$?

As to the first question, we obtained that:

$$h(\theta) = f_\lambda(\theta) \quad e^{i\lambda} \text{ eigenvalue of } \mathcal{R}^2 \tag{3.2}$$

This says that the observed pattern, $f_\lambda(\theta)$, is the same ‘shifted’ pattern one would find in the abelian theory where the shift was caused by a phase factor $e^{i\lambda}$. But this particular phase factor $e^{i\lambda}$ is an eigenvalue of the monodromy-operator \mathcal{R}^2 .

Concerning the second question about what happened to the state of the system: the two-particle internal state will be projected onto the eigenspace corresponding to the eigenvalue $e^{i\lambda}$.

As \mathcal{R}^2 can have distinct eigenvalues, different eigenvalue-patterns $f_\lambda(\theta)$, or ‘eigen-patterns’ in short, can be found in this one-to-one experiment. If E_λ is the projection operator, which projects the initial two-particles’ internal state $|\psi_{\text{in}}\rangle$ onto the eigenspace of the \mathcal{R}^2 -eigenvalue $e^{i\lambda}$, then the probability p_λ of observing the eigenpattern $f_\lambda(\theta)$ associated with a particular eigenvalue $e^{i\lambda}$ is:

$$p_\lambda = \langle \psi_{\text{in}} | E_\lambda | \psi_{\text{in}} \rangle \quad (3.3)$$

The final internal state $|\psi_{\text{final}}\rangle$ of the two particles A and B , when in the limit of $N \rightarrow \infty$ the eigenpattern $f_\lambda(\theta)$ has been observed, can be written as:

$$|\psi_{\text{final}}\rangle = \frac{E_\lambda |\psi_{\text{in}}\rangle}{\sqrt{\langle \psi_{\text{in}} | E_\lambda | \psi_{\text{in}} \rangle}} \quad (3.4)$$

The square root in the denominator is needed to normalize $|\psi_{\text{final}}\rangle$.

Now we will verify the above statements by explicit calculation.

3.1.2 The one-to-one experiment in more detail

There is an initial two-particles’ internal state $|\psi_{\text{in}}\rangle \in V^B \otimes V^A$. Call this state the in-state for the first ‘run’ of the experiment:

$$|\psi_{\text{in}}\rangle_1 \equiv |\psi_{\text{in}}\rangle$$

This first run yields an observed angle $\theta_{t_1} \equiv \theta^1$ and an out-state $|\psi_{\text{out}}\rangle_1$. We know from chapter 2 (see table 2.1, p. 28) what this out-state looks like:

$$\begin{aligned} |\psi_{\text{out}}\rangle_1 &= \frac{1}{\sqrt{K}} [c_{\text{above}}^{t_1} \mathcal{R}^{-1} + c_{\text{below}}^{t_1} \mathcal{R}] |\psi_{\text{in}}\rangle \\ &\equiv \frac{1}{\sqrt{K}} [c_{\text{above}}^1 \mathcal{R}^{-1} + c_{\text{below}}^1 \mathcal{R}] |\psi_{\text{in}}\rangle \end{aligned} \quad (3.5)$$

Here we wrote the normalizing denominator as \sqrt{K} , for compact notation.

Next we bring back B to its original position in a counterclockwise way, by performing an \mathcal{R} , see fig. 3.1. The resulting state will be the in-state for the second run of the experiment:

$$|\psi_{\text{in}}\rangle_2 := \mathcal{R} |\psi_{\text{out}}\rangle_1$$

And this we can continue for every k ’th run:

$$|\psi_{\text{in}}\rangle_k := \mathcal{R} |\psi_{\text{out}}\rangle_{k-1}$$

So, this means that:

$$\begin{aligned} |\psi_{\text{in}}\rangle_2 &= \frac{1}{\sqrt{K_1}} [c_{\text{above}}^1 + c_{\text{below}}^1 \mathcal{R}^2] |\psi_{\text{in}}\rangle \\ |\psi_{\text{in}}\rangle_{N+1} &= \frac{1}{\sqrt{K_N}} [c_{\text{above}}^N + c_{\text{below}}^N \mathcal{R}^2] \dots [c_{\text{above}}^1 + c_{\text{below}}^1 \mathcal{R}^2] |\psi_{\text{in}}\rangle \end{aligned} \quad (3.6)$$

Furthermore, $|\psi_{\text{in}}\rangle_{N+1}$ is thus a function of the N observed (somewhat random) angles $\theta^1 \dots \theta^N$. The normalization factors K are now labeled by 1 and N to indicate that $K_1 \neq K_N$.

Now let’s rewrite these equations by introducing the projection operator E_λ , which projects any two-particle internal state $|\psi\rangle \in V^B \otimes V^A$ onto the $e^{i\lambda}$ eigenspace of the monodromy-operator \mathcal{R}^2 .

$$\mathcal{R}^2 = \sum_j e^{i\lambda_j} E_{\lambda_j} \quad \sum_j E_{\lambda_j} = \mathbb{1}_B \otimes \mathbb{1}_A = \mathbb{1}$$

The operators E_λ obey the *projector algebra*:

$$E_\lambda E_\mu = E_\mu E_\lambda = \delta_{\lambda\mu} E_\lambda \quad (E_\lambda)^2 = E_\lambda = (E_\lambda)^\dagger$$

Then:

$$\left[c_{\text{above}}^k + c_{\text{below}}^k \mathcal{R}^2 \right] = \left[c_{\text{above}}^k \mathbb{1} + c_{\text{below}}^k \mathcal{R}^2 \right] = \sum_j \left[c_{\text{above}}^k + c_{\text{below}}^k e^{i\lambda_j} \right] E_{\lambda_j}$$

Now we may recast (3.6) into the following form:

$$\begin{aligned} |\psi_{\text{in}}\rangle_{N+1} &= \sum_{j_1, j_2, \dots, j_N} \frac{1}{\sqrt{K_N}} \left[c_{\text{above}}^N + c_{\text{below}}^N e^{i\lambda_{j_N}} \right] \dots \left[c_{\text{above}}^1 + c_{\text{below}}^1 e^{i\lambda_{j_1}} \right] E_{\lambda_{j_N}} \dots E_{\lambda_{j_1}} |\psi_{\text{in}}\rangle \\ &= \sum_j \frac{1}{\sqrt{K_N}} \left[c_{\text{above}}^N + c_{\text{below}}^N e^{i\lambda_j} \right] \dots \left[c_{\text{above}}^1 + c_{\text{below}}^1 e^{i\lambda_j} \right] E_{\lambda_j} |\psi_{\text{in}}\rangle \\ &\equiv \frac{1}{\sqrt{K_N}} \sum_j \mathcal{F}_{\lambda_j}^N \dots \mathcal{F}_{\lambda_j}^2 \mathcal{F}_{\lambda_j}^1 E_{\lambda_j} |\psi_{\text{in}}\rangle \end{aligned} \quad (3.7)$$

We introduced $\mathcal{F}_{\lambda_j}^k$ for compact notation. $\mathcal{F}_{\lambda_j}^k$ is a known function of θ^k and $e^{i\lambda_j}$. The normalization factor, K_N , can also be expressed with these $\mathcal{F}_{\lambda_j}^k$'s:

$$\mathcal{F}_{\lambda_j}^k = \left[c_{\text{above}}^k + c_{\text{below}}^k e^{i\lambda_j} \right] \quad K_N = \sum_j \left| \mathcal{F}_{\lambda_j}^N \dots \mathcal{F}_{\lambda_j}^2 \mathcal{F}_{\lambda_j}^1 \right|^2 \langle \psi_{\text{in}} | E_{\lambda_j} | \psi_{\text{in}} \rangle \quad (3.8)$$

To justify the claim of (3.4), it remains to be shown that (up to an overall phase factor):

$$\lim_{N \rightarrow \infty} \frac{1}{\sqrt{K_N}} \sum_j \mathcal{F}_{\lambda_j}^N \dots \mathcal{F}_{\lambda_j}^2 \mathcal{F}_{\lambda_j}^1 E_{\lambda_j} |\psi_{\text{in}}\rangle = \frac{E_\mu}{\sqrt{\langle \psi_{\text{in}} | E_\mu | \psi_{\text{in}} \rangle}} |\psi_{\text{in}}\rangle \quad (3.9)$$

This implies that for large N :

$$\left| \mathcal{F}_\mu^N \dots \mathcal{F}_\mu^2 \mathcal{F}_\mu^1 \right|^2 \gg \left| \mathcal{F}_{\lambda_j}^N \dots \mathcal{F}_{\lambda_j}^2 \mathcal{F}_{\lambda_j}^1 \right|^2 \quad \forall \lambda_j \neq \mu \quad (3.10)$$

Note that since:

$$\left| \mathcal{F}_{\lambda_j}^k \right|^2 = \left| c_{\text{above}}^k + c_{\text{below}}^k e^{i\lambda_j} \right|^2 = \left| c_{\text{above}}^{t_k} \right|^2 + \left| c_{\text{below}}^{t_k} \right|^2 + 2\text{Re} \left(c_{\text{above}}^{t_k*} c_{\text{below}}^{t_k} e^{i\lambda_j} \right) = f_{\lambda_j}(\theta_{t_k}),$$

we have that:

$$\left| \mathcal{F}_{\lambda_j}^N \dots \mathcal{F}_{\lambda_j}^2 \mathcal{F}_{\lambda_j}^1 \right|^2 = f_{\lambda_j}(\theta^N) \dots f_{\lambda_j}(\theta^2) f_{\lambda_j}(\theta^1). \quad (3.11)$$

We prove (3.10) in appendix A. In this proof we will also need the probability P_N of measuring the sequence of angles $\theta^1, \theta^2, \dots, \theta^N$. One can always construct a sequence for which (3.10) does not hold. But the probability of actually observing such a sequence goes to zero.

The probability P_N to find these specific angles is a rather complicated factor. The probability $P^{(k)}$ to observe particle B at the k th run at a specific angle depends on the outcomes of the preceding outcomes $\theta^1, \dots, \theta^{k-1}$. When we write P_N as the product of probabilities $P^{(k)}$, the expression for P_N becomes intractable.

The key observation however is that this probability P_N turns out to be also equal to the normalization factor K_N . This is even true for all k :

$$P_k = K_k,$$

as is shown in the appendix.

3.1.3 The resulting state is locked in an eigenspace of the monodromy operator

The final state then becomes, as stated in (3.4):

$$|\psi_{\text{final}}\rangle = \lim_{N \rightarrow \infty} |\psi_{\text{in}}\rangle_{N+1} = \frac{E_{\mu}|\psi_{\text{in}}\rangle}{\sqrt{\langle \psi_{\text{in}} | E_{\mu} | \psi_{\text{in}} \rangle}} \quad (3.12)$$

But this will also be the case for finite (but relatively large) N ; the sequence of measurements ‘locks’ the two-particle system in a specific state which it cannot escape anymore, at least not during the one-to-one experiment.

After reaching projection in N steps, the experiment can be repeated for an infinite number of times M (well at least $M \gg N$), where the probability distribution $f(\theta_t)$ for each next measurement does not change anymore, and remains equal to $f_{\mu}(\theta_t)$. Also, the state is then locked into the state (3.12). And since $M \gg N$ the contribution of the first N particles in the interference pattern vanishes and an ‘eigenpattern’ will be found:

$$\lim_{M \rightarrow \infty} \frac{M_t}{M} := h(\theta_t) = f_{\mu}(\theta_t) \quad (3.13)$$

Each eigenvalue can occur with probability p_{μ} as we stated in (3.3).

We make the following observations concerning our results:

- The convergence is fast (roughly exponential), and depends on the observable difference between $f_{\lambda_1}(\theta)$ and $f_{\lambda_2}(\theta)$ for $\lambda_1 \neq \lambda_2$ (or the difference between eigenvalue patterns).
- Beforehand it is impossible to tell which \mathcal{R}^2 -eigenvalue one will find, unless the two-particle state is already an \mathcal{R}^2 -eigenstate, which is what one expects for any quantum system.
- This experiment is the same if the role of A and B are swapped: it does not matter which of the two is the projectile or the target.
- The choice to use \mathcal{R} or \mathcal{R}^{-1} to bring back particle B to its original position (i.e. clockwise or counterclockwise) is an arbitrary one and does not affect the result.
- One could also not bring back B to its original position, but just place the double slit to the right of A and shoot particle B from the right at the double slit. The result remains.
- The result can be easily verified by a numerical simulation on a computer (monte-carlo).

3.1.4 An example

Let’s illustrate the projection process with an hypothetical example. Here, \mathcal{R}^2 has two distinct eigenvalues: $e^{i\lambda_1} = 1$ and $e^{i\lambda_2} = -1$. The double-slit-geometry is that of the ideal experiment, as in section 2.2. The ideal eigen-patterns are $f_{e^{i\lambda=1}}(\theta) \equiv f_1(\theta) = 2 \cos^2(\pi\theta)$ and $f_{-1}(\theta) = 2 \sin^2(\pi\theta)$, $\theta \in [0, 1]$. As initial probabilities we choose $p_1 = 0.6$ and $p_{-1} = 0.4$. A particular sequence of measurements is shown in figs. 3.2, 3.3 and 3.4.

This ends our discussion of the ‘one-to-one’ experiment. We are now ready for the ‘many-to-one’ version, which is somewhat more difficult but in the end will allow us to use the same convergence-theorem.

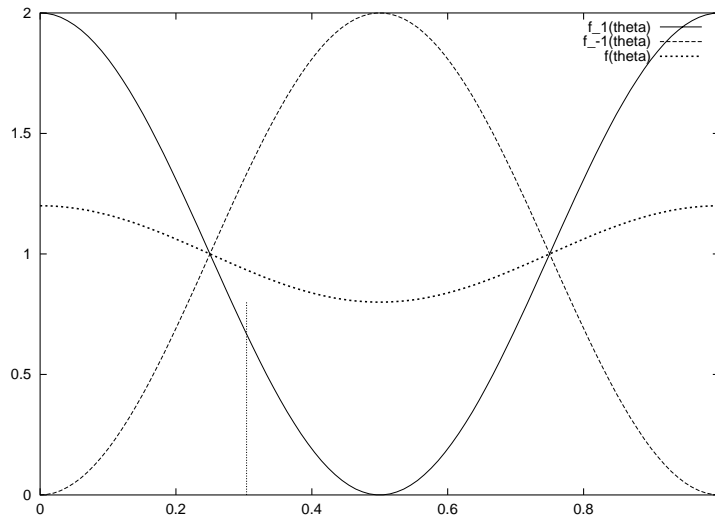


Figure 3.2: The probability of finding $e^{i\lambda} = 1$ is 0.6, that of $e^{i\lambda} = -1$ is 0.4. The first measurement is at $\theta = 0.30$ (where $f_{-1}(\theta) = 2f_1(\theta)$). p_1 now changes to 0.43, p_{-1} to 0.57.

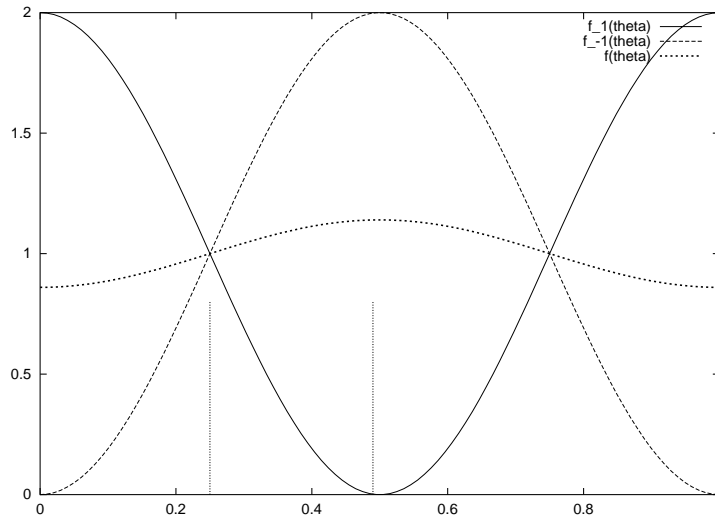


Figure 3.3: The next measured particle is found at an angle $\theta = 0.25$, for which $f_1(\theta) = f_{-1}(\theta)$. The p_{λ_i} 's do not change now, because this specific point does not favour one of the two eigenvalues. The third point is at $\theta = 0.49$, where $f_{-1}(\theta) = 1000f_1(\theta)$. This causes a great change: $p_1 \rightarrow 0.001$, $p_{-1} \rightarrow 0.999$

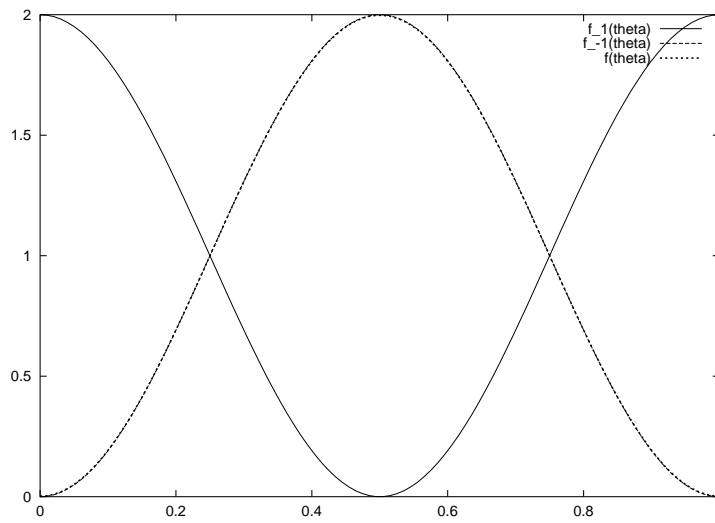


Figure 3.4: The system is now (almost totally) projected on $e^{i\lambda} = -1$, which could result from the beginning with chance 0.4. The probability of measuring a lot of points at $\theta \approx 1$ or $\theta \approx 0$ (which would favour the other eigenvalue) is very small.

3.2 The many-to-one experiment: probe one particle with many identical other particles

We will now discuss the 'many-to-one' experiment which we mentioned in chapter 2. This involves a more sophisticated analysis than that of the 'one-to-one', with a lot of, sometimes even rather large, equations (so be warned, but there are also some cute pictures). We will start by describing the experiment in section 3.2.1. Then, in section 3.2.2, it is argued that there are specific final states that do not change when continuing the experiment. These fixed final states will be eigenstates of some operator U which will be described. Arbitrary initial states will be projected onto these U eigenstates, which we will show in section 3.2.3. We will have to introduce some restrictions on the particles to be able to solve the problem, so in a sense we have not solved the many-to-one experiment for arbitrary particles in complete generality.

3.2.1 Description of the experiment

In the many-to-one experiment, one uses the same target particle A behind the slits (the 'one' part), but a whole lot (N) of identical projectile particles B (the 'many' part). We furthermore *assume* that the B particles have *identical* internal states¹.

So there are $N + 1$ particles. One can define this initial multi-particle internal state as:

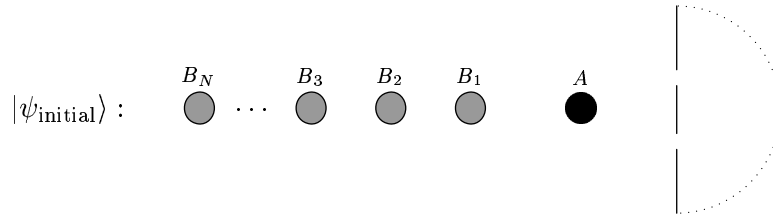
$$\begin{aligned}
 |\psi_{\text{initial}}\rangle &\in V_N^B \otimes \dots \otimes V_2^B \otimes V_1^B \otimes V_\alpha^A \\
 |\psi_{\text{initial}}\rangle &= \psi_{\text{initial}}^{i_N \dots i_2 i_1 \alpha} |e_{i_N}^B\rangle \dots |e_{i_2}^B\rangle |e_{i_1}^B\rangle |e_\alpha^A\rangle
 \end{aligned}
 \tag{3.14}$$

From here on, we will also assume the B 's not to be entangled with each other nor with A , so that $\psi_{\text{initial}}^{i_N \dots i_2 i_1 \alpha}$ can be factorised:

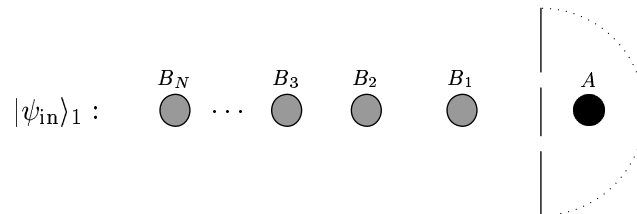
$$\psi_{\text{initial}}^{i_N \dots i_2 i_1 \alpha} = y^{i_N} \dots y^{i_2} y^{i_1} x^\alpha \quad y \text{ and } x \text{ fixed vectors}
 \tag{3.15}$$

The y^{i_k} assure that the B particles have identical internal states, x^α denotes the internal state of particle A .

We may schematically represent this as:



Now we can start the experiment by positioning A behind the two slits and prepare to direct the first projectile particle B at the double slit. We will call the state of the system $|\psi_{\text{in}}\rangle_1 = |\psi_{\text{initial}}\rangle$:



¹The condition that the B particles have identical internal states need not always be physically implementable, for example if the internal degeneracy is related with a local gauge invariance. We return to this point in our discussion of the Discrete Gauge Theories in chapter 4.

Next we direct B_1 at the double slit and detect B_1 again behind the double slit at an angle θ_1 . We have a new state now:

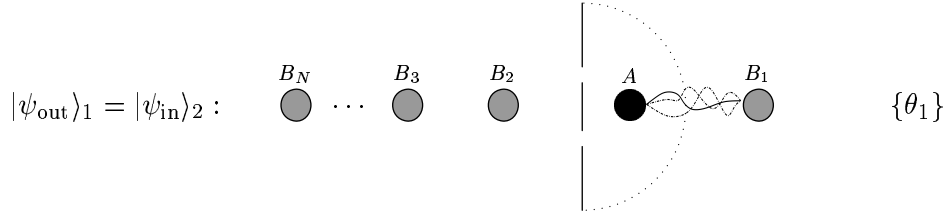
$$|\psi_{\text{out}}\rangle_1 \in V_N^B \otimes \dots \otimes V_2^B \otimes V_\alpha^A \otimes V_1^B$$

$$|\psi_{\text{out}}\rangle_1 = \psi_1^{i_N \dots i_2 \alpha j_1} |e_{i_N}^B\rangle \dots |e_{i_2}^B\rangle |e_\alpha^A\rangle |e_{j_1}^B\rangle \quad (3.16)$$

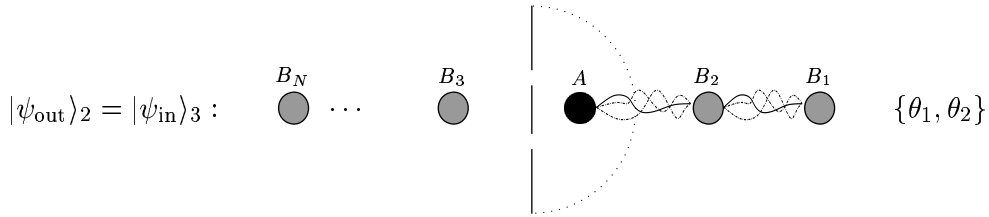
Particle A and B will be entangled, so $\psi_1^{i_N \dots i_2 \alpha j_1}$ factorizes as:

$$\psi_1^{i_N \dots i_2 \alpha j_1} = y^{i_N} \dots y^{i_2} z^{\alpha j_1}$$

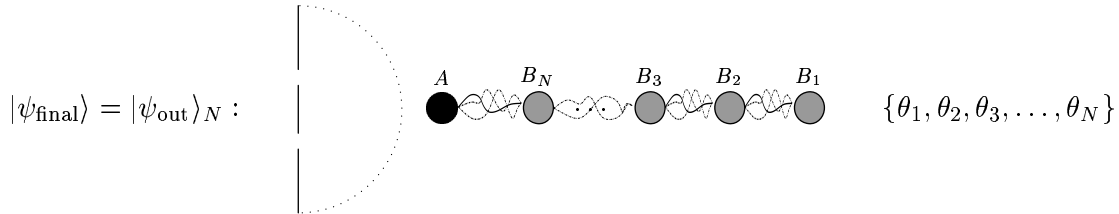
This resulting out-state is the in-state for the measurement of the next particle, B_2 :



We continue this process



.....until we have had all N particles, and detected them at angles $\theta_1 \dots \theta_N$:



We end up with a, fairly entangled, final state $|\psi_{\text{final}}\rangle$:

$$|\psi_{\text{final}}\rangle = |\psi_{\text{out}}\rangle_N \in V_\alpha^A \otimes V_N^B \otimes \dots \otimes V_2^B \otimes V_1^B$$

$$|\psi_{\text{final}}\rangle = (\psi_N)^{\alpha j_N \dots j_2 j_1} |e_\alpha^A\rangle |e_{j_N}^B\rangle \dots |e_{j_2}^B\rangle |e_{j_1}^B\rangle \quad (\psi_N)^{\alpha j_N \dots j_2 j_1} \text{ is no longer factorizable} \quad (3.17)$$

After we have measured the angles $\theta_1 \dots \theta_N$, we are mainly interested in what we can say about the internal state of particle A in the multi-particle state $|\psi_{\text{final}}\rangle$. But since the particle A is now entangled (with N other particles), it is convenient to look at its density matrix ρ_A instead of $(\psi_N)^{\alpha j_N \dots j_2 j_1}$.

$$(\rho_{AN})_\beta^\alpha = (\psi_N)^{\alpha j_N \dots j_2 j_1} (\psi_N)_{\beta j_N \dots j_2 j_1} \quad (3.18)$$

As we will show below, the conclusion is that in a particular basis of the internal state of A , most of the diagonal elements of the density matrix will vanish. If N becomes large then ρ_{AN} ,

which is N -dependent, converges (rapidly) to a final matrix: $\lim_{N \rightarrow \infty} \rho_{AN} = \rho_{A\text{final}}$ which is N -independent! So there is indeed a final state. The information can be obtained from the collection of measured angles $\theta_1 \dots \theta_N$. In this particular basis the matrix U will be diagonal.

We have now described the many-to-one experiment. We are now ready to perform some calculations. We will determine when a density-matrix ρ_A is final, i.e. when it does not change anymore after a next particle has been measured.

As announced, we have only been able to obtain the result if a restriction is satisfied by the type of the B particles: *these B particles should have trivial braiding amongst each other* (braiding is then nothing more than a permutation of these particles):

$$\begin{aligned} \mathcal{R}|B_i\rangle|B_j\rangle &= \mathcal{R}^{-1}|B_i\rangle|B_j\rangle = \sigma|B_i\rangle|B_j\rangle = |B_j\rangle|B_i\rangle \\ \Rightarrow \quad \mathcal{R}^2 &= \mathbb{1} \quad \text{when working on } B\text{'s} \end{aligned} \quad (3.19)$$

To simplify notation, we use $\tilde{\mathcal{R}}$ as the inverse of \mathcal{R} , so:

$$\mathcal{R}^{-1} \equiv \tilde{\mathcal{R}} \quad (3.20)$$

3.2.2 Final states

A final state is a state where the outcome of a measurement of an incoming particle B_k does not depend on the outcome of the previous particle B_{k-1} . The outcome-probability of a double slit experiment depends on the \mathcal{R}^2 expectation value. So for a final state of an entangled particle A , the expectation value of an \mathcal{R}^2 working on particles B_2 and A should be independent of the measured angle θ_t of the first particle.

Let the three particles A, B_1, B_2 be unentangled with each other but all possibly entangled with other particles, and let B_1 and B_2 have the same internal state, i.e. the three particle state can be written as:

$$|\psi\rangle = y^{jn} y^{im} x^{\alpha p} |e_j^{B_2}\rangle |e_i^{B_1}\rangle |e_\alpha^A\rangle \otimes |e_n^{O(B_2)}\rangle |e_m^{O(B_1)}\rangle |e_p^{O(A)}\rangle \quad (3.21)$$

Where $x^{\alpha p} |e_\alpha^A\rangle |e_p^{O(A)}\rangle$ stands for the internal state of particle A and all other particles A is entangled with (with multi-particle orthonormal base $|e_p^{O(A)}\rangle$), and likewise with y^{im} for B_1 and B_2 . The total state $|\psi\rangle$ is still factorised in the same way as in (3.15), but the fixed vectors y and x have now been replaced by fixed tensors y and x .

After the incoming particle B_1 has been detected at an angle θ_t the state has changed to:

$$\begin{aligned} |\psi_{\text{out}}\rangle_1^t &= \frac{c_{\text{above}}^t \tilde{\mathcal{R}}_1 + c_{\text{below}}^t \mathcal{R}_1}{\sqrt{K^t}} |\psi_{\text{in}}\rangle \\ K^t &= |c_{\text{above}}^t|^2 + |c_{\text{below}}^t|^2 + 2\text{Re}(c_{\text{above}}^{*t} c_{\text{below}}^t \langle \psi_{\text{in}} | (\mathcal{R}_1)^2 | \psi_{\text{in}} \rangle) \end{aligned} \quad (3.22)$$

K^t is the normalization factor. We explicitly show the dependence on the measured angle θ^t of $|\psi_{\text{out}}\rangle_1^t$ and K^t .

We will count from right to left when numbering both the particles and the exchange operators. This means that an \mathcal{R}_2 on the initial state exchanges B_1 and $B_2 \dots$. Furthermore, we will use \mathcal{R}^2 to indicate the tensor (matrix) components of any \mathcal{R}^2 -operator operating on a particle B and A :

$$(\mathcal{R}_1)^2 |e_i^{B_1}\rangle |e_\alpha^A\rangle = (\mathcal{R}^2)_{i\alpha}^{k\beta} |e_k^{B_1}\rangle |e_\beta^A\rangle \quad (3.23)$$

In this way we can discriminate between physically different operators $\mathcal{R}_{(i)}^2$ that have the same tensor components \mathcal{R}^2 .

The expectation value for $(\mathcal{R}_1)^2$ becomes:

$$\begin{aligned}
 |\psi_{\text{in}}\rangle &= y^{jn} y^{im} x^{\alpha p} |j i \alpha n m p\rangle \quad (\text{compact notation}) \\
 \langle \psi_{\text{in}} | (\mathcal{R}_1)^2 | \psi_{\text{in}} \rangle &= \langle \hat{j} \hat{\alpha} \hat{n} \hat{m} \hat{p} | y_{j\hat{n}} y_{i\hat{m}} x_{\hat{\alpha}\hat{p}} (\mathbb{R}^2)^{k\beta}_{i\alpha} y^{jn} y^{im} x^{\alpha p} |j k \beta n m p\rangle \\
 &= (y^{jn} y_{jn}) (y^{im} y_{km}) (x^{\alpha p} x_{\beta p}) (\mathbb{R}^2)^{k\beta}_{i\alpha} \\
 &= (\text{Tr}_B \rho_B) (\rho_B^i_k) (\rho_A^\alpha_\beta) (\mathbb{R}^2)^{k\beta}_{i\alpha} \\
 &= (1) (\rho_A^\alpha_\beta) (U^\beta_\alpha) \\
 &= \text{Tr}_A (U \rho_A)
 \end{aligned} \tag{3.24}$$

where we used the definitions (Tr indicates the trace of a matrix, i.e. the sum of the diagonal elements):

$$\rho_B^i_k = y^{im} y_{km} \quad \rho_A^\alpha_\beta = x^{\alpha p} x_{\beta p} \quad \text{Tr}_A(\rho_A) = 1 \quad \text{Tr}_B(\rho_B) = 1 \tag{3.25}$$

$$U^\beta_\alpha \equiv \rho_B^i_k (\mathbb{R}^2)^{k\beta}_{i\alpha} = [\text{Tr}_B(\rho_B \mathbb{R}^2)]^\beta_\alpha \quad U: V^A \rightarrow V^A \tag{3.26}$$

Here we see the U -matrix for the first time, and it will not be the last. U is the \mathcal{R}^2 matrix traced partially with respect to the internal state of B and B 's density matrix, and so is a matrix-valued object on A 's internal space.

Now, if $|\psi_{\text{in}}\rangle = |\psi_{\text{final}}\rangle$ then ${}^t_1 \langle \psi_{\text{out}} | (\mathcal{R}_2)^2 | \psi_{\text{out}} \rangle_1^t$ should be independent of t . Then all the terms with t -dependence should cancel each other, including the t -dependent normalization factor K^t .

So,

$$\begin{aligned}
 {}^t_1 \langle \psi_{\text{out}} | (\mathcal{R}_2)^2 | \psi_{\text{out}} \rangle_1^t &= \frac{1}{K^t} \left(\langle \psi_{\text{in}} | \mathcal{R}_1 (\mathcal{R}_2)^2 \tilde{\mathcal{R}}_1 | \psi_{\text{in}} \rangle |c_{\text{above}}^t|^2 + \langle \tilde{\mathcal{R}}_1 (\mathcal{R}_2)^2 \mathcal{R}_1 | c_{\text{below}}^t|^2 + \right. \\
 &\quad \left. + \langle \mathcal{R}_1 (\mathcal{R}_2)^2 \mathcal{R}_1 \rangle c_{\text{above}}^{*t} c_{\text{below}}^t + \langle \tilde{\mathcal{R}}_1 (\mathcal{R}_2)^2 \tilde{\mathcal{R}}_1 \rangle c_{\text{above}}^t c_{\text{below}}^{*t} \right)
 \end{aligned} \tag{3.27}$$

should be independent of t .

The expression (3.27) involves four different expectation values of braiding operators, which can be rewritten using braid relations as illustrated in fig. 3.5. If furthermore a braid of the two B particles is just the trivial exchange, $\mathcal{R} |B_i\rangle |B_j\rangle = \sigma |B_i\rangle |B_j\rangle$, and also $\tilde{\mathcal{R}} = \sigma = \mathcal{R}$ (which we demanded in (3.19)) then these expectation values simplify to:

$$\langle \psi_{\text{in}} | \mathcal{R}_1 (\mathcal{R}_2)^2 \tilde{\mathcal{R}}_1 | \psi_{\text{in}} \rangle = \langle \psi_{\text{in}} | \sigma_2 (\mathcal{R}_1)^2 \sigma_2 | \psi_{\text{in}} \rangle \tag{3.28}$$

$$\langle \psi_{\text{in}} | \tilde{\mathcal{R}}_1 (\mathcal{R}_2)^2 \mathcal{R}_1 | \psi_{\text{in}} \rangle = \langle \psi_{\text{in}} | \sigma_2 (\mathcal{R}_1)^2 \sigma_2 | \psi_{\text{in}} \rangle \tag{3.29}$$

$$\langle \psi_{\text{in}} | \mathcal{R}_1 (\mathcal{R}_2)^2 \mathcal{R}_1 | \psi_{\text{in}} \rangle = \langle \psi_{\text{in}} | [(\mathcal{R}_1)^2] [\sigma_2 (\mathcal{R}_1)^2 \sigma_2] | \psi_{\text{in}} \rangle \tag{3.30}$$

$$\langle \psi_{\text{in}} | \tilde{\mathcal{R}}_1 (\mathcal{R}_2)^2 \tilde{\mathcal{R}}_1 | \psi_{\text{in}} \rangle = \langle \psi_{\text{in}} | [(\tilde{\mathcal{R}}_1)^2] [\sigma_2 (\mathcal{R}_1)^2 \sigma_2] | \psi_{\text{in}} \rangle \tag{3.31}$$

Where the operators at the right hand side are products of maps from $V_{2\beta}^B \otimes V_{1\beta}^B \otimes V_\alpha^A$ to itself. We can substitute the appropriate \mathbb{R}^2 components for these operators, through:

$$\begin{aligned}
 (\mathcal{R}_1)^2 |e_j^{B_2}\rangle |e_i^{B_1}\rangle |e_\alpha^A\rangle &= (\mathbb{R}^2)^{k\beta}_{i\alpha} |e_j^{B_2}\rangle |e_k^{B_1}\rangle |e_\beta^A\rangle \\
 [\sigma_2 (\mathcal{R}_1)^2 \sigma_2] |e_j^{B_2}\rangle |e_i^{B_1}\rangle |e_\alpha^A\rangle &= (\mathbb{R}^2)^{k\beta}_{j\alpha} |e_k^{B_2}\rangle |e_i^{B_1}\rangle |e_\beta^A\rangle
 \end{aligned}$$

If we use the formal sum notation used in quantum group theory, then:

$$\begin{aligned}
 (\mathcal{R}_1)^2 &= \sum \mathbb{1} \otimes \mathbb{R}_{(1)}^2 \otimes \mathbb{R}_{(2)}^2 \\
 \sigma_2 (\mathcal{R}_1)^2 \sigma_2 &= \sum \mathbb{R}_{(1)}^2 \otimes \mathbb{1} \otimes \mathbb{R}_{(2)}^2
 \end{aligned}$$

Figure 3.5: Identities for (representations of) the braid group. All relations can be found using $\mathcal{R}_1\mathcal{R}_2\mathcal{R}_1 = \mathcal{R}_2\mathcal{R}_1\mathcal{R}_2$. The relations are valid for arbitrary particles, i.e. without writing explicitly the labels A , B_1 and B_2 . Recall that we number from right to left.

Let us write the in-state again as $|\psi_{\text{in}}\rangle = y^{jn}y^{im}x^{\alpha p}|ji\alpha nmp\rangle$. Then (3.28)...(3.31) become:

$$\begin{aligned}
 \langle\psi_{\text{in}}|\sigma_2(\mathcal{R}_1)^2\sigma_2|\psi_{\text{in}}\rangle &= (y^{jn}y_{kn})(y^{im}y_{im})(x^{\alpha p}x_{\beta p})(\mathcal{R}^2)^{k\beta}_{i\alpha} \\
 &= \rho_B^j{}_k\rho_B^i{}_i\rho_A^\alpha{}_\beta(\mathcal{R}^2)^{k\beta}_{j\alpha} \\
 &= U^\beta{}_\alpha\rho_A^\alpha{}_\beta \\
 &= \text{Tr}_A(U\rho_A)
 \end{aligned} \tag{3.32}$$

$$\begin{aligned}
 \langle\psi_{\text{in}}|[(\mathcal{R}_1)^2][\sigma_2(\mathcal{R}_1)^2\sigma_2]|\psi_{\text{in}}\rangle &= (y^{jn}y_{kn})(y^{im}y_{lm})(x^{\alpha p}x_{\gamma p})(\mathcal{R}^2)^{k\beta}_{j\alpha}(\mathcal{R}^2)^{l\gamma}_{i\beta} \\
 &= \rho_B^j{}_k\rho_B^i{}_l\rho_A^\alpha{}_\gamma(\mathcal{R}^2)^{k\beta}_{j\alpha}(\mathcal{R}^2)^{l\gamma}_{i\beta} \\
 &= U^\beta{}_\alpha\rho_A^\alpha{}_\gamma U^\gamma{}_\beta \\
 &= \text{Tr}_A(UU\rho_A)
 \end{aligned} \tag{3.33}$$

$$\begin{aligned}
 \langle\psi_{\text{in}}|[(\tilde{\mathcal{R}}_1)^2][\sigma_2(\mathcal{R}_1)^2\sigma_2]|\psi_{\text{in}}\rangle &= \rho_B^j{}_k\rho_B^i{}_l\rho_A^\alpha{}_\gamma(\mathcal{R}^2)^{k\beta}_{j\alpha}(\mathcal{R}^{-2})^{l\gamma}_{i\beta} \\
 &= U^\beta{}_\alpha\rho_A^\alpha{}_\gamma(U^\dagger)^\gamma{}_\beta \\
 &= \text{Tr}_A(U^\dagger U\rho_A)
 \end{aligned} \tag{3.34}$$

We can now reformulate equation (3.27) to:

$${}_1^t\langle\psi_{\text{out}}|(\mathcal{R}_2)^2|\psi_{\text{out}}\rangle_1^t = \frac{1}{K^t} \left(\text{Tr}_A(U\rho_A)|c_{\text{above}}^t|^2 + \text{Tr}_A(U\rho_A)|c_{\text{below}}^t|^2 + \right)$$

$$\text{Tr}_A(UU\rho_A)c_{\text{above}}^{*t}c_{\text{below}}^t + \text{Tr}_A(U^\dagger U\rho_A)c_{\text{above}}^tc_{\text{below}}^{*t} \quad (3.35)$$

And (3.35) becomes independent of t if:

$$\text{Tr}_A(UU\rho_A) = \text{Tr}_A(U\rho_A)\text{Tr}(U\rho_A) \quad \text{Tr}_A(U^\dagger U\rho_A) = \text{Tr}_A(U^\dagger\rho_A)\text{Tr}_A(U\rho_A) \quad (3.36)$$

Because then, with K^t explicitly given:

$$K^t = |c_{\text{above}}^t|^2 + |c_{\text{below}}^t|^2 + 2\text{Re}(c_{\text{above}}^{*t}c_{\text{below}}^t\text{Tr}_A(U\rho_A)),$$

the t -dependent terms in the nominator and denominator of equation (3.35) cancel each other:

$$\begin{aligned} {}_1^t\langle\psi_{\text{out}}|(\mathcal{R}_2)^2|\psi_{\text{out}}\rangle_1^t &= \text{Tr}_A(U\rho_A)\frac{|c_{\text{above}}^t|^2 + |c_{\text{below}}^t|^2 + \text{Tr}_A(U\rho_A)c_{\text{above}}^{*t}c_{\text{below}}^t + \text{Tr}_A(U\rho_A)^*c_{\text{above}}^tc_{\text{below}}^{*t}}{K^t} \\ &= \text{Tr}_A(U\rho_A) \end{aligned} \quad (3.37)$$

So the remaining question is: when is $\text{Tr}_A(U^2\rho_A)$ equal to $(\text{Tr}_A(U\rho_A))^2$? Because ρ_A is a density matrix, we can reformulate the question to one for expectation values, for an arbitrary operator A :

$$\langle A^2 \rangle \stackrel{?}{=} \langle A \rangle^2 \quad \langle A \rangle = \text{Tr}(A\rho)$$

The answer: this is true if and only if the system is in an eigenstate of operator A .

This means that for $|\psi_{\text{in}}\rangle$ to be a final state, $|\psi_{\text{final}}\rangle$, the diagonal of the matrix $\rho_A^{\alpha\beta}$, written in an eigenbasis of the matrix U^β_α , should have only nonzero elements in an eigenspace of U with eigenvalue κ , so that:

$$\text{Tr}_A(U\rho_A) = \kappa\text{Tr}_A(\rho_A) = \kappa \quad (3.38)$$

Note that U , because of its definition (3.26), depends explicitly on the chosen internal state of the B particles, and so do its eigenvalues.

So we have determined U eigenstates to be 'fixed' or 'stable' states, we will now prove that arbitrary initial states, will be projected on such an eigenstate. In that sense, one can think of an arbitrary density matrix ρ_A to be a superposition of U eigen-density-matrices.

3.2.3 Every initial state will end up on a final state in some U eigenspace

We will now prove that every initial state will converge to a final state, which is a U -eigenstate. This is not so hard to see if we work with the initial state in the U -eigenbasis. In this base the matrix U is diagonal with entries $\kappa_1, \kappa_2, \dots, \kappa_m$ where m is the dimension of particle A 's internal state:

$$U_{\text{diag}} = \begin{pmatrix} \kappa_1 & 0 & \dots & 0 \\ 0 & \kappa_2 & \dots & 0 \\ \vdots & \vdots & \ddots & 0 \\ 0 & 0 & 0 & \kappa_m \end{pmatrix}$$

In this basis, the density matrix ρ_A has the form:

$$\rho_{A\text{diag}} \equiv \begin{pmatrix} p_1 & * & \dots & * \\ * & p_2 & \dots & * \\ \vdots & \vdots & \ddots & * \\ * & * & \dots & p_m \end{pmatrix} \quad \text{Tr}(\rho_A) = \text{Tr}(\rho_{A\text{diag}}) = \sum_{i=1}^m p_i = 1$$

Although $\rho_{A\text{diag}}$ is *not* a diagonal matrix, we are only interested in its diagonal elements p_i .

In this basis, the trace of U and ρ_A becomes equal to a trace over two 'diagonal' matrices:

$$\text{Tr}(U\rho_A) = \text{Tr}(U_{\text{diag}}\rho_{A\text{diag}}) = \sum_{i=1}^m p_i \kappa_i$$

Let us write ρ_{A0} for the initial internal state of particle A , i.e. its initial density matrix, before we start the experiment. Then the expectation value of the operator \mathcal{R}^2 operating on A and the first particle, B_1 , becomes:

$$\begin{aligned} \langle \psi_{\text{in}} | (\mathcal{R}_1)^2 | \psi_{\text{in}} \rangle &= {}_1 \langle \psi_{\text{in}} | (\mathcal{R}_1)^2 | \psi_{\text{in}} \rangle_1 \\ &= \text{Tr}(U\rho_{A0}) \\ &= \text{Tr}(U_{\text{diag}}(\rho_{A0})_{\text{diag}}) \\ &= \sum_{i=1}^m \kappa_i p_i^0 \end{aligned} \quad (3.39)$$

$$(\rho_{A0})_{\text{diag}} = \begin{pmatrix} p_1^0 & * & \dots & * \\ * & p_2^0 & \dots & * \\ \vdots & \vdots & \ddots & * \\ * & * & \dots & p_m^0 \end{pmatrix}$$

Now we plug in $(\rho_{A1})_{\text{diag}}$ via the expectation value of \mathcal{R}^2 operating on A and the next particle, B_2 :

$${}_2 \langle \psi_{\text{in}} | (\mathcal{R}_2)^2 | \psi_{\text{in}} \rangle_2 = \text{Tr}(U_{\text{diag}}(\rho_{A1})_{\text{diag}}) \quad (3.40)$$

$$= \sum_{i=1}^m \kappa_i p_i^1 \quad (3.41)$$

But, according to (3.35), this expectation value is also equal to:

$$\begin{aligned} {}_2 \langle \psi_{\text{in}} | (\mathcal{R}_2)^2 | \psi_{\text{in}} \rangle_2 &= {}_1^t \langle \psi_{\text{out}} | (\mathcal{R}_2)^2 | \psi_{\text{out}} \rangle_1^t \\ &= \frac{1}{K^t} \left(\text{Tr}(U\rho_{A0}) |c_{\text{above}}^t|^2 + \text{Tr}(U\rho_{A0}) |c_{\text{below}}^t|^2 + \right. \\ &\quad \left. \text{Tr}(UU\rho_{A0}) c_{\text{above}}^{*t} c_{\text{below}}^t + \text{Tr}(U^\dagger U\rho_{A0}) c_{\text{above}}^t c_{\text{below}}^{*t} \right) \\ &= \frac{1}{K^t} \left(\sum_{i=1}^m p_i^0 \kappa_i |c_{\text{above}}^t|^2 + \sum_{i=1}^m p_i^0 \kappa_i |c_{\text{below}}^t|^2 + \right. \\ &\quad \left. \sum_{i=1}^m p_i^0 \kappa_i^2 c_{\text{above}}^{*t} c_{\text{below}}^t + \sum_{i=1}^m p_i^0 \kappa_i \kappa_i^* c_{\text{above}}^t c_{\text{below}}^{*t} \right) \\ &= \frac{1}{K^t} \sum_{i=1}^m \kappa_i p_i^0 \left(|c_{\text{above}}^t|^2 + |c_{\text{below}}^t|^2 + \kappa_i c_{\text{above}}^{*t} c_{\text{below}}^t + \kappa_i^* c_{\text{above}}^t c_{\text{below}}^{*t} \right) \\ &= \sum_{i=1}^m \kappa_i \frac{p_i^0}{K^t} \left(|c_{\text{above}}^t|^2 + |c_{\text{below}}^t|^2 + 2\text{Re}(c_{\text{above}}^{*t} c_{\text{below}}^t \kappa_i) \right) \end{aligned} \quad (3.42)$$

And now we can identify p_i^1 as:

$$p_i^1 = \frac{p_i^0}{K^t} \left(|c_{\text{above}}^t|^2 + |c_{\text{below}}^t|^2 + 2\text{Re}(c_{\text{above}}^{*t} c_{\text{below}}^t \kappa_i) \right) \quad (3.43)$$

Let us rewrite P_i^1 with:

$$f_{\kappa_i}(\theta^t = \theta_1) = f_{\kappa_i}(\theta_1) = |c_{\text{above}}^t|^2 + |c_{\text{below}}^t|^2 + 2\text{Re}(c_{\text{above}}^{*t} c_{\text{below}}^t \kappa_i) \quad (3.44)$$

$$K^t = \sum_{i=1}^m p_i^0 f_{\kappa_i}(\theta_1) \equiv K_1$$

to:

$$p_i^1 = \frac{p_i^0 f_{\kappa_i}(\theta_1)}{\sum_{j=1}^m p_j^0 f_{\kappa_j}(\theta_1)} \quad \sum_{i=1}^m p_i^1 = 1 \quad (3.45)$$

Now we can also apply this method to arbitrary many other particles B_2, \dots, B_N :

$$p_i^2 = \frac{p_i^0 f_{\kappa_i}(\theta_1) f_{\kappa_i}(\theta_2)}{K_2} \quad K_2 = \sum_{i=1}^m p_i^0 f_{\kappa_i}(\theta_1) f_{\kappa_i}(\theta_2)$$

$$\dots = \dots$$

$$p_i^N = p_i^0 \frac{f_{\kappa_i}(\theta_1) f_{\kappa_i}(\theta_2) \dots f_{\kappa_i}(\theta_N)}{K_N} \quad K_N = \sum_{i=1}^m p_i^0 \prod_{l=1}^N f_{\kappa_i}(\theta_l) \quad (3.46)$$

If all the κ_i are different, then with probability p_i^0 one projects out the corresponding eigenstate when the number of probing particles N becomes large:

$$\lim_{N \rightarrow \infty} p_i^N = 1 \quad p_j^N = 0 \quad \forall j \neq i \quad (3.47)$$

If some of the κ_i are the same, i.e. the eigenvalues of the matrix U are degenerate: $\kappa_{i_1} = \kappa_{i_2} = \dots = \kappa_{i_k}$ (but $\kappa_{i_x} \neq \kappa_{j_y}$ if $i \neq j$), then, with probability $\sum_x p_{i_x}^0$:

$$\lim_{N \rightarrow \infty} \sum_x p_{i_x}^N = 1 \quad p_{j_y}^N = 0 \quad \forall j \neq i \quad (3.48)$$

$$\frac{p_{i_x}^N}{p_{i_y}^N} = \frac{p_{i_x}^0}{p_{i_y}^0} \quad \forall N$$

So in the degenerate case one projects onto an U eigenspace (instead of an eigenstate) with the associated probability.

The proof of (3.47) and (3.48) is the same as that of the convergence in the 'one-to-one' experiment. The only difference lies in the eigenvalues: these no longer need to be roots of unity, but the proof (see appendix A) does not depend on that. One can replace each $e^{i\lambda_j}$ by a κ_j and see that every statement in there remains true. In the end, the coefficient p_{κ}^N of one of the eigenpattern $f_{\kappa}(\theta)$ will become infinitely (at least much) larger than the coefficients of the other eigenpatterns, and this specific eigenpattern will then 'rule' the observed interference pattern.

The final state, or final density matrix $\rho_{A \text{ final}}$ is thus (in the limit of $N \rightarrow \infty$):

$$\rho_{A \text{ final}} = \frac{E_{\kappa} \rho_A E_{\kappa}}{\text{Tr}(E_{\kappa}) \rho_A} \quad (3.49)$$

where E_{κ} is the projection operator projecting in the vector space V^A onto the κ -eigenspace of the matrix U . The probability p_{κ} to find a specific eigenvalue κ is then:

$$p_{\kappa} = \text{Tr}(E_{\kappa} \rho_A) \quad (3.50)$$

And this eigenvalue κ will become apparent in the observed interference pattern $g(\theta)$, which is the eigen-pattern $f_\kappa(\theta)$:

$$g(\theta) = f_\kappa(\theta) \quad (3.51)$$

This almost concludes the part of the many-to-one experiment. We will now investigate what the eigenvalues U look like, and relax the condition on the braiding of the B 's, from (3.19). In the end we will summarize the results concerning (non-abelian) double slit experiments presented in this chapter.

3.2.4 Eigenvalues of the U -matrix

We have been referring to the eigenvalues of the matrix U defined in (3.26). For the unitary \mathcal{R}^2 , we know that all eigenvalues are phase factors. What can we say about the eigenvalues of U ?

Well, although U is neither unitary nor hermitian, it is 'normal' in the sense that it commutes with its adjoint:

$$UU^\dagger = U^\dagger U \quad (3.52)$$

this is so, because every unitary operator can be written as an imaginary exponential of a hermitian operator:

$$\begin{aligned} \mathcal{R}^2 &= e^{iS} & S^\dagger &= S \\ U &= \text{Tr}_B(e^{iS} \rho_B) \end{aligned}$$

And then (3.52) follows:

$$UU^\dagger = \text{Tr}_B(e^{iS} \rho_B) \text{Tr}_B(e^{-iS} \rho_B) = \text{Tr}_B(e^{-iS} \rho_B) \text{Tr}_B(e^{iS} \rho_B) = U^\dagger U$$

The spectral theorem for normal matrices states that U can be diagonalized by a unitary (basis) transformation. So, U can be completely diagonalized, but its eigenvalues have no further restrictions due to 'normality', as eigenvalues of hermitian and unitary operators have. In appendix D we present an alternative proof by using a graphical notation.

Since U is constructed from \mathcal{R}^2 , the expectation value of \mathcal{R}^2 for a final state is equal to both:

$$\langle \mathcal{R}^2 \rangle = \text{Tr}_A(U \rho_A) = \kappa \quad (3.53)$$

and:

$$\langle \mathcal{R}^2 \rangle = \text{Tr}_A \text{Tr}_B(\mathcal{R}^2(\rho_A \otimes \rho_B)) = \sum_j p_{\lambda_j} e^{i\lambda_j} \quad \sum_j p_{\lambda_j} = 1 \quad (3.54)$$

This means each eigenvalue κ of the matrix U can be written as a weighed sum of eigenvalues of the \mathcal{R}^2 -operator. Furthermore, since the p_{λ_j} are normalized:

$$|\kappa| \leq 1, \quad (3.55)$$

which assures that the eigenpattern $f_\kappa(\theta)$ is non-negative for all θ :

$$f_\kappa(\theta) \geq 0 \quad \forall \theta. \quad (3.56)$$

The U -eigenpattern can be written as the weighed sum of \mathcal{R}^2 -eigenpatterns, in the same way as the corresponding eigenvalues:

$$f_\kappa(\theta) = \sum_j p_{\lambda_j} f_{\lambda_j}(\theta) \quad \kappa = \sum_j p_{\lambda_j} e^{i\lambda_j} \quad (3.57)$$

3.2.5 Relaxing the constraint $\mathcal{R} = \mathcal{R}^{-1}$

When examining the equalities in (3.28) . . . (3.31) and the braid relations in fig 3.5 we conclude that we can relax the demand of (3.19), namely that of the B particles having trivial braiding, to B 's having abelian braiding, or:

$$\mathcal{R}|B_i\rangle|B_j\rangle = e^{i\mu}\sigma|B_i\rangle|B_j\rangle = e^{i\mu}|B_j\rangle|B_i\rangle \quad (3.58)$$

$$\mathcal{R}^{-1}|B_i\rangle|B_j\rangle = e^{-i\mu}\sigma|B_i\rangle|B_j\rangle = e^{-i\mu}|B_j\rangle|B_i\rangle \quad (3.59)$$

Now $\mathcal{R} \neq \mathcal{R}^{-1}$, but (3.28) . . . (3.31) remain valid, because the opposite phase factors $e^{\pm i\mu}$ cancel each other.

This means that the statements about the many-to-one experiment are also true for all B particles that have the property that they cannot become entangled with each other by braiding amongst each other (of course one B could be entangled to another B , but this entanglement is then due to other reasons than braiding of these two B 's).

The general case of the many-to-one experiment, with no constraint on A nor on B nor on their specific internal state (possibly terribly entangled) remains an unsolved problem for the moment. The answer to this question, whatever it may turn out to be, should of course be compatible with the answers in this chapter. We will, later, come back to this question of restrictions on the many-to-one experiment, but this will be for non-abelian anyons described by the quantum double $D(H)$; since $D(H)$ is to explained in chapter 4, this is not the good place to treat this subject; therefore, this discussion of the generic many-to-one experiment is postponed to section 8.1, p. 94.

3.3 Summary

The results for this chapter are conveniently summarized in table 3.1.

Also the name ‘many-to-many’ is introduced for the experiment where the probability distribution $f(\theta)$ is determined, with the use of many identically prepared systems with both an A and a B . (So this name fits naturally in between ‘one-to-one’ and ‘many-to-one’.)

The most important operator is the monodromy operator \mathcal{R}^2 , working on both A and B , and on which there are no constraints (well to ‘enjoy’ all the different outcomes the \mathcal{R}^2 -matrix should be something more than an identity-matrix). It is \mathcal{R}^2 that supplies the possible outcomes and eigenvalues (directly or indirectly).

The *average* of the outcomes of the three experiments is the same, namely $\langle \mathcal{R}^2 \rangle$. This is nice in two ways, because:

- it resembles the case of the abelian theory (Aharonov-Bohm) and the free theory (ordinary double slit) where the results for these three are always the same.
- it is a kind of probability conservation: the probability $f(\theta)$ for the *first* particle B to go through the double slit and be detected at an angle θ is the same in all three experiments (when using the same internal states of course).

#B-#A (name of experiment)	many-to-many	one-to-one	many-to-one $\rho_{AB} = \rho_A \otimes \rho_B$ $\mathcal{R} B\rangle B\rangle = e^{i\mu} \mathbb{1} B\rangle B\rangle$
Interference pattern	$f(\theta) = \sum_i p_{\lambda_i} f_{\lambda_i}(\theta)$	$h(\theta) = f_{\lambda_i}(\theta)$	$g(\theta) = f_{\kappa_j}(\theta)$
In terms of eigenvalues (e.v.s)	$\langle \mathcal{R}^2 \rangle$ $= \langle \psi_{\text{in}} \mathcal{R}^2 \psi_{\text{in}} \rangle$ $= \text{Tr}(\mathcal{R}^2 \rho_{AB})$	$e^{i\lambda_i}$ is e.v. of \mathcal{R}^2 : $V^A \otimes V^B \rightarrow V^A \otimes V^B$	κ_j is e.v. of $U = \text{Tr}_B(\mathcal{R}^2 \rho_B)$ $U: V^A \rightarrow V^A$
Probability for each value	1	$p_{\lambda_i} = \langle \psi_{\text{in}} E_{\lambda_i} \psi_{\text{in}} \rangle$ $= \text{Tr}(E_{\lambda_i} \rho_{AB})$	$p_{\kappa_j} = \text{Tr}_A(E_{\kappa_j} \rho_A)$
Expectation value (average)	$1 \cdot \langle \mathcal{R}^2 \rangle$ $= \langle \mathcal{R}^2 \rangle$	$\langle \mathcal{R}^2 \rangle = \sum_i p_{\lambda_i} e^{i\lambda_i}$ $= \langle \mathcal{R}^2 \rangle$	$\langle U \rangle = \sum_j p_{\kappa_j} \kappa_j$ $= \text{Tr}_A(U \rho_A)$ $= \text{Tr}_A \text{Tr}_B(\mathcal{R}^2 [\rho_B \otimes \rho_A])$ $= \langle \mathcal{R}^2 \rangle$
Change of system (projection)	not relevant	$ \psi_{\text{in}}\rangle \rightarrow \frac{E_{\lambda_i} \psi_{\text{in}}\rangle}{\sqrt{\langle \psi_{\text{in}} E_{\lambda_i} \psi_{\text{in}} \rangle}}$	$\rho_A \rightarrow \frac{E_{\kappa_j} \rho_A E_{\kappa_j}}{\text{Tr}_A(E_{\kappa_j} \rho_A)}$ ρ_B not relevant
Abelian Theory $\mathcal{R}^2 = e^{i\lambda} \mathbb{1}_A \otimes \mathbb{1}_B$	$f(\theta) = f_{\lambda}(\theta)$	$h(\theta) = f_{\lambda}(\theta)$	$g(\theta) = f_{\lambda}(\theta)$
Free Theory $\mathcal{R}^2 = \mathbb{1}_A \otimes \mathbb{1}_B$	$f(\theta) = f_0(\theta)$	$h(\theta) = f_0(\theta)$	$g(\theta) = f_0(\theta)$

Table 3.1: Schematic results for this chapter. When particles can entangle there is a great difference in what way the experiment is performed (or repeated). The ‘one-to-one’ measures a combined property of two particles. The ‘many-to-one’ measures the internal state of a particle, but in a specific basis, depending on the internal state of the probing particles. The ‘many-to-many’ does not measure anything about the internal state of the particles. It is only in the non-abelian theory that these three experiments yield different results; in the free and abelian theory (the original double slit, and the Aharonov-Bohm case) these would give the same result. Only when averaging the measurements in the non-abelian case they all return the same value $\langle \mathcal{R}^2 \rangle$.

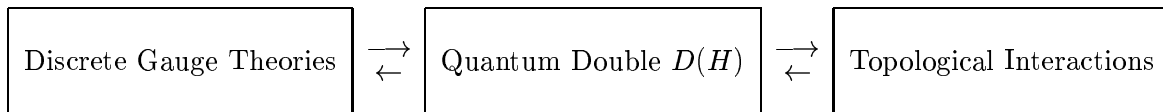
CHAPTER 4

DISCRETE GAUGE THEORIES

In this chapter we will give some physical and mathematical background on topologically interacting particles. We base the behaviour of these exotic particles in this thesis mainly on the mathematical structure $D(H)$, the quantum double of a finite group H . We will describe $D(H)$ extensively in section 4.2. To support the usage of $D(H)$ *physically*, we will glance at a specific case of spontaneously broken gauge theories, in which the structure of $D(H)$ can be identified. We will look at these *discrete gauge theories* in section 4.1. The identifications with $D(H)$ will be made in section 4.2.

To describe double slit experiments as in chapters 2 and 3 we also require, apart from an internal state on which the topological interaction acts, a description of an external state. We, as thought-experimenters, want to be able to manipulate this external state, for instance to move particles. This cannot be done with $D(H)$ alone. This external state is supplied by the discrete gauge theories though. On the other hand we will often omit the external states.

At first sight then, topological interaction follows from $D(H)$, and $D(H)$ follows from discrete gauge theories, but on second thoughts this is not a strict one-way direction.



There may be other physical theories than the discrete gauge theories, from which the structure $D(H)$ emerges. Results of this thesis will probably be also valid for such theories. Perhaps even, the possible physical implementation for these may be more realistic.

Although $D(H)$ can be viewed separately from discrete gauge theories, this chapter is named ‘discrete gauge theories’, after the title of Propitius and Bais [11] which treats both the gauge theory and $D(H)$, and on which most of this chapter is based.

4.1 Spontaneously broken discrete gauge theories

We will now present, briefly, some aspects of spontaneously broken gauge theories which produce a non-abelian discrete gauge theory. We will step over many non-trivial details. For any questions concerning these details, one should consult Propitius and Bais [11] and references

therein. Reference [11] is a review of discrete gauge theories, based on Bais [17], Bais, van Driel, and de Wild Propitius [18, 19].

We will show that, for this specific case in two spatial dimensions, such broken gauge theories yield stable solutions that behave as point-like particles: fluxes, charges and dyons. These particles are labeled by conjugacy classes of a *finite* group H and the irreducible representations of their centralizers.

4.1.1 Yang-Mills Higgs action

The 2+1 dimensional model of the gauge theories that break to a finite group, has an action of the form:

$$S = S_{\text{YMH}} + S_{\text{matter}} \quad (4.1)$$

First, we will focus on the Yang-Mills Higgs part of this action:¹

$$S_{\text{YMH}} = \int d^3x \left(-\frac{1}{4} F^a{}_{\kappa\nu} F^a{}_{\kappa\nu} + (\mathcal{D}^\kappa \Phi)^\dagger \cdot \mathcal{D}_\kappa \Phi - V(\Phi) \right)$$

The Higgs field Φ transforms as a higher dimensional representation of a continuous non-abelian gauge group G . The potential $V(\Phi)$ breaks the symmetry to a finite group: there is a degenerate set of ground states which are invariant under a finite, or discrete, non-abelian subgroup H of G . The ground state manifold is isomorphic to the quotient G/H .

4.1.2 Classifying vortex solutions: fluxes

In the low energy regime of this theory, stable vortices can be formed, which behave as point-like particles. They are labeled by the fundamental group of G/H :

$$\pi_1(G/H) \simeq H \quad (4.2)$$

Which is isomorphic to the discrete group H itself. This means different vortices, which are called *fluxes*, can be labeled by the elements of H .

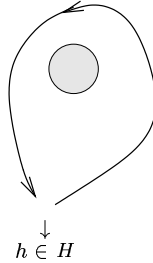


Figure 4.1: We associate an element h of the discrete group H with each (global) counterclockwise loop that we draw. A product-loop is assigned the group-product of the elements of the individual loops. (We are actually using the Wilson loop operator here; we will not explain the Wilson loop operator.)

This label is not gauge-invariant though. Under a residual global gauge transformations $g \in H$ a flux h changes to:

$$g: h \mapsto ghg^{-1} \quad (4.3)$$

¹We will not use the explicit form of this action any further, neither will we use the field-strength $F^a{}_{\kappa\nu}$ and the covariant derivative \mathcal{D}_κ . Actually, in two spatial dimensions one may add the so-called Chern Simons action which does affect the topological interactions between the particles.

The action of g conjugates h . So a better, gauge-invariant, label is the conjugacy class ${}^A C$, where $h \in {}^A C$. Each vortex solution has – apart from an external state – an internal state which changes under a residual global gauge transformation. An orthonormal basis for this internal space, which we will call V^A , is $\{|h\rangle, h \in {}^A C\}$. The action of a residual global gauge transformation g on these basisvectors is equal to the action of (4.3). We still call these particles ‘fluxes’.

There can be multiple vortices. If we locally exchange two vortices, their internal states change. If we call this exchange-operation \mathcal{R} , which we choose to be a counterclockwise exchange, then:

$$\mathcal{R}|h_1, \vec{y}\rangle|h_2, \vec{z}\rangle = |h_1 h_2 h_1^{-1}, \vec{y}\rangle|h_1, \vec{z}\rangle \quad \vec{y}, \vec{z} \text{ denote the external states} \quad (4.4)$$

Effectively, the flux of the particle at the right gets conjugated by the flux of the particle at the left and then they are interchanged. The operation of \mathcal{R} has the form as in (4.4), because it should conserve the ‘total’ flux $(h_1 h_2)$ of the two-vortices-state: $(h_1)(h_2) = (h_1 h_2 h_1^{-1})(h_1)$. This ‘conservement-of-flux’ can be illustrated if we assign a flux to a global loop. The local exchange cannot change this global flux, see figs. 4.1 and 4.2.

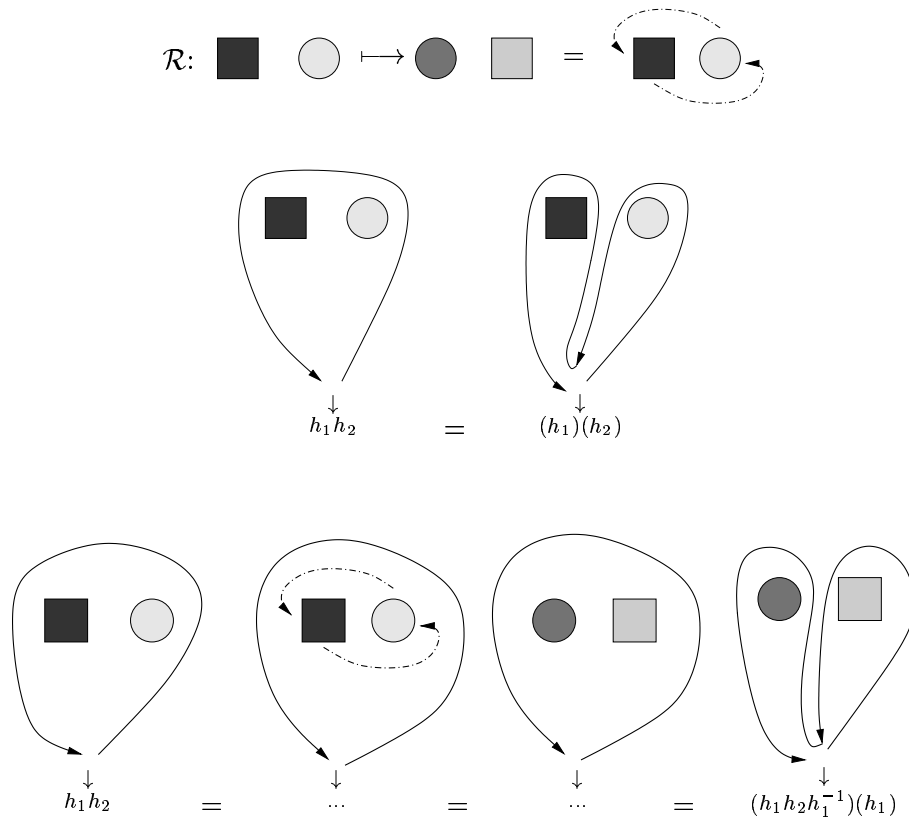


Figure 4.2: The total flux is invariant under a local exchange of two vortices.

One can now also define a clockwise exchange \mathcal{R}^{-1} , which also is the inverse of \mathcal{R} :

$$\mathcal{R}^{-1}|h_3, \vec{y}\rangle|h_1, \vec{z}\rangle = |h_1, \vec{y}\rangle|h_1^{-1} h_3 h_1, \vec{z}\rangle \quad h_3 = h_1 h_2 h_1^{-1} \Rightarrow \mathcal{R}^{-1} \mathcal{R} = \mathbb{1} \quad (4.5)$$

A counterclockwise *monodromy* \mathcal{R}^2 is the result of two successive \mathcal{R} -exchanges, thereby moving one particle counterclockwise around the other particle and returning it back to its original position:

$$\begin{aligned} \mathcal{R}^2|h_1, \vec{y}\rangle|h_2, \vec{z}\rangle &= |(h_1 h_2) h_1 (h_1 h_2)^{-1}, \vec{y}\rangle |(h_1 h_2) h_2 (h_1 h_2)^{-1}, \vec{z}\rangle \\ &= |(h_1 h_2) h_1 (h_1 h_2)^{-1}, \vec{y}\rangle |h_1 h_2 h_1^{-1}, \vec{z}\rangle \end{aligned} \quad (4.6)$$

Effectively, both fluxes have been conjugated by the total flux ($h_1 h_2$).

We will omit the external states, \vec{y} and \vec{z} , from now on.

The action of a residual global gauge transformation g is a conjugation of both fluxes by g :

$$g : |h_1\rangle|h_2\rangle \mapsto |gh_1g^{-1}\rangle|gh_2g^{-1}\rangle \quad (4.7)$$

4.1.3 Other particles: charges and dyons

If we add to the Yang-Mills Higgs action a matter term S_{matter} , which describes additionally matter fields minimally coupled to the gauge fields, then this gives rise to *charges*. Charges are particles transforming as irreducible representations (irreps) of the finite gauge group H . These charges also behave as point-like particles.

A residual global gauge transformation g changes the internal state $|v\rangle$ of a charge according to its irrep:

$$g : |h\rangle|v\rangle \mapsto |ghg^{-1}\rangle|\Gamma(g)v\rangle \quad (4.8)$$

Where $\Gamma(g)$ is the irrep matrix associated with $g \in H$.

One can argue that if a flux h is moved around a charge, the internal state of the charge is changed by $\Gamma(h)$:

$$\mathcal{R}^2|h\rangle|v\rangle = |h\rangle|\Gamma(h)v\rangle \quad (4.9)$$

One can check that the operator \mathcal{R}^2 , when operating on fluxes and/or charges, commutes with residual global gauge transformations, indicating that \mathcal{R}^2 expectation values are invariant under the action of a residual global gauge transformation g :

$$\mathcal{R}^2g = g\mathcal{R}^2 \quad (4.10)$$

$$g : \langle u_2|\langle u_1|\mathcal{R}^2|u_1\rangle|u_2\rangle \mapsto \langle u_2|\langle u_1|\mathcal{R}^2|u_1\rangle|u_2\rangle \quad |u_i\rangle: \text{flux or charge} \quad (4.11)$$

Apart from fluxes and charges there can also be *dyons*: particles with both flux and charge. The flux of a dyon is, still, labeled by a conjugacy class ${}^A C$ of H . The charge of a dyon is not an irrep of H , but an irrep of the *centralizer*² ${}^A N$ of that conjugacy class ${}^A C$. A residual global symmetry transformation effects this particle's internal state $|h, v\rangle$ through:

$$g : |h, v\rangle \mapsto |ghg^{-1}, \Gamma(\tilde{g})v\rangle \quad \tilde{g} = \tilde{g}(g) \in N^A \quad (4.12)$$

where Γ is the centralizer irrep-matrix and \tilde{g} is an element of the centralizer; we will specify \tilde{g} later.

Theories like this have been called *discrete gauge theories*, for obvious reasons.

The complete spectrum of this discrete H gauge theory then consists of particles labeled by:

$$({}^A C, \alpha) \quad (4.13)$$

where A runs over the different conjugacy classes of H and $\alpha = \alpha(A)$ stands for the different irreps of the centralizer ${}^A N$ of the conjugacy class ${}^A C$. ‘Pure’ fluxes are dyons where the centralizer irrep is the trivial irrep (i.e. the identity matrix). ‘Pure’ charges are dyons of which

²The centralizer ${}^h N$ of an element h of a group H is the subgroup of H consisting of all elements that commute with h : ${}^h N = \{g \in H | ghg^{-1} = h\}$. The centralizers of different elements in the same conjugacy class are isomorphic. Therefore we can assign one centralizer ${}^A N$ to each conjugacy class ${}^A C$.

the conjugacy class is the identity element $e \in H$. The centralizer of e is the whole group H . Although all particles are dyons, we will mainly use the term ‘dyon’ to indicate particles which are neither a pure flux nor a pure charge.

We will show later what the effect of exchanging dyons is, i.e. the explicit operation of \mathcal{R} , \mathcal{R}^2 and \mathcal{R}^{-1} on states of multiple dyons. The dyons affect each other only by these exchanges, and the effect depends only on the number and order of exchanges (or braids, or windings). Therefore these particles exhibit a topological interaction, but this was presumably already clear.

We should note that we will use the operators \mathcal{R} , \mathcal{R}^{-1} and \mathcal{R}^2 as dynamical operators that can be used to actually exchange two particles, while the discrete gauge theories are merely a static theory; in the discrete gauge theories the operators \mathcal{R} , \mathcal{R}^{-1} and \mathcal{R}^2 indicate the change of the wave-function if one particle is adiabatically transported around another particle, there is not yet a description of dynamical processes. But we will use the exchange operators as if they are the correct dynamical operators.

It turns out that there is an algebraic structure in which we can identify both the same spectrum as that of (4.13) and the same exchange operations \mathcal{R} , \mathcal{R}^2 and \mathcal{R}^{-1} as described in this section. This structure is the quantum double $D(H)$ of the finite group H . We will give an extensive description of $D(H)$ in the following section.

4.2 Quantum double $D(H)$

Here we will describe many aspects concerning the quantum double $D(H)$ of a finite group H . It will be more thorough compared to the brief review of spontaneously broken gauge theories in the previous section. The quantum double $D(H)$ of a discrete group H is a quantum group. Here we will describe what $D(H)$ is: its algebraic structure, its irreducible representations, its universal R -element, its braid group representations and many more. The quantum double of a discrete group was introduced by Roche, Pasquier, and Dijkgraaf [20].

As many of the available textbooks on the subject of quantum groups are very mathematically involved, we attempt in this section a rather pedestrian but also hamhanded introduction to the subject. One of the from the physicist’s point of view more accessible books is Majid [21].

Though $D(H)$ is a quantum group, $D(H)$ is *not* a group, it rather is an algebra.

4.2.1 Algebras

An **algebra** A is a vectorspace V^A (there is abelian addition of vectors, scalar multiplication, there is a null-vector) equipped with a linear associative, possibly commutative, product m and a unit³ $\mathbb{1}_A$ with respect to this product:

$$m : V^A \otimes V^A \rightarrow V^A \quad m(a, b) = a \cdot b \quad a, b \in A \quad (4.14)$$

$$a \cdot \mathbb{1}_A = \mathbb{1}_A \cdot a = a \quad \forall a \in A \quad (4.15)$$

One can completely specify the product by its operation on basisvectors. Let $\{|e_i\rangle\}$ be an orthonormal basis for V^A , then:

$$m(|e_i\rangle, |e_j\rangle) = m_{ij}^k |e_k\rangle \quad (4.16)$$

³In fact some similar structures that do not have a unit are also called algebras. A Lie algebra, for instance, does not have a unit. We will always demand, that what we call an algebra, has a unit.

$$m(x^i|e_i), y^j|e_j) = x^i y^j m_{ij}^k |e_k) \quad \forall x^i|e_i), y^j|e_j) \in A$$

Associativity means:

$$a \cdot (b \cdot c) = (a \cdot b) \cdot c \quad m_{il}^m m_{jk}^l = m_{ij}^n m_{nk}^m \quad (4.17)$$

One can always make an algebra out of a finite group H , the **group algebra** $\mathbb{C}[H]$. An orthonormal basis for $V^{\mathbb{C}[H]}$ is $\{|h)\}, h \in H$, meaning $\langle h'|h) = \delta_{h'h}$. The multiplication of basisvectors of the algebra is the product of the group:

$$|h_1) \cdot |h_2) = |h_1 h_2) \quad |h_1), |h_2), |h_1 h_2) \in V^{\mathbb{C}[H]}$$

and this extends naturally to all complex linear combinations of basisvectors. Of course, $|e)$ is the unit-element of the group algebra. If H is non-abelian then also the group algebra is non-commutative.

An example of an abelian algebra is $\mathcal{F}(H)$, the algebra of functions on H (or functions on $V^{\mathbb{C}[H]}$). Its basis is $\{P_h\}, h \in H$. $\mathcal{F}(H)$ is further specified by:

$$\begin{aligned} f : H &\rightarrow \mathbb{C} \\ (f_1 + f_2)(h) &= f_1(h) + f_2(h) & f, f_1, f_2, P_k \in \mathcal{F}(H) \\ (f_1 \cdot f_2)(h) &= f_1(h) f_2(h) & g, h \in H \\ P_g(h) &= \delta_{gh} \\ P_h \cdot P'_h &= \delta_{hh'} P_h \\ \mathbb{1} &= \sum_h P_h \end{aligned}$$

From two algebras A and B one can create another algebra C , the **tensor product** of A and B :

$$\begin{aligned} C &= A \otimes B \\ V^C &= V^A \otimes V^B \\ (a_1 \otimes b_1) \cdot (a_2 \otimes b_2) &= (a_1 \cdot a_2) \otimes (b_1 \cdot b_2) \quad a_1, a_2 \in A; b_1, b_2 \in B \end{aligned}$$

Where the product on C is just the tensor product of the multiplications on A and B .

The quantum double $D(H)$ looks like the tensor product of $\mathbb{C}[H]$ and $\mathcal{F}(H)$, but its is so only as a vector space:

$$V^{D(H)} = V^{\mathcal{F}(H)} \otimes V^{\mathbb{C}[H]} \quad (4.18)$$

For it has another product than that of the tensor product:

$$(P_h \otimes |g) \cdot (P_{h'} \otimes |g') = (\delta_{h,gh'g^{-1}}) P_h \otimes |g \cdot g') \quad (4.19)$$

where we used $\{P_h \otimes |g)\}$ as the orthonormal basis for $D(H)$. This also implies that if the group H has order $|H|$, then $D(H)$ is a $|H|^2$ -dimensional algebra. We can adapt a shorter notation:

$$P_h \otimes |g) = P_h g \quad (4.20)$$

$$\mathbb{1}_{\mathcal{F}(H)} \otimes g = \sum_h P_h g = g \quad (4.21)$$

$$P_h \otimes \mathbb{1}_{\mathbb{C}[H]} = P_h e = P_h \quad (4.22)$$

The unit element of the algebra $D(H)$ is the tensor product of the two units of the subspaces:

$$\mathbb{1}_{D(H)} = \mathbb{1}_{\mathcal{F}(H)} \otimes \mathbb{1}_{\mathbb{C}[H]} \quad (4.23)$$

Algebras can act on other structures. Algebras usually only become physically interesting when they act on other structures. The ‘action’ of $P_h g$ can be thought of as a residual global symmetry transformation g , followed by a projection onto the flux h . Crucial is that these two separate actions do not commute:

$$gP_h = P_{ghg^{-1}}g \quad (4.24)$$

$D(H)$ is more than just an algebra, but we will come to that later. Let us now first classify the irreducible representations of $D(H)$ as an algebra.

4.2.2 Irreps of algebras

A n -dimensional representation of a group G is a map from G to $GL(n, \mathbb{C})$, the group of non-singular $n \times n$ matrices. It is a homomorphism, which means that the product of the group is mapped onto the product of $GL(n, \mathbb{C})$, i.e. the matrix multiplication. Shown explicitly, with $T(g)$ the matrix-representation of an element g :

$$T(g \cdot h) = T(g) \cdot T(h) \quad (4.25)$$

Now the group G has no addition and no scalar multiplication, but $GL(n, \mathbb{C})$ does have addition of matrices and scalar multiplication. So there is no problem of extending the idea of representations to algebras: a map from the algebra to $GL(n, \mathbb{C})$ which not only respects the product but also addition and scalar multiplication.

Groups have irreducible representations (irreps): basic building blocks for all other representations. Also algebras have irreps, which means practically that the representation matrices of an irrep cannot be turned into block-diagonal matrices for all basisvectors of the algebra when performing orthonormal basis transformations. Every algebra-representation is a direct sum of irreps of the algebra⁴.

For instance, consider the irreps of the group algebra $\mathbb{C}[H]$. These are the same as the irreps of the group H itself. The sum of the squared dimensions of the irreps is equal to the order of the group H and is thereby also equal to the dimension of the group algebra (let $\{T^i\}$ denote the set of irreps):

$$\sum_i [\dim(T^i)]^2 = |H| = \dim(\mathbb{C}[H]) \quad (4.26)$$

The irreps of $D(H)$ are, not to our surprise, labeled by the conjugacy class ${}^A C$ and the irrep α of the centralizer ${}^A N$, just as in (4.13). Also now, the sum of the squared dimensions of the irreps is equal to the dimension of the algebra (we use $|{}^A C| |{}^A N| = |H|$):

$$\begin{aligned} \sum_{A, \alpha} \dim(\Pi_\alpha^A)^2 &= \sum_{A, \alpha} [|{}^A C| \dim(\alpha)]^2 \\ &= \sum_A |{}^A C|^2 \sum_\alpha \dim(\alpha)^2 \\ &= \sum_A |{}^A C|^2 |{}^A N| \\ &= |H| \sum_A |{}^A C| \\ &= |H|^2 \end{aligned} \quad (4.27)$$

⁴As in the case of groups, where this statement is true for finite and compact groups, we will restrict ourselves to finite dimensional algebras. Generalizations of the quantum double to the case of continuous groups have been given by Koornwinder, Bais, and Muller [22]

Here we already used Π_α^A to indicate the different irreps of $D(H)$. Let us explicitly write the matrix entries for these irreps:

$$\Pi_\alpha^A(P_h g) |^A h_i, \alpha v_j\rangle = \delta_{h, g A h_i g^{-1}} |g A h_i g^{-1}, \alpha(\tilde{g})_{mj} \alpha v_m\rangle \quad (4.28)$$

where

$$\{|^A h_i, \alpha v_j\rangle\}_{j=1, \dots, \dim \alpha}^{i=1, \dots, k} \quad (4.29)$$

is a basis for the vector space V_α^A on which the irreps act. The v_j are basis vectors of the centralizer irrep α . The group elements, or fluxes, h_i are elements of the conjugacy class ${}^A C$ which contains k elements:

$${}^A C = \{{}^A h_1, {}^A h_2, \dots, {}^A h_k\} \quad (4.30)$$

We will now specify \tilde{g} . If one chooses a set of k elements $\{{}^A x_1, {}^A x_2, \dots, {}^A x_k\}$ such that ${}^A h_i = {}^A x_i {}^A h_1 {}^A x_i^{-1}$ (with ${}^A x_1 = e$) then one can express \tilde{g} as:

$$\tilde{g} = {}^A x_l^{-1} g {}^A x_l \quad {}^A h_l = g {}^A h_i g^{-1} \quad (4.31)$$

The element \tilde{g} is constructed in such a way, that it will be an element of the centralizer of ${}^A h_1$. Different choices for ordering of the ${}^A h_i$ and choices of the ${}^A x_j$ give equivalent representations.

One can and should check that Π_α^A of (4.28) forms a representation of $D(H)$.

We can also consider the character of the representation Π_α^A : the trace of the matrices $\Pi_\alpha^A(P_h g)$. If we do this, we can conclude that:

$$\frac{1}{H} \sum_{h, g} \text{Tr}(\Pi_\alpha^A(P_h g)) \text{Tr}(\Pi_\beta^B(P_h g))^* = \delta^{A, B} \delta_{\alpha, \beta} \quad (4.32)$$

This result, see Roche et al. [20], implies that the set $\{\Pi_\alpha^A\}$ is the complete set of irreps of $D(H)$.

The irrep Π_α^A also induces a, possibly reducible, representation T of the group H by:

$$T_\alpha^A(g) = \sum_h \Pi_\alpha^A(P_h g) = \Pi_\alpha^A\left(\sum_h P_h g\right) = \Pi_\alpha^A(g) \quad (4.33)$$

We will from now on identify different particles of the discrete H gauge theory with the different irreps of $D(H)$, and label them accordingly. The vector space V_α^A on which the irreps act, serves as the internal space of the particles.

The operation of $T_\alpha^A(g) = \Pi_\alpha^A(g)$ of (4.33) on a particle Π_α^A is that of the residual global gauge transformation g . A pure flux, for instance, gets conjugated by g : $\Pi_\alpha^A(g)|h\rangle = |ghg^{-1}\rangle$, where α should be the trivial irrep to make sure that Π_α^A is a pure flux.

Let us now consider a system of two particles (at least more than one), where the two particles are labeled by Π_α^A and Π_β^B . Then we want the combined internal state $|\psi\rangle$, i.e. the tensor product of Π_α^A and Π_β^B : $|\psi\rangle \in V_\alpha^A \otimes V_\beta^B$, to also be a representation of $D(H)$. This will probably be a reducible representation.

For irreps $T^1(g)$ and $T^2(g)$ of a group G the tensor product representation $M(g)$ is the tensor product of the T^i : $M(g) = T^1(g) \otimes T^2(g)$. But such a construction is not possible for algebras,

because it is contradicted by the scalar multiplication. Let T^1 and T^2 be two irreps of an algebra A , let a be an arbitrary element of A , and M the tensor product of T^1 and T^2 , then:

$$\begin{aligned} M(a) &= T^1(a) \otimes T^2(a) \\ &\Rightarrow \\ M(2a) &= T^1(2a) \otimes T^2(2a) \\ &= 4 T^1(a) \otimes T^2(a) \\ &= M(4a) \\ &\neq M(2a), \end{aligned}$$

indicating that M is *not* a representation of the algebra A .

For algebra A with basis $\{|e_i\rangle\}$, the representation M of the tensor product $T^1 \otimes T^2$ should have the general form:

$$M(|e_i\rangle) = M_i^{jk} T^1(|e_j\rangle) \otimes T^2(|e_k\rangle) \quad (4.34)$$

which is a linear map from $V_\alpha^A \otimes V_\beta^B$ to itself and *is* a representation of A . This property, indicated by (4.34), actually requires the algebra A to be a *bialgebra*.

Indeed, $D(H)$ is a bialgebra. But to understand what a bialgebra is, one needs to know what a *coalgebra* is.

4.2.3 Coalgebras, bialgebras

A **coalgebra** C is a complex⁵ vectorspace V^C equipped with a linear co-associative, possibly cocommutative, *coproduct* (or comultiplication) Δ and a *counit* ε .

$$\Delta : C \rightarrow C \otimes C \quad (4.35)$$

The operation of the coproduct can be written in the basis $\{|e_i\rangle\}$ as:

$$\Delta(|e_i\rangle) = M_i^{jk} |e_j\rangle \otimes |e_k\rangle \quad (4.36)$$

But Δ is usually written without an explicit basis and in a short notation:

$$\begin{aligned} \Delta(c) &= \sum_i c_{i(1)} \otimes c_{i(2)} \quad c, c_x \in C \\ &= \sum c_{(1)} \otimes c_{(2)} \end{aligned} \quad (4.37)$$

Coassociativity means:

$$(\mathbb{1} \otimes \Delta) \circ \Delta(c) = (\Delta \otimes \mathbb{1}) \circ \Delta(c) = \sum c_{(1)} \otimes c_{(2)} \otimes c_{(3)} \quad (4.38)$$

$$M_l^{ij} M_m^{lk} = M_m^{in} M_n^{jk}$$

Notice the difference between the unit-*element* of an algebra $\mathbb{1}$ and the identity *map* or unit-matrix $\mathbb{1}$, which operates on the same algebra. There are more occasions where the difference between elements and operators tends to fade.

⁵We will only consider algebras, coalgebras and bialgebras etcetera over the field of complex numbers. But one can replace \mathbb{C} by \mathbb{R} in all the definitions to obtain the real counterparts. One could also replace it by a general field K .

The counit is a linear map from C to \mathbb{C} :

$$\varepsilon : C \rightarrow \mathbb{C} \quad \varepsilon(|e_i\rangle) = \varepsilon_i \in \mathbb{C} \quad (4.39)$$

It is called a *counit* because it has to obey:

$$(\mathbb{1} \otimes \varepsilon) \circ \Delta(c) = (\varepsilon \otimes \mathbb{1}) \circ \Delta(c) = c \quad \forall c \in C \quad (4.40)$$

$$M_k^{ij} \varepsilon_j = \delta_k^i \quad M_k^{ij} \varepsilon_i = \delta_k^j$$

One can write something similar for an algebra A with unit $\mathbb{1}_A = \eta^l |e_l\rangle$, then: $m_{il}^k \eta^l = \delta_i^k$ and $m_{ij}^k \eta^l = \delta_j^k$.

If C is cocommutative, then, with τ as a swapping operator on $C \otimes C$:

$$\Delta(c) = \tau \circ \Delta(c) = \sum c_{(1)} \otimes c_{(2)} = \sum c_{(2)} \otimes c_{(1)} \quad (4.41)$$

For a structure B to be an algebra and a bialgebra at the same time, in a compatible way, it needs to be a **bialgebra**. So B has a unit, counit, product, coproduct, that are compatible with each other in the sense:

$$\Delta(hg) = \Delta(h) \cdot \Delta(g) \quad \Delta(\mathbb{1}) = \mathbb{1} \otimes \mathbb{1} \quad \varepsilon(hg) = \varepsilon(h)\varepsilon(g) \quad \varepsilon(\mathbb{1}) = 1 \quad \forall g, h \in B \quad (4.42)$$

Where the product $\Delta(h) \cdot \Delta(g)$ is the true tensor-product multiplication of the bialgebra $B \otimes B$.

The quantum double $D(H)$ is a bialgebra. Its coproduct and counit are:

$$\Delta(P_h g) = \sum_{h' \cdot h'' = h} P_{h'} g \otimes P_{h''} g \quad \varepsilon(P_h g) = \delta_{h,e} \quad (4.43)$$

The action of the quantum double $D(H)$ on the system of two particles Π_α^A and Π_β^B , or the representation M on the combined internal states in other words, thus becomes:

$$M(P_h g) \quad : \quad V_\alpha^A \otimes V_\beta^B \rightarrow V_\alpha^A \otimes V_\beta^B \quad (4.44)$$

$$M(P_h G) = (\Pi_\alpha^A \otimes \Pi_\beta^B) \Delta(P_h g) \quad (4.45)$$

$$= \sum_{h' \cdot h'' = h} \Pi_\alpha^A(P_{h'} g) \otimes \Pi_\beta^B(P_{h''} g) \quad (4.46)$$

We observe that:

$$\Delta(g) = g \otimes g \quad (4.47)$$

This means that the action of a residual global gauge transformation g of the group H on the combined internal states, is the usual tensor-product-representation action for groups (see (4.33)):

$$M(g) = \Pi_\alpha^A(g) \otimes \Pi_\beta^B(g) = T_\alpha^A(g) \otimes T_\beta^B(g) \quad (4.48)$$

A residual global gauge transformation g on a system of two pure fluxes conjugates both fluxes separately, which it should do as explained in section 4.1.

We can decompose the tensor product representation $M(P_h g)$ of $D(H)$ in irreps of $D(H)$:

$$\Pi_\alpha^A \otimes \Pi_\beta^B = \bigoplus_{C, \gamma} N_{\alpha\beta C}^{AB\gamma} \Pi_\gamma^C \quad (4.49)$$

$$N_{\alpha\beta C}^{AB\gamma} = \frac{1}{|H|} \sum_{h, g} \text{Tr} (\Pi_\alpha^A \otimes \Pi_\beta^B (\Delta(P_h g))) \text{Tr} (\Pi_\gamma^C (P_h g))^* \quad (4.50)$$

This decomposition of the tensor product is also referred to as the **fusion rules**. We will use fusion later as an additional tool to the double slit measurements of chapter 3 and the exchange operators \mathcal{R} , which we will come to in a moment, to manipulate the internal quantum states of particles.

By *fusion* we mean we can bring two particles Π_α^A and Π_β^B close together and merge them to find another particle Π_γ^C . Possible outcomes for (C, γ) are given by the fusion rules. Probabilities for specific outcomes require detailed knowledge of the quantum states.

Bialgebras can be (co)commutative or non(co)commutative. We are especially interested in those which are ‘almost’ cocommutative, like quasitriangular bialgebras.

4.2.4 Quasitriangular bialgebras

A bialgebra where there can be found an invertible element R of $B \otimes B$ with the properties:

$$\tau \circ \Delta(b) = R\Delta(b)R^{-1} \quad \forall b \in B \quad \tau \text{ as in (4.41)} \quad (4.51)$$

$$(\Delta \otimes \mathbb{1})R = R_{13}R_{23} \quad (\mathbb{1} \otimes \Delta)R = R_{13}R_{12} \quad (4.52)$$

$$R = \sum R^{(1)} \otimes R^{(2)} \quad R_{13} = \sum R^{(1)} \otimes \mathbb{1} \otimes R^{(2)} \quad R_{ij} = \dots\dots$$

is called a **quasitriangular bialgebra**, and R is its *quasitriangular structure*. Equation (4.51) indicates that B is ‘almost’ cocommutative, i.e. it is cocommutative up to conjugation by the element R . Further properties of a quasitriangular bialgebra are:

$$(\varepsilon \otimes \mathbb{1})R = (\mathbb{1} \otimes \varepsilon)R = \mathbb{1} \quad (4.53)$$

$$R_{12}R_{13}R_{23} = R_{23}R_{13}R_{12} \quad (4.54)$$

Where (4.54) is known as the quantum Yang-Baxter equation.

For the quantum double $D(H)$ the quasitriangular structure $R \in D(H) \otimes D(H)$ and its inverse are:

$$R = \sum_g P_g \otimes g \quad R^{-1} = \sum_g P_g \otimes g^{-1} = \sum_g P_{g^{-1}} \otimes g \quad (4.55)$$

Let us check that these indeed yield the right cocommutation-relations:

$$\begin{aligned} \tau \circ \Delta(P_h g) &= \sum_{h' \cdot h'' = h} P_{h''} g \otimes P_{h'} g \\ R\Delta(P_h g)R^{-1} &= \sum_{k, f' \cdot f'' = h, l} P_k P_{f'} g P_l \otimes k P_{f''} g l^{-1} \\ &= \sum_{k, f' \cdot f'' = h, l} P_k P_{f'} P_{g l g^{-1}} g \otimes P_{k f'' k^{-1}} k g l^{-1} \\ &= \sum_{f' \cdot f'' = h, l} P_{f'} P_{g l g^{-1}} g \otimes P_{g l g^{-1} f'' g l^{-1} g^{-1}} g \\ &= \sum_l P_{g l g^{-1}} g \otimes P_{g l g^{-1} (g l^{-1} g^{-1} h) g l^{-1} g^{-1}} g \\ &= \sum_m P_m g \otimes P_{h m^{-1}} g \\ &= \sum_{m' \cdot m'' = h} P_{m''} g \otimes P_{m'} g \\ &= \tau \circ \Delta(P_h g) \end{aligned}$$

The element R of a quasitriangular bialgebra is not unique. For a given R , we can always construct another quasitriangular structure R' , which is:

$$R' = \tau \circ R^{-1} \tag{4.56}$$

Sometimes, the element R is referred to as the ‘universal R -element’ or ‘universal R -matrix’.

4.2.5 Exchange operators \mathcal{R}

We will now construct some linear operators that map a tensor product of two vector spaces, V_α^A, V_β^B , to the swapped tensor product:

$$V_\alpha^A \otimes V_\beta^B \rightarrow V_\beta^B \otimes V_\alpha^A$$

A relatively simple operator with this property, is the permutation operator σ , which only exchanges left and right, or, when it operates on basisvectors:

$$\sigma : |e_i^{A\alpha}\rangle \otimes |e_j^{B\beta}\rangle \mapsto |e_j^{B\beta}\rangle \otimes |e_i^{A\alpha}\rangle \tag{4.57}$$

Let us define another map which we call \mathcal{R} . We use the operator σ , the quasitriangular structure R and the irreps $\Pi_\alpha^A, \Pi_\beta^B$ of the quantum double $D(H)$ in its construction:

$$\begin{aligned} \mathcal{R} &= \sigma \circ (\Pi_\alpha^A \otimes \Pi_\beta^B) (R) \\ &= \sigma \circ \sum_g \Pi_\alpha^A(P_g) \otimes \Pi_\beta^B(g) \end{aligned} \tag{4.58}$$

Remember that R is an element, but \mathcal{R} is an operator. This operator \mathcal{R} has exactly the same effect on a state of two particles as the counterclockwise exchange operator we introduced in section 4.1.

But the quasitriangular structure R is not unique, what happens if we use $R' = \tau \circ R^{-1}$ instead of R ?

$$\sigma \circ (\Pi_\alpha^A \otimes \Pi_\beta^B) (\tau \circ R^{-1}) = \mathcal{R}^{-1} \tag{4.59}$$

Then we find that this operator is equal to the clockwise exchange operator \mathcal{R}^{-1} , the inverse of \mathcal{R} .

Although we have to make a choice of which R -element to associate with a counterclockwise or clockwise exchange, physics is independent of this choice.

As an example to explicitly check the correct⁶ function of \mathcal{R} , according to (4.4), let \mathcal{R} work on two pure fluxes, $|h_1\rangle \otimes |h_2\rangle$:

$$\begin{aligned} \mathcal{R}(|h_1\rangle|h_2\rangle) &= \sigma \circ \sum_g \Pi(P_g)|h_1\rangle \otimes \Pi(g)|h_2\rangle \\ &= \sigma \circ \sum_g \delta_{gh_1}|h_1\rangle \otimes |gh_2g^{-1}\rangle \\ &= |h_1h_2h_1^{-1}\rangle|h_1\rangle \end{aligned} \tag{4.60}$$

Apart from the three exchange operators $\sigma, \mathcal{R}, \mathcal{R}^{-1}$ there is the monodromy operator \mathcal{R}^2 , which is not truly an exchange operator, because it maps a tensor product-space to itself:

$$\mathcal{R}^2: V_\alpha^A \otimes V_\beta^B \rightarrow V_\alpha^A \otimes V_\beta^B$$

⁶‘Correct’ according to the physically irrelevant choices that we made.

$$\mathcal{R}^2 = (\mathcal{R})^2 = (\Pi_\alpha^A \otimes \Pi_\beta^B) \left(\sum_{h,g} h P_g \otimes P_{hg} \right) = \sum_{h,g} (\Pi_\alpha^A \otimes \Pi_\beta^B) (P_{hgh^{-1}h} \otimes P_{hg}) \quad (4.61)$$

We will now study some of the braid-aspects of the exchange operators.

4.2.6 Truncated braid group representations

Because the R element obeys the quantum Yang-Baxter equation, there is a similar equation for the \mathcal{R} operators, when they work on three (or more) particles:

$$\mathcal{R}_1 \mathcal{R}_2 \mathcal{R}_1 = \mathcal{R}_2 \mathcal{R}_1 \mathcal{R}_2 \quad (4.62)$$

$$\mathcal{R}_1 = \mathcal{R} \otimes \mathbb{1} \quad \mathcal{R}_2 = \mathbb{1} \otimes \mathcal{R}$$

Equation (4.62) is the (ordinary) Yang-Baxter equation. The exchange operators define, thus, representations of the braid group B_n . Therefore the operators \mathcal{R} and \mathcal{R}^{-1} are also called *braid operators*.

The braid operation also commutes with the action of the quantum double because of $\tau \circ \Delta R = R \Delta$ (as in (4.51)):

$$\mathcal{R} \circ [(\Pi_\alpha^A \otimes \Pi_\beta^B) \Delta(P_{hg})] = [(\Pi_\beta^B \otimes \Pi_\alpha^A) \Delta(P_{hg})] \circ \mathcal{R} \quad (4.63)$$

Here, we used this extended form, instead of just $\Delta \mathcal{R} = \mathcal{R} \Delta$, to once more discriminate clearly between elements of the algebra, P_{hg} , operators on the algebra, Δ , representation-matrices of the algebra, $\Pi_{\alpha/\beta}^{A/B}$, and operators on the representation-space, \mathcal{R} .

To be concrete, systems containing n particles are (reducible) representations of both the quantum double $D(H)$ and the braid group B_n . Because the actions of these two commute, the multiple particle state can be decomposed into a direct sum of irreps of both $D(H)$ and B_n at the same time. And it is this all important property which makes $D(H)$ into a powerful mathematical tool in the analysis of topological interactions.

When H is a discrete group, to which we always restrict ourselves, there exists an m such that:

$$\mathcal{R}^m = \mathbb{1} \otimes \mathbb{1} \quad m \in \mathbb{N} \quad (4.64)$$

This means we are actually working with a representation of a subset of the braid group B_n . These subsets, generated by the braid operators with the extra relation of (4.64), are called *truncated braid groups*. Truncated braid groups can be finite, whereas the braid group itself has infinite order. So we are dealing with irreps of truncated braid groups rather than irreps of the full braid group.

Appendix C describes the braid group, the truncated braid group and also the (partially) colored braid group.

4.2.7 Hopf algebras

It turns out that we can assign to every element b in the quantum double $D(H)$ another element $S(b) \in D(H)$ with the following properties:

$$\cdot (S \otimes \mathbb{1}) \circ \Delta(b) = \cdot (\mathbb{1} \otimes S) \circ \Delta(b) = \eta \circ \varepsilon(b) \quad (4.65)$$

$$\sum S(b_{(1)}) \cdot b_{(2)} = \sum b_{(1)} \cdot S(b_{(2)}) = \eta(\varepsilon(b)) = \varepsilon_k b^k \eta^l |_{e_l} = \varepsilon(b) \mathbb{1}$$

$$S(b_1 b_2) = S(b_2) S(b_1) \quad S(\mathbb{1}) = \mathbb{1} \quad (S \otimes S) \circ \Delta(b) = \tau \circ \Delta \circ S(b) \quad \varepsilon(S(b)) = \varepsilon(b) \quad (4.66)$$

This map S , which is linear, is called the *antipode*. Its role is like that of an inverse (although we do not demand that $S^2 = \mathbb{1}$). A bialgebra B with such an antipode is called a **Hopf algebra**. For the quantum double $D(H)$ the operation of the antipode is:

$$S(g) = g^{-1} \quad S(P_h) = P_{h^{-1}} \quad S(P_h g) = S(g) \cdot S(P_h) = P_{g^{-1} h^{-1} g} g^{-1} \quad (4.67)$$

If there exist a universal R -element in B , then B is called a *quasitriangular Hopf algebra*, and:

$$R^{-1} = (S \otimes \mathbb{1})R \quad (\mathbb{1} \otimes S)R^{-1} = R \quad (S \otimes S)R = R \quad (4.68)$$

For our purposes with the quantum double $D(H)$ we do not need the antipode explicitly, so although $D(H)$ is a quasitriangular *hopf* algebra we will only use the properties it has as being a quasitriangular *bialgebra*.

CHAPTER 5

AN EXAMPLE: MANIPULATION WITH $D(S_3)$


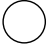


We will give various examples of thought experiments, including the *one-to-one* and *many-to-one* double slit experiments, in this chapter. The non-abelian anyons we use for this purpose are based on the discrete gauge theory with $D(S_3)$ as the associated quantum double.

The examples will not only show the one-to-one and many-to-one experiments in ‘practice’, but other interesting results as well. After some preparations in section 5.1, we will walk through a sequence of experiments based on a single particle with initially known internal state in section 5.2. It turns out, that the outcomes of this sequence is independent of the initial internal state, as we show in section 5.3, and especially the vacuum-state is also allowed as initial state. In section 5.4 we introduce a global quantum double transformation to understand the similarity between the sequence of experiments for different initial states. The end-result of the described sequence is some kind of ordering of the particles. We can label such a collection of ordered particles by unentangled basis-states, even if the particles were originally created from the vacuum. This relabeling, which cannot be directly described by a global quantum double transformation, is introduced in section 5.6. Along the way, we find evidence to relax the restrictions on the many-to-one experiment. Furthermore, we also introduce a pictorial language to illustrate the various worked out examples.

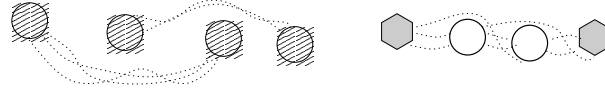
5.1 Preliminaries for experiments with $D(S_3)$

The examples of experiments in this chapter can only be understood by using results of other parts of this thesis. The measurement-aspect of experiments is described in chapter 3. Quantum doubles and its global transformations are treated in chapter 4. The complete spectrum and further properties of $D(S_3)$ are combined in appendix B. We will not explicitly refer to these chapters anymore in the following sections.

The spectrum of $D(S_3)$ consists of eight particle types. We will use the following of those:

particle	type	dimension	graphic	basis for the internal state
$ \mathbb{1}\rangle$	vacuum	1		$ \mathbb{1}\rangle$
$ B\rangle$	charge	2		$ b_+\rangle, b_-\rangle$; or $ a_+\rangle, a_-\rangle$ or $ c_+\rangle, c_-\rangle$ or $ B_1\rangle, B_2\rangle$
$ (12)\rangle$	flux	3		$ 12\rangle, 13\rangle, 23\rangle$
$ (123)\rangle$	flux	2		$ 123\rangle, 132\rangle$

Notice that we use a ket $|\dots\rangle$ to indicate both the particle and the state it is in. In the table above, we also introduce a graphical representation for $D(S_3)$ -particles. We will sometimes explicitly display entanglement of particles in the upcoming pictorial descriptions. Although in the ‘real’ thought experiment there is of course no direct way to ‘see’ entanglement of particles, we will indicate it with dotted lines between particles as indicated below:



In the following sections we will be conducting various one-to-one and many-to-one experiments. One-to-one projects on an eigenspace of the monodromy operator \mathcal{R}^2 . Many-to-one project the density-matrix of particle A on an eigenspace of the operator U , where $U = \text{Tr}_B(\mathcal{R}^2 \rho_B)$.

A first experiment with $D(S_3)$ particles

We begin with a simple thought-experiment of which the results are not interesting, but which is nevertheless representative for the other upcoming experiments.

Let us create a pair of $|(12)\rangle$ out of the vacuum, which we indicate by:

$$|\mathbb{1}\rangle \rightarrow |(12)\rangle|(12)\rangle$$

The state $|\psi\rangle$ of the total two particle system is as follows:

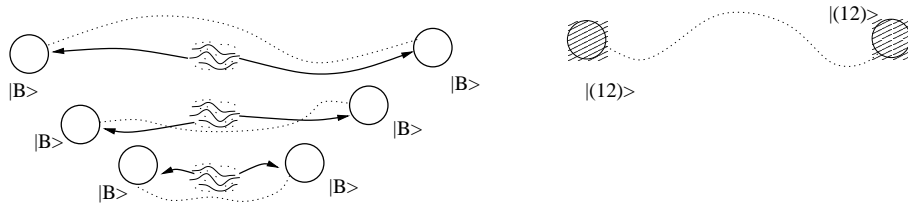
$$|\psi\rangle = \frac{1}{\sqrt{3}} [|(12)\rangle|12\rangle + |13\rangle|13\rangle + |23\rangle|23\rangle]$$

In the pictorial language, this pair-creation is indicated by:

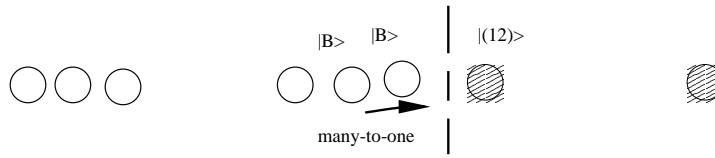


We continue by pulling a pair of $|B\rangle$ from the vacuum, and we do this often.

$$|\mathbb{1}\rangle \rightarrow |B\rangle|B\rangle \quad |\psi\rangle = \frac{1}{\sqrt{2}} [|b_+\rangle|b_+\rangle + |b_-\rangle|b_-\rangle]$$



Now we will commence a many-to-one experiment where we will use one $|(12)\rangle$ as the ‘ A ’ particle and $|B\rangle$ ’s as the ‘ B ’ particles. Note that $|B\rangle$ ’s are charges and they have trivial braiding amongst each-other, and these ‘ B ’ particles are not entangled with each other, so they satisfy the restrictions from chapter 3 to perform the ‘many-to-one’ and to calculate its result using $U = \text{Tr}_B(\mathcal{R}^2 \rho_B)$.



Let us specify ρ_A , ρ_B , \mathcal{R}^2 and the U -matrix. The $|a_+\rangle|12\rangle$ etc. indicate the basisvectors of the basis in which the matrix-elements of \mathcal{R}^2 are written¹.

$$\rho_A = \frac{1}{3}\mathbb{1} \quad \rho_B = \frac{1}{2}\mathbb{1} \quad \mathcal{R}^2 = \begin{pmatrix} 1 & 0 & 0 & 0 \\ 0 & -1 & 0 & 0 \\ 0 & 1 & 0 & 0 \\ 0 & 0 & -1 & 0 \\ 0 & 0 & 1 & 0 \\ 0 & 0 & 0 & -1 \end{pmatrix} \begin{matrix} |a_+\rangle|12\rangle \\ |a_-\rangle|12\rangle \\ |b_+\rangle|13\rangle \\ |b_-\rangle|13\rangle \\ |c_+\rangle|23\rangle \\ |c_-\rangle|23\rangle \end{matrix} \quad U = \begin{pmatrix} 0 & 0 & 0 \\ 0 & 0 & 0 \\ 0 & 0 & 0 \end{pmatrix} \quad (5.1)$$

So, U has three zero eigenvalues. Since there are no different eigenvalues, there is no further projection nor measurement. This is also observed in the interference pattern $g(\theta)$ which always will be:

$$g(\theta) = f_{\kappa=0}(\theta) = \frac{1}{2}f_1(\theta) + \frac{1}{2}f_{-1}(\theta) = |c_{\text{above}}^t|^2 + |c_{\text{below}}^t|^2 \quad (5.2)$$

Our first try did not bring us any ‘success’. So we will try something else and we will begin with a particle which is not pair-created from the vacuum.

5.2 Special $|13\rangle$ flux state as a starting point of a sequence of experiments

We will perform a different thought experiment now, actually a sequence of experiments. It is more interesting, but perhaps physically impossible, because we assume we know a particle’s internal state².

Step 0: one particle in a specific state

We will begin this sequence of experiments with a particle $|12\rangle$ of which we know its internal state and it happens to be $|13\rangle$. We say nothing whatsoever about how we obtained this knowledge or this particle.

$|13\rangle$

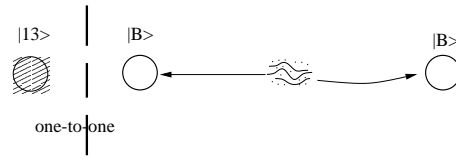


Step 1: a ‘one-to-one’ experiment

We will draw a pair of $|B\rangle$ ’s from the vacuum and perform a ‘one-to-one’ experiment on the $|12\rangle$, with internal state $|13\rangle$, and one of the $|B\rangle$ ’s.

¹So, we are actually using the same notation ‘ \mathcal{R}^2 ’ for the monodromy operator \mathcal{R}^2 and the matrix elements of \mathcal{R}^2 when it operates on two particles of known type.

²This naturally depends on how the quantum double symmetry is realized physically. A pair-creation from the vacuum is generally supposed to be ‘possible’ in theory. But there might be other realizations in which the internal state of a particle is known. However, in the forthcoming sections the states which were created from the vacuum, show the same properties as the particle with specified internal state which we are about to describe.



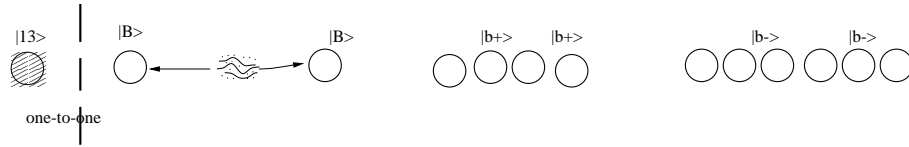
Its \mathcal{R}^2 is the same as that of (5.1) but now there are two possible outcomes:

Probability	Observed pattern	Resulting state
$\frac{1}{2}$	$f_1(\theta)$	$ 13\rangle b_+\rangle b_+\rangle$
$\frac{1}{2}$	$f_{-1}(\theta)$	$ 13\rangle b_-\rangle b_-\rangle$

So there are two distinct results. If we find $f_{-1}(\theta)$ as the interference pattern we move the two $|B\rangle$ charges, which we now know to be in the state $|b_-\rangle$, to the far right. If we find the '+1' pattern we will also move the $|B\rangle$'s to the right but not so far away. We will repeat this process often: drawing a pair of $|B\rangle$'s from the vacuum and performing a 'one-to-one' on one of the $|B\rangle$ particles and the $|12\rangle$ probability. The probabilities to find either $f_1(\theta)$ or $f_{-1}(\theta)$ remain the same.

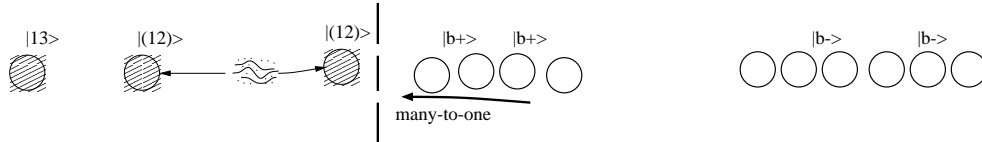
When we are done with this, we still have a particle $|12\rangle$ in the state $|13\rangle$ on the left. On the right we have first a pile of $|B\rangle$'s in the state $|b_+\rangle$ and more to the right we have a stock of them with internal state $|b_-\rangle$. There is no entanglement between the $|b_-\rangle$ and the $|b_+\rangle$ because, although they exchanged with one another, they are charges and thus have trivial braiding. The systems total internal state is now:

$$|13\rangle|b_+\rangle|b_+\rangle \dots |b_+\rangle|b_+\rangle|b_-\rangle|b_-\rangle \dots |b_-\rangle \quad (5.3)$$



Step 2: a 'many-to-one' experiment

We will use a number of the charges $|B\rangle$ with internal state $|b_+\rangle$ to perform a 'many-to-one' experiment, where they will of course serve as the 'many'-side. Just to the right of the $|13\rangle$ we will pull a pair of $|12\rangle$ from the vacuum and use the right one of these two as the 'one'-side.



Although \mathcal{R}^2 is the same as in (5.1) we will write it in another basis, ρ_B is certainly different now:

$$\rho_B = \begin{pmatrix} 1 & 0 \\ 0 & 0 \end{pmatrix} \begin{matrix} |b_+\rangle \\ |b_-\rangle \end{matrix} \quad \mathcal{R}^2 = \begin{pmatrix} -\frac{1}{2} & \frac{1}{2}\sqrt{3} & 0 & 0 \\ \frac{1}{2}\sqrt{3} & \frac{1}{2} & 0 & 0 \\ 0 & 1 & 0 & 0 \\ 0 & 0 & -1 & 0 \\ 0 & 0 & 0 & -\frac{1}{2} \\ & & & -\frac{1}{2}\sqrt{3} \\ & & & \frac{1}{2} \end{pmatrix} \begin{matrix} |b_+\rangle|12\rangle \\ |b_-\rangle|12\rangle \\ |b_+\rangle|13\rangle \\ |b_-\rangle|13\rangle \\ |b_+\rangle|23\rangle \\ |b_-\rangle|23\rangle \end{matrix} \quad (5.4)$$

The associated U -matrix is:

$$U = \begin{pmatrix} -\frac{1}{2} & 0 & 0 \\ 0 & 1 & 0 \\ 0 & 0 & -\frac{1}{2} \end{pmatrix} \begin{matrix} |12\rangle \\ |13\rangle \\ |23\rangle \end{matrix} \quad (5.5)$$

U is diagonal and has two distinct eigenvalues:

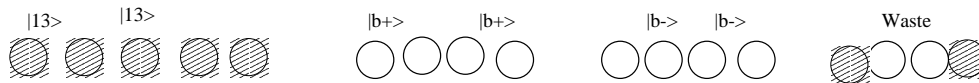
Probability	Observed pattern	Resulting state	Resulting density matrix
$\frac{1}{3}$	$f_1(\theta)$	$ 13\rangle b_+\rangle \dots b_+\rangle 13\rangle b_+\rangle \dots b_+\rangle$	$\rho_A = \begin{pmatrix} 0 & 0 & 0 \\ 0 & 1 & 0 \\ 0 & 0 & 0 \end{pmatrix} \begin{matrix} 12\rangle \\ 13\rangle \\ 23\rangle \end{matrix}$
$\frac{2}{3}$	$f_{-\frac{1}{2}}(\theta)$	$\approx \frac{1}{\sqrt{2}} 12\rangle[\dots] 12\rangle + \frac{e^{i\phi}}{\sqrt{2}} 23\rangle[\dots] 23\rangle$	$\rho_A = \frac{1}{2} \begin{pmatrix} 1 & 0 & 0 \\ 0 & 0 & 0 \\ 0 & 0 & 1 \end{pmatrix} \begin{matrix} 12\rangle \\ 13\rangle \\ 23\rangle \end{matrix}$

With a chance of two-third we will find a ‘one-half’-pattern. The resulting state is entangled and is best described by the density matrix. We do not want to use the particles associated with this outcome further (not yet at this stage that is). The collection of two fluxes and used charges, i.e. $|(12)\rangle|B\rangle \dots |B\rangle|(12)\rangle$ combined (or even fused) is a charge (it has no flux). We can safely move charges in a way that does not change the internal state of other dyons. We will move this collection beyond the stack of $|b_-\rangle$ particles to form a charge-waste-bin of some sort at the far right.

If the outcome is the ‘one’-pattern we are left with a pure (i.e. a non-entangled) state and we can move the charges $|b_+\rangle$ safely back to their pile without changing any internal state. In that case we are left with: $|13\rangle|13\rangle|13\rangle|b_+\rangle \dots |b_+\rangle|b_-\rangle \dots |b_-\rangle$.

We will also repeat this process. If we find $f_{1/2}(\theta)$ we put our particles on the charge-dump, else we add the fluxes to the $|13\rangle$ set. Now we have a total system of the form:

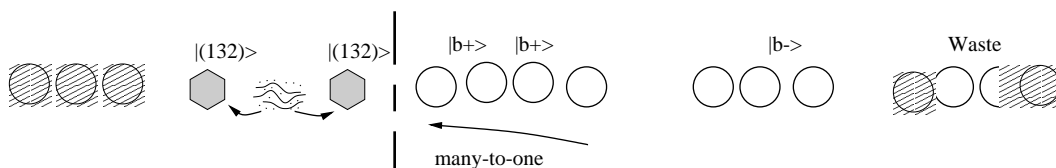
$$|13\rangle|13\rangle \dots |13\rangle |b_+\rangle|b_+\rangle \dots |b_+\rangle |b_-\rangle|b_-\rangle \dots |b_-\rangle |charge - waste\rangle \quad (5.6)$$



Step 3: another many-to-one experiment?

Can we also use the $|b_+\rangle$ to measure the internal state of another flux than $|(12)\rangle$? Let us try it with a particle $|(123)\rangle$, of which we pull a pair out of the vacuum:

$$|1\rangle \rightarrow |(123)\rangle|(123)\rangle \quad |\psi\rangle = \frac{1}{\sqrt{2}}[|(123)\rangle|132\rangle + |132\rangle|(123)\rangle]$$



We try a many-to-one with the $|b_+\rangle$ charges onto one $|123\rangle$; $\rho_A, \rho_B, \mathcal{R}^2$ and U are:

$$\rho_A = \frac{1}{2} \mathbb{1} \quad \rho_B = \frac{1}{2} \begin{pmatrix} 1 & 1 \\ 1 & 1 \end{pmatrix} \begin{matrix} |B_1\rangle \\ |B_2\rangle \end{matrix} \quad \mathcal{R}^2 = \begin{pmatrix} e^{2\pi i/3} & 0 & 0 & 0 \\ 0 & e^{4\pi i/3} & 0 & 0 \\ 0 & 0 & e^{4\pi i/3} & 0 \\ 0 & 0 & 0 & e^{2\pi i/3} \end{pmatrix} \begin{matrix} |123\rangle|B_1\rangle \\ |123\rangle|B_2\rangle \\ |132\rangle|B_1\rangle \\ |132\rangle|B_2\rangle \end{matrix}$$

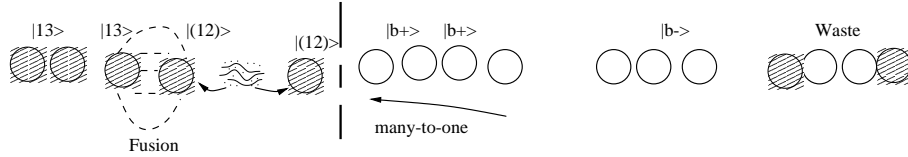
$$U = \begin{pmatrix} -\frac{1}{2} & 0 \\ 0 & -\frac{1}{2} \end{pmatrix} \begin{matrix} |123\rangle \\ |132\rangle \end{matrix} \quad (5.7)$$

But U is a multiple of the unit-matrix, so we cannot measure anything we do not know yet. We will pretend³ we never did this step and we certainly will not repeat it.

Step 4: fusion

We will look closer at the previous step where we measured with $|b_+\rangle$ at a pair $|12\rangle|12\rangle$ from the vacuum. We use the one at the right as the ‘one’-side of the ‘many-to-one’ measurement. But suppose we fused the left $|12\rangle$ particle with one of the already present $|13\rangle$ particles during (just before, during, or after) the ‘many-to-one’ experiment.

$$|13\rangle|12\rangle : \quad |\psi\rangle = |13\rangle \otimes \frac{1}{\sqrt{3}} [|12\rangle + |13\rangle + |23\rangle] \quad (5.8)$$



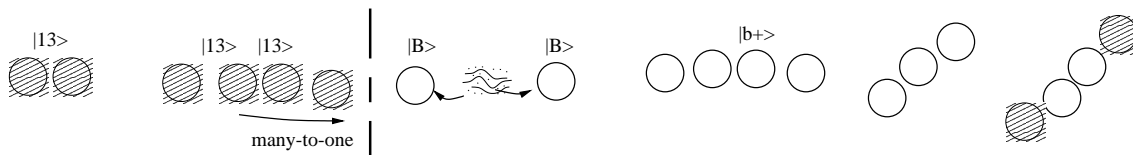
Before starting the experiment we would find with probability $\frac{1}{3}$ a charge ($|1\rangle$ or $|B\rangle$ to be precise) as the fusion product. With probability $\frac{2}{3}$ we would find a particle that does have flux ($|123\rangle, |D\rangle, \text{ or } |E\rangle$). At the end of the ‘one-many’-experiment, if the outcome was $f_1(\theta)$ with 100% chance a charge will be found when fusing the two particles. If the outcome were $f_{1/2}(\theta)$ then with complete certainty a particle with non-trivial flux is found after fusion.

So, the fusion probabilities completely follow the outcome-probabilities of the ‘many-to-one’-experiment.

Step 5: a forbidden ‘many-to-one’?

Until this point we have only conducted thought-experiments as explained in chapter 3 and under the restrictions as we put them there. This meant, for instance, that when doing a ‘many-to-one’ the ‘many’ particles should have trivial braiding. We will now deviate from this rule.

We will use $|12\rangle$ -fluxes as ‘many’ particles; these fluxes will in general have non-trivial braiding. But the fluxes we will use, have a specific internal state, which gives them trivial braiding nonetheless. So, with this restriction on the internal states, these particles have trivial braiding.



³This is one of the benefits of doing thought-experiments.

These particles are the $|13\rangle$ particles, of which we have created quite a lot in the steps above. As the ‘one’-side we will pull a pair of $|B\rangle$ particles from the vacuum. Then ρ_A , ρ_B , \mathcal{R}^2 and U become (where we still use the same \mathcal{R}^2 as in (5.1) but in a suitably reshuffled basis):

$$\rho_A = \frac{1}{2}\mathbb{1} \quad \rho_B = \begin{pmatrix} 0 & 0 & 0 \\ 0 & 1 & 0 \\ 0 & 0 & 0 \end{pmatrix} \begin{matrix} |12\rangle \\ |13\rangle \\ |23\rangle \end{matrix} \quad \mathcal{R}^2 = \begin{pmatrix} -\frac{1}{2} & 0 & 0 & \frac{1}{2}\sqrt{3} & 0 & 0 \\ 0 & 1 & 0 & 0 & 0 & 0 \\ 0 & 0 & -\frac{1}{2} & 0 & 0 & \frac{1}{2}\sqrt{3} \\ \frac{1}{2} & 0 & 0 & \frac{1}{2}\sqrt{3} & 0 & 0 \\ 0 & 0 & 0 & 0 & -1 & 0 \\ 0 & 0 & \frac{1}{2}\sqrt{3} & 0 & 0 & \frac{1}{2} \end{pmatrix} \begin{matrix} |12\rangle|b_+\rangle \\ |13\rangle|b_+\rangle \\ |23\rangle|b_+\rangle \\ |12\rangle|b_-\rangle \\ |13\rangle|b_-\rangle \\ |23\rangle|b_-\rangle \end{matrix}$$

$$U = \begin{pmatrix} 1 & 0 \\ 0 & -1 \end{pmatrix} \begin{matrix} |b_+\rangle \\ |b_-\rangle \end{matrix} \quad (5.9)$$

From which we conclude that in 50% of the times we will end up with a new $|b_+\rangle|b_+\rangle$ and in the other case with $|b_-\rangle|b_-\rangle$. This creates no new states, but we can also ‘make’ $|b_+\rangle$ particles by doing a ‘many-to-one’ with $|13\rangle$ ’s instead of a ‘one-to-one’ with a $|13\rangle$ particle. So the resulting particles (and their internal states) are not new, but the fact that we performed a ‘many-to-one’ with fluxes is a new result. Remember though that we started this section with the assumption that we already had a $|12\rangle$ particle with specific internal state $|13\rangle$.

We will next assume that we have a particle of type $|12\rangle$ but its internal state can be arbitrary. We will then perform *exactly* the same steps as we did here, where we base actions, like putting particles on specific piles, on the *observed* interference patterns.

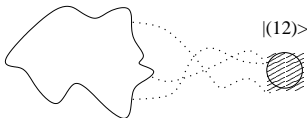
5.3 Arbitrary $|12\rangle$ state as a starting point of the same sequence

We will repeat all the steps of the previous section. Also here, we start with a single particle $|12\rangle$ with known *but arbitrary* internal state. It turns out that in this sequence of experiments the observations, i.e. the interference patterns, do not depend on this initial internal state.

Step 0: a single particle with arbitrary state

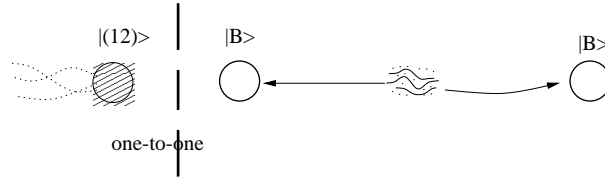
Now we start with a $|12\rangle$ with arbitrary initial state which we will denote by:

$$\zeta|\dots\rangle|12\rangle + \eta|\dots\rangle|13\rangle + \theta|\dots\rangle|23\rangle \quad |\zeta|^2 + |\eta|^2 + |\theta|^2 = 1 \quad (5.10)$$



Since this particle might be entangled (with particles we assume to lie at the left) it is perhaps even better to talk about an arbitrary initial density matrix. Notice that the case that $|12\rangle$ has internal state $|13\rangle$ and the case that it is pulled from the vacuum are covered by this arbitrary initial state.

Step 1: one-to-one with charges from the vacuum



Step one is to draw a pair $|B\rangle|B\rangle$ from the vacuum and to perform a ‘one-to-one’ with the particle $|(12)\rangle$, just as before. The internal state of the vacuum-pair is:

$$|\psi\rangle = \frac{1}{\sqrt{2}} [|a_+\rangle|a_+\rangle + |a_-\rangle|a_-\rangle] = \frac{1}{\sqrt{2}} [|b_+\rangle|b_+\rangle + |b_-\rangle|b_-\rangle] = \frac{1}{\sqrt{2}} [|c_+\rangle|c_+\rangle + |c_-\rangle|c_-\rangle] \quad (5.11)$$

The density matrix for both of the $|B\rangle$ particles is:

$$\rho = \frac{1}{2}\mathbb{1},$$

and it obviously has this form in each basis. The probability of finding eigenpattern $f_1(\theta)$ is (see chapter 3):

$$p_1 = \text{Tr}(E_1\rho_{AB}) = \text{Tr}_A\text{Tr}_B [E_1(\rho_A \otimes \rho_B)] \quad (5.12)$$

We calculate p_1 after writing down E_1 in the basis in which it is diagonal:

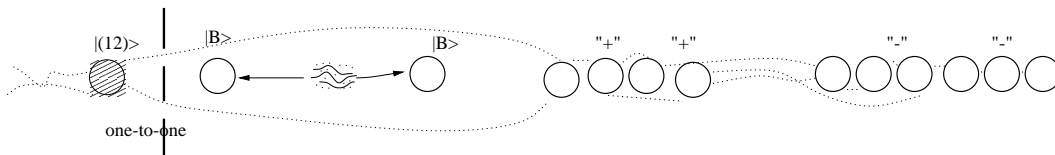
$$E_1 = \begin{pmatrix} 1 & & & & & \\ & 0 & & & & \\ & & 1 & & & \\ & & & 0 & & \\ & & & & 1 & \\ & & & & & 0 \end{pmatrix} \begin{matrix} |a_+\rangle|12\rangle \\ |a_-\rangle|12\rangle \\ |b_+\rangle|13\rangle \\ |b_-\rangle|13\rangle \\ |c_+\rangle|23\rangle \\ |c_-\rangle|23\rangle \end{matrix} \quad |(12)\rangle \rightarrow \rho_A \quad |B\rangle \rightarrow \rho_B \quad (5.13)$$

$$p_1 = \text{Tr}_A\text{Tr}_B [E_1(\rho_A \otimes \rho_B)] = \frac{1}{2}\text{Tr}_A(\rho_A \mathbb{1}) = \frac{1}{2} \quad (5.14)$$

So, this probability p_1 is independent of the (arbitrary) density matrix of particle $|(12)\rangle$. Likewise for the eigenvalue -1 .

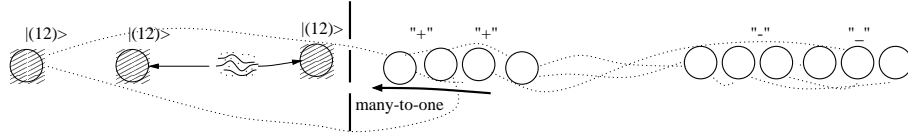
We repeat this step and we move all the charges which yielded $f_1(\theta)$ to the ‘+1’-pile, and the minus-ones to the ‘-1’-mountain. All particles are now entangled with each other. We can explicitly write the total systems state:

$$|\psi\rangle = \begin{aligned} & \zeta |\dots\rangle|12\rangle |a_+\rangle|a_+\rangle \dots |a_+\rangle |a_-\rangle|a_-\rangle \dots |a_-\rangle \\ & + \eta |\dots\rangle|13\rangle |b_+\rangle|b_+\rangle \dots |b_+\rangle |b_-\rangle|b_-\rangle \dots |b_-\rangle \\ & + \theta |\dots\rangle|23\rangle |c_+\rangle|c_+\rangle \dots |c_+\rangle |c_-\rangle|c_-\rangle \dots |c_-\rangle \end{aligned} \quad (5.15)$$



Step 2: ‘many-to-one’ with the ‘+1’ charges

The next step is to use the particles from the +1-pile to perform a ‘many-to-one’ on one member of a pair $|12\rangle|12\rangle$ from the vacuum. This is something which we have not done before. Although the particles $|B\rangle$ do have trivial braiding the density matrix ρ_B for each consecutive particle of the ‘many’-side is not a constant any more. Both ρ_A and ρ_B will change with each measurement of the angle. We nevertheless do the experiment in this example, which we worked out by hand. The outcomes do not depend on the initial state.



We will find the same patterns as before, when we started with $|13\rangle$:

Probability	Observed pattern
$\frac{1}{3}$	$f_1(\theta)$
$\frac{2}{3}$	$f_{-1/2}(\theta)$

If the ‘plus’ pattern is found, the (not yet normalized) state has become:

$$\begin{aligned}
 & \frac{\zeta}{\sqrt{3}} |\dots\rangle |12\rangle |12\rangle |12\rangle |a_+\rangle |a_+\rangle \dots |a_+\rangle |a_-\rangle |a_-\rangle \dots |a_-\rangle \\
 + & \frac{\eta}{\sqrt{3}} |\dots\rangle |13\rangle |13\rangle |13\rangle |b_+\rangle |b_+\rangle \dots |b_+\rangle |b_-\rangle |b_-\rangle \dots |b_-\rangle \\
 + & \frac{\theta}{\sqrt{3}} |\dots\rangle |23\rangle |23\rangle |23\rangle |c_+\rangle |c_+\rangle \dots |c_+\rangle |c_-\rangle |c_-\rangle \dots |c_-\rangle
 \end{aligned} \tag{5.16}$$

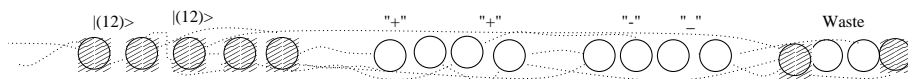
The ‘minus-one-half’ state is really ugly, and contains terms like (with ϕ and $\hat{\phi}$ some unknown and uninteresting values):

$$\zeta |12\rangle \left(|13\rangle |13\rangle + e^{i\phi} |23\rangle |23\rangle \right) |\dots\rangle \quad \eta |13\rangle \left(|12\rangle |12\rangle + e^{i\hat{\phi}} |23\rangle |23\rangle \right) |\dots\rangle \quad \dots\dots$$

which are some sort of ‘cross-terms’, because $|12\rangle$ is not entangled with another $|12\rangle$ but with the other two of the basis-vectors, $|13\rangle$ and $|23\rangle$.

Just like in the previous section, we move the to eigenvalue $-\frac{1}{2}$ associated particles to the charge-dump. After repeating this often, the normalized total internal state becomes (pretty entangled):

$$\begin{aligned}
 |\psi\rangle = & \zeta |\dots\rangle |12\rangle |12\rangle |12\rangle \dots |12\rangle |a_+\rangle |a_+\rangle \dots |a_+\rangle |a_-\rangle |a_-\rangle \dots |a_-\rangle |waste\rangle \\
 + & \eta |\dots\rangle |13\rangle |13\rangle |13\rangle \dots |13\rangle |b_+\rangle |b_+\rangle \dots |b_+\rangle |b_-\rangle |b_-\rangle \dots |b_-\rangle |waste\rangle \\
 + & \theta |\dots\rangle |23\rangle |23\rangle |23\rangle \dots |23\rangle |c_+\rangle |c_+\rangle \dots |c_+\rangle |c_-\rangle |c_-\rangle \dots |c_-\rangle |waste\rangle
 \end{aligned} \tag{5.17}$$

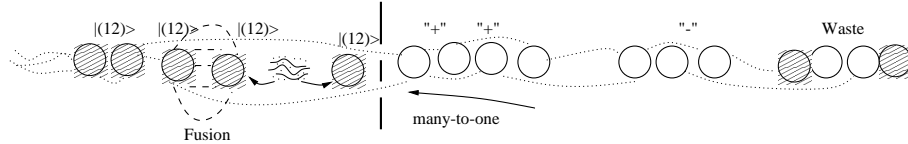


Step 3: still nothing

We could again try to use the +1 charges to scatter of a $|123\rangle$ particle from the vacuum. But also in this case this will give one possible eigenvalue ($-\frac{1}{2}$) and thus no real measurement. We totally skip this step.

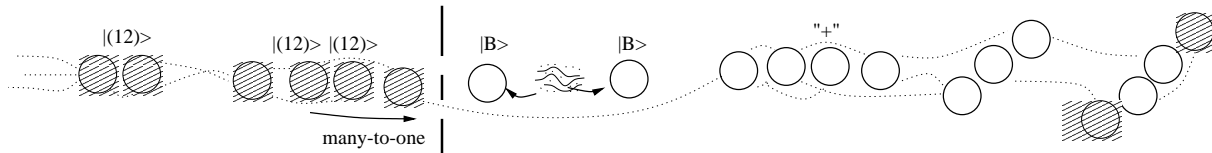
Step 4: fusion results also remain the same

If we consider again to fuse a $|12\rangle$ particle, which forms a pair with another that is used in a ‘many-to-one’, with an already present $|12\rangle$ particle, then we will find the same probabilities as in the previous section. So, also with an arbitrary initial state, the fusion probabilities follow the outcome of the many-to-one experiment of step 2.



Step 5: many-to-one with fluxes

This experiment creates, not to our surprise, again plus and minus eigenpatterns and ditto charges, although this result is obtained after explicit calculation by hand.



By now, we have probably illustrated enough the fact that the outcomes of measurements do not depend on the initially chosen internal state of the first particle $|12\rangle$. They are, of course, the same if we start with $|13\rangle$ as the initial internal state, but the measurements are also the same if we pull the first $|12\rangle$ in a pair from the vacuum.

Let us now search for a (mathematically supported) reason to explain the peculiar similarity between the outcomes of the experiments with different, even arbitrary, initial conditions. We will find an answer to this question in global transformations of the quantum double.

5.4 Global $D(S_3)$ transformations explain similarity

It seems rather peculiar that the results of sections 5.2 and 5.3 are exactly the same. That is, the interference patterns we would find are the same; their internal states are not. The state of the first is completely unentangled, the other more entangled than one can ever get, in a way of speaking.

$$|\psi_1\rangle = |13\rangle|13\rangle \dots |13\rangle |b_+\rangle|b_+\rangle \dots |b_+\rangle |b_-\rangle|b_-\rangle \dots |b_-\rangle |charge - waste\rangle \quad (5.18)$$

$$|\psi_2\rangle = \begin{aligned} & \zeta | \dots \rangle |12\rangle |12\rangle |12\rangle \dots |12\rangle |a_+\rangle|a_+\rangle \dots |a_+\rangle |a_-\rangle|a_-\rangle \dots |a_-\rangle |waste\rangle \\ & + \eta | \dots \rangle |13\rangle |13\rangle |13\rangle \dots |13\rangle |b_+\rangle|b_+\rangle \dots |b_+\rangle |b_-\rangle|b_-\rangle \dots |b_-\rangle |waste\rangle \\ & + \theta | \dots \rangle |23\rangle |23\rangle |23\rangle \dots |23\rangle |c_+\rangle|c_+\rangle \dots |c_+\rangle |c_-\rangle|c_-\rangle \dots |c_-\rangle |waste\rangle \end{aligned} \quad (5.19)$$

And the only difference at the beginning was in the internal state of one particle of type $|(12)\rangle$:

$$|\psi_{\text{initial } 1}\rangle = |13\rangle \quad |\psi_{\text{initial } 2}\rangle = \frac{1}{\sqrt{3}} [|12\rangle + |13\rangle + |23\rangle] \quad (5.20)$$

if we take $\zeta = \eta = \theta = \frac{1}{\sqrt{3}}$ for simplicity.

We can relate these two initial states to each other by some unitary transformation. But there is another transformation that turns $|\psi_{\text{initial } 1}\rangle$ into $|\psi_{\text{initial } 2}\rangle$. This transformation is:

$$\begin{aligned} \Pi(\bar{g}) \quad \bar{g} \in D(S_3) \quad \bar{g} &= \frac{1}{\sqrt{3}}(13) + \frac{1}{\sqrt{3}}(12) + \frac{1}{\sqrt{3}}(23) \quad (12), (13), (23) \in S_3 \quad (5.21) \\ \Pi(\bar{g})|13\rangle &= \frac{1}{\sqrt{3}} [|12\rangle + |13\rangle + |23\rangle] \end{aligned}$$

When doing a residual global gauge transformation, one uses $\Pi(g)$ where $g \in S_3$ is an *element* of the discrete *group*. Here, we take a linear combination of elements of the group, which of course are contained in $D(S_3)$.

This transformation $\Pi(\bar{g})$ is not unitary. As a matrix it has the form:

$$\Pi(\bar{g}) = \frac{1}{\sqrt{3}} \begin{pmatrix} 1 & 1 & 1 \\ 1 & 1 & 1 \\ 1 & 1 & 1 \end{pmatrix} \quad \bar{g} \text{ fixed as in (5.21)}$$

Nevertheless, we assume for now that $\Pi(\bar{g})$ is some sort of allowed global transformation. Let this global transformation now work on the state $|13\rangle|b_+\rangle|b_+\rangle$:

$$\bar{g} : \quad |13\rangle|b_+\rangle|b_+\rangle \rightarrow (\Pi \otimes \Pi \otimes \Pi) ((\Delta \otimes \mathbf{1})\Delta(\bar{g})|13\rangle|b_+\rangle|b_+\rangle) \quad (5.22)$$

$$\Delta(\bar{g}) = \frac{1}{\sqrt{3}}(13) \otimes (13) + \frac{1}{\sqrt{3}}(12) \otimes (12) + \frac{1}{\sqrt{3}}(23) \otimes (23)$$

$$(\Delta \otimes \mathbf{1})\Delta(\bar{g}) = \frac{1}{\sqrt{3}}(13) \otimes (13) \otimes (13) + \frac{1}{\sqrt{3}}(12) \otimes (12) \otimes (12) + \frac{1}{\sqrt{3}}(23) \otimes (23) \otimes (23)$$

$$\begin{aligned} \bar{g} : \quad |13\rangle|b_+\rangle|b_+\rangle \rightarrow & + \frac{1}{\sqrt{3}}|13\rangle|b_+\rangle|b_+\rangle \\ & + \frac{1}{\sqrt{3}}|12\rangle|a_+\rangle|a_+\rangle \\ & + \frac{1}{\sqrt{3}}|23\rangle|c_+\rangle|c_+\rangle \end{aligned} \quad (5.23)$$

This means \bar{g} is a global transformation and it transforms $|\psi_1\rangle$ of (5.18) into $|\psi_2\rangle$ of (5.19), with proper adjustments for ζ, η, θ of course. This transformation is linear, but it has no inverse, since \bar{g} has no inverse in the algebra. Since all group-like elements of $D(H)$ act on the vacuum as the identity, this also means that the global \bar{g} transformation leaves the vacuum intact, up to a constant factor:

$$\Pi(\bar{g})|\mathbf{1}\rangle = \frac{3}{\sqrt{3}}|\mathbf{1}\rangle \quad (5.24)$$

All elements of $D(H)$ commute with all \mathcal{R}^2 , especially group-like-elements like \bar{g} ; therefore the action of \bar{g} also commutes with all \mathcal{R}^2 . All measurements with one-to-one and many-to-one experiments depend only on expectation values of \mathcal{R}^2 and are thus invariant under the action of \bar{g} .

So, we found a way to transform a simple problem, i.e. experiments with unentangled particles, into a more complex problem, i.e. experiments with initially entangled particles. The simple problem we can solve using techniques as described in chapter 3, using the U -matrix for instance. The complex problem cannot be handled by these techniques, but the outcomes are the same as that of the simple problem. The corresponding total system's internal state of the more complex problem can at any time be calculated after the global transformation under \bar{g} .

5.5 A similar ordering with the flux $|{(123)}\rangle$

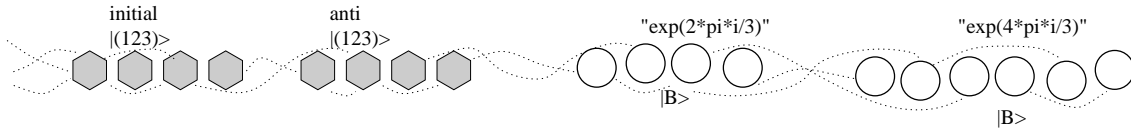
The sequence of experiments as described in section 5.3 is some kind of ordering process, in which we make piles of particles with equal internal states, i.e. outcomes of experiments are the same for these particles. We are not restricted to the use of particles of type $|{(12)}\rangle$ in this ordering process. There is also a flux $|{(123)}\rangle$ in the spectrum of $D(S_3)$, on which we can base our ordering.

The flux $|{(123)}\rangle$ has a two-dimensional internal space and has trivial braiding with other $|{(123)}\rangle$ particles independent of internal states. If we start with an initial state:

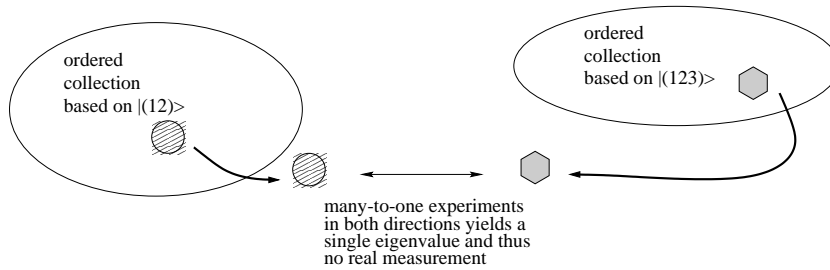
$$\psi = \alpha|\dots\rangle|123\rangle + \beta|\dots\rangle|132\rangle \quad |\alpha|^2 + |\beta|^2 = 1, \tag{5.25}$$

we can, after doing ‘one-to-one’ and ‘many-to-one’ experiments similar to those in section 5.3, make a collection of particles ordered on outcomes of measurement. This collection exists out of: initial fluxes of type $|{(123)}\rangle$, ‘anti-fluxes’ of the same type $|{(123)}\rangle$, $e^{2\pi i/3}$ charges of type $|B\rangle$ and $e^{4\pi i/3}$ of type $|B\rangle$. The total system’s internal state is:

$$|\psi\rangle = \begin{matrix} \alpha|\dots\rangle & |123\rangle\dots|123\rangle & |132\rangle\dots|132\rangle & |B_1\rangle\dots|B_1\rangle & |B_2\rangle\dots|B_2\rangle \\ + \beta|\dots\rangle & |132\rangle\dots|132\rangle & |123\rangle\dots|123\rangle & |B_2\rangle\dots|B_2\rangle & |B_1\rangle\dots|B_1\rangle \end{matrix} \tag{5.26}$$



But, if we built collections with only particles that were pulled from the vacuum, we cannot combine this ordering based on $|{(123)}\rangle$ with the one based on the $|{(12)}\rangle$ flux of section 5.3: if we use the $e^{2\pi i/3}$ charges to do a ‘many-to-one’ on a $|{(12)}\rangle$ flux, there is but a single outcome of the experiment, just like in step 3 of sections 5.2 and 5.3. Other possible measurements also yield no particles with different internal states than the ones we already obtained.



There is, however, a way to build a collection in which there are both $|{(123)}\rangle$ and $|{(12)}\rangle$ fluxes. This ordered collection is built from (highly entangled) vacuum-pairs, but can equally well be described by unentangled particles, as we will now demonstrate.

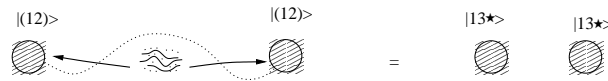
5.6 Identifying unentangled basis-states by relabeling

Let us pull a pair of $|{(12)}\rangle$ fluxes from the vacuum, which we know is in the state:

$$\frac{1}{\sqrt{3}} [|12\rangle|12\rangle + |13\rangle|13\rangle + |23\rangle|23\rangle]$$

but we label this state with:

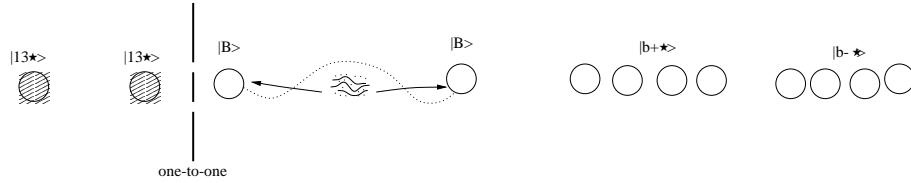
$$|13\star\rangle|13\star\rangle$$



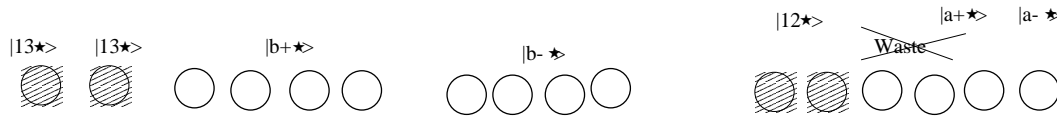
where we use the star \star to indicate that we use another ‘basis’ than the standard one, although this label is certainly not the result of a basis transformation. Basis transformations cannot change an unentangled state into an entangled one or vice versa.

We pull multiple pairs of $|B\rangle$ particles from the vacuum, in the state $|b_+\rangle|b_+\rangle + |b_-\rangle|b_-\rangle$, and perform a ‘one-to-one’ on the $|13\star\rangle$ and one of the $|B\rangle$ particles. The corresponding eigenvalues can be plus or minus one. If we find plus we call the state $|b_+\star\rangle$, and $|b_-\star\rangle$ for the minus-case. The total, unentangled state becomes:

$$|13\star\rangle |b_+\star\rangle|b_+\star\rangle \dots |b_+\star\rangle |b_-\star\rangle|b_-\star\rangle \dots |b_-\star\rangle \tag{5.27}$$



Next, we pull a new pair of $|12\rangle$ particles from the vacuum. And we perform a ‘many-to-one’ on one of them with the $|b_+\star\rangle$ -charges. If U -eigenvalue $+1$ is found (with probability $\frac{1}{3}$), we know that these $|12\rangle$ particles have internal state equal to $|13\star\rangle$. If we find eigenvalue $-\frac{1}{2}$ this internal state is not $|13\star\rangle$ but some other. This, eigenvalue $-\frac{1}{2}$, was the outcome we threw on the charge-waste-dump in sections 5.2 and 5.3. Here, we will use it further and we will call the internal state of this particle $|12\star\rangle$.



We can pull more pairs of $|12\rangle$ and $|B\rangle$ from the vacuum and do more ‘one-to-one’ and ‘many-to-one’ experiments and create a total state of the form:

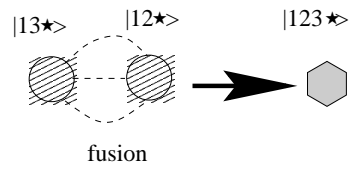
$$\begin{aligned} &|13\star\rangle \dots |13\star\rangle|b_+\star\rangle \dots |b_+\star\rangle|b_-\star\rangle \dots |b_-\star\rangle \otimes \\ &\otimes |12\star\rangle \dots |12\star\rangle|a_+\star\rangle \dots |a_+\star\rangle|a_-\star\rangle \dots |a_-\star\rangle \otimes \\ &\otimes |23\star\rangle \dots |23\star\rangle|c_+\star\rangle \dots |c_+\star\rangle|c_-\star\rangle \dots |c_-\star\rangle \end{aligned} \tag{5.28}$$

This state is *unentangled* in the relabeled basis, even though we only used particles pulled from the vacuum. In terms of the $|12\rangle, |13\rangle, |23\rangle$ basis this state is extremely entangled and almost impossible to write on one sheet of paper. But in terms of the basis $|12\star\rangle, |13\star\rangle, |23\star\rangle$ it can be written on one line (but we used three.....).

Although this relabeling is very close to the global \bar{g} transformation which transforms an unentangled state into an entangled one, as described in sections 5.4 and 5.2, 5.3, this relabeling *cannot be described* by a global $D(H)$ transformation alone⁴.

What about particles of type $|123\rangle$? We create them by merging already existing starred fluxes: If we fuse one $|13\star\rangle$ with one $|12\star\rangle$ we obtain the state: $|123\star\rangle$ of particle type $|123\rangle$. If this has been done we can create more $|123\star\rangle$ and also $|132\star\rangle$ by pulling pairs of $|123\rangle$ from the vacuum. But it is important that the first $|123\star\rangle$ is created by fusion, for only this state acts correctly with the other starred basis-vectors.

⁴This is because global $D(H)$ transformations cannot create crossterms which occurred in the ‘ugly’ charge-waste-terms of sections 5.2 and 5.3. The relabeling is however very close to a global $D(H)$ transformation.



We note already at this moment, that pairs pulled from the vacuum usually have a density matrix which is a multiple of the identity matrix and thus have the same form in any basis, including the ‘starred’ basis. Meaning for instance, that a vacuum-pair $|(12)\rangle|(12)\rangle$ also has the form:

$$\frac{1}{\sqrt{3}} [|12^*\rangle|12^*\rangle + |13^*\rangle|13^*\rangle + |23^*\rangle|23^*\rangle]$$

We will come back to this later, in chapter 7.

CHAPTER 6

QUBITS, GATES AND MEASUREMENTS WITH $D(H)$

There is but one reason why this chapter, of such modest size, should stand on its own and not merely figure as a section somewhere else. For in here, we make a start with unifying the contents of all previous chapters: Quantum computation, double-slit experiments and discrete gauge theories. With non-abelian anyons emerging from $D(H)$ -symmetries we want to construct qubits, gates on those qubits and measurements of those qubits. Although this subject is crucial to quantum computation with non-abelian anyons, our main efforts have not been concentrated on this aspect. It is certainly a non-trivial subject, that deserves an in depth analysis on its own.

In section 6.1 we construct a qubit with $D(S_3)$ -particles from a pair of fluxes of which the total flux vanishes. These qubits can be measured on the standard basis. We construct a *Not*-gate in section 6.2. If we work in a ‘re-labeled’ basis, we can create two superpositions of $|0\rangle$ and $|1\rangle$, as shown in section 6.3. This is all that can be achieved with the particular content of $D(S_3)$. So, for this example the resulting set (of gates, measurements and qubits) is certainly not a universal set, but it is all we have been able to investigate in detail up to this moment. From this exercise it does become clear however, that much more can be achieved for larger groups.

We continue in section 6.4 by giving an example of how one should not mix definitions of qubits and gates. In section 6.5 we state that gates, qubits and measurements with $D(H)$ -particles, with $H \neq S_3$, should at least be compatible with each other; but we can say little more about a general $D(H)$ -theory at least as universal sets are concerned.

6.1 Fluxless pairs as measurable qubits

As suggested by Preskill [10], it might be clever to work with pairs of fluxes of which the total flux vanishes¹. A pair $|13\rangle \otimes |13\rangle$, or $|123\rangle|132\rangle$ (where we dropped the ‘ \otimes ’), or $\alpha|123\rangle|132\rangle + \beta|132\rangle|123\rangle$ are all good examples, as are the pairs which we pull from the vacuum.

If we make the following identifications:

$$|123\rangle|132\rangle \equiv |0\rangle \quad |132\rangle|123\rangle \equiv |1\rangle, \quad (6.1)$$

¹Fluxless pairs are nice, because as a total they behave as charges; charges do not influence (do not interact with) each other when they are moved around (exchanged) in the two-dimensional setup. Working with charges relieves us of the job to keep track of every particle and how it affects and is affected by the other particles.

then we may consider this as a qubit, because the internal state of flux-less pairs of two $|123\rangle$ particles is two dimensional². Since the two fluxes combined have zero flux, if we call one of them ‘flux’ the other may be called ‘anti-flux’.

We can measure such a qubit, with arbitrary³ state $\alpha|0\rangle + \beta|1\rangle$, by performing a many-to-one experiment with for instance $|B\rangle$ charges that were taken from the pile labeled by $e^{2\pi i/3}$ (as in section 5.5). This experiment uses only one of the pairs out of which the qubits is made, but projects the qubit on either $|0\rangle$ or $|1\rangle$, with the proper probability.

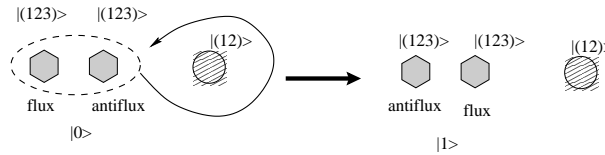
6.2 The *Not*-gate

We can perform an operation on these qubits, by doing an \mathcal{R}^2 -operation with an arbitrary $|12\rangle$ -particle.

The result is:

$$\mathcal{R}^2(|0\rangle|12\rangle) = \mathcal{R}^2(|1\rangle|12\rangle) \tag{6.2}$$

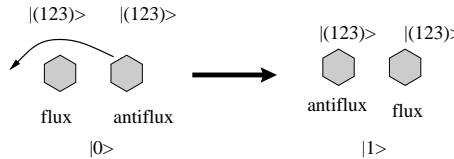
$$\mathcal{R}^2(|1\rangle|12\rangle) = \mathcal{R}^2(|0\rangle|12\rangle) \tag{6.3}$$



So this is a linear operation, because \mathcal{R}^2 is linear, that interchanges $|0\rangle$ and $|1\rangle$. This operation is also called the *Not*-gate. So, when the *Not*-gate operates on a linear combination of $|0\rangle$ and $|1\rangle$, then:

$$Not(\alpha|0\rangle + \beta|1\rangle) = \alpha|1\rangle + \beta|0\rangle \tag{6.4}$$

But there is another way to achieve the same thing: by just interchanging the flux and its anti-flux, in either direction.



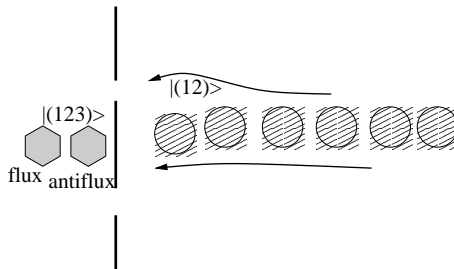
The *Not*-gate is nevertheless a real, and our first, 1-qubit-gate, although the *Not*-gate does not gain us anything, in the sense that it does not create new states that we cannot create otherwise.

²The flux-less pair of two $|123\rangle$ particles is three dimensional and thus not directly useful to function as a qubit.

³At this point we do not have the ability to create arbitrary states, we can only prepare states with α and β equal to 0 or 1.

6.3 Creating combinations of $|0\rangle$ and $|1\rangle$ in the relabeled basis

But what if we put a pair, a qubit, behind the double slit and perform a ‘many-to-one’ experiment with many $|1(2)\rangle$ fluxes?



The associated U -matrix has two distinct eigenvalues ± 1 . Then we can ‘make’, apart from $|0\rangle$ and $|1\rangle$ also the following superpositions:

$$\frac{1}{\sqrt{2}} [|0\rangle + |1\rangle] \quad \frac{1}{\sqrt{2}} [|0\rangle - |1\rangle] \tag{6.5}$$

Where we can discriminate between the two by the observed interference pattern: $f_1(\theta)$ for the ‘+’-result and $f_{-1}(\theta)$ for the minus-result. The probabilities for either eigenvalue *do* however depend on the internal states of the particles.

Furthermore, this many-to-one requires both a $|1(2)\rangle$ and a $|1(23)\rangle$ flux. This is not yet a problem, because we can create two separate collections, one based on a pair of $|1(2)\rangle$ particles drawn from the vacuum and another collection based on a $|1(23)\rangle$ -vacuum-pair. We will use $|1(2)\rangle$ particles from the first collection and a $|1(23)\rangle$ particle from the second. But we will *always* find $f_1(\theta)$ as the interference pattern. This means that we can actually create only qubits with internal states $|0\rangle$ or $|1\rangle$, which is not really interesting.

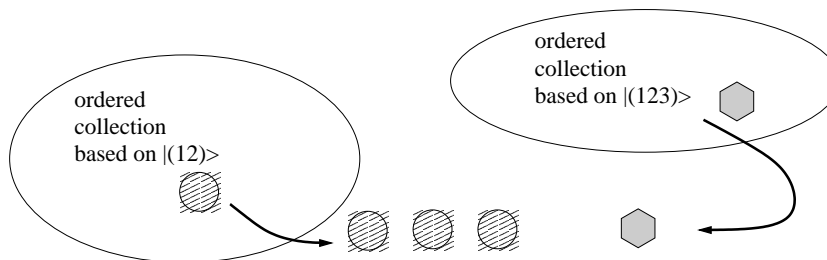


Figure 6.1: If the $|1(2)\rangle$ and the $|1(23)\rangle$ come from two different collections, but both created from the vacuum, then no new qubit-state can be created.

But as showed explicitly in chapter 5, we could order our particles in another way, and after relabeling to the ‘starred’ basis obtain basis-states for both $|1(23)\rangle$ and $|1(2)\rangle$ types of particles. So, let us continue in the relabeled, ‘starred’, basis.

We now identify a qubit as the flux-less combinations of two $|1(23)\rangle$ particles in the starred basis:

$$|0\rangle \equiv |123\star\rangle|132\star\rangle \quad |1\rangle \equiv |132\star\rangle|123\star\rangle \tag{6.6}$$

The *Not*-gate stays the same: an \mathcal{R}^2 -operator with any particle of type $|1(2)\rangle$ and the qubit or just an exchange of the two fluxes that form the qubit; both change $|0\rangle$ into $|1\rangle$ and vice versa.

Let us now do the ‘many-to-one’ with these states with many of the $|13\star\rangle$ and the pair $|123\star\rangle|132\star\rangle = |0\rangle$. With this experiment, the two plus/minus states from (6.5), which are additional states, *can now* be observed, with equal probability of $\frac{1}{2}$.

Note that these states were created by measurements, not by unitary transformation. Apart from the *Not*-gate, there is no other possible transformation in the scala of $D(S_3)$ -operations to operate on these qubits.

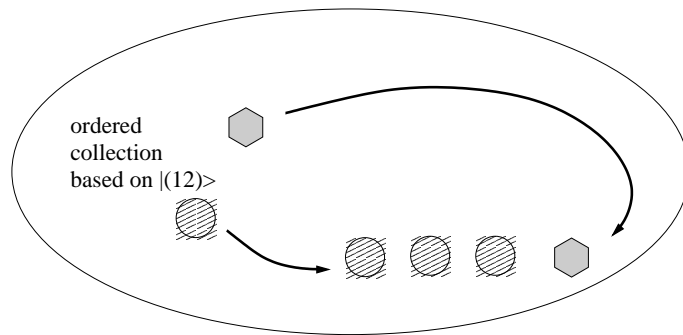


Figure 6.2: In the relabeled basis, all particles are aligned to one initial particle that may have been created from the vacuum. The plus/minus qubit combinations from (6.5) can be obtained in this setup.

6.4 Example of a suggestive mistake

We will now give an example of how one can make errors in defining gates, qubits, etc., which shows the subtlety of the subject we are dealing with. The example we use here continues using fluxless pairs of particles of type $|(123)\rangle$ as a qubit. A basis for the internal state of such a pair is $\{|123\rangle|132\rangle, |132\rangle|123\rangle\}$. We still use these basisvectors as qubit-basisvectors $|0\rangle$ and $|1\rangle$, but we write them as a primed qubit-basis: $\{|0'\rangle, |1'\rangle\}$.

We can measure the state of the qubit in this primed standard-basis by performing a many-to-one experiment with an appropriate $|B\rangle$ charge on *one* of the members of the pair. Furthermore, we know⁴ that in this particular basis we have the ability to make from a state of one qubit $\alpha|0'\rangle + \beta|1'\rangle$ a state of two qubits of the form: $\alpha|0'\rangle|0'\rangle + \beta|1'\rangle|1'\rangle$.

Let us now consider another choice of basis for these qubits and define the qubits 0 and 1 in the hat basis by $|\hat{0}\rangle = (|0'\rangle + |1'\rangle)/\sqrt{2}$, $|\hat{1}\rangle = (|0'\rangle - |1'\rangle)/\sqrt{2}$. We can measure the state of the qubit in the hat basis $\{|\hat{0}\rangle, |\hat{1}\rangle\}$ by doing a many-to-one experiment with $|(12)\rangle$ fluxes and *both* particles that form the fluxless pair. Furthermore, in the hat basis, if we have two pairs, i.e. two qubits, we can consider this as a single qubit state under the following identifications:

$$|\hat{0}\rangle|\hat{0}\rangle \simeq |\hat{0}\rangle \quad |\hat{0}\rangle|\hat{1}\rangle \simeq |\hat{1}\rangle \quad |\hat{1}\rangle|\hat{0}\rangle \simeq |\hat{1}\rangle \quad |\hat{1}\rangle|\hat{1}\rangle \simeq |\hat{0}\rangle \quad , \quad (6.7)$$

so this is some kind of merging⁵ process.

If we would mix up these two bases, and both call them $\{|0\rangle, |1\rangle\}$ by dropping the hat and the prime, we would think we could perform a controlled not. For let there be two unknown qubits,

⁴We know this from thought-experiments that are similar to the examples in chapter 5. Here, we will not show or prove this explicitly.

⁵This ‘merging’ might be understood as some kind of fusion process of the two pairs. However, the merge-identifications in the ‘hat’-basis do not depend on the kind of fusion, as the measurement of the qubit in the ‘hat’-basis uses the whole pair (or pairs) between the double slit, and not a single particle.

$\alpha|0\rangle + \beta|1\rangle$ and $\gamma|0\rangle + \delta|1\rangle$, then their combined state becomes:

$$\begin{aligned} \alpha|0\rangle + \beta|1\rangle \otimes \gamma|0\rangle + \delta|1\rangle &= \alpha\gamma|00\rangle \\ &+ \beta\gamma|10\rangle \\ &+ \alpha\delta|01\rangle \\ &+ \beta\delta|11\rangle \end{aligned} \tag{6.8}$$

Now, we start with the same two qubits; from the first qubit, we make a two-qubit state:

$$\begin{aligned} \alpha|0\rangle + \beta|1\rangle \otimes \gamma|0\rangle + \delta|1\rangle &\longrightarrow \alpha|00\rangle + \beta|11\rangle \otimes \gamma|0\rangle + \delta|1\rangle, \end{aligned} \tag{6.9}$$

and then we merge the second and third qubit:

$$\begin{aligned} \alpha|00\rangle + \beta|11\rangle \otimes \gamma|0\rangle + \delta|1\rangle &\longrightarrow \alpha\gamma|00\rangle \\ &+ \beta\gamma|11\rangle \\ &+ \alpha\delta|01\rangle \\ &+ \beta\delta|10\rangle \end{aligned} \tag{6.10}$$

If we compare (6.8) and (6.10) we see that the latter is equal to the first state to which a *Controlled Not*⁶-gate has been applied, with the first qubit as the control-qubit.

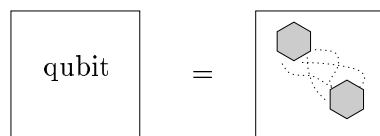
But this is not possible, since we mixed operations that are valid in only one particular basis. For example, although two pairs, and thus two qubits, both in the state $|\hat{0}\rangle$ may be considered as a single qubit in state $|\hat{0}\rangle$, this latter state is not equal to $(|0'\rangle + |1'\rangle)/\sqrt{2}$. For this qubit exists out of four $|(123)\rangle$ particles and such a state is not measurable in the basis $\{|0'\rangle, |1'\rangle\}$. Measurement in the basis $\{|0'\rangle, |1'\rangle\}$ can be done with one member of a pair, not with one member of four particles and certainly not with two members of two pairs.

We hope that the example in this section has been an instructive one but also sufficient warning.

6.5 Constructing compatible qubits, gates and measurements is non-trivial

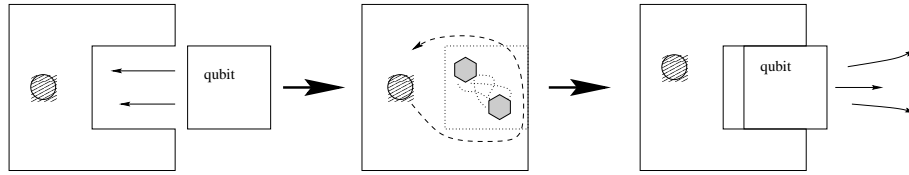
If we want to do quantum computation with non-abelian anyons, we need qubits, gates and measurements as we explained in chapter 1. What we have shown is that non-abelian anyons are governed by the quantum double $D(H)$; that particles are described by $D(H)$ -irreps, that internal states can be changed by exchanging particles through the operators \mathcal{R} and \mathcal{R}^{-1} , and that the internal state can be measured through double slit interference experiments. Furthermore we have described a way of creating particles with a known internal state by the ordering process (which will be described in more detail in section 7.6). The question remains, how to turn these non-abelian anyons into a quantum computer, because there seems to be no one to one correspondence.

Most likely, each qubit, gate and measurements will be a *fixed* combination of some particles and actions with these particles. Qubits, gates and measurements will then be some sort of higher-level objects or boxes, where the boxes are made of the non-abelian anyons and \mathcal{R} operations and measurements. For example let the box labeled by ‘qubit’ be made of a fluxless pair of particles of type $|(123)\rangle$:



⁶The ‘Controlled Not’ is discussed in chapter 1.

A gate is a box that operates on a qubit box and returns a qubit box. We could graphically represent the *Not*-gate of the previous example of section 6.2 and its operation on a qubit as follows:



What is really important in such a framework is that *all boxes have to be compatible*. If some box returns a qubit, this qubit should behave as a qubit for all other boxes. In the example of the previous section, 6.4, the merging of two qubits into one in the hat-basis was obviously not compatible with the measurement of a qubit in the prime-basis.

6.6 Does $D(H)$ become universal for some H ?

Still unanswered, at least in this thesis, is if there exists a finite group H , for which the particles in the $D(H)$ -spectrum supply a universal set with which quantum computation is possible. For $H = S_3$, which is a very small group, we never expected to find a universal set. It is reasonable to assume that for larger groups, more gates can be constructed, and probably also more types of measurements. Whether the set of qubits, gates and measurements will become universal for sufficiently large H is not known.

Of course, Kitaev and Preskill have claimed that the groups S_5 and A_5 allow the construction of a universal set. But their initial assumptions, especially concerning the ability to measure the internal state of particles, seem different from ours⁷, and may thus not be directly applicable to our setup; This, however, does not rule out that their results are correct.

It will be an entirely different story if there exists a global analogue of the Aharonov-Bohm effect. If that is the case, then the internal states of the non-abelian anyons are measurable for sure. We can then skip the whole problem of initial states or how to measure states and only concern ourselves with gate construction. But as for now, a local gauge description is all we have.

⁷Mostly due to the fact that both Kitaev and Preskill refer to unpublished work; details concerning the underpinning of their claims is therefore hard to get at.

CHAPTER 7

DO VACUUMSTATES EXHIBIT THE WHOLE STRUCTURE OF $D(H)$?

The examples with $D(S_3)$ in chapter 5 show that if we do experiments with vacuumpairs alone, non-trivial outcomes of the experiments can be obtained, even stronger: the same results are found if we begin with a particle in a specific, unentangled, internal state. But strictly, the vacuumstate is a singlet state. It is reasonable to think that a system consisting only of vacuumpairs will be restricted to some ‘substructure’ of $D(H)$, in the sense that only some facets of the full, unrestricted, quantum double $D(H)$ can be seen, perhaps even a trivial substructure. Nevertheless, the examples with $D(S_3)$ show otherwise. Furthermore, the examples show a kind of ordering process, where identical particles with equivalent internal states were put on piles.

The behaviour of non-abelian anyons in the $D(S_3)$ -examples lead us to believe that some of it should be true for general $D(H)$. But it is not completely clear yet what ‘some of it for general $D(H)$ ’ is, so we will not make a statement about ordering and behaviour of outcomes of experiments for general $D(H)$ vacuumpairs. In this chapter we will present some smaller claims; these, more simple, claims support, when they are combined, the description of the ordering process as a whole. These smaller claims are mainly concerned with the assumption that particles in a vacuumstate have a unital density matrices (this is the first claim). We have been unable to solve our claims (except one) for general $D(H)$, which turns these claims into conjectures. So, this chapter mainly consists out of conjectures for general $D(H)$ that are checked for $D(S_3)$. In that sense, this chapter should be considered as being speculative.

At the end, in section 7.7, we briefly turn to a paradox that rises in the ordering process for vacuumstates: as the non-abelian anyons are described by a local gauge theory it seems odd that we can determine their internal states. We apparently solve this paradox by stating that we do not need the description with known internal states of non-abelian anyons: physical results depend rather on the *representation-theory* of the underlying model.

Although we are not ready yet to make a solid statement about the ordering process as a whole, the conjectures of the following sections are concrete statements; we regret that we have not been able to prove them. But, there is another known theorem, which we failed to prove by ourselves. This is the fact that the exchange and monodromy operators are of finite order:

$$\mathcal{R}^m = \mathbb{1} \otimes \mathbb{1} \quad \text{for some } m \in \mathbb{N}$$

Techniques to prove this statement might also be useful to prove the conjectures in this chapter.

7.1 Vacuumstates have a unital density-matrix

In the spectrum of particles of the quantum double of a finite group H , the members of a pair drawn from the vacuum have a density matrix which is a multiple of the unit matrix $\mathbb{1}$. A pair is ‘in the vacuum state’ when, upon fusing the two particles, the vacuum channel will appear with unit probability.

For pure fluxes it is easily shown that the density matrix is equal to $\lambda\mathbb{1}$. The state $|\psi\rangle$ of the two particles, of which the first is labeled by the conjugacy class ${}^A C$, has the following form:

$$|\psi\rangle = \frac{1}{\sqrt{|{}^A C|}} \sum_{h \in {}^A C} |h\rangle |h^{-1}\rangle \quad (7.1)$$

This state $|\psi\rangle$ has all the properties of the singlet vacuum state and therefore is the vacuum state. The density matrix for both particles is $\rho = \frac{1}{|{}^A C|} \mathbb{1}$.

We could use a similar construction for pure charges to show that a vacuum-pair has $\rho = \lambda\mathbb{1}$. For dyons however, such a construction is perhaps less obvious, but always possible given an explicit finite group H . We will now try a more general way by considering the behaviour of the density matrix under the action of the quantum double $D(H)$. But let us first look at density matrices for particles labeled by irreps of a *group*, instead of a quantum group.

Let there be particles labeled by irreps of a finite group G . Furthermore there exists a ‘vacuum’ state which is invariant under the the action of the group G . This means that for a single particle labeled by irrep D , in the (pure) state $|\psi\rangle$:

$$D(g)|\psi\rangle = |\psi\rangle \quad \forall g \in G \quad (7.2)$$

The density matrix is given by $\rho = |\psi\rangle\langle\psi|$. Because the action of the group $D(g)$ leaves the state $|\psi\rangle$ invariant, it should also leave the density matrix invariant, which implies that:

$$D(g)\rho D(g)^\dagger = \rho \quad \forall g \in G, \quad (7.3)$$

since the action of $g \in G$ sandwiches ρ between $D(g)$ and its adjoint. But G is a finite group, therefore $D(g)$ can be chosen to be unitary. We multiply (7.3) from the right by $D(g)$ and obtain:

$$D(g)\rho = \rho D(g) \quad \forall g \in G \quad (7.4)$$

Now, Schur’s lemma tells us that ρ is a multiple of the unit matrix, because $D(g)$ is an irreducible representation of the group G :

$$\rho = \lambda\mathbb{1} \quad (\text{Tr}\rho = 1 \Rightarrow \lambda = 1/\dim D) \quad (7.5)$$

The density matrix has this form also, if there is more than one particle. With two particles, one labeled by irrep D^A , the other by D^B , the vacuum state $|\psi\rangle$ is invariant under every g in G , which operates as the tensor product of the two irreps:

$$D^A(g) \otimes D^B(g)|\psi\rangle = |\psi\rangle \quad \forall g \in G \quad (7.6)$$

The density matrix ρ_A for the first particle is given by:

$$\rho_A = \text{Tr}_B |\psi\rangle\langle\psi| \quad (7.7)$$

Because the trace has the cyclic property, ρ_A changes in the same way under the action of G as in the case of the single particle:

$$\rho_A \xrightarrow{g} \text{Tr}_B D^A(g) \otimes D^B(g) |\psi\rangle\langle\psi| D^A(g)^\dagger \otimes D^B(g)^\dagger \quad (7.8)$$

$$= \text{Tr}_B D^A(g) \otimes [D^B(g)^\dagger D^B(g)] |\psi\rangle\langle\psi| D^A(g)^\dagger \quad (7.9)$$

$$= \text{Tr}_B D^A(g) |\psi\rangle\langle\psi| D^A(g)^\dagger \quad (7.10)$$

$$= D^A(g) \rho_A D^A(g)^\dagger \quad (7.11)$$

Because of Schur's lemma, if ρ_A is invariant under the action of G , it should be a multiple of the unit matrix.

Now for the quantum group $D(H)$. If a particle in the spectrum of $D(H)$ is labeled by irrep Π_α^A , and this is a vacuum state $|\psi\rangle$, does this mean that for the density matrix ρ :

$$\rho \stackrel{?}{=} \Pi_\alpha^A(P_h g) \rho \Pi_\alpha^A(P_h g)^\dagger \quad \forall P_h g \in D(H) \quad (7.12)$$

and does this imply that $\rho = \lambda \mathbb{1}$? Does Schur's lemma exist for algebra irreps? At first sight no positive answer to these three questions can be given. As for (7.12), there are many elements $P_h g$ for which $\Pi_\alpha^A(P_h g) = 0$ and thus the equation fails. But let us examine this problem closer.

If a system $|\psi\rangle$ of multiple particles is the vacuum state, then the action of the quantum double on this multi-particle state is:

$$P_h g: |\psi\rangle \mapsto |\psi'\rangle = \Pi_{\mathbb{1}}^e(P_h g) |\psi\rangle \quad (7.13)$$

$$\Pi_{\mathbb{1}}^e(P_h g) = \begin{cases} 1 & \text{if } h = e \\ 0 & \text{if } h \neq e \end{cases} \quad (7.14)$$

Let us call one particle A and label the other particles by B (so multiple particles are labeled by a single B). The density matrix ρ_A for particle A is:

$$\rho_A = \text{Tr}_B |\psi\rangle\langle\psi| \quad (7.15)$$

Let $P_h g$ operate on ρ_A

$$P_h g: \rho_A \mapsto \rho_A' = \text{Tr}_B |\psi'\rangle\langle\psi'| = \begin{cases} \rho_A & \text{if } h = e \\ 0 & \text{if } h \neq e \end{cases} \quad (7.16)$$

We can sum over h :

$$\sum_h P_h g: \rho_A \mapsto \rho_A' = \text{Tr}_B \sum_h |\psi'\rangle\langle\psi'| = \rho_A \quad (7.17)$$

But since $\sum_h P_h g = g$, $g \in H$ this is the action of the finite group H itself, by the induced representation $T^A(g)$:

$$\rho_A' = \text{Tr}_B \sum_{h,h'} (\Pi^A \otimes \Pi^B)(\Delta(P_h g)) |\psi\rangle\langle\psi| [(\Pi^A \otimes \Pi^B)(\Delta(P_{h'} g))]^\dagger \quad (7.18)$$

$$= \text{Tr}_B T^A(g) \otimes T^B(g) |\psi\rangle\langle\psi| T^A(g)^\dagger \otimes T^B(g)^\dagger \quad (7.19)$$

$$= T^A(g) \rho_A T^A(g)^\dagger \quad (7.20)$$

$$= \rho_A \quad (7.21)$$

However, since $T^A(g)$ is in general reducible we cannot claim ρ_A as a multiple of the unit matrix. We can, of course, decompose¹ $T^A(g)$ in irreps $D(g)$ of the group H . If we look at ρ_A in this particular basis, we find ρ_A to be block-unital:

$$\rho_A = \begin{pmatrix} \lambda_1 \mathbb{1}_1 & 0 & \cdots & 0 \\ 0 & \lambda_2 \mathbb{1}_2 & \cdots & 0 \\ \vdots & \vdots & \ddots & 0 \\ 0 & 0 & 0 & \lambda_n \mathbb{1}_n \end{pmatrix} \quad T^A(g) = D_1(g) \oplus D_2(g) \oplus \cdots \oplus D_n(g) \quad (7.22)$$

We obtained this result by applying both the Schur lemmas². The $\lambda_i \in [0, 1]$ have to obey the unit trace of a density matrix:

$$\sum_i \lambda_i \dim D_i = 1 \quad (7.23)$$

The states with density matrices like in (7.22) are invariant under a residual global gauge transformation $g \in H$, but are not necessarily vacuum states. A nice proof of the fact that pairs pulled from the vacuum have a unital density matrix still lacks, which implicitly makes this fact a conjecture.

Although we found no true proof, we did gain something. For we let B , in (7.15) and (7.18), indicate an arbitrary number of particles. This leads to the conjecture that not only vacuum pairs have a unit density matrix, but *all* particles of a multi-particle vacuum state have a density matrix equal to a multiple of $\mathbb{1}$. This is illustrated in fig. 7.1.

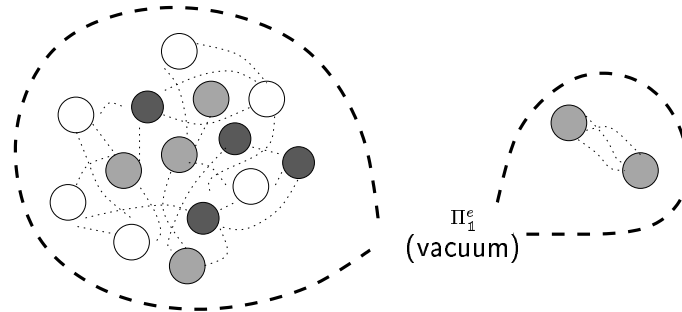


Figure 7.1: No matter how entangled particles can be with each-other, if their total system state is the vacuum state, then all these particles have a density matrix which is a multiple of the unit matrix $\mathbb{1}$. This is especially true for pairs which are pulled from the vacuum.

Let us for clarity, repeat the conjecture that we make in this section:

¹Perhaps a more proper notation for this decomposition is $T^A(g) = \bigoplus_i n_i D^i(g)$, but the notation of (7.22) is suitable enough for the moment.

²The first lemma is well known: for an irrep $D(g)$ of a group G , if $D(g)A = AD(g)$ for all $g \in G$, then the operator A is a multiple of the unit matrix. The second lemma states that, for inequivalent irreps $D(g)$ and $D'(g)$, if $BD(g) = D'(g)B$, for all $g \in G$, then the operator B is a zero operator.

Given a system with n particles, $n \geq 2$, of which the total system's state $|\psi\rangle$ can be written, with basisvectors $|i_k\rangle$ for particle k , as:

$$|\psi\rangle = \psi^{i_1 i_2 \dots i_n} |i_1\rangle \otimes |i_2\rangle \otimes \dots \otimes |i_n\rangle$$

If under global transformations $P_{hg} \in D(H)$ the total systems transforms as the vacuum:

$$P_{hg}: |\psi\rangle \mapsto \Pi_{\mathbb{1}}^e(P_{hg})|\psi\rangle,$$

then the density matrix ρ_j for each particle j is a multiple of the unit matrix:

$$\rho_j = \frac{\text{Tr}_{i_k, k \neq j} |\psi\rangle\langle\psi|}{\dim j} = \lambda_j \mathbb{1}_j \quad \forall j \quad \left(\lambda_j = \frac{1}{\dim j}\right).$$

7.2 Fusion of, or \mathcal{R}^2 on two vacuumstates yields all channels

If we use two particles, which are not entangled with each-other and both have a density matrix proportional to the unit matrix, to perform an one-to-one double slit experiment or a fusion of the two particles, all possible outcomes have equal probability. We will begin with the one-to-one experiment.

In the one-to-one double slit experiment we measure the eigenvalue $e^{i\lambda}$ of the monodromy operator \mathcal{R}^2 . We can write \mathcal{R}^2 as a sum over projection operators E_λ and eigenvalues:

$$\mathcal{R}^2 = \sum_{\lambda} e^{i\lambda} E_\lambda$$

We perform the one-to-one experiment for two particles, A and B , in a multiple-particles state labeled by $|\psi\rangle$. The probability p_λ to observe eigenvalue λ is equal to the expectation value of E_λ :

$$p_\lambda = \langle\psi|E_\lambda|\psi\rangle \tag{7.24}$$

$$= \text{Tr}(\rho_{AB} E_\lambda) \tag{7.25}$$

$$= \frac{\dim \lambda}{\dim A \dim B} \quad \text{if } \rho_{AB} = \mathbb{1}_A \otimes \mathbb{1}_B / \dim A \cdot \dim B \tag{7.26}$$

Where $\dim \lambda = \dim E_\lambda = \text{Tr} E_\lambda$. So, if ρ_{AB} is factorisable into $\rho_A \otimes \rho_B$ (A and B are unentangled) and ρ_A and ρ_B are proportional to the unit matrices, we find that each eigenvalue λ has weighed equal probability, weighed with respect to the dimension of the eigenspace of λ .

For fusion processes this, (7.26), is also true, but λ and E_λ are different now. We now indicate by λ the type of the resulting particle after fusing A and B ; usually we use C (or Π_γ^C) to indicate the observed fusion result. We construct E_λ from the *Clebsch-Gordan coefficients* $C_{\alpha i}^{\lambda \mu}$. If $\{|\alpha\rangle\}$ is a basis for the internal state of particle A , $\{|i\rangle\}$ a basis for B , and $\{|\lambda_\mu\rangle\}$ a basis for particle λ , then:

$$|\alpha\rangle|i\rangle = C_{\alpha i}^{\lambda \mu} |\lambda_\mu\rangle \quad |\lambda_\mu\rangle = C_{\lambda_\mu}^{-1 \beta j} |\beta\rangle|j\rangle \tag{7.27}$$

The projection operator E_λ which projects onto the eigenspace of λ is the product of C^{-1} and C for fixed λ :

$$E_\lambda^{\beta j}_{\alpha i} = (C_\lambda^{-1})_{\mu}^{\beta j} (C_\lambda)_{\alpha i}^{\mu} \tag{7.28}$$

The probability p_λ to observe particle λ is again evenly spread:

$$p_\lambda = \text{Tr}(\rho_{AB} E_\lambda) = \frac{\dim \lambda}{\dim A \dim B} \quad \text{if } \rho_{AB} = \mathbb{1}_A \otimes \mathbb{1}_B / \dim A \cdot \dim B \tag{7.29}$$

Since vacuum states exist out of particles with unital density matrices, this means that if we do experiments with particles drawn from the vacuum, we are not restricted to a subset of possible outcomes: even with vacuumstates, the full spectrum of experiment-outcomes for quantum double particles is observable. Let us repeat our statement:

Let the fusion product of particle (A, α) and (B, β) be given by (i.e. the Clebsch-Gordan series):

$$\Pi_\alpha^A \otimes \Pi_\beta^B = N_{\alpha\beta C}^{AB\gamma} \Pi_\gamma^C$$

The probability $p_{(C,\gamma)}$ to observe Π_γ^C (i.e. particle (C, γ)) upon fusion is given by:

$$p_{(C,\gamma)} = \text{Tr}(\rho_{AB} E_{(C,\gamma)})$$

If (A, α) and (B, β) are not entangled with each-other and both have a density matrix that is the multiple of the unit matrix, then the probability $p_{(C,\gamma)}$ is:

$$p_{(C,\gamma)} = \frac{\dim(C, \gamma)}{\dim(A, \alpha) \dim(B, \beta)} \quad \text{if } \rho_{AB} = \rho_A \otimes \rho_B \quad \rho_A = \lambda_A \mathbb{1}_A, \quad \rho_B = \lambda_B \mathbb{1}_B.$$

This is (naturally) only true if $N_{\alpha\beta C}^{AB\gamma}$ is non-zero.

7.3 Projection E_λ commutes with group-action, but not always with action of $D(H)$

Until this point, we have not considered the compatibility of experiments (fusion or double slit) with for instance residual global gauge transformations. Of course these are compatible, since \mathcal{R}^2 commutes with a residual global gauge transformation $g \in H$ and \mathcal{R}^2 is build out of E_λ : $\mathcal{R}^2 = \sum_\lambda e^{i\lambda} E_\lambda$. Given the fact that E_λ is a projection-operator and that the \mathcal{R}^2 eigenvalues are roots of unity it is not difficult to show that E_λ also commutes with every residual global gauge transformation $g \in H$.

One could also view the many-to-one double slit experiment as a large sequence of different E_λ . So, all experiments, as described in this thesis, commute with residual global gauge transformations. But what about the action of the full quantum double $D(H)$? If a multi-particle system $|\psi\rangle$ has a total has the following decomposition into $D(H)$ -irreps:

$$|\psi\rangle \simeq \bigoplus_{C,\gamma} \Pi_\gamma^C \quad P_h g: |\psi\rangle \mapsto \bigoplus_{C,\gamma} \Pi_\gamma^C (P_h g) |\psi\rangle, \tag{7.30}$$

does the local projection E_λ operator (operating on two particles) change this decomposition? The answer to this question is yes, but with a few exceptions. One of the exceptions is when the total state is a single, pure, irrep (and not a sum):

$$|\psi\rangle \simeq \Pi_\gamma^C \quad \Rightarrow \quad E_\lambda: |\psi\rangle \mapsto |\psi'\rangle \simeq \Pi_\gamma^C \tag{7.31}$$

Especially, if the total system is the vacuum state, then (local) E_λ projections leave the total state as a vacuum. In other words, we can use particles that we draw from the vacuum for all kinds of experiments while if we fuse them in the end they will with complete certainty return to the vacuum, as depicted in fig. 7.2.

Perhaps it seems almost natural that local experiments should not change the systems' total decomposition if it is pulled from the vacuum, but since there are examples of states (not

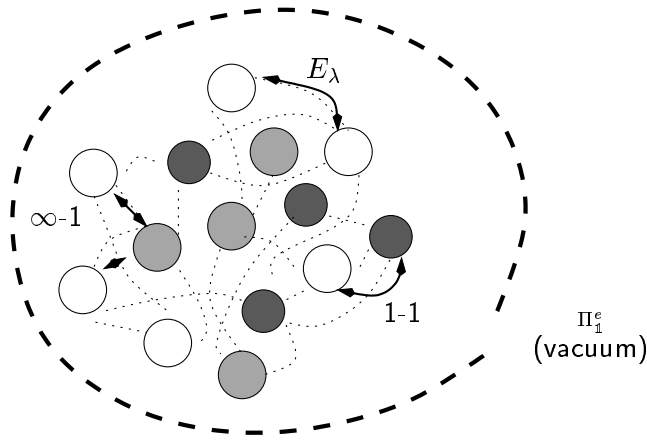


Figure 7.2: If we do experiments with particles originally drawn from the vacuum, the total multi-particle state remains in this vacuum state. We abbreviated one-to-one and many-to-one with 1-1 and $\infty-1$.

vacuum states of course) for which the decomposition does change³, this is not a trivial point. Nevertheless we also do not work out this problem any further and regard it as a conjecture, which we now repeat:

If the state $|\psi\rangle$ of a multiple particle system behaves as the vacuum:

$$P_{hg}: |\psi\rangle \mapsto \Pi_{\mathbb{1}}^e(P_{hg})|\psi\rangle$$

then a local non-zero, normalized, projection $E_{(C,\gamma)}$ on two particles in the system, which operates as follows:

$$E_{(C,\gamma)}: |i_k\rangle \otimes |i_l\rangle \mapsto \frac{E_{(C,\gamma)}|i_k\rangle \otimes |i_l\rangle}{\sqrt{\text{Tr}(\rho_{kl}E_{(C,\gamma)})}} \quad p_{(C,\gamma)} \neq 0,$$

changes the state $|\psi\rangle$ to $|\psi'\rangle$, but the new state still behaves as the vacuum:

$$E_{(C,\gamma)}|\psi\rangle = |\psi'\rangle \quad P_{hg}: |\psi'\rangle \mapsto \Pi_{\mathbb{1}}^e(P_{hg})|\psi'\rangle.$$

7.4 All channels are possible if only one particle is a vacuum-state

In section 7.2 we showed that if we use two particles with unital density matrix for a one-to-one or fusion experiment, all possible outcomes (channels) could occur with ‘equal’ probability. If only one of the two particles has a unit density matrix, then this seems also to be the case, in other words the conjecture is:

$$\rho_{AB} = \rho_A \otimes \rho_B \quad \rho_B = \frac{\mathbb{1}_B}{\dim B} \quad \Rightarrow \quad p_\lambda = \text{Tr}(E_\lambda \rho_{AB}) = \frac{\dim \lambda}{\dim A \dim B} \quad (7.32)$$

³For example in $D(S_3)$, consider the tensor product of $|13\rangle$ and $(|12\rangle + |13\rangle)/\sqrt{2}$, and the fusion- or one-to-one experiment on these two particles.

What needs to be proven is that $\text{Tr}_A(\rho_A F_\lambda) = \frac{\dim \lambda}{\dim A}$ for all ρ_A . Here F_λ is defined by:

$$F_\lambda := \text{Tr}_B(E_\lambda) \tag{7.33}$$

This F_λ is a hermitian and positive operator, it has trace $\text{Tr}_A F_\lambda = \dim \lambda$ and it is complete, in the sense that $\sum_\lambda F_\lambda = \mathbb{1}_A$. Unfortunately, these properties of F_λ are not enough to prove (7.32).

Residual global gauge transformations might be the missing link. A residual global gauge transformation leaves p_λ invariant but changes ρ_A (one can also say that after the action of $g \in H$, E_λ changed and ρ_A remained the same). Nevertheless, a closer examination is needed. This conjecture resembles the statement from section 7.2 (but that wasn't a conjecture):

Let the fusion product of particle (A, α) and (B, β) be given by (i.e. the Clebsch-Gordan series):

$$\Pi_\alpha^A \otimes \Pi_\beta^B = N_{\alpha\beta C}^{AB\gamma} \Pi_\gamma^C$$

The probability $p_{(C,\gamma)}$ to observe Π_γ^C (i.e. particle (C, γ)) upon fusion is given by:

$$p_{(C,\gamma)} = \text{Tr}(\rho_{AB} E_{(C,\gamma)})$$

If (A, α) and (B, β) are not entangled with each-other and *one* of them, we choose (B, β) , has a density matrix that is the multiple of the unit matrix, then the probability $p_{(C,\gamma)}$ is:

$$p_{(C,\gamma)} = \frac{\dim(C, \gamma)}{\dim(A, \alpha) \dim(B, \beta)} \quad \text{if } \rho_{AB} = \rho_A \otimes \rho_B, \rho_B = \lambda_B \mathbb{1}_B.$$

(If $N_{\alpha\beta C}^{AB\gamma}$ is non-zero.)

7.5 Relabeling leaves unital density-matrices invariant

We introduced a relabeling of particles in section 5.6. This relabeling is not a basistransformation because the relabeling can change unentangled states into entangled ones, which basistransformations cannot. There is however a common property: both this relabeling and basistransformations leave density matrices which are a multiple of $\mathbb{1}$ invariant.

In other words, in a setup after relabeling, one can pull again pairs from the vacuum and these pairs have a density matrix which is $\lambda \mathbb{1}$ in either basis, especially the relabeled basis.

Let us repeat the example we already gave in chapter 5, with two $|(12)\rangle$ fluxes that ere created from the vacuum. Before relabeling this pair has a state $|\psi\rangle$ given by:

$$|\psi\rangle = \frac{1}{\sqrt{3}} [|12\rangle|12\rangle + |13\rangle|13\rangle + |23\rangle|23\rangle]$$

This vacuum pair is part of a large system with state $|\Psi\rangle$, which can be factorised into $|\Psi\rangle = |\phi\rangle \otimes |\psi\rangle$. After relabeling, which relabels the $|\phi\rangle$ -part of the total system, the $|\psi\rangle$ -part becomes:

$$|\psi\rangle = \frac{1}{\sqrt{3}} [|12^\star\rangle|12^\star\rangle + |13^\star\rangle|13^\star\rangle + |23^\star\rangle|23^\star\rangle],$$

and this vacuum pair still has a unital density matrix after relabeling.

7.6 Ordering process for particles pulled from the vacuum

Let us now combine the properties of particles in the spectrum of $D(H)$ which were all drawn from the vacuum once. So, there are multiple particles and we allow for exchanges of particles by means of \mathcal{R} , \mathcal{R}^{-1} and/or \mathcal{R}^2 and furthermore experiments like many-to-one, one-to-one and fusion. At a certain moment we can schematically represent this situation as in fig. 7.3.

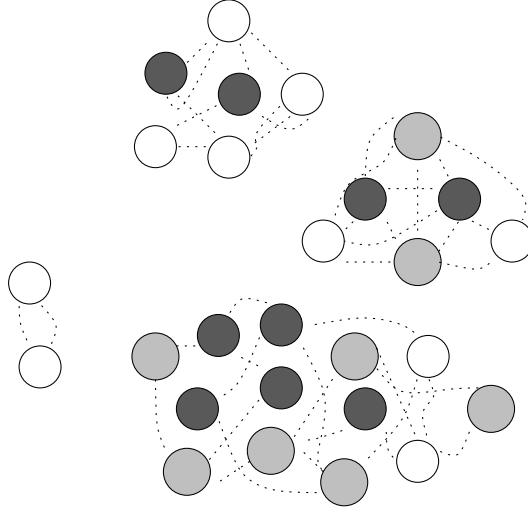


Figure 7.3: A sketch of a possible situation of a system with particles in it that were originally pulled from the vacuum but afterwards have been manipulated with, either by exchanges or by experiments.

One can always divide such a system in parts based on entanglement. Particles that are entangled with each-other are in the same part, particles that are not entangled *with each-other* reside in different parts. The total system is the tensor product of these parts, which are genuine subsystems. Each subsystem total decomposition in $D(H)$ irreps is the vacuum, see fig. 7.4.

But, as stated in section 7.1, particles in a (sub)system which behaves as a whole as the vacuum, have a density matrix ρ which is a multiple of $\mathbb{1}$. This means that for all experiments of a particle A in one subsystem with particles B from other subsystems, the combined density matrix ρ_{AB} is factorisable into $\rho_{AB} = \rho_A \otimes \rho_B$. In our setup, particle B can only come from another subsystem with the vacuum-decomposition which leaves its density matrix $\rho_B = \lambda \mathbb{1}$, and the density matrix ρ_{AB} which governs the outcomes of all experiments is:

$$\rho_{AB} = \rho_A \otimes \rho_B = \frac{1}{\dim A \dim B} \mathbb{1}_A \otimes \mathbb{1}_B \quad (7.34)$$

For the one-to-one experiment and the fusion experiment, this means that all outcomes are possible with ‘equal’ probability, as explained in section 7.2. For the many-to-one experiment the U -matrix has only one eigenvalue, or equivalently is a multiple of the unit matrix⁴, which means no extra information can be gained.

In each subsystem we can do a relabeling. This relabeling within a subsystem has the advantage that the highly entangled state describing the subsystem may be ‘converted’ to an unentangled

⁴This statement is also a conjecture. It is furthermore assumed that all B particles have $\rho_B \propto \mathbb{1}$, so the next B particle has to come from a different subsystem than the first. The matrix U is then proportional to the partial trace of the monodromy operator \mathcal{R}^2 : $U \propto \text{Tr}_B(\mathcal{R}^2) = \sum_{h,g} \Pi_\alpha^A(hP_g) \cdot M_\beta^B(P_hg)$, where $M_\beta^B = \text{Tr}_B \Pi_\beta^B$ as explained in appendix B. Perhaps some equivalent to the Schur lemma can prove $\text{Tr}_B(\mathcal{R}^2)$ proportional to $\mathbb{1}_A$.

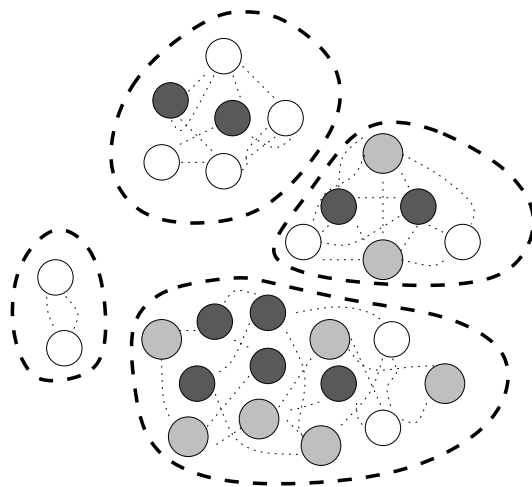


Figure 7.4: Every such system can be divided in parts or subsystem, where different subsystems are unentangled, whereas all particles in a subsystem are entangled with each-other. Each subsystem as a whole behaves as the vacuum; if all particles in a subsystem are fused the vacuum will come out with unit probability. To the outside world, each particle has a density matrix which is a multiple of the unit matrix. The outside world consists of all particles which are not in the first particle's subsystem.

state. The outcomes of experiments with only particles from within this subsystem should yield the same result in both bases, the one before and the one after relabeling. The relabeling may also cause the decomposition into $D(H)$ irreps of a single subsystem to be different from the vacuum state. But the relabeling is only valid *within* the subsystem. On the level of subsystems, each other subsystem still behaves as the vacuum! See also fig. 7.5 for an illustration.

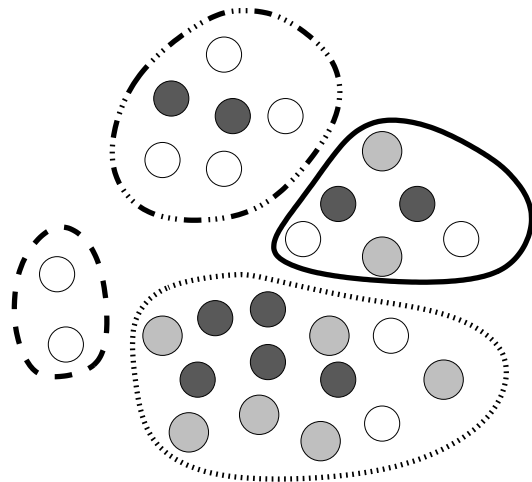


Figure 7.5: In each subsystem one can perform a relabeling. This relabeling changes the entangled state of a system into a completely unentangled state, which nevertheless gives the same results for outcomes of experiments as the previous entangled state. However, the relabeling is bound to the subsystem, and so are the experiments based on the relabeled state. Other subsystems still behave as the vacuum and its particles have a unital density matrix.

As stated in sections 7.4 and 7.5, this leaves us no problem if we concern ourselves with the

relabeling of only one subsystem. We can now also perform experiments with other subsystems that give the same result as before relabeling. Before relabeling both particles had a unital density matrix, but the outcomes of experiments are the same if only one of the two particles has a unital density matrix. After relabeling one subsystem, particles from the other subsystems still have a unital density matrix, since this is also true after relabeling.

What we are effectively doing is a process where we align or gauge⁵ all subsystems to one subsystem, as shown in fig. 7.6. The relabeling within this subsystem then, is probably based on one particle. So we are aligning all particles to one single particle. All aligned particles are unentangled with each-other in the relabeled basis, while in the basis before relabeling they are all entangled with each-other, because alignment is only possible by doing experiments with the particles. These experiments naturally entangle the particles, at least in the standard basis. Particles that have not (yet) been aligned, form a subsystem with other unaligned particles. The fusion of all unaligned particles always yields the vacuum and each unaligned particle has the unit density matrix with respect to all aligned particles.

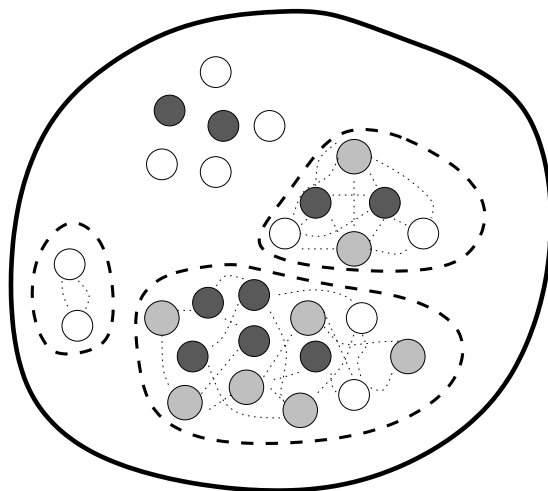
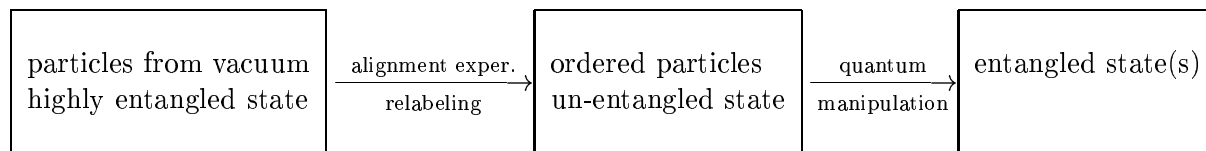


Figure 7.6: We relabel one of the subsystems, which becomes unentangled. The other subsystems are still internally entangled in the new relabeled basis. All outcomes of experiments are the same as they would be without any relabeling.

So, we can align all the different particles and label them by unentangled states. But we are not restricted to unentangled states. Certainly, if we want to do quantum computation, we like to be able to create and work with states of entangled particles. It is only in the ordering, or alignment process, that we like the particles to be unentangled, because this simplifies the description of the outcomes of manipulation with these particles. To show this schematically:



If there were an ordering (relabeling) that simplifies the outcomes of quantum manipulation with these particles, this ordering would ofcourse be preferable to the one described above which uses unentangled states.

⁵Perhaps the word 'gauge' is too confusing to be used here, although its meaning is correct.

It is important that the ‘first’ particle, to which the other particles are to be aligned, is chosen with care. For example with $H = S_3$, as in chapter 5, if we start the alignment with a flux of type $|(123)\rangle$, we can not identify after ordering a flux of type $|(12)\rangle$ with internal state $|13\rangle$. While if we start the ordering process with a flux of type $|(12)\rangle$, we can identify all fluxes $|12\rangle$, $|13\rangle$, $|23\rangle$, $|123\rangle$ and $|132\rangle$. This seems due to the fact that the members of the conjugacy class $\{(12), (13), (23)\}$ generate the whole group S_3 , while the conjugacy class $\{(123), (132)\}$ fails to do so.

When we continue the ordering process further, we discover that we are building piles of particles, where each pile consists of equivalent particles; for all experiments it does not matter which particle of a pile we use, all particles of a pile yield the same result. This means especially that many-to-one experiments use particles of one pile as the many part of the experiment! We can also add the comment that within each pile the canonical spin-statistics connection (section B.2) is restored.

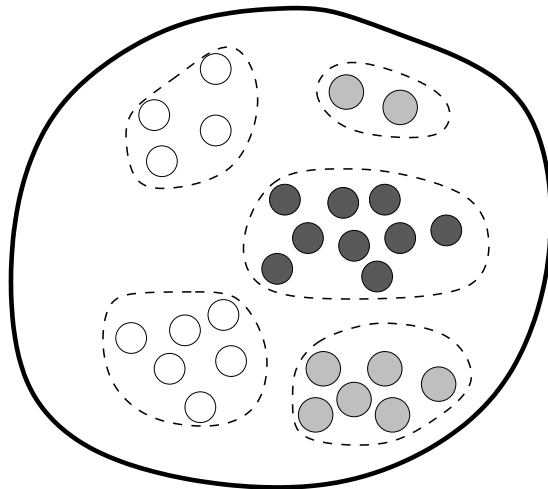


Figure 7.7: In the end of the ordering process, piles have formed of identical particles with identical internal states; these particles are truly equivalent or indistinguishable. There may be particles on other piles of identical type, but these particles have another internal state. Many-to-one experiments use particles from a single pile as the ‘many’ particles.

7.7 Representation-theory instead of description with states

At this point we have created a paradox. The discrete gauge theories are *local* gauge theories. With a local gauge, it is *impossible* to determine the internal state of a particle. Quarks are the obvious analogue: it is not possible to determine the color of a quark; neither can you pretend that one quark is red and that therefore another one should be green. One does need colors to describe the quarks consistently, but in calculations the colors are always summed out. But here, with non-abelian anyons that were created from the vacuum in a local gauge theory, we seem to be able to determine the ‘color’ of the particles after all. So, what is wrong?

Well, we do not suspect the quarks to be in error. So it is our description of the internal state of the non-abelian anyons. If we look closer, we see that we make a choice of ‘color’ for one particle, say ‘red’; but the results of the following experiments are independent of this color, a choice of ‘green’ would have yielded the same results; we could as well sum over all possible choices of colors for the particular particle. In other words, the results of experiments *can* be described by

choosing the ‘color’ of one non-abelian anyon, but this is just a coincidental side-effect of what is really important: the experiments can be described without colors by *representation theory* alone, for example through calculations with the different channels of the braid-operators or of the fusion rules; a small demonstration of where we are pointing to, is given in fig. 7.8.

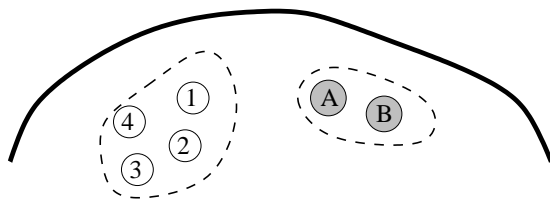


Figure 7.8: We can view the resulting system of the ordering process as some eigenstate of many exchange operators \mathcal{R} . If we indicate the total system’s state by $|\psi\rangle$, then $|\psi\rangle$ is, because of the abelian braiding, an eigenstate of \mathcal{R}_{12} , \mathcal{R}_{23} , \mathcal{R}_{34} and therefore also of \mathcal{R}_{13} and \mathcal{R}_{24}^2 , and likewise for \mathcal{R}_{AB} , \mathcal{R}_{AB}^{-1} etc. Furthermore, the expectation value for a monodromy on particle ‘1’ and particle ‘A’ is the same as that of particle ‘3’ and ‘B’ etc.: $\langle \mathcal{R}_{1A}^2 \rangle = \langle \mathcal{R}_{3B}^2 \rangle = \langle \mathcal{R}_{1B}^2 \rangle = \dots$. The state $|\psi\rangle$ is a specific state in the space of all vacuumstates. In such a way, we work only with eigenstates of braid-operators and we do not need to specify the internal states.

The quest for a universal set for quantum computation should therefore also be pursued in the context of representations, instead of a description with dyons in specific internal states. The mathematical framework will probably also be more solid with representation-theory. As we have no experience with computational problems and representation-theory, we do not know where this quest may lead: there are representations of the group H itself, representations of the quantum double group $D(H)$ and there are the (truncated) braid group representations. Together, they form a very non-trivial team. Even if all our speculations in this chapter turn out to be wrong.

CHAPTER 8

CONCLUSIONS

This chapter concludes this thesis. Some discussion already took place at the end of chapters 6 and 7, especially about the ability of non-abelian anyons for quantum computation and the role of states that were created from the vacuum. Here we will discuss two subjects that are not directly connected to the quantum computation aspect of non-abelian anyons. Afterwards, in section 8.3, we will summarize our findings, as described in this thesis.

We start in section 8.1 by describing some aspects of the many-to-one experiment. The restrictions to the many-to-one experiment, as we put them in chapter 3, may be loosened a bit, for which we saw indications in the examples with S_3 in chapter 5. This leads to the concept of a generic many-to-one experiment, part of which is a conjecture. In section 8.2 we explain why we used double slit interference experiments throughout this thesis instead of scattering interference experiments.

8.1 The generic many-to-one experiment

The many-to-one experiment as discussed in section 3.2 was solved under certain restrictions. With the example manipulations of chapter 5 it became clear that these restrictions may be relaxed a bit. We will now present the relaxed restrictions, under which we believe¹ the many-to-one experiment can always be solved and produces physically sensible output². However, under the new restrictions (in short: the ‘many’ particles need to be ‘truly indistinguishable’ particles) we have not yet found explicit answers to all valid inputs, i.e. an answer in the sense of the eigenvalue-pattern that will be observed and the associated projection. We also lay a link with the canonical spin-statistics connection.

The generic many-to-one experiment is performed with N particles of type (B, β) , or B for short, and one particle of type (A, α) , or A . These $N + 1$ particles may be part of system containing more particles. The total system should be ordered in such a way that the B particles are next to each-other; the A particle should be next to the ‘pile’ of B particles. In other words, for the total systems internal state $|\psi\rangle$:

$$|\psi\rangle \in \dots V_{\text{particles}}^{\text{other}} \otimes V_{\beta}^B \otimes \dots \otimes V_{\beta}^B \otimes \underbrace{V_{\beta}^B \otimes V_{\beta}^B \otimes V_{\beta}^B \otimes V_{\alpha}^A}_{\mathcal{R}_2} \otimes V_{\text{particles}}^{\text{other}} \dots \quad (8.1)$$

¹This believe is based upon countless explicitly worked out examples.

²There may exist *input* for the many-to-one experiment which is un-physical, but which is not rejected by the new restrictions.

We number the exchange operators \mathcal{R}_i in such a way that \mathcal{R}_1 exchanges particle A and the first adjacent particle B . The first and second B particles are exchanged by \mathcal{R}_2 , etcetera.

The N particles have to have abelian braiding, i.e. exchanging two B particles in a counter-clockwise fashion, via the \mathcal{R} -operator, should yield the spin factor $e^{2\pi s_{B,\beta}}$. This should be true for all N particles.

$$\mathcal{R}_j|\psi\rangle = e^{2\pi i s_{B,\beta}} \sigma_j|\psi\rangle = e^{2\pi i s_{B,\beta}} |\psi\rangle \quad \forall j \geq 2 \quad (j < N) \quad (8.2)$$

$$\tilde{\mathcal{R}}_j|\psi\rangle = e^{-2\pi i s_{B,\beta}} \sigma_j|\psi\rangle = e^{-2\pi i s_{B,\beta}} |\psi\rangle \quad (\mathcal{R}^\dagger = \mathcal{R}^{-1} \equiv \tilde{\mathcal{R}}) \quad (8.3)$$

The B particles should also have the same internal state, in the sense that moving a B particle around the A particle should yield the same result for all B particles. This means that the expectation value for all these operation should be equal:

$$\langle B_i \text{ around } A \rangle = \langle B_j \text{ around } A \rangle \quad \text{for all } i \text{ and } j$$

If we exchange particle B_i with particle A we should first move B_i close to particle A , perform the monodromy \mathcal{R}^2 , and then move the B particle back to the i th position, but along the same way. We indicate this operation by Γ_i :

$$\Gamma_i = \mathcal{R}_i \dots \mathcal{R}_3 \mathcal{R}_2 \mathcal{R}_1^2 \tilde{\mathcal{R}}_2 \tilde{\mathcal{R}}_3 \dots \tilde{\mathcal{R}}_i \quad (8.4)$$

In the context of partially colored braid groups, as discussed in appendix C, this operation is similar to the γ_{ij} operation.

$$\tau_i \longleftrightarrow \mathcal{R}_i \quad \gamma_{(i+1)1} \longleftrightarrow \Gamma_i$$

We can then formulate the requirement of identical internal state as follows:

$$\langle \psi | \Gamma_i | \psi \rangle = \langle \psi | \Gamma_j | \psi \rangle \quad \forall i, j \quad (1 \leq i, j \leq N) \quad (8.5)$$

We could alternatively work with the tensor-components of $|\psi\rangle$ for some basis and demand that this tensor is symmetric in all B -indices, of which there are N .

This, abelian-braiding of (8.2) together with identical expectation values of (8.5), means that all B particles are really equal or even *indistinguishable*, in the sense that even the *order* in which we use the B particles for experiments does not matter, since all expectation values are equal, for instance:

$$\langle \psi | \Gamma_2 | \psi \rangle = \langle \psi | (\tilde{\mathcal{R}}_2 \mathcal{R}_1^2 \mathcal{R}_2 | \psi \rangle = \langle \psi | \sigma_2 \mathcal{R}_1^2 \sigma_2 | \psi \rangle = \langle \psi | \mathcal{R}_1^2 | \psi \rangle = \langle \psi | \Gamma_1 | \psi \rangle, \quad (8.6)$$

but because of the abelian braiding this is independent of the exact path. We could also have defined Γ_2 by: $\Gamma_2 = \mathcal{R}_2 \mathcal{R}_1^2 \tilde{\mathcal{R}}_2$; this yields the same expectation value. In other words, it does not matter how we pick any particle from the B pile: all different paths and particles give the same result, as illustrated in fig. 8.1.

We replace \mathcal{R}_j by $e^{2\pi i s_{B,\beta}} \sigma_j$ in other expectation values also. We assume that this is allowed, but have not yet proven this. For instance, we use the following ‘equality’:

$$\langle \psi | (\mathcal{R}_1^2 \tilde{\mathcal{R}}_2 \mathcal{R}_1^2 \mathcal{R}_2 | \psi \rangle \stackrel{?}{=} \langle \psi | \mathcal{R}_1^2 \sigma_2 \mathcal{R}_1^2 \sigma_2 | \psi \rangle \quad (8.7)$$

So, the restrictions for the system’s state $|\psi\rangle$ of a generic many-to-one experiment are that the B particles should have abelian braiding and an ‘identical’ internal state to the extent that they give equal expectation values. The various ways to solve the generic many-to-one experiment can be divided in three ‘classes’ depending on the mutual entanglement:

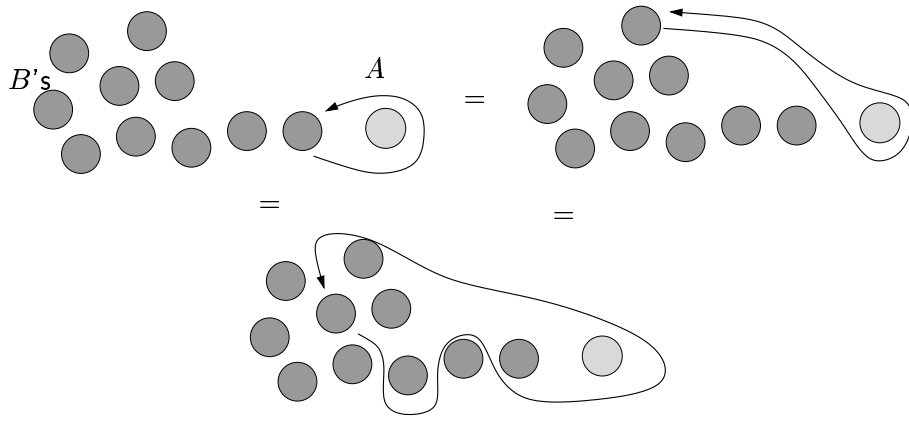


Figure 8.1: The B particles in the many-to-one experiment form a pile of truly identical, i.e. indistinguishable, particles when interacting with particle A .

- (i) **All particles are not entangled with each-other:** The many-to-one where the particles are not mutually entangled, i.e. in terms of density matrices:

$$\rho_{BBBB} = \rho_B \otimes \rho_B \otimes \rho_B \otimes \rho_A,$$

is actually the problem that has been solved in section 3.2. Possibly observed eigenpatterns are associated with eigenvalues μ of the matrix U :

$$U = \text{Tr}_B(\mathcal{R}^2 \rho_B) \tag{8.8}$$

The density matrix ρ_A is projected onto the eigenspace of eigenvalue μ :

$$\rho_A \rightarrow \frac{E_\mu \rho_A E_\mu}{\text{Tr}(E_\mu \rho_A)} \tag{8.9}$$

- (ii) **The B particles are entangled with each-other, but not with A :** If the B particles are already entangled, which does not contradict the given restrictions, the density-matrix can be written as:

$$\rho_{BBBB} = \rho_{BBB} \otimes \rho_A$$

At the end of the experiment however, particle A will be entangled with all remaining B particles. This means we end up with a density matrix $\hat{\rho}_{BBBB}$ that cannot be factorised.

If the initial ρ_A density matrix is a multiple of the identity:

$$\rho_A = \lambda \mathbb{1}, \tag{8.10}$$

then we can possibly obtain the result by a global quantum double $D(H)$ transformation \bar{g} , which changes the (unentangled) tensor product of ρ_B' density matrices to ρ_{BBB} :

$$\bar{g} \in D(H): \rho_B' \otimes \rho_B' \otimes \rho_B' \otimes \rho_A \mapsto \rho_{BBB} \otimes \rho_A \tag{8.11}$$

We then compute the U -eigenvalues relative to ρ_B' :

$$U = \text{Tr}_B(\mathcal{R}^2 \rho_B') \tag{8.12}$$

Next, we project ρ_A onto the μ -eigenspace and then transform back by \bar{g} to obtain $\hat{\rho}_{BBBB}$:

$$\rho_{BBB} \otimes \rho_A \rightarrow \left[\rho_B' \otimes \rho_B' \otimes \rho_B' \otimes \frac{E_\mu \rho_A E_\mu}{\text{Tr}(E_\mu \rho_A)} \xrightarrow{\bar{g}} \right] \hat{\rho}_{BBBB} \tag{8.13}$$

If $\rho_A \neq \lambda \mathbb{1}$ the problem is also solvable, but we do not have a ready-to-use scheme to do this.

(iii) **All particles are entangled with each-other:** For the case that ρ_{BBBB} is not factorisable at all, we have no direct solution. At the end of the experiment the resulting final density matrix will still be unfactorisable. Our best clue is that the initial density matrix ρ_{BBBB} will probably be a sum of such final density matrices:

$$\rho_{BBBB} \simeq \hat{\rho}_{BBBB} + \check{\rho}_{BBBB} + \dots$$

The statements above that we have not solved or proved explicitly, should therefore be considered conjectures.

The formulation of ‘allowed’ particles for the ‘many’-side of the man-to-one experiment may also be interesting from the point of view of the discrete gauge theories, as the *canonical spin-statistics connection*, see section B.2 of the appendix, is concerned; the state of the ‘many’ particles is such that it obeys the canonical spin-statistics connection. This is worth mentioning and perhaps even of physical significance as well, since arbitrary states usually violate the canonical spin-statistics connection.

8.2 Scattering versus double slit experiments

One good question not considered until now is: why do other articles about measurements with non-abelian anyons always use a scattering experiment and is the double slit experiment used in this thesis? Well, for various reasons:

- the scattering experiment is often used because it is easy to solve when there is an incoming plane wave. For experiments involving only one incoming particle it is invalid to assume an incoming plane wave.
- the calculated cross sections are a first order effect: the main part of the incoming beam passes the scatterer without being disturbed. Only a small percentage gets scattered and is measured; this happens at angles ‘far away’ from the direction of the main beam (for which $\theta = 0$). The double slit experiment, on the contrary, uses a zeroth order effect and especially measures at angles around $\theta = 0$.
- the many-to-many experiment is good to compare a scattering with a double slit experiment. Observed patterns for both experiments depend on $\langle \mathcal{R}^2 \rangle$, but for scattering only the amplitude of the pattern can change, while for the double slit the pattern both can shift and change amplitude.
- the double slit guarantees that the incoming particle never comes in contact with the target particle between the two slits. For Aharonov-Bohm double slit experiments with electrons and magnetic fields etcetera this requirement turned out to be unnecessary, but for particles of the $D(H)$ spectrum there exists no description how to deal with such a situation, which we therefore happily avoid where we can.
- finally there is the problem that particles need to be re-used after they have been detected. In all ‘regular’ scattering experiments detected particles are lost. Introducing ‘particle-recycling’ may encounter less resistance from physicists when doing it in a less known experiment like the double slit instead of scattering. Another similar question is what would happen to the incoming particle if it would not pass the double slit, but bounce of the wall; is it re-usable then or does it stuck to the wall?

The above arguments do not rule out useful scattering experiments with non-abelian anyons. Cross sections also have, in the many-to-many experiment for example, a decomposition in eigenpatterns. Let σ_λ indicate the cross section measured for an eigenstate of \mathcal{R}^2 with eigenvalue λ . Then for another state, with $\langle \mathcal{R}^2 \rangle = \sum_l p_\lambda \lambda$, σ is the same weighed sum of eigenpatterns: $\sigma = \sum_\lambda p_\lambda \sigma_\lambda$. Preskill [10] applies a Mach-Zender interferometer, which is yet another description of an interference experiment that will probably yield the same results as the double slit experiment.

So, the above arguments just try to explain why the double slit experiment was preferable to the scattering experiment in this thesis.

8.3 Summary

In this summary, we will stroll through all preceding chapters in ascending order. We will highlight important aspects, specify our own contributions and indicate some directions for future research.

Quantum computation is a fascinating field of research, with the perspective of vastly increased computational power. Chapter 1 figures as the introduction to both this thesis and relevant aspects of quantum computation. A quantum computer is made of a few elementary objects and operations on those objects: qubits, gates and measurements. Together they form a set and if the set allows quantum computation it constitutes a universal set (see page 7 where we give the definition of a universal set). The major difference with conventional computers, is that quantum computers use quantum properties of nature at the fundamental level. Building a quantum computer in practice is very difficult, because carefully prepared quantum states tend to decohere, due to interactions with the noisy environment. Any practical set-up that is decoherence free is a very good candidate to become a real quantum computer. A decoherence free abstract model for a quantum computer is suggested by Kitaev and Preskill through using non-abelian anyons. It is a promising set-up, although many aspects remain unclear (also because both Kitaev and Preskill abundantly refer to unpublished work). An important question of principle is what properties of the internal state of non-abelian anyons can be determined and how we can measure the internal states. Another practical problem is that non-abelian anyons as such have never been observed in nature, but indications do exist. Preskill has claimed that the quantum double of the group A_5 yields a universal set. In chapter 6 we continue on quantum computation; first we treat non-abelian anyons and various interference experiments.

We analyzed the double slit experiment for non-abelian anyons in chapter 2. We started with merely two-dimensional free point-particles, which were used in an idealized interference experiment. We introduce a notation that hides the details that depend on the practical set-up of the double slit experiment. The observed pattern and probability distribution can now easily be written as a sum of separate contributions from each slit and an interference term. We already distinguish between the interference pattern and the probability distribution, although these two are still equal at this point. We introduce abelian anyons, which are particles with a topological interaction via phase factors. Anyons are a generalization of bosons and fermions and emerge from theories like the discrete gauge theories that are described in chapter 4. The interaction is topological, because it only depends on the topology of the multiparticle configuration space, or in simple words, it depends on the number of times that the particles are wound around each-other. This winding is efficiently described by the braid operators \mathcal{R} , \mathcal{R}^{-1} and \mathcal{R}^2 , the monodromy operator. The phase factors resulting from the interaction cause the interference term for the double slit experiment to change. The double slit interference experiment with abelian anyons is equivalent to the well-known Aharonov-Bohm effect. Non-abelian

anyons, however, do not interact via mere phase factors (the interaction is still topological though); these particles have non-trivial internal degrees of freedom on which the braid operators act, which can cause the particles to become entangled. For double slit experiments with non-abelian anyons, the probability distribution and the interference pattern are certainly not equal anymore in general, due to the entanglement of particles in the experiment. In the probability distribution, it is again only the interference term that is changed by the topological interaction, through the expectation value of the monodromy operator. Table 2.1 (p. 28) efficiently summarizes this chapter on topologically interacting particles and interference in two spatial dimensions. As for the interference pattern, there are various inequivalent schemes that produce one, and these are treated in the subsequent chapter.

We develop two different schemes for a double slit experiment with non-abelian anyons in chapter 3. We call the first ‘one-to-one’ and the second ‘many-to-one’. The one-to-one experiment describes a set-up with two particles: one of which is located behind and between the two slits, while the other is directed at the double slit, and detected at a specific angle behind the double slit, after which it is returned to its original position where it will be re-used as incident particle. In other words, the two-particle out-state of one measurement (of the angle of the incoming particle) is the two-particle in-state for the next measurement. The combined sequence of angular measurements results in some interference pattern. We derive an expression for this interference pattern and conclude that the two-particle system becomes projected onto an eigenspace of some eigenvalue of the monodromy operator \mathcal{R}^2 during the experiment. The eigenvalue can be determined through the observed interference pattern, that may carry the name of ‘eigenpattern’. This result of projection is the statistical average over the sequence of angular measurements, which apparently locks the two-particle system in an eigensubspace. Which eigenvalue of \mathcal{R}^2 is determined by the usual probabilities for quantum measurements (via expectation values of the eigenspace-projection operators). The major part of the rather elaborate proof is given in appendix A. The second double slit experiment we describe, is the many-to-one experiment. Here we direct many identically prepared particles at the double slit, behind which one other particle resides. We measure the angle of the ‘many’ particles as they show up behind the double slit. This sequence defines an interference pattern. We determine the interference pattern to be an eigenpattern of an operator that we call the U -matrix. The U matrix is defined as the partial trace over the monodromy operator \mathcal{R}^2 and the density matrix of the incoming particle (and since all incoming particles are identically prepared, the U -matrix is the same for all these particles) and may operate on the internal space of the ‘one’ particle that sits between the two slits. The result of the many-to-one experiment is also a projection: the density matrix of the ‘one’ particle becomes projected onto the eigenspace that is associated with the eigenvalue (and eigenpattern) of U . It turns out that we can use almost the same proof for the many-to-one experiment as that of the one-to-one experiment. However, we can solve the many-to-one experiment only if we pose a restriction on the ‘many’ particles, which should have abelian braiding amongst each-other. We have summarized the results for both the one-to-one and the many-to-one experiment in table 3.1 (p. 46), where we introduced the name ‘many-to-many’ to indicate the double slit experiment that yields the probability density distribution as the interference pattern. Obviously, the theory of non-abelian anyons embraces that of abelian anyons; since abelian anyons have a trivial internal state there is nothing to measure of it. Only with non-abelian anyons, the double slit experiments one-to-one and many-to-one can be used as quantum measurements.

We leave the double slit experiment for a while in chapter 4. Here, we briefly review discrete gauge theories, from which non-abelian anyons emerge naturally. This leads mathematically from a spontaneously broken gauge theory (broken to a discrete finite group H) to the use of the quantum double $D(H)$ of that finite group H . The non-abelian anyons, traditionally divided into fluxes, charges and dyons (which have both charge and flux), can be labeled by the irreducible

representations of $D(H)$. The topological interaction, i.e. the braid-operators, is implemented through the quasi-triangular structure on $D(H)$. We supply a pedestrian introduction to quasi-triangular hopf algebras, in particular $D(H)$, thereby discussing algebras, irreps of algebras, coalgebras, bialgebras, quasitriangular bialgebras and the fusion rules. The braid operators form representations of truncated braid groups. Braid groups, and its colored, partially colored, truncated and partially colored truncated variants, are described in appendix C. The discrete gauge theories also give a description on how to create non-abelian anyons; they can be created from the vacuum in entangled pairs, where the total pair still has the quantum numbers of the vacuum, but its individual members need not of course.

We combine the one-to-one and many-to-one double slit experiments with the quantum double $D(H)$ through various worked out examples in chapter 5, where as example we use the quantum double $D(H)$ of the smallest non-abelian group H , which is S_3 . Details concerning the construction of the spectrum of $D(H)$, and particularly the spectrum of $D(S_3)$, are relegated to appendix B. In the examples, we basically perform the same sequence of experiments twice. The first time we start with some flux in a specific given unentangled state, the second run we allow the initial state to be arbitrary, which includes an entangled particle like a particle created from the vacuum. Both sequences seem very different but yield the same observable result, i.e. the same interference patterns. We explain this resemblance between the sequences by a global quantum double transformation, which indeed leaves the observable outcomes of experiments invariant. Furthermore, the examples with $D(S_3)$ will provide evidence for more general $D(H)$ properties: (1) the many-to-one experiments seems possible under more relaxed restrictions; (2) vacuumstates, i.e. particles that were once created from the vacuum, seem equally useful for quantum manipulation as the special unentangled initial states; we construct a ‘relabeling’ of the particles which maps the highly entangled vacuumstates to a completely unentangled system. Although this relabeling looks like a basis transformation, it cannot be one, since basis transformations cannot change an entangled system into an unentangled one.

We describe the link of non-abelian anyons with quantum computation in chapter 6. We construct a qubit with the non-abelian anyons that are described by $D(S_3)$; this qubit exists out of two particles, which together are fluxless. We can measure the value of a qubit on the standard basis, through a many-to-one experiment. We can apply a simple gate, the *Not*-gate, to a qubit by acting with the monodromy operator, and we can create a simple plus or minus superposition of the states $|0\rangle$ and $|1\rangle$ by measuring the qubit in another basis than the standard one. The quantum double $D(S_3)$ obviously does not supply a universal set, but $D(H)$ may very well become universal for some larger group H . As we have not considered other groups, we can not make a decisive statement about this question. It is clear however, that qubits, gates and measurements can be constructed as objects that are build of combinations of particles, measurement experiments and monodromies. These objects should be completely compatible with each other, which is not a trivial point, as we demonstrate with an example of a subtle mistake. We would have liked to compare our results with those of Kitaev and Preskill on this matter of universality, but we did not get to that point.

Multiparticle states in the vacuumchannel form a special subset in the theory, as for now they form the only description on how to create non-abelian anyons, but vacuumstates behave roughly the same as particles with other internal states as became clear in the examples with $D(S_3)$. In chapter 7 we speculate on some of these seemingly remarkable properties of vacuumstates. We state several conjectures, which are mainly concerned with the density matrices of particles in vacuumstates that are a multiple of the unit matrix. Unital density matrices can no doubt simplify certain expressions, for example the fusion probabilities, that can be written as a trace over projection operators and the two-particle density matrix. We also describe an ordering process, that starts with particles that are pair-created from the vacuum and ends with piles of particles with ‘truly identical’ internal states that can be labeled by unentangled states. We have

not been able to prove our conjectures for general $D(H)$, however they are correct for $D(S_3)$. Furthermore, the conjectures (if they are true) seem to be in conflict with well-known results for local gauge theories (one cannot determine a quark's color). We do offer an explanation for this paradox, by saying that we are really using only the representation-theory. This statement actually renders the description via explicit states, either vacuumstates or unentangled states, obsolete. But as for now, this chapter 7 is a chapter of speculations.

The final chapter of this thesis, chapter 8, treats two subjects on double slit interference experiments. The first deals with the generic many-to-one experiment, which is the many-to-one experiment with more relaxed restrictions, as already indicated by the examples with $D(S_3)$; In the generic many-to-one experiments, the 'many' particles need to be truly equivalent or truly identical particles (for which the canonical spin-statistics connection is restored) and that is the only restriction. This allows for many-to-one experiments with initially highly entangled particles. We present some hints to solve the generic many-to-one experiment; solving the problem can be divided in three classes, based on the initial entanglement. We fail to solve all three classes explicitly. On the second subject, we discuss a matter which could as well have been put at the start of chapter 2, namely why we chose to use the double slit interference experiments instead of ordinary scattering experiments. Next, and finally, we present an extensive summary of the thesis, which is about to end with some remarks regarding future research.

Perhaps the question one most urgently wants to be answered, is for which group H the quantum double $D(H)$ supplies a universal set, in particular, if there exists such a group at all. But just trying a few groups (which of course would include A_5 or S_5 and \bar{D}_2 ³) and eventually finding such a group may not directly lead to new insights (although it may very well indicate how the complexity of gates may grow with the order of the group). It is probably preferable to continue the quest for universality through representation-theory. The link between the theory of quantum doubles $D(H)$ and that of computational complexity (like the ability for universal quantum computation) might be far more clear or obvious, than if we would continue using the description with specific internal states. Hopefully, the construction of compatible qubits, gates and measurements may also become less dependent on small details, although it will probably remain a non-trivial job. Of course, a description in terms of representation-theory should of course include examples of $D(S_3)$ (and probably also of $D(A_5)$, $D(\bar{D}_2)$).

A starting point for future research might be to prove the conjectures of chapter 7. Although this is a speculative chapter, the conjectures therein are concrete enough to be proven or be discarded. We are rather confident that the manifestation of a quantum double of a finite group through non-abelian anyons yields more nice properties than we were able to reveal (prove) in this thesis, especially in terms of expectation values of braid operators. In this context, also the global quantum double transformations that leave the outcomes of experiments invariant, deserve a closer look. An almost trivial but nevertheless useful starting point, is rewriting the discrete gauge theories (e.g. fusion probabilities) in terms of density matrices, since the description of an entangled particle via the density matrix is superior.

The two double slit experiments, one-to-one and many-to-one, yield remarkable results. But these results were solved in a semi-classical context; apart from the assumption that the measurement of the angle projects on a momentum-eigenstate, the non-abelian anyons are treated as classical, dynamical, point-particles. Under these conditions the results for the one-to-one and many-to-one are perfectly valid. But the discrete gauge theories do not yet supply a dynamical description of non-abelian anyons. So, it is an interesting question, if these conditions are still valid in a proper dynamical theory of non-abelian anyons, and how this change would affect the

³The group \bar{D}_2 , which is a non-abelian group of order eight (so it is a small group), is taken as example to illustrate discrete gauge theories in Propitius and Bais [11]

results for double slit experiments. In other, impatient, experimental, words, let us search for a physical realization of non-abelian anyons where we can put the double slit experiments into practice, and compare the result with the theory. Anyway, a theoretical model for non-abelian anyons including a dynamical description could be useful. Another, more simple, question is, if there are other schemes for double slit experiments than the one-to-one, the many-to-one and the many-to-many experiments, that yield interesting results.

The research on non-abelian anyons and there application for quantum computation definitely deserves further study.

Acknowledgements

And here it is, my 'afstudeerscriptie', the result of spending some (and some more) time at the institute for theoretical physics in that room on the fourth floor. I would like to thank my supervisor Sander Bais: although sessions with him tend to take lots of time and can get 'rough' every now and then, the net result has always been positive, taking care of all (by now formerly) unclear aspects. One of the side-effects is the rather large size of my thesis (but I thus do not pity him to have to read through all of it.). I'd like to thank Joost Slingerland for some less tense discussion on the subject and for the idea of partial projection. My room mates Matthijs Randsdorp and 'm'n makkertje' Bastian Wemmenhove have accompanied me for the past $1\frac{1}{2}$ years and together, especially through our famous blackboard sessions, we have become the physicists we are today. I am very grateful that I have been able to combine the work on this thesis with my daily training in the swimming-pool without destructive interference. Let me conclude by thanking all 'theorie-studenten' and those I haven't mentioned yet that deserve this credit nevertheless.

APPENDIX A

PROOF OF PROJECTION (LOCKING) FOR DOUBLE SLIT EXPERIMENTS

This appendix is devoted to the proof of the projection and convergence statements of chapter 3, and while it is purely mathematical, it certainly should be considered as a core element of this thesis. The proof is rather elegant, for it involves no tricks or conditions on the eigenvalues, for instance. The results of the proof can be illustrated easily, which of course we will do. In section A.1.1 we will recast our problem and claims in a notationally suitable form and we will try some (unsuccessful) ways to solve our problem. Subsequently, in section A.1.2, we will create a new probability density distribution, with which we will solve our problem for two eigenvalues in section A.1.3. We will supply plenty of examples and pictures in section A.2. Finally we will consider the case for arbitrary many eigenvalues in section A.3, but this follows straight from the case of two eigenvalues.

We will not explicitly summarize our findings for this chapter, as we have done so already in the main text.

Perhaps the most interesting thing of the whole proof is that a quantum mechanical measurement of an eigenvalue accompanied by a projection on the eigenspace of that eigenvalue, is the statistical result of an experiment which is repeated often. So the quantum measurement does not happen instantaneously, but is the average over many single observations.

We worked it out ourselves, so there are no references to others. Techniques used are found in mathematical textbooks (analysis, statistics). Our own efforts to accomplish this proof will probably accentuate the style in which this chapter has been written.

A.1 Solving the problem for two eigenvalues

A.1.1 Translating the problem from physics to mathematics

Let us first restate what we will proof but thereby change notation a bit. Let:

$$p_{\lambda_j} = \langle \psi_{\text{in}} | E_{\lambda_j} | \psi_{\text{in}} \rangle$$

Then the statement is (see (3.9), p. 32) that with unit probability up to an overall phase factor:

$$\lim_{N \rightarrow \infty} \sum_j \frac{\mathcal{F}_{\lambda_j}^N \dots \mathcal{F}_{\lambda_j}^2 \mathcal{F}_{\lambda_j}^1}{\sqrt{\sum_i |\mathcal{F}_{\lambda_i}^N \dots \mathcal{F}_{\lambda_i}^2 \mathcal{F}_{\lambda_i}^1|^2 p_{\lambda_i}}} E_{\lambda_j} = \frac{1}{\sqrt{p_\mu}} E_\mu \quad (\text{A.1})$$

for some μ . Each μ has a probability p_μ . This expression (A.1) is independent of $|\psi_{\text{in}}\rangle$. Properties and definitions of the above arguments, which have been introduced in chapters 2 and 3, are:

$$\begin{aligned} \sum_j p_{\lambda_j} &= 1 \\ \mathcal{F}_{\lambda_j}^k &= c_{\text{above}}^{t_k} + c_{\text{below}}^{t_k} e^{i\lambda_j} \\ |\mathcal{F}_{\lambda_j}^k|^2 &= |c_{\text{above}}^{t_k}|^2 + |c_{\text{below}}^{t_k}|^2 + 2\text{Re}\left(c_{\text{above}}^{t_k*} c_{\text{below}}^{t_k} e^{i\lambda_j}\right) = f_{\lambda_j}(\theta_{t_k}) \\ \sum_{t_k} |c_{\text{above}}^{t_k}|^2 + |c_{\text{below}}^{t_k}|^2 &= 1 \quad \sum_{t_k} c_{\text{above}}^{t_k*} c_{\text{below}}^{t_k} = 0 \\ \Rightarrow \sum_{t_k} f_{\lambda_j}(\theta_{t_k}) &= \sum_{t_k} |\mathcal{F}_{\lambda_j}^k|^2 = 1 \quad \forall k, \lambda_j \end{aligned}$$

The probability to observe the sequence $\theta^1, \dots, \theta^N$ is:

$$P_N(\theta^1, \dots, \theta^N) = \sum_i |\mathcal{F}_{\lambda_i}^N \dots \mathcal{F}_{\lambda_i}^2 \mathcal{F}_{\lambda_i}^1|^2 p_{\lambda_i} = \sum_j f_{\lambda_j}(\theta^N) \dots f_{\lambda_j}(\theta^1) p_{\lambda_j} \quad (\text{A.2})$$

With probability one the particle will be detected at some angle, or:

$$\begin{aligned} 1 &\equiv \sum_{\theta^1, \dots, \theta^N} P_N(\theta^1, \dots, \theta^N) \\ &= \sum_{\theta^1, \dots, \theta^N, j} f_{\lambda_j}(\theta^N) \dots f_{\lambda_j}(\theta^1) p_{\lambda_j} \\ &= \sum_j p_{\lambda_j} = 1 \end{aligned} \quad (\text{A.3})$$

Now let's for convenience change notation, and furthermore, for simplicity, assume that there are only two eigenvalues: λ_1 and λ_2 .

$$\begin{aligned} \theta_t &\rightarrow x \text{ (continuous)} \\ f_{\lambda_1}(\theta) &\rightarrow A(x) \quad A(x) \geq 0 \quad \forall x \\ f_{\lambda_2}(\theta) &\rightarrow B(x) \quad B(x) \geq 0 \quad \forall x \\ p_{\lambda_1} &\rightarrow \alpha^2 \\ p_{\lambda_2} &\rightarrow \beta^2 \quad \alpha^2 + \beta^2 = 1 \\ \sum_{\theta} f_{\lambda_1}(\theta) = 1 &\rightarrow \int A(x) dx = 1 \\ \sum_{\theta} f_{\lambda_2}(\theta) = 1 &\rightarrow \int B(x) dx = 1 \\ N &\rightarrow n \\ P_N(\theta^1, \dots, \theta^N) &\rightarrow p(x_1, \dots, x_n) \\ &= \alpha^2 A(x_1) A(x_2) \dots A(x_n) + \beta^2 B(x_1) B(x_2) \dots B(x_n) \\ \int \int \dots \int p(x_1, x_2, \dots, x_n) dx_1 dx_2 \dots dx_n &= \alpha^2 + \beta^2 = 1 \end{aligned}$$

We define α_n^2 and β_n^2 by:

$$\alpha_n^2(x_1, x_2, \dots, x_n) := \alpha^2 \frac{A(x_1)A(x_2) \dots A(x_n)}{p(x_1, x_2, \dots, x_n)} \quad (\text{A.4})$$

$$\beta_n^2(x_1, x_2, \dots, x_n) := \beta^2 \frac{B(x_1)B(x_2) \dots B(x_n)}{p(x_1, x_2, \dots, x_n)} \quad (\text{A.5})$$

Here one can consider α_n^2 to be that part of the wave function that is in a λ_1 eigenstate after n observations. Where $\alpha_n^2 + \beta_n^2 = 1$ of course.

Then the claim states that in the limit of n to infinity projection takes place:

$$\begin{array}{llll} \text{either} & \alpha_n^2 \rightarrow 1 & \beta_n^2 \rightarrow 0 & \text{with probability } \alpha^2 \\ \text{or} & \alpha_n^2 \rightarrow 0 & \beta_n^2 \rightarrow 1 & \text{with probability } \beta^2 \end{array}$$

But the problem remains to prove this. We start with some instructive attempts:

1. We calculate the expectation value of α_n^2 and see if it contradicts projection.

$$\begin{aligned} \langle \alpha_n^2 \rangle &= \int p(\vec{x}_n) \alpha_n^2(\vec{x}_n) d\vec{x}_n & (\vec{x}_n) &= (x_1, x_2, \dots, x_n) \\ &= \int \alpha^2 A(x_1)A(x_2) \dots A(x_n) d\vec{x}_n = \alpha^2 & (\forall n) \end{aligned} \quad (\text{A.6})$$

This is the same answer as in the case of projection, because then:

$$\langle \alpha_n^2 \rangle = \alpha^2 \cdot 1 + \beta^2 \cdot 0 = \alpha^2 \quad (n \rightarrow \infty)$$

This contradicts neither confirms projection.

2. Let's construct a function that is 1 if $\alpha_n^2 = 0$ or $\alpha_n^2 = 1$: the function $f = (2\alpha_n^2 - 1)^2$ for example. We calculate its expectation value (it should be 1 for $n \rightarrow \infty$):

$$\begin{aligned} \langle f \rangle &= \int p(x_1, x_2, \dots, x_n) (2\alpha_n^2 - 1)^2 d\vec{x}_n \\ &= \int p(\vec{x}_n) \left(\frac{2\alpha^2 A(x_1)A(x_2) \dots A(x_n) - p(\vec{x}_n)}{p(\vec{x}_n)} \right)^2 d\vec{x}_n \\ &= \int \frac{(\alpha^2 A_1 A_2 \dots A_n - \beta^2 B_1 B_2 \dots B_n)^2}{\alpha^2 A_1 A_2 \dots A_n + \beta^2 B_1 B_2 \dots B_n} d\vec{x}_n \end{aligned}$$

One can evaluate this integral numerically (with $A = \cos^2$ and $B = \sin^2$ for example) and it tends to 1, but this is still no analytical proof; dependence of α^2 and β^2 does not become clear either. Besides, there is a better way:

3. One can also say that in the end $\alpha_n^2 \gg \beta_n^2$ or $\beta_n^2 \gg \alpha_n^2$, so why not look at $\frac{\alpha_n^2}{\beta_n^2}$. This is not yet good enough, because the denominator could become zero. Instead, one should look at the logarithm:

$$\ln \frac{\alpha_n^2}{\beta_n^2} = \ln \frac{\alpha^2 \frac{A(x_1)A(x_2) \dots A(x_n)}{p(x_1, x_2, \dots, x_n)}}{\beta^2 \frac{B(x_1)B(x_2) \dots B(x_n)}{p(x_1, x_2, \dots, x_n)}} = \ln \frac{\alpha^2 A_1 A_2 \dots A_n}{\beta^2 B_1 B_2 \dots B_n} = \ln \frac{\alpha^2}{\beta^2} + \ln \frac{A_1}{B_1} + \dots + \ln \frac{A_n}{B_n}$$

This has some advantages: the normalization factors $p(x_1, x_2, \dots, x_n)$ cancel each other; it now becomes a sum of terms, where each term depends on only one x -variable. It is 'symmetric' for $\beta_n^2 > \alpha_n^2$ or $\alpha_n^2 > \beta_n^2$ (gives a minus sign, so perhaps anti-symmetric would be more correct). So the logarithm is clearly preferable and will be used.

A.1.2 A new probability distribution: $P_n(z)$

With the probability that $\ln \frac{\alpha_n^2}{\beta_n^2} = z$ we associate the probability density distribution $P_n(z)$ ($z \in \mathbb{R}$). In other words, with the old probability distribution, $p(\vec{x}_n)$, we create a new one by:

$$\int_a^b P_n(z) dz = \int \dots \int p(\vec{x}_n) H\left(a < \ln \frac{\alpha_n^2}{\beta_n^2} < b\right) d\vec{x}_n \quad H(\text{true}) = 1 \quad H(\text{false}) = 0 \quad (\text{A.7})$$

and define $P_n(z)$ itself (in the usual way in statistics) by:

$$P_n(z) = \lim_{\Delta z \rightarrow 0} \frac{\int_z^{z+\Delta z} P_n(\hat{z}) d\hat{z}}{\Delta z}$$

This gives:

$$P_n(z) = \int \dots \int p(\vec{x}_n) \delta\left(z - \ln \frac{\alpha_n^2}{\beta_n^2}\right) d\vec{x}_n \quad (\text{A.8})$$

Which can be expanded into:

$$\begin{aligned} P_n(z) &= \int \dots \int (\alpha^2 A_1 A_2 \dots A_n + \beta^2 B_1 B_2 \dots B_n) \delta\left(z - \ln \frac{\alpha^2}{\beta^2} - \ln \frac{A_1 A_2 \dots A_n}{B_1 B_2 \dots B_n}\right) d\vec{x}_n \\ &\equiv \alpha^2 P_n^A\left(z - \ln \frac{\alpha^2}{\beta^2}\right) + \beta^2 P_n^B\left(z - \ln \frac{\alpha^2}{\beta^2}\right) \end{aligned} \quad (\text{A.9})$$

Here, we introduced two new functions, $P_n^A(z)$ and $P_n^B(z)$, which are truly independent of α^2 and β^2 .

$$P_n^A(z) = \int \dots \int A_1 A_2 \dots A_n \delta\left(z - \ln \frac{A_1 A_2 \dots A_n}{B_1 B_2 \dots B_n}\right) d\vec{x}_n \quad (\text{A.10})$$

$$P_n^B(z) = \int \dots \int B_1 B_2 \dots B_n \delta\left(z - \ln \frac{A_1 A_2 \dots A_n}{B_1 B_2 \dots B_n}\right) d\vec{x}_n \quad (\text{A.11})$$

The dependence of $P_n(z)$ on α^2 and β^2 enters the equation (A.9) only in a, α^2 - and β^2 -dependent, scaling of $P_n^A(z)$ and $P_n^B(z)$.

To achieve projection, the probability that α_n^2 and β_n^2 are roughly equal, or $\alpha_n^2 \approx \beta_n^2$, should tend to zero, so $P_n(z)$ should vanish in an environment of $z = 0$ when n grows larger:

$$n \rightarrow \infty : \quad P_n(z) \Big|_{z=0} \downarrow 0$$

It would be nice to know $P_n^A(z)$ for all n (as an explicit function of z). Let's start with $P_1^A(z)$, which can be determined using:

$$\delta(f(x)) = \sum_{x_i} \frac{\delta(x_i)}{|f'(x_i)|} \quad f(x_i) = 0$$

$$\begin{aligned} P_1^A(z) &= \int A(x) \delta\left(z - \ln \frac{A(x)}{B(x)}\right) dx \\ &= \sum_{x_i} \int A(x) \frac{\delta(x_i)}{\left|-\frac{A'B - B'A}{AB}\right|} dx \\ &= \sum_{x_i} A(x_i) \frac{A(x_i)B(x_i)}{|A(x_i)'B(x_i) - B(x_i)'A(x_i)|} \end{aligned} \quad (\text{A.12})$$

$$x_i : \quad z - \ln \frac{A(x_i)}{B(x_i)} = 0 \Leftrightarrow e^z = \frac{A(x_i)}{B(x_i)}$$

When $A(x)$ and $B(x)$ are given, the $x_i(z)$ can be determined and with it the explicit z -dependence of $P_1^A(z)$. Having found $P_1^A(z)$, one can continue with P_2^A :

$$P_2^A(z) = \int A(x) P_1^A(z - \ln \frac{A(x)}{B(x)}) dx \quad (\text{A.13})$$

And likewise for arbitrary $n \dots$. But this is an integral-equation and is not easy to solve, even when $A(x)$ and $B(x)$ are explicitly given. One can verify this using Maple (for instance) for various examples; troubles start when $n > 2$. For such examples, with $n = 1$ or $n = 2$, we found that $P_n^A(z)$ was definitely not even near zero. So proof of projection is still far away.

A.1.3 Scaling of $P_n^A(z)$ and $P_n^B(z)$ with n yields solution

$P_n^A(z)$ and $P_n^B(z)$ can both be considered as probability density distributions, in the sense that (which one can easily check):

$$\begin{aligned} P_n^A(z) &\geq 0 & P_n^B(z) &\geq 0 \\ \int_{-\infty}^{\infty} P_n^A(z) dz &= 1 & \int_{-\infty}^{\infty} P_n^B(z) dz &= 1 \end{aligned}$$

One can calculate mean values (expectation values) associated with these probability distributions:

$$\langle z \rangle_{1A} = \int_{-\infty}^{\infty} P_1^A(z) z dz \equiv \mu_A > 0 \quad \langle z \rangle_{1B} = \int_{-\infty}^{\infty} P_1^B(z) z dz \equiv -\mu_B < 0 \quad (\text{A.14})$$

$$\langle z^2 \rangle_{1A} = \int_{-\infty}^{\infty} P_1^A(z) z^2 dz \equiv \sigma_A^2 + \mu_A^2 \quad \langle z^2 \rangle_{1B} = \int_{-\infty}^{\infty} P_1^B(z) z^2 dz \equiv \sigma_B^2 + \mu_B^2 \quad (\text{A.15})$$

These integrals can also be solved in x -space:

$$\langle z \rangle_{1A} = \int_{-\infty}^{\infty} P_1^A(z) z dz = \int_{-\infty}^{\infty} \int A(x) \delta(z - \ln \frac{A(x)}{B(x)}) z dx dz = \int A(x) \ln \frac{A(x)}{B(x)} dx > 0$$

$$A \ln \frac{A}{B} + B \ln \frac{B}{A} = (A - B) \left(\ln \frac{A}{B} \right) = (A - B) (\ln A - \ln B) \geq 0$$

One also determines the other ‘means’ by first performing the z integral. For example:

$$\langle z^2 \rangle_{1A} = \int A(x) \ln^2 \frac{A(x)}{B(x)} dx \quad (\text{A.16})$$

Next, we calculate $\langle z \rangle_{nA}$:

$$\langle z \rangle_{nA} = \int_{-\infty}^{\infty} P_n^A(z) z dz = n \langle z \rangle_{1A} = n \mu_A \quad \langle z \rangle_{nB} = \int_{-\infty}^{\infty} P_n^B(z) z dz = -n \mu_B \quad (\text{A.17})$$

$$\langle z^2 \rangle_{nA} = \int_{-\infty}^{\infty} P_n^A(z) z^2 dz = n\sigma_A^2 + n^2\mu_A^2 \quad \langle z^2 \rangle_{nB} = \int_{-\infty}^{\infty} P_n^B(z) z^2 dz = n\sigma_B^2 + n^2\mu_B^2 \quad (\text{A.18})$$

Now we found that both the mean and the variance scale with a factor n :

$$\langle z \rangle_{nA} = n\langle z \rangle_{1A} \quad \langle z \rangle_{nB} = n\langle z \rangle_{1B} \quad (\text{A.19})$$

$$\sigma_{1A}^2 = \langle z^2 \rangle_{1A} - \langle z \rangle_{1A}^2 \quad \sigma_{1B}^2 = \langle z^2 \rangle_{1B} - \langle z \rangle_{1B}^2 \quad (\text{A.20})$$

$$\mu_n = n\mu \quad (\text{A.21})$$

$$\sigma_{nA}^2 = \langle z^2 \rangle_{nA} - \langle z \rangle_{nA}^2 = n\sigma_{1A}^2 \quad \sigma_{nB}^2 = n\sigma_{1B}^2 \quad (\text{A.22})$$

Let us show this explicitly for $\langle z \rangle_{nA}$:

$$\begin{aligned} \langle z \rangle_{nA} &= \int_{-\infty}^{\infty} P_n^A(z) z dz \\ &= \int_{-\infty}^{\infty} \int \int \dots \int A(x_1)A(x_2)\dots A(x_n)\delta(z - \ln \frac{A(x_1)}{B(x_1)} - \dots - \ln \frac{A(x_n)}{B(x_n)})z d\vec{x}_n dz \\ &= \int \int \dots \int A(x_1)A(x_2)\dots A(x_n)(\ln \frac{A(x_1)}{B(x_1)} + \ln \frac{A(x_2)}{B(x_2)} \dots + \ln \frac{A(x_n)}{B(x_n)}) d\vec{x}_n \\ &= n \int \int \dots \int A(x_1) \ln \frac{A(x_1)}{B(x_1)} dx_1 A(x_2)\dots A(x_n) d\vec{x}_{n-1} \\ &= n \cdot 1^{n-1} \cdot \int A(x) \ln \frac{A(x)}{B(x)} dx \\ &= n\mu_A \end{aligned}$$

When doing the other mean $\langle z^2 \rangle_{nA}$ one encounters $(\ln \frac{A(x_1)}{B(x_1)} + \ln \frac{A(x_2)}{B(x_2)} \dots + \ln \frac{A(x_n)}{B(x_n)})^2$. This yields a total of n^2 terms (when expanding), of which n are of the form $\int A(x) \ln^2 \frac{A(x)}{B(x)} dx$; the others, which are $n^2 - n$ in number, are of the form $(\int A(x) \ln \frac{A(x)}{B(x)} dx)(\int A(y) \ln^2 \frac{A(y)}{B(y)} dy)$. Combined, these yield:

$$\langle z^2 \rangle_{nA} = n\langle z^2 \rangle_{1A} + (n^2 - n)(\langle z \rangle_{1A})^2 = n\sigma_A^2 + n^2\mu_A^2$$

What has been found is that the peak (when plotting the function) of $P_n^A(z)$ moves to the right and $P_n^B(z)$ moves to the left, and $P_n(z)$ becomes zero in a neighbourhood of $z = 0$. While (the mean of) the peak moves (scales) with n , the width of the peak (width \approx standard deviation $= \sigma = \sqrt{\sigma^2}$) scales with \sqrt{n} . So for $n = 100$, the peak of the function lies a hundred times more to the right (or left for $P^B(z)$) whilst the width has only increased by a factor ten.

Projection has been proved.

We can consider α_n^2 and β_n^2 as explicit functions of z . Since:

$$\frac{\alpha_n^2}{\beta_n^2} = e^z \quad \alpha_n^2 + \beta_n^2 = 1, \quad (\text{A.23})$$

this means that $\alpha_n^2(z)$ and $\beta_n^2(z)$ are of the following form:

$$\alpha_n^2(z) = \frac{1}{1 + e^{-z}} \quad \beta_n^2(z) = \frac{1}{1 + e^z} \quad \forall n \quad (\text{A.24})$$

By plotting $\alpha_n^2(z)$, $\beta_n^2(z)$ and $P_n(z)$ in the same figure we can illustrate the projection-process, as shown in fig. A.1.

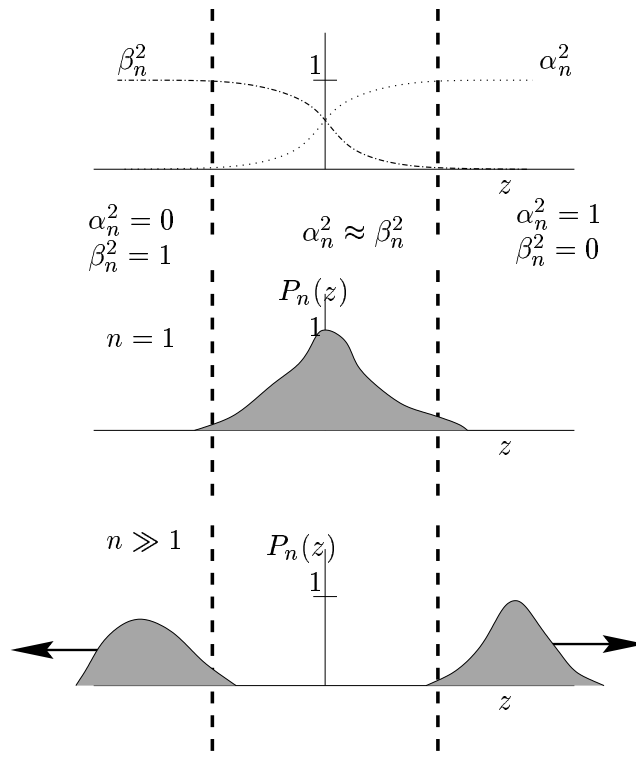


Figure A.1: The real axis can be divided into three parts: one where α_n^2 and β_n^2 are roughly the same and two where $\alpha_n^2 = 0$ (1) and $\beta_n^2 = 1$ (0). $P_1(z)$ might ‘fool’ you because it lies in the ‘roughly the same’ part. When n grows, $P_n(z)$ appears to be a sum of two peaks, which both move away from the origin, and projection becomes a fact. The area under the right peak is α^2 , under the left peak β^2 .

Rate of projection

How fast is projection? For the variety of examples we have considered, it is extremely fast.

The answer to this question is not easy. It involves integrals of tails of probability distributions, and even in the simple case of gaussian normal distributions this becomes analytically unsolvable, and typically involves the error-function (erf). Nevertheless we can estimate it.

Let the probability that after n steps the system has *not* been projected yet be given by Q_n . Then:

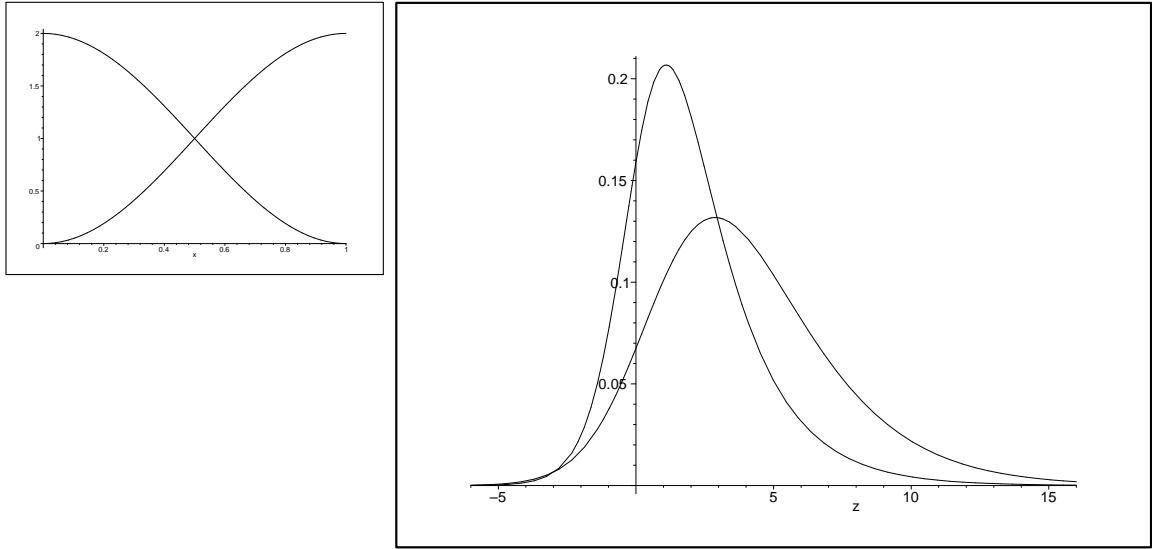
$$Q_n < c_1 e^{c_2 \frac{n\mu}{\sigma}} = c_1 \exp\left(c_2 \frac{n\mu}{\sigma}\right) \quad (\text{A.25})$$

where c_1 and c_2 are constants, μ and σ are the mean value and width of the $P_1^{A,B,\dots}(z)$, or in x -space:

$$\mu = \int A(x) \ln \frac{A(x)}{B(x)} dx \quad \sigma^2 = \int A(x) \ln^2 \frac{A(x)}{B(x)} dx - \mu^2$$

So the rate of convergence is likely to be exponential, possibly faster. This is a conjecture however, since this is not a calculated estimate, but it’s a really estimated estimate.

Perhaps this is not a relevant question. What is relevant is that the rate of convergence depends on the ‘difference’ between $A(x)$ and $B(x)$, of which μ is a measure.

Figure A.2: $A(x)$ and $B(x)$ (l), $P_1^A(z)$ and $P_2^A(z)$ (r), from example (1)

A.2 Examples and more for the case of two eigenvalues

We will give some examples and corresponding figures of typical functions for $A(x)$ and $P_n^A(z)$ etcetera. These examples give rise to other general properties which will be discussed.

Example (1)

For this example we used the following form of $A(x)$ and $B(x)$:

$$A = 2 \cos^2\left(\frac{\pi}{2}x\right) \quad B = 2 \sin^2\left(\frac{\pi}{2}x\right) \quad x \in [0, 1]$$

We explicitly calculated μ , σ^2 , $P_1^A(z)$ and $P_2^A(z)$:

$$\mu = 2 \quad \sigma^2 = \pi^2 - \mu^2 \quad \sigma \approx 2,42$$

$$P_1^A(z) = \frac{2}{\pi} \frac{e^{\frac{3}{2}z}}{(1+e^z)^2} \quad P_2^A(z) = \frac{4}{\pi^2} \frac{e^{\frac{3}{2}z}(ze^z - 2e^z + z + 2)}{(e^z - 1)^3}$$

These results are plotted in fig. A.2. For higher values of n than two, $P_n^A(z)$ is hard to solve analytically; therefore we computed $P_n^A(z)$, $n \geq 2$ by numerical integration. Figures A.3 and A.4 plot $P_n^A(z)$ for some values of n .

Furthermore, we found a kind of symmetry between P_n^A and P_n^B :

$$P_n^A(-z) = P_n^B(z)$$

This is not a coincidence, because $A(x)$ and $B(x)$ resemble each other. In most of the following examples $A(x)$ looks like $B(x)$: translation or mirroring of $A(x)$ yields $B(x)$. For such cases one usually finds that $P_n^A(-z) = P_n^B(z)$.

Figure A.3: Numerical calculation (Monte-Carlo) of $P_8^A(z)$ from example (1)

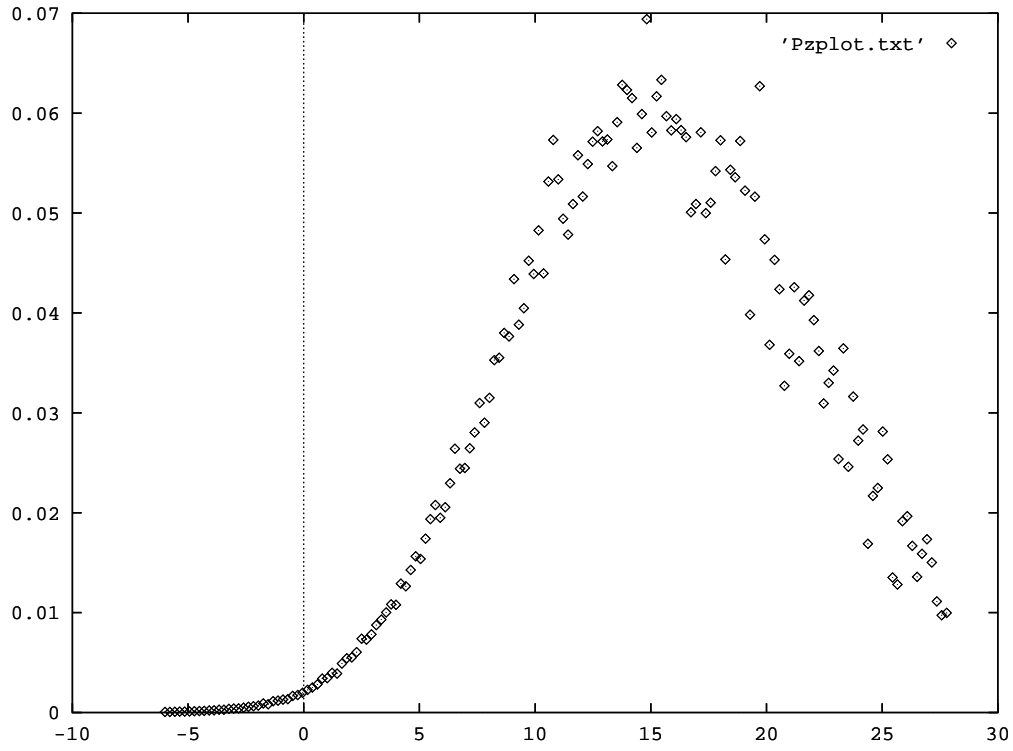


Figure A.4: Numerical calculation of $P_n^A(z)$ for $n = 1, 3, 8$ from example (1)

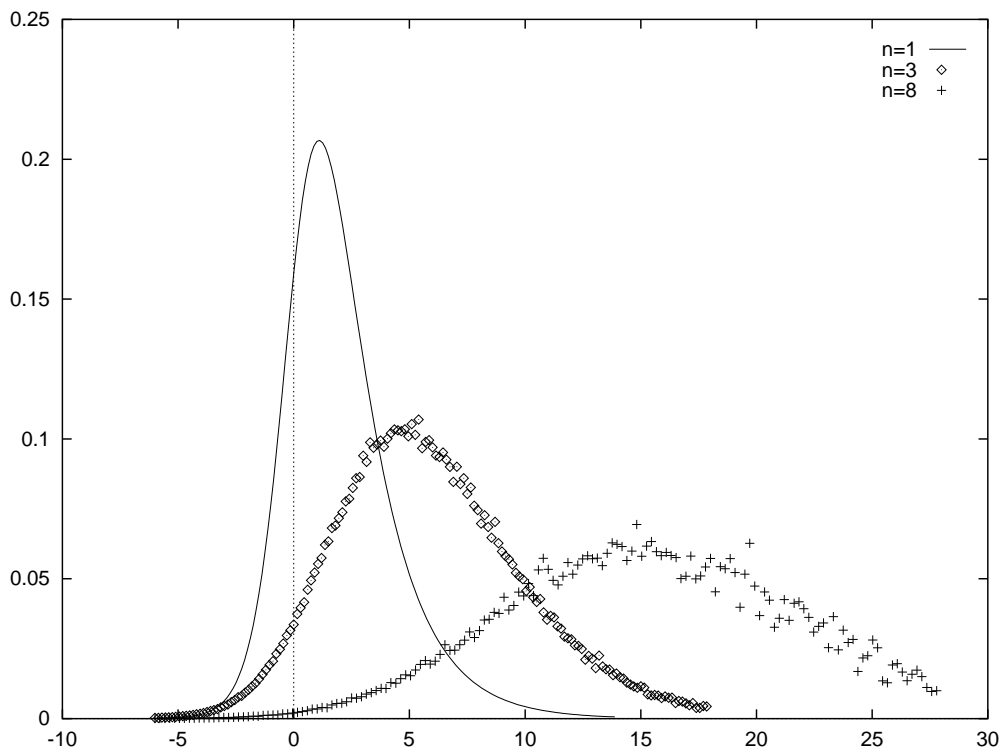
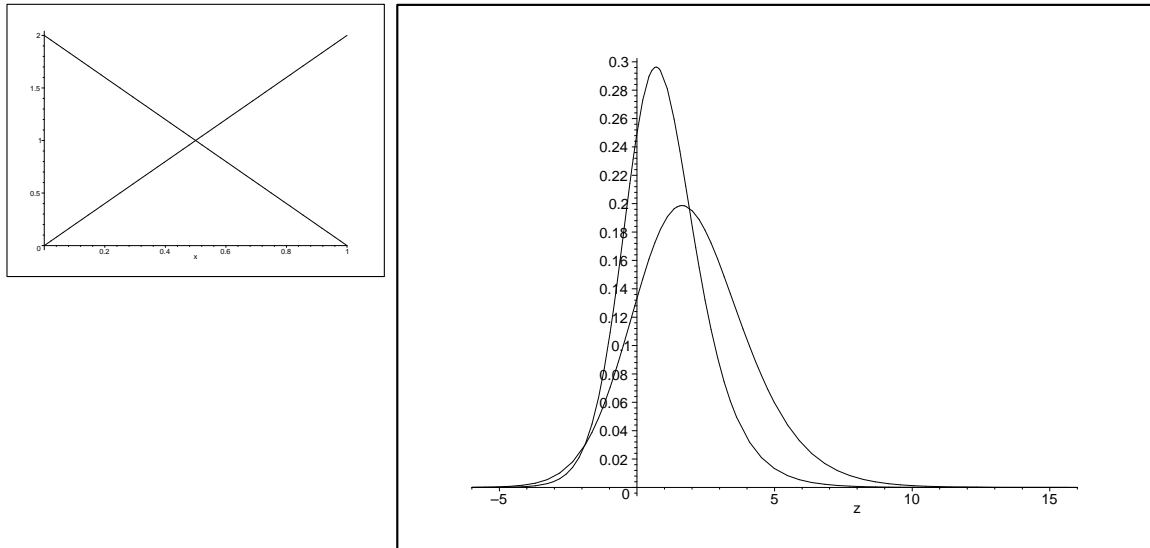


Figure A.5: $A(x)$ and $B(x)$ (l), $P_1^A(z)$ and $P_2^A(z)$ (r), from example (2)



Example (2)

Instead of using sines for $A(x)$ and $B(x)$, we use straight lines in this example:

$$A = 2x \quad B = 2 - 2x$$

Explicit values of μ etcetera differ from example (1), but the overall from is the same:

$$\mu = 1 \quad \sigma^2 = \frac{1}{3}\pi^2 - \mu^2 \quad \sigma \approx 1,51$$

$$P_1^A(z) = 2 \frac{e^{2z}}{(1 + e^z)^3} \quad P_2^A(z) = 4 \frac{e^{2z}(ze^{2z} - 3e^{2z} + 4ze^z + z + 3)}{(e^z - 1)^5}$$

Also now, there is the symmetry between P_n^A and P_n^B :

$$P_n^A(-z) = P_n^B(z)$$

This example is illustrated in fig. A.5.

Example (3)

In this example, we return to cosines for the functions $A(x)$ and $B(x)$, but both are shifted compared with example (1):

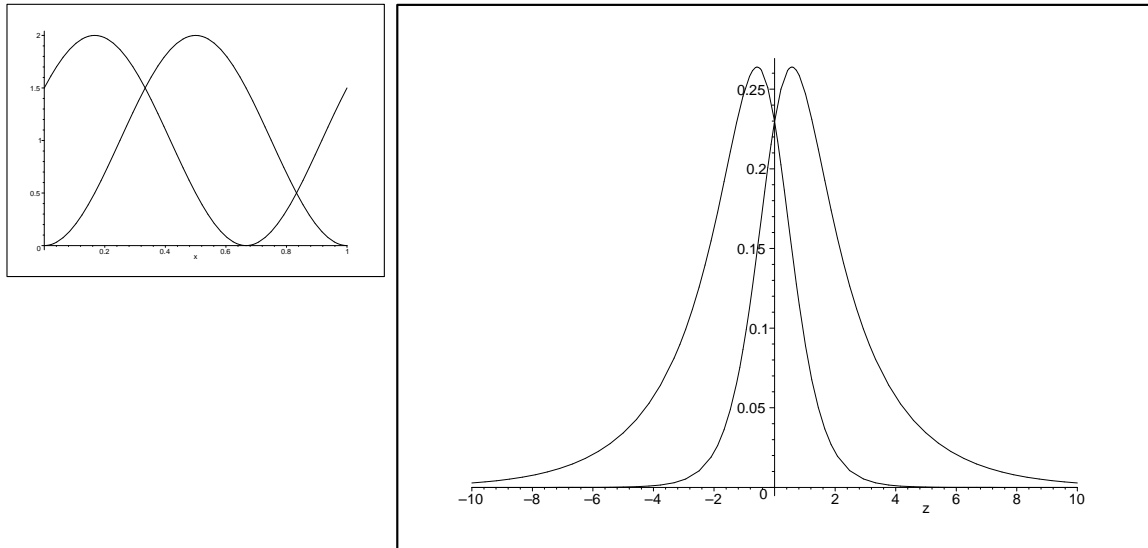
$$A = 2 \cos^2(\pi(x - \frac{1}{2})) \quad B = 2 \cos^2(\pi(x - \frac{1}{2} - \frac{2}{3}))$$

Characteristic values for this example are:

$$\mu = \frac{3}{2} \quad \sigma^2 + \mu^2 \approx 6,959 \quad \sigma \approx 2,17$$

Expressions for $P_n^{A/B}(z)$ are not nice to write down. Therefore we plotted them in fig. A.6.

Figure A.6: $A(x)$ and $B(x)$ (l), $P_1^A(z)$ and $P_1^B(z)$ (r), from example (3)



Example (4)

Now, we choose different forms for $A(x)$ and $B(x)$:

$$A = 2x \quad B = 1$$

B is now the most simple probability distribution one can imagine: a constant one. This is no obstruction whatsoever, and we calculated $P_1^A(z)$:

$$P_1^A(z) = \frac{1}{2}e^{2z} \cdot \theta(\ln 2 - z) \quad P_1^B(z) = \frac{1}{2}e^z \cdot \theta(\ln 2 - z)$$

With θ as the Heaviside step-function. For higher n this step becomes smoothed. $P_n^A(z)$ and $P_n^B(z)$ have different, i.e. not opposite, means now:

$$\mu_A = \ln 2 - \frac{1}{2} \approx 0,19 \quad \mu_B = \ln 2 - 1 \approx -0,31$$

$$\sigma_A^2 = \frac{1}{4} \quad \sigma_B^2 = 1$$

$$P_2^A(z) = \frac{1}{4}e^{2z}(2 \ln 2 - z)\theta(2 \ln 2 - z) \quad P_2^B(z) = \frac{1}{4}e^z(2 \ln 2 - z)\theta(2 \ln 2 - z)$$

See fig. A.7 for $P_1^A(z)$ and $P_1^B(z)$.

Example (5)

In the previous examples we only showed $P_n^A(z)$ or $P_n^B(z)$, but not $P_n(z)$ itself. In fig. A.8 we do show $P_n(z)$ and its dependence on α^2 and β^2 . For simplicity, We used gaussian normal distributions for $P_n^A(z)$ and $P_n^B(z)$.

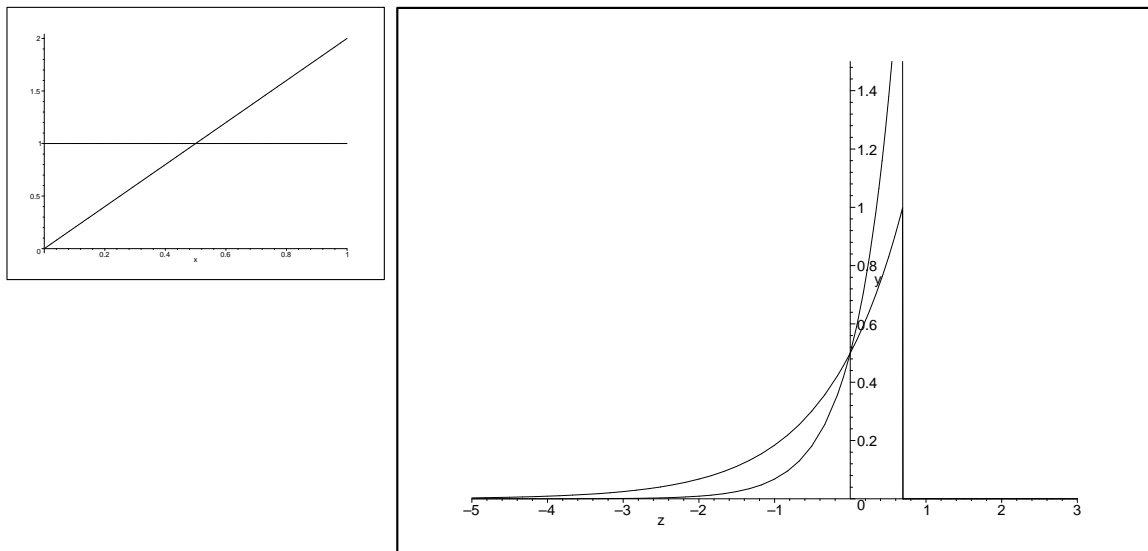
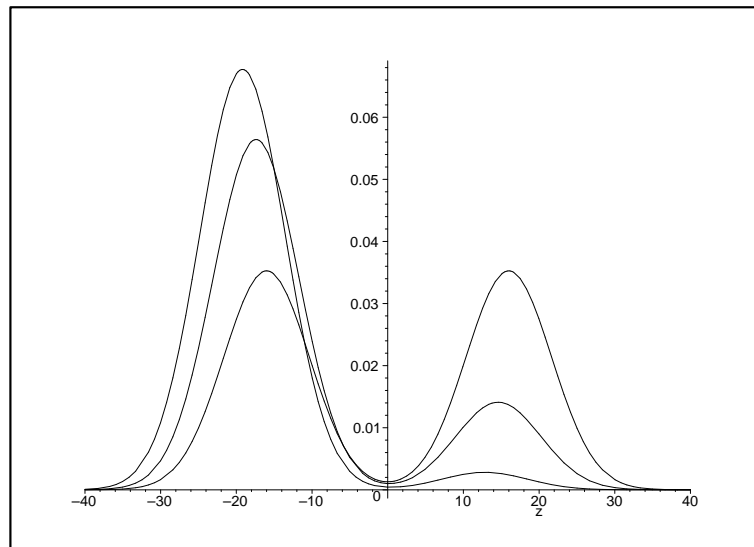
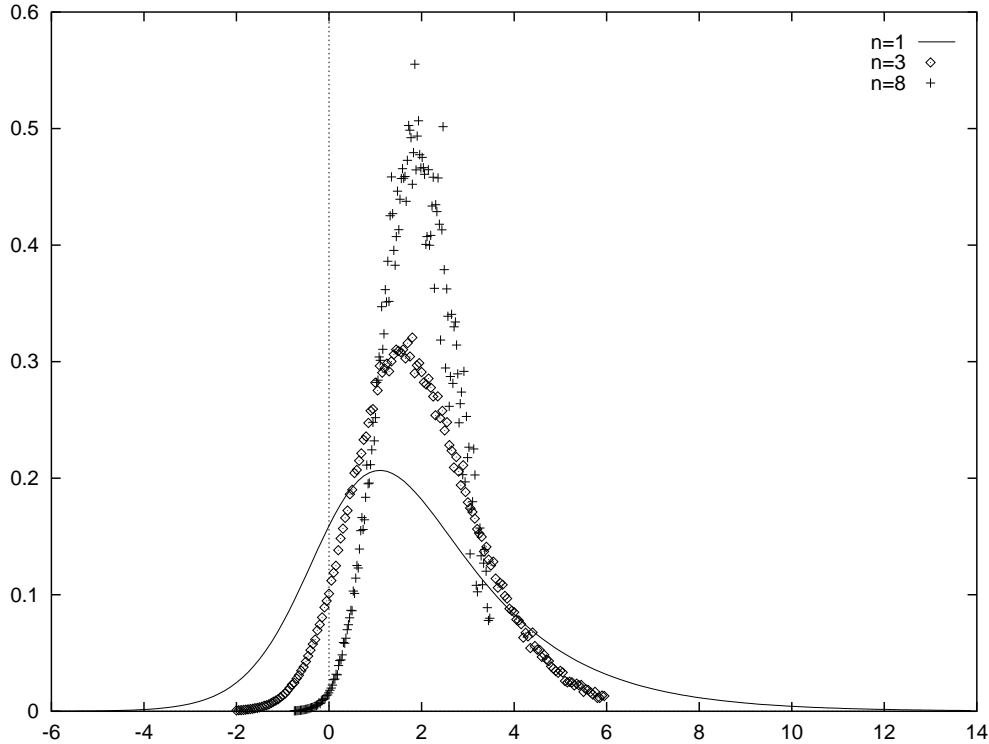
Figure A.7: $A(x)$ and $B(x)$ (l), $P_1^A(z)$ and $P_1^B(z)$ (r), from example (4)Figure A.8: This is what $P_n(z)$ looks like, for $n = 8$ and $\alpha^2 = \frac{1}{2}$; 0,2 and 0,04 (used $P^A(z)$ and $P^B(z)$ are gaussian normal distributions, with $\mu = \pm 2$ and $\sigma^2 = 4$)

Figure A.9: Numerical calculation of $nP_n^A(\frac{z}{n})$ for $n = 1, 3, 8$ from example (1); it approaches a delta-function.



Having seen a few examples, there seem to be further general properties for $P_n^A(z)$ and $P_n^B(z)$ than just the fact that sometimes $P_n^A(-z) = P_n^B(z)$. We will work out some of these properties now.

Limit $n \rightarrow \infty$ is a delta-function

We like to rescale $P_n^A(z)$ to make its mean value a constant. Because $\langle z \rangle_{nA} = n\mu_A$, and $\langle \frac{z}{n} \rangle_{nA} = \mu_A$ one should try $P_n^A(z) = P_n^A(\frac{z}{n})$; this function has a mean of μ_A for all n , but is not yet normalized, so we use instead:

$$\hat{P}_n^A(z) = nP_n^A\left(\frac{z}{n}\right) \quad (\text{A.26})$$

This function is normalized and has constant mean:

$$\int_{-\infty}^{\infty} \hat{P}_n^A(z) dz = 1 \quad \int_{-\infty}^{\infty} \hat{P}_n^A(z) z dz = \mu_A \quad (\text{A.27})$$

When n goes to infinity, this becomes a delta function:

$$\lim_{n \rightarrow \infty} \hat{P}_n^A(z) = \lim_{n \rightarrow \infty} n P_n^A\left(\frac{z}{n}\right) = \delta(z - \mu_A) \quad (\text{A.28})$$

In terms of $A(x)$ and $B(x)$:

$$\lim_{n \rightarrow \infty} n \int A_1 A_2 \dots A_n \delta\left(\frac{z}{n} - \ln \frac{A_1}{B_1} - \ln \frac{A_2}{B_2} \dots - \ln \frac{A_n}{B_n}\right) d\vec{x}_n = \delta\left(z - \int A \ln \frac{A}{B} dx\right) \quad (\text{A.29})$$

As there is no proof as yet, this is a conjecture. Figure A.9 clearly shows the basic idea.

P_1 yields P_2 : $P_2 = P_1 \circ P_1$

Intuitively one may think that $P_2(z)$ is somehow a combination of $P_1(z)$'s. This appears to be the case for $P^A(z)$ and $P^B(z)$ (but not for $P(z)$ itself):

$$P_2^A(z) = \int_{-\infty}^{\infty} P_1^A(z-w)P_1^A(w) dw \quad (\text{A.30})$$

because (the righthandside is equal to):

$$\begin{aligned} &= \int_{-\infty}^{\infty} \int \int A(x_1)\delta(z-w-\ln\frac{A(x_1)}{B(x_1)})A(x_2)\delta(w-\ln\frac{A(x_2)}{B(x_2)})dx_1dx_2dw \\ &= \int \int A(x_1)A(x_2)\delta(z-\ln\frac{A(x_1)A(x_2)}{B(x_1)B(x_2)})dx_1dx_2 = P_2^A(z) \end{aligned}$$

In the same way one can form $P_n^A(z)$ out of P_1^A 's and of course this is also true for $P_1^B(z)$ and $P_n^B(z)$. But this is *not* true for $P_n(z)$.

The $P_n^A(z)$ are thus of a form to which the central limit theorem (from statistics) applies, which also supports the conjecture of taking the form of a delta-function.

P^A and P^B have more similarity: $P^A = e^z P^B$

$P_n^A(z)$ and $P_n^B(z)$ have the, seemingly peculiar, property that:

$$P_n^A(z) = e^z P_n^B(z) \quad \forall n \quad (\text{A.31})$$

With $z \simeq \ln \frac{A}{B}$ this says that roughly $P^A = \frac{A}{B} P^B$.

Proof:

$$\begin{aligned} \frac{P_1^A(z)}{P_1^B(z)} &= \frac{\sum_{x_i} A(x_i) \frac{A(x_i)B(x_i)}{|A(x_i)'B(x_i)-B(x_i)'A(x_i)|}}{\sum_{x_j} B(x_j) \frac{A(x_j)B(x_j)}{|A(x_j)'B(x_j)-B(x_j)'A(x_j)|}} \\ &e^z = \frac{A(x_k)}{B(x_k)} \quad \forall k \\ &= \frac{\sum_{x_i} e^z B(x_i) \frac{A(x_i)B(x_i)}{|A(x_i)'B(x_i)-B(x_i)'A(x_i)|}}{\sum_{x_j} B(x_j) \frac{A(x_j)B(x_j)}{|A(x_j)'B(x_j)-B(x_j)'A(x_j)|}} = e^z \end{aligned}$$

For arbitrary n , using $P_1^A(z) = e^z P_1^B(z)$:

$$\begin{aligned} P_n^A(z) &= \int A(x_1) \dots A(x_n) P_1^A(z - \ln \frac{A(x_1)}{B(x_1)} \dots - \ln \frac{A(x_n)}{B(x_n)}) d\vec{x}_n \\ &= \int A_1 \dots A_n e^{z - \ln \frac{A_1}{B_1} \dots - \ln \frac{A_n}{B_n}} P_1^B(z - \ln \frac{A(x_1)}{B(x_1)} \dots - \ln \frac{A(x_n)}{B(x_n)}) d\vec{x}_n \\ &= e^z \int B(x_1) \dots B(x_n) P_1^B(z - \ln \frac{A(x_1)}{B(x_1)} \dots - \ln \frac{A(x_n)}{B(x_n)}) d\vec{x}_n \\ &= e^z P_n^B(z) \end{aligned}$$

This also implies that we can write $P_n(z)$ in terms of only $P_n^A(z)$ or $P_n^B(z)$:

$$\begin{aligned}
P_n(z, \alpha^2, \beta^2 = 1 - \alpha^2) &= \alpha^2 P_n^A(z - \ln \frac{\alpha^2}{\beta^2}) + \beta^2 P_n^B(z - \ln \frac{\alpha^2}{\beta^2}) \\
&= \beta^2 (1 + e^z) P_n^B(z - \ln \frac{\alpha^2}{\beta^2}) \\
&= \alpha^2 (1 + e^{-z}) P_n^A(z - \ln \frac{\alpha^2}{\beta^2})
\end{aligned} \tag{A.32}$$

Furthermore, if we use the z -dependent forms for α_n^2 and β_n^2 :

$$\alpha_n^2 = \frac{1}{1 + e^{-z}} \quad \beta_n^2 = \frac{1}{1 + e^z},$$

we can easily calculate their expectation values:

$$\begin{aligned}
\langle \alpha_n^2 \rangle &= \int_{-\infty}^{\infty} \alpha_n^2(z) P_n(z, \alpha^2, \beta^2) dz \\
&= \int_{-\infty}^{\infty} \frac{1}{1 + e^{-z}} \alpha^2 (1 + e^{-z}) P_n^A(z - \ln \frac{\alpha^2}{\beta^2}) dz \\
&= \alpha^2 \int_{-\infty}^{\infty} P_n^A(w) dw = \alpha^2
\end{aligned} \tag{A.33}$$

A.3 The case for arbitrary many eigenvalues extends easily from that of two eigenvalues

We now solve the problem, i.e. give the proof, for more than two eigenvalues, but this is almost a trivial job.

A.3.1 Three eigenvalues

Let's tackle the problem with three instead of two eigenvalues. This requires $A(x)$, $B(x)$ and $C(x)$. And $\alpha_n^2(\vec{x}_n)$, $\beta_n^2(\vec{x}_n)$ and $\gamma_n^2(\vec{x}_n)$ and a probability density distribution $p_n(\vec{x}_n)$:

$$p_n(\vec{x}) = \alpha^2 A(x_1) A(x_2) \dots A(x_n) + \beta^2 B(x_1) \dots B(x_n) + \gamma^2 C(x_1) \dots C(x_n) \tag{A.34}$$

As a reminder:

$$\gamma_n^2 = \frac{C(x_1) \dots C(x_n)}{p_n(\vec{x}_n)} \tag{A.35}$$

Again we will create a new probability distribution, but it will now be dependent of two variables, z and w , instead of only z , and it indicates the probability that at the same time $\frac{\alpha_n^2}{\beta_n^2} = e^z$ and $\frac{\alpha_n^2}{\gamma_n^2} = e^w$:

$$P_n(z, w) = \int P(\vec{x}_n) \delta(z - \ln \frac{\alpha_n^2}{\beta_n^2}) \delta(w - \ln \frac{\alpha_n^2}{\gamma_n^2}) d\vec{x}_n \tag{A.36}$$

$$\begin{aligned}
&= \alpha^2 P_n^A(z - \ln \frac{\alpha^2}{\beta^2}, w - \ln \frac{\alpha^2}{\gamma^2}) + \beta^2 P_n^B(z - \ln \frac{\alpha^2}{\beta^2}, w - \ln \frac{\alpha^2}{\gamma^2}) \\
&\quad + \gamma^2 P_n^C(z - \ln \frac{\alpha^2}{\beta^2}, w - \ln \frac{\alpha^2}{\gamma^2})
\end{aligned} \tag{A.37}$$

With of course:

$$P_n^A(z, w) = \int A(x_1)A(x_2) \dots A(x_n) \delta(z - \ln \frac{A(x_1) \dots A(x_n)}{B(x_1) \dots B(x_n)}) \delta(w - \ln \frac{A(x_1) \dots A(x_n)}{C(x_1) \dots C(x_n)}) d\vec{x}_n$$

For $P_n^B(z, w)$ and $P_n^C(z, w)$ one should replace some of the $A(x)$'s with $B(x)$'s or $C(x)$'s. We continue as in the case of two eigenvalues:

$$P_2^A(z, w) = \int \int P_1^A(z - \hat{z}, w - \hat{w}) P_1^A(\hat{z}, \hat{w}) d\hat{z} d\hat{w} \tag{A.38}$$

and similar for P^B and P^C .

$$\langle z \rangle_n^A = \int \int P_n^A(z, w) z dz dw = n \langle z \rangle_1^A > 0 \tag{A.39}$$

$$\langle w \rangle_n^A = n \langle w \rangle_1^A > 0 \tag{A.40}$$

$$\sigma_n^{A^2}(z) = n \sigma_1^{A^2}(z) \quad \sigma^2(z) = \langle z^2 \rangle - \langle z \rangle^2 \tag{A.41}$$

and likewise for w , and B and C , with the exception of:

$$\langle z \rangle_1^B < 0 \quad \langle w \rangle_1^B > \langle z \rangle_1^B$$

$$\langle w \rangle_1^C < 0 \quad \langle z \rangle_1^C > \langle w \rangle_1^C$$

which one should be able to show using previous techniques.

$$\alpha_n^2(z, w) = \frac{1}{1 + e^{-z} + e^{-w}} \quad \beta_n^2 = \frac{1}{1 + e^z + e^{z-w}} \quad \gamma_n^2 = \frac{1}{1 + e^w + e^{w-z}} \tag{A.42}$$

Projection can again be made visible as in fig. A.10.

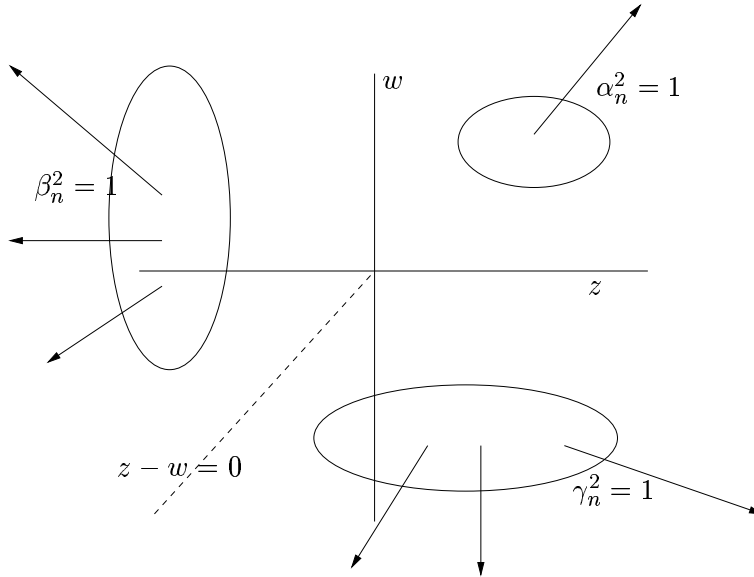


Figure A.10: The two dimensional $z-w$ -plane becomes divide into three parts. In each part one of $\alpha_n^2, \beta_n^2, \gamma_n^2$ becomes 1, the other two vanish. $P_n(z)$ is a sum of three terms, $P_n^A(z), P_n^B(z), P_n^C(z)$ which all 'float' in their own direction, away from the origin. For the precise directions, $A(x), B(x), C(x)$ have to be known.

One can also rewrite $P_n(z, w, \alpha^2, \beta^2, \gamma^2 = 1 - \alpha^2 - \beta^2)$ to:

$$P_n(z, w) = \alpha^2(1 + e^{-z} + e^{-w})P_n^A(z - \ln \frac{\alpha^2}{\beta^2}, w - \ln \frac{\alpha^2}{\gamma^2}) \tag{A.43}$$

A.3.2 M eigenvalues

The extension to M eigenvalues becomes almost trivial now: this requires M coefficients $\alpha_n^{i,2}$ and M functions $A^i(x)$ ($i \in \{1, 2, \dots, M\}$). Next, we define a new probability distribution as the chance that:

$$\frac{\alpha_n^{1,2}}{\alpha_n^{i,2}} = e^{z_i} \quad \forall i \in \{2, 3, \dots, M\}$$

We call this probability distribution $P_n(z_2, z_3, \dots, z_M) = P_n(\vec{z})$.

$$P_n(\vec{z}) = \sum_{i=1}^M \alpha_n^{i,2} P_n^i(\vec{z} - \vec{v}) \quad \vec{v} = \left(\ln \frac{\alpha_n^{1,2}}{\alpha_n^{2,2}}, \dots, \ln \frac{\alpha_n^{1,2}}{\alpha_n^{M,2}} \right)$$

and furthermore:

$$\int P_n^i(\vec{z}) d\vec{z} = 1 \quad P_2^i(\vec{z}) = \int P_1^i(\vec{z} - \vec{w}) P_1^i(\vec{w}) d\vec{w}$$

$$\langle z_j \rangle_n^i = \int P_n^i(\vec{z}) z_j d\vec{z} = n \langle z_j \rangle_1^i$$

$$\sigma_{jn}^{i,2} = \langle z_j^2 \rangle_n^i - (\langle z_j \rangle_n^i)^2 = n \sigma_{j1}^{i,2}$$

So much for that.

The conclusion remains that projection will take place, if and only if the functions $A(x)$, $B(x)$, $C(x)$ etcetera (the eigenvalue ‘patterns’) are different.

APPENDIX B

THE SPECTRUM OF $D(H)$, WITH $H = S_3$ AS AN EXAMPLE

In this appendix, we discuss the spectrum and structure of a the quantum double $D(H)$ of a finite group H . We use $H = S_3$ as a model; the choice for S_3 has not been because of the relation between the braid group and the permutation group, but because S_3 is the smallest finite non-abelian group.

B.1 The group S_3 , irreps of $D(S_3)$

The group that we will use to show the structure of a $D(H)$ explicitly is S_3 , which is the group of permutations on three objects. It is also isomorphic to D_3 . S_3 contains six elements. Elements of S_3 are written using the so called *cycle notation*. For instance, (123) means: move the object on the first position to position two, that of two to position three, and move the object of position three to the first position.

$$S_3 = \{e, (12), (13), (23), (123), (132)\} \simeq D_3 = \{e, r, r^2, q, qr, qr^2\} \quad (\text{B.1})$$

Multiplication of cycles, i.e. the group multiplication, is easy in cycle notation.

$$(13)(12) = (123) \quad e = () \quad (12)(12) = e = (1)(2) \quad (\text{B.2})$$

We will not give a complete multiplication table, because this is not necessary for $D(S_3)$. The *conjugation* table however, is important. It describes how group-elements change when conjugated by another element.

Table B.1: Conjugation table of S_3 : vuv^{-1}

$v \backslash u$	e	(12)	(13)	(23)	(123)	(132)
e	e	12	13	23	123	132
(12)	e	12	23	13	132	123
(13)	e	23	13	12	132	123
(23)	e	13	12	23	132	123
(123)	e	23	12	13	123	132
(132)	e	13	23	12	123	132

Table B.2: Conjugacy classes and centralizers.

${}^1C = \{e\}$	${}^eN = \{e, (12), (13), (23), (123), (132)\}$	${}^1N = S_3$
${}^2C = \{(12), (13), (23)\}$	${}^{(12)}N = \{e, (12)\}$ ${}^{(13)}N = \{e, (13)\}$ ${}^{(23)}N = \{e, (23)\}$	${}^2N \simeq \mathbb{Z}_2 = \{e, a\}$
${}^3C = \{(123), (132)\}$	${}^{(123)}N = \{e, (123), (132)\}$ ${}^{(132)}N = \{e, (132), (123)\}$	${}^3N \simeq \mathbb{Z}_3 = \{e, z, z^2\}$

When the conjugation table is given, one can determine the different conjugacy classes ${}^A C$ and centralizers ${}^h N$ of elements $h \in H$ and centralizers ${}^A N$ of classes ${}^A C$.

Next, we calculate the character-tables for the centralizers of the conjugacy classes. These centralizers are probably isomorphic to other well-known finite groups, of which the character tables are also known.

Table B.3: Character-tables for S_3 , \mathbb{Z}_2 and \mathbb{Z}_3 , with $\omega = e^{2\pi i/3}$.

S_3	1C	2C	3C	\mathbb{Z}_2	e	a	\mathbb{Z}_3	e	z	z^2
$\mathbb{1}$	1	1	1	$\mathbb{1}$	1	1	$\mathbb{1}$	1	1	1
A	1	-1	1	C	1	-1	D	1	ω	ω^2
B	2	0	-1				E	1	ω^2	ω

We can now classify the different particles in the spectrum of $D(S_3)$ by combining a conjugacy class with one of its centralizer irreps. We can conclude that there are eight different particles in $D(S_3)$.

Table B.4: Particles in the spectrum of $D(S_3)$: (${}^A C$, irrep of ${}^A N$).

$ \mathbb{1}\rangle$:=	$(e, \mathbb{1})$	$ (12)\rangle$:=	$({}^2C, \mathbb{1})$	$ (123)\rangle$:=	$({}^3C, \mathbb{1})$
$ A\rangle$:=	(e, A)	$ C\rangle$:=	$({}^2C, C)$	$ D\rangle$:=	$({}^3C, D)$
$ B\rangle$:=	(e, B)				$ E\rangle$:=	$({}^3C, E)$

B.2 Character matrices for $D(H)$ irreps, spin

We now construct the character tables for the different irreps Π_α^A of $D(S_3)$, i.e. the traces of irreps of the algebra $D(S_3)$. Let us write the matrix-components of $\Pi_\alpha^A(P_h g)$ once more:

$$\Pi_\alpha^A(P_h g)|{}^A h_i, \alpha v_j\rangle = \delta_{h, g A h_i g^{-1}} |g A h_i g^{-1}, \alpha(\tilde{g})_{mj} \alpha v_m\rangle \quad (\text{B.3})$$

We observe that quite often the matrix $\Pi_\alpha^A(P_h g)$ is equal to the null matrix. This is when h is not an element of the conjugacy class ${}^A C$. Then, also the character of $\Pi_\alpha^A(P_h g)$ vanishes.

$$\Pi_\alpha^A(P_h g) = 0 \text{ if: } h \notin {}^A C \quad \Rightarrow \quad \text{Tr}(\Pi_\alpha^A(P_h g)) = 0 \quad (\text{B.4})$$

But the trace of $\Pi_\alpha^A(P_h g)$ is equal to zero at more occasions, namely if h and g do not commute.

$$\text{Tr}(\Pi_\alpha^A(P_h g)) = 0 \text{ (also), if: } gh \neq hg \tag{B.5}$$

So, there are a few h and g for which $\text{Tr}(\Pi_\alpha^A(P_h g))$ is non-zero. In those cases it is equal to a particular value of the character table of the irrep α .

$$h \in {}^A C, g \in {}^h N \Rightarrow \text{Tr}(\Pi_\alpha^A(P_h g)) = \text{Tr}[\alpha(g)] \text{ with } \alpha \text{ irrep of } {}^h N \simeq {}^A N \tag{B.6}$$

The character-table for the irreps of $D(S_3)$ can be conveniently written as character-matrices M_α^A .

$$M_\alpha^A(P_h g) = \text{Tr}(\Pi_\alpha^A(P_h g)) = (M_\alpha^A)_g^h \tag{B.7}$$

We will now give these character-matrices for $D(S_3)$. We use a ‘-’ to indicate that $\Pi_\alpha^A(P_h g)$ is the null matrix, of which the trace is of course also zero.

$M_{1/A/B}^1(P_h g) =$	$P_h \backslash g$	e	(12)	(13)	(23)	(123)	(132)
	e	${}^1 C$	${}^2 C$	${}^2 C$	${}^2 C$	${}^3 C$	${}^3 C$
	(12)	-	-	-	-	-	-
	(13)	-	-	-	-	-	-
	(23)	-	-	-	-	-	-
	(123)	-	-	-	-	-	-
	(132)	-	-	-	-	-	-
$\sum_h P_h$		${}^1 C$	${}^2 C$	${}^2 C$	${}^2 C$	${}^3 C$	${}^3 C$
$M_{1/C}^2(P_h g) =$	$P_h \backslash g$	e	(12)	(13)	(23)	(123)	(132)
	e	-	-	-	-	-	-
	(12)	1	a	0	0	0	0
	(13)	1	0	a	0	0	0
	(23)	1	0	0	a	0	0
	(123)	-	-	-	-	-	-
	(132)	-	-	-	-	-	-
$\sum_h P_h$		3	a	a	a	0	0
$M_{1/C/D}^3(P_h g) =$	$P_h \backslash g$	e	(12)	(13)	(23)	(123)	(132)
	e	-	-	-	-	-	-
	(12)	-	-	-	-	-	-
	(13)	-	-	-	-	-	-
	(23)	-	-	-	-	-	-
	(123)	1	0	0	0	z	z^2
	(132)	1	0	0	0	z^2	z
$\sum_h P_h$		2	0	0	0	$z + z^2$	$z + z^2$

If we sum up all rows of the matrix M_α^A , we find the the character for the induced representation $T_\alpha^A(g)$ of the group S_3 , induced from the quantum double irrep Π_α^A . The decomposition of Π_α^A in irreps of S_3 can now be easily calculated using the character-table of S_3 and orthogonality of characters.

$$T_\alpha^A(g) = \sum_h \Pi_\alpha^A(P_h g) \tag{B.8}$$

$$\mathrm{Tr}(T_\alpha^A(g)) = \mathrm{Tr}\left(\sum_h \Pi_\alpha^A(P_h g)\right) = \sum_h M_\alpha^A(P_h g) \quad (\text{B.9})$$

If we trace the matrix M_α^A , we find a multiple of the *spin* $e^{2\pi i s_{A,\alpha}}$ of the particle Π_α^A . Each centralizer hN has a central element: h commutes by definition with all other elements of the centralizer. The hN -irrep-matrix for h is therefore always a multiple of the unit matrix. This multiplicity-value is the spin of the particle Π_α^A .

$$\mathrm{Tr}(M_\alpha^A) = \sum_g M_\alpha^A(P_g g) = |{}^A C| e^{2\pi i s_{A,\alpha}} \quad (\text{B.10})$$

It is called spin, because if we rotate particle Π_α^A counterclockwise over 360 degrees, its wave-function gets multiplied by the factor $e^{2\pi i s_{A,\alpha}}$. Also if we exchange to identical particles Π_α^A counterclockwise then the two-particle wave function obtains this phase factor. However this last equality turns out to be *only* true for specific internal states of the identical particles Π_α^A . For such cases, it is called the *canonical spin-statistics connection*, see Propitius and Bais [11][p. 52], and the two particle state $|\psi\rangle$ usually is entangled:

$$|\psi\rangle = \sum_{i: {}^A h_i \in {}^A C} c_i |{}^A h_i\rangle |{}^A h_i\rangle \quad \sum_i |c_i|^2 = 1 \quad (\text{B.11})$$

$$\mathcal{R}|\psi\rangle = e^{2\pi i s_{A,\alpha}} |\psi\rangle \quad (\text{B.12})$$

Bosons have integral spin, fermions have spin 1/2, anyons (both abelian and non-abelian) have any fractional spin.

We will now state both the induced $H = S_3$ -group-representation decomposition and the spin of the particles Π_α^A . We also give the dimension of the internal states of the eight different particles

Table B.5: Spin and group-irrep decomposition for the particles of $D(S_3)$.

particle	dimension	$e^{2\pi i s}$	spin s	H irrep decomposition
$ \mathbb{1}\rangle$	1	1	0	$ \mathbb{1}\rangle$
$ A\rangle$	1	1	0	$ A\rangle$
$ B\rangle$	2	1	0	$ B\rangle$
$ (12)\rangle$	3	1	0	$ \mathbb{1}\rangle + B\rangle$
$ C\rangle$	3	-1	1/2	$ A\rangle + B\rangle$
$ (123)\rangle$	2	1	0	$ \mathbb{1}\rangle + A\rangle$
$ D\rangle$	2	$e^{2\pi i/3}$	2/3	$ B\rangle$
$ E\rangle$	2	$e^{4\pi i/3}$	4/3	$ B\rangle$

B.3 S -matrix, fusion rules and \mathcal{R}^2 -eigenvalues

We would like to calculate the fusion rules now. This calculation is simplified by using the so called S -matrix:

$$S_{\alpha\beta}^{AB} = \frac{1}{|H|} \mathrm{Tr}(\mathcal{R}^{-2AB}_{\alpha\beta}) \quad (\text{B.13})$$

For $H = S_3$, $S_{\alpha\beta}^{AB}$ is thus a 8×8 matrix.

It turns out that the S -matrix itself can easily be calculated with the character-matrices M_α^A . Traces of $D(H)$ -irreps are the same for $P_h g$ and $g P_h$ although these are not the same elements in $D(H)$:

$$P_h g \neq g P_h \quad (\text{B.14})$$

$$\text{Tr}(\Pi_\alpha^A(P_h g)) = \text{Tr}(\Pi_\alpha^A(P_{ghg^{-1}g})) = \text{Tr}(\Pi_\alpha^A(g P_h)) \quad (\text{B.15})$$

With this relation, S_α^{AB} is the trace of the product of M_α^A and M_β^B :

$$|H| S_{\alpha\beta}^{AB} = \text{Tr}((\mathcal{R}^{-2})_{\alpha\beta}^{AB}) \quad (\text{B.16})$$

$$= \text{Tr}((\mathcal{R}^2)_{\alpha\beta}^{AB})^* \quad (\text{B.17})$$

$$= \text{Tr}(\Pi_\alpha^A \otimes \Pi_\beta^B (\sum_{h,g} h P_g \otimes P_h g))^* \quad (\text{B.18})$$

$$= \left[\sum_{h,g} \text{Tr}(\Pi_\alpha^A(h P_g)) \text{Tr}(\Pi_\beta^B(P_h g)) \right]^* \quad (\text{B.19})$$

$$= \left[\sum_{h,g} (M_\alpha^A)^g_h (M_\beta^B)^h_g \right]^* \quad (\text{B.20})$$

$$= \text{Tr}(M_\alpha^A M_\beta^B)^* \quad (\text{B.21})$$

We can also write the orthogonality relations for the characters of $D(H)$ -irreps in matrix-form:

$$\frac{1}{|H|} \text{Tr}[M_\alpha^A (M_\beta^B)^\dagger] = \delta_{A,B} \delta_{\alpha,\beta}, \quad (\text{B.22})$$

but this is not relevant at the moment.

The S -matrix now takes the following form:

Table B.6: S -matrix: $|H| S_{\alpha\beta}^{AB}$

		B, β							
		$ \mathbb{1}\rangle$	$ A\rangle$	$ B\rangle$	$ (12)\rangle$	$ C\rangle$	$ (123)\rangle$	$ D\rangle$	$ E\rangle$
A, α	$ \mathbb{1}\rangle$	1	1	2	3	3	2	2	2
	$ A\rangle$	1	1	2	-3	-3	2	2	2
	$ B\rangle$	2	2	4	0	0	-2	-2	-2
	$ (12)\rangle$	3	-3	0	3	-3	0	0	0
	$ C\rangle$	3	-3	0	-3	3	0	0	0
	$ (123)\rangle$	2	2	-2	0	0	4	-2	-2
	$ D\rangle$	2	2	-2	0	0	-2	-2	4
	$ E\rangle$	2	2	-2	0	0	-2	4	-2

With the S -matrix, the fusion rules, i.e. the coefficients $N_{\alpha\beta C}^{AB\gamma}$ follow from multiplication of its rows:

$$\Pi_\alpha^A \otimes \Pi_\beta^B = \bigoplus_{C,\gamma} N_{\alpha\beta C}^{AB\gamma} \Pi_\gamma^C \quad (\text{B.23})$$

$$N_{\alpha\beta C}^{AB\gamma} = \sum_{D,\delta} \frac{S_{\alpha\delta}^{AD} S_{\beta\delta}^{BD} (S^*)_{\gamma\delta}^{CD}}{S_{1\delta}^{eD}} \quad (\text{B.24})$$

Table B.7: Fusion rules for $D(S_3)$.

$A \times A = 1$		
$A \times B = B$	$B \times B = 1 + A + B$	
$A \times (12) = C$	$B \times (12) = (12) + C$	$(12) \times (12) = 1 + B + (123) + D + E$
$A \times C = (12)$	$B \times C = (12) + C$	$(12) \times C = A + B + (123) + D + E$
$A \times (123) = (123)$	$B \times (123) = D + E$	$(12) \times (123) = (12) + C$
$A \times D = D$	$B \times D = (123) + E$	$(12) \times D = (12) + C$
$A \times E = E$	$B \times E = (123) + D$	$(12) \times E = (12) + C$
$D \times D = 1 + A + D$	$(123) \times (123) = 1 + A + (123)$	$C \times C = 1 + B + (123) + D + E$
$D \times E = B + (123)$	$(123) \times D = B + E$	$C \times (123) = (12) + C$
	$(123) \times E = B + D$	$C \times D = (12) + C$
$E \times E = 1 + A + E$		$C \times E = (12) + C$

We calculated the fusion rules for S_3 . Fusion of Π_α^A with the vacuum $|\mathbb{1}\rangle$ always yields Π_α^A .

The fusion rules in this form are just a blob of information. However, the fusion rules can be written more compact, if we make the following identifications:

$$\begin{aligned}
 \mathbb{1} &:= 1 \\
 A &:= A \\
 K^{a/b} &:= (12), C \\
 J^{w/x/y/z} &:= B, (123), D, E
 \end{aligned}$$

The fusion rules now compactify to:

$$\begin{aligned}
 A \times A &= \mathbb{1} \\
 A \times K^a &= T^b \\
 A \times J^w &= J^w \\
 \\
 K^a \times K^a &= \mathbb{1} + J^w + J^x + J^y + J^z \\
 K^a \times K^b &= A + J^w + J^x + J^y + J^z \\
 K^a \times K^w &= K^a + K^b \\
 \\
 J^w \times J^w &= \mathbb{1} + A + J^w \\
 J^w \times J^x &= J^y + J^z
 \end{aligned}$$

Of real interest are the various \mathcal{R}^2 -matrices. With the fusion rules and the spin of the particles, we can determine the eigenvalues for \mathcal{R}^2 -matrices. The eigenvalues for \mathcal{R}^2 operating on Π_α^A and Π_β^B are the spins for the particles Π_γ^C appearing in the fusion channel, corrected for the spins of Π_α^A and Π_β^B :

$$\mathcal{R}^2|\lambda_{A,\alpha,B,\beta}\rangle = \lambda|\lambda_{A,\alpha,B,\beta}\rangle \quad \lambda = e^{2\pi i(s_C - s_A - s_B)} \tag{B.25}$$

Most of the different possible \mathcal{R}^2 operators are equal to the identity operator. Those that are not are combined in the following table:

particles on which \mathcal{R}^2 operates	$n \cdot \lambda$: n fold degeneracy of \mathcal{R}^2 -eigenvalue λ
A, K^a	$2 \cdot -1$
$K^a, K^{a/b}$	$5 \cdot 1 + 2 \cdot e^{2\pi i/3} + 2 \cdot e^{4\pi i/3}$
K^a, J^w	$3 \cdot 1 + 3 \cdot -1$
J^w, J^w	$2 \cdot 1 + 2 \cdot e^{-2\pi i s_w}$
J^w, J^x	$\{4 \cdot 1\}$ or $\{2 \cdot e^{2\pi i/3} + 2 \cdot e^{4\pi i/3}\}$ depending on w and x $= 2 \cdot e^{2\pi i(s_y - s_w - s_x)} + 2 \cdot e^{2\pi i(s_z - s_w - s_x)}$

Explicit forms of matrices, of both the irreps $\Pi_\alpha^A(P_{hg})$ and \mathcal{R}^2 -operators have to be worked out further, and this cannot be done generically. One can use a computer-program and the construction with \tilde{g} (see (4.31), p. 54) to do this. One can also construct these matrices by hand, where the decomposition into group-irreps is a valuable tool.

However, both methods, by computer and by hand, require the explicit forms of irrep-matrices of the centralizers ${}^A N$. One-dimensional irreducible representations are equal to the characters, but higher-dimensional irreps are not, of course. For $H = S_3$, there is one two-dimensional irrep, which we will give now, written in various different bases:

Table B.8: The 2-dimensional irrep of S_3 (B) in explicit matrices and some basis transformations.

	(12)	(13)	(23)	(123)	(132)
$ b_+\rangle$ $ b_-\rangle$	$\begin{pmatrix} -\frac{1}{2} & \frac{1}{2}\sqrt{3} \\ \frac{1}{2}\sqrt{3} & \frac{1}{2} \end{pmatrix}$	$\begin{pmatrix} 1 & 0 \\ 0 & -1 \end{pmatrix}$	$\begin{pmatrix} -\frac{1}{2} & -\frac{1}{2}\sqrt{3} \\ -\frac{1}{2}\sqrt{3} & \frac{1}{2} \end{pmatrix}$	$\begin{pmatrix} -\frac{1}{2} & \frac{1}{2}\sqrt{3} \\ -\frac{1}{2}\sqrt{3} & -\frac{1}{2} \end{pmatrix}$	$\begin{pmatrix} -\frac{1}{2} & -\frac{1}{2}\sqrt{3} \\ \frac{1}{2}\sqrt{3} & -\frac{1}{2} \end{pmatrix}$
$ B_1\rangle$ $ B_2\rangle$	$\begin{pmatrix} 0 & e^{4\pi i/3} \\ e^{2\pi i/3} & 0 \end{pmatrix}$	$\begin{pmatrix} 0 & 1 \\ 1 & 0 \end{pmatrix}$	$\begin{pmatrix} 0 & e^{2\pi i/3} \\ e^{4\pi i/3} & 0 \end{pmatrix}$	$\begin{pmatrix} e^{2\pi i/3} & 0 \\ 0 & e^{4\pi i/3} \end{pmatrix}$	$\begin{pmatrix} e^{4\pi i/3} & 0 \\ 0 & e^{2\pi i/3} \end{pmatrix}$
$ a_+\rangle$ $ a_-\rangle$	$\begin{pmatrix} 1 & 0 \\ 0 & -1 \end{pmatrix}$	$\begin{pmatrix} -\frac{1}{2} & -\frac{1}{2}\sqrt{3} \\ -\frac{1}{2}\sqrt{3} & \frac{1}{2} \end{pmatrix}$	$\begin{pmatrix} -\frac{1}{2} & \frac{1}{2}\sqrt{3} \\ \frac{1}{2}\sqrt{3} & \frac{1}{2} \end{pmatrix}$	$\begin{pmatrix} -\frac{1}{2} & \frac{1}{2}\sqrt{3} \\ -\frac{1}{2}\sqrt{3} & -\frac{1}{2} \end{pmatrix}$	$\begin{pmatrix} -\frac{1}{2} & -\frac{1}{2}\sqrt{3} \\ \frac{1}{2}\sqrt{3} & -\frac{1}{2} \end{pmatrix}$
$ c_+\rangle$ $ c_-\rangle$	$\begin{pmatrix} -\frac{1}{2} & -\frac{1}{2}\sqrt{3} \\ -\frac{1}{2}\sqrt{3} & \frac{1}{2} \end{pmatrix}$	$\begin{pmatrix} -\frac{1}{2} & \frac{1}{2}\sqrt{3} \\ \frac{1}{2}\sqrt{3} & \frac{1}{2} \end{pmatrix}$	$\begin{pmatrix} 1 & 0 \\ 0 & -1 \end{pmatrix}$	$\begin{pmatrix} -\frac{1}{2} & \frac{1}{2}\sqrt{3} \\ -\frac{1}{2}\sqrt{3} & -\frac{1}{2} \end{pmatrix}$	$\begin{pmatrix} -\frac{1}{2} & -\frac{1}{2}\sqrt{3} \\ \frac{1}{2}\sqrt{3} & -\frac{1}{2} \end{pmatrix}$
	$ a_+\rangle = \begin{pmatrix} b_+\rangle & b_-\rangle \\ \frac{1}{2} & \frac{1}{2}\sqrt{3} \\ -\frac{1}{2}\sqrt{3} & \frac{1}{2} \end{pmatrix}$	$ c_+\rangle = \begin{pmatrix} b_+\rangle & b_-\rangle \\ \frac{1}{2} & -\frac{1}{2}\sqrt{3} \\ \frac{1}{2}\sqrt{3} & \frac{1}{2} \end{pmatrix}$		$ B_1\rangle = \begin{pmatrix} b_+\rangle & b_-\rangle \\ \frac{1}{\sqrt{2}} & \frac{i}{\sqrt{2}} \\ \frac{1}{\sqrt{2}} & -\frac{i}{\sqrt{2}} \end{pmatrix}$	$ B_2\rangle = \begin{pmatrix} b_+\rangle & b_-\rangle \\ \frac{1}{\sqrt{2}} & \frac{i}{\sqrt{2}} \\ \frac{1}{\sqrt{2}} & -\frac{i}{\sqrt{2}} \end{pmatrix}$

B.4 An alternative $D(H)$ character-table

It is possible to construct a character-table for $D(S_3)$ that differs from the character-matrices M_α^A . We already observed that the character of $\Pi_\alpha^A(P_{hg})$ is zero when h and g do not commute. Let us then restrict ourselves to P_{hg} with $hg = gh$. If such a pair (h, g) , or (h_1, h_2) , is conjugated by another element, then the resulting pair is still a commuting pair:

$$g: (h_1, h_2) \mapsto (gh_1g^{-1}, gh_2g^{-1}) \tag{B.26}$$

$$h_1h_2 = h_2h_1 \Rightarrow (gh_1g^{-1})(gh_2g^{-1}) = (gh_2g^{-1})(gh_1g^{-1}) \tag{B.27}$$

But under this conjugation-action of g , the trace of the matrix $\Pi_\alpha^A(P_{h_1} h_2)$ is invariant:

$$\text{Tr}(\Pi_\alpha^A(P_{h_1} h_2)) = \text{Tr}(\Pi_\alpha^A(P_{gh_1g^{-1}} gh_2g^{-1})) \quad (\text{B.28})$$

Some sort of conjugation classes of commuting pairs can be formed:

$$C^{(h_1, h_2)} = \{(gh_1g^{-1}, gh_2g^{-1}) \mid g \in H\} \quad (\text{B.29})$$

A character-*table* of $D(H)$ is a matrix, where the rows are labeled by the irreps of $D(H)$ and the columns by the different conjugation classes of commuting pairs. The order can always be chosen in such a way, that this is a block diagonal matrix, where the blocks are the character tables of the centralizers.

Table B.9: Character-table for $D(S_3)$.

	e, e	$e, (12)$	$e, (123)$	$(12), e$	$(12), (12)$	$(123), e$	$(123), (123)$	$(123), (132)$
$\mathbb{1}$	1	1	1	-	-	-	-	-
A	1	-1	1	-	-	-	-	-
B	2	0	-1	-	-	-	-	-
(12)	-	-	-	1	-1	-	-	-
C	-	-	-	1	-1	-	-	-
(123)	-	-	-	-	-	1	1	1
D	-	-	-	-	-	1	ω	ω^2
E	-	-	-	-	-	1	ω^2	ω
$ C^{(h, g)} $	1	3	2	3	3	2	2	2

The rows and columns of the character-table are orthogonal, when taking the number of elements $|C^{(h, g)}|$ in each conjugacy class of commuting pairs in account.

Calculating the S -matrix is simplified as well. Let P be the matrix that permutes the conjugacy class of a pair, in the sense that it exchanges its members:

$$P: (h_1, h_2) \mapsto (h_2, h_1) \quad (\text{B.30})$$

Let furthermore D be the diagonal matrix with the number of elements $|C^{(h, g)}|$ in each conjugacyclass, then, with C as the character-table, then:

$$S^* = CPDC^T \quad (\text{B.31})$$

$$S_{\alpha\beta}^{AB} = \left(C_{\alpha I_1}^A P_{I_1}^{I_2} D_{I_2}^{I_3} (C^T)_{I_3 \beta}^B \right)^* \quad (\text{B.32})$$

$$[P, D] = 0, P^T = P, P^2 = \mathbb{1}, D^T = D \quad \Rightarrow \quad S = S^T \quad (\text{B.33})$$

For $H = S_3$ the orthogonal symmetric ‘permutation’-matrix P is:

$$P = \begin{matrix} & e, e & e, (12) & e, (123) & (12), e & (12), (12) & (123), e & (123), (123) & (123), (132) \\ \begin{matrix} e, e \\ e, (12) \\ e, (123) \\ (12), e \\ (12), (12) \\ (123), e \\ (123), (123) \\ (123), (132) \end{matrix} & \left(\begin{array}{cccccccc} 1 & 0 & 0 & 0 & 0 & 0 & 0 & 0 & 0 \\ 0 & 0 & 0 & 1 & 0 & 0 & 0 & 0 & 0 \\ 0 & 0 & 0 & 0 & 0 & 0 & 1 & 0 & 0 \\ 0 & 1 & 0 & 0 & 0 & 0 & 0 & 0 & 0 \\ 0 & 0 & 0 & 0 & 1 & 0 & 0 & 0 & 0 \\ 0 & 0 & 1 & 0 & 0 & 0 & 0 & 0 & 0 \\ 0 & 0 & 0 & 0 & 0 & 0 & 0 & 1 & 0 \\ 0 & 0 & 0 & 0 & 0 & 0 & 0 & 0 & 1 \end{array} \right) & \end{matrix} \quad (\text{B.34})$$

Although the S -matrix can be calculated easier with the character-table C , the decomposition into group-irreps can not. So, both methods, with character-matrices M_α^A or character-table C , have their advantages.

APPENDIX C

BRAID GROUP B_n

The *braid group* B_n is a discrete group of infinite order. It is generated by $n - 1$ elements $\tau_1, \tau_2, \dots, \tau_{n-1}$ and their inverses. The generators are subject to the relations:

$$\begin{aligned} \tau_i \tau_{i+1} \tau_i &= \tau_{i+1} \tau_i \tau_{i+1} & i = 1, \dots, n - 2 \\ \tau_i \tau_j &= \tau_j \tau_i & |i - j| \geq 2 \end{aligned} \quad (\text{C.1})$$

These relations are well known as the Yang–Baxter equation. The generators can be presented graphically by counterclockwise (for the τ_i) and clockwise (for the τ_i^{-1}) braids of n ‘strings of rope’, as is shown in figs. C.1 and C.2

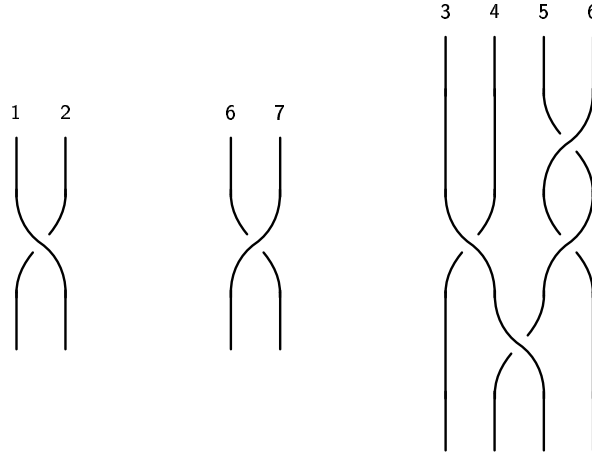


Figure C.1: A graphical representation for generators τ_i, τ_i^{-1} , with from left to right: τ_1, τ_6^{-1} and $\tau_5^{-1} \tau_3 \tau_5^{-1} \tau_4$ which is equal to $\tau_5^{-2} \tau_3 \tau_4$. The pictures themselves have to be read up-down to ‘see’ the associated clock- or counterclockwise directions of the braids.

The braid group is frequently used for describing exchanges of objects or particles in a two-dimensional space. Particles may be distinguishable or not. In physics of two-dimensions, n indistinguishable particles can behave as some representation of the braid group B_n . Distinguishable particles are more likely to be described by a subgroup P_n of the braid group B_n . This subgroup is usually called the *colored braid group*. It is generated by the monodromy operators γ_{ij} and their inverses, defined by:

$$\gamma_{ij} = \tau_i \dots \tau_{j-2} \tau_{j-1}^2 \tau_{j-1}^{-1} \dots \tau_i^{-1} \quad \text{with } 1 \leq i \leq j \leq n \quad (\text{C.2})$$

The monodromy operator γ_{ij} takes particle i around particle j and follows a specific path to ‘bring’ i next to j and the same path for the ‘way back’, which is illustrated in fig. C.3. There can

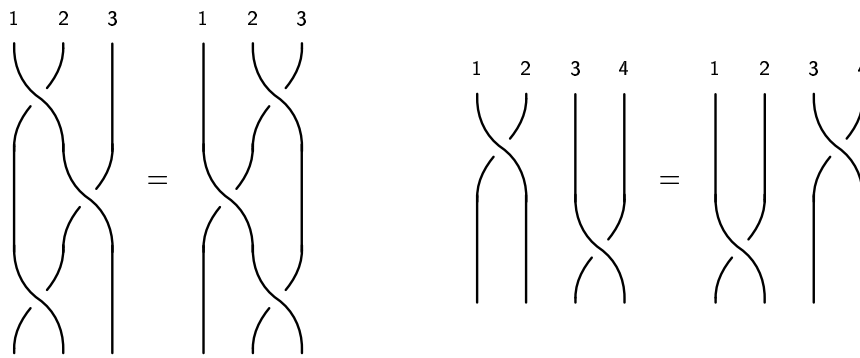


Figure C.2: These braids represent the Yang–Baxter relations: $\tau_1\tau_2\tau_1 = \tau_2\tau_1\tau_2$ and $\tau_1\tau_3 = \tau_3\tau_1$.

also be *partially colored braid group*, which describes a system of particles formed by different subsystems of identical particles. The many-to-one experiment as described in chapter 3 fits this description: there is one particle of type A , and n identical particles of type B .

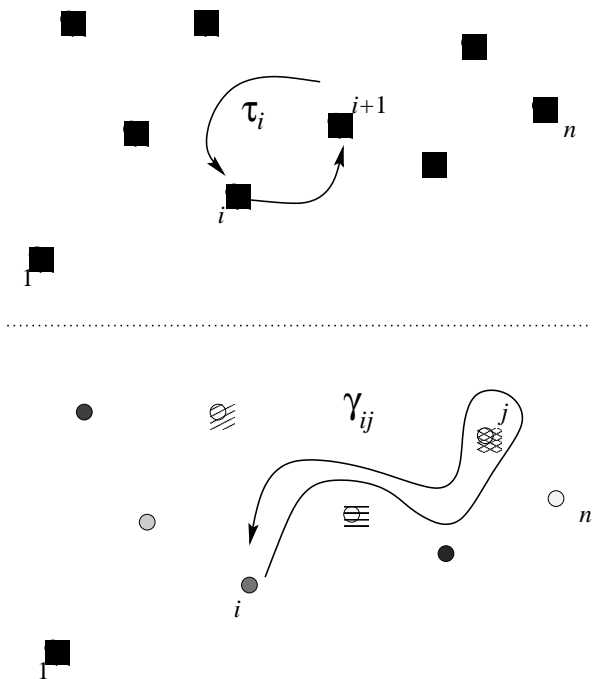


Figure C.3: The operations τ_i and γ_{ij} in the context of the ordinary and colored braid group with indistinguishable and distinguishable particles respectively.

Usually there are more restrictions or relations than just the Yang–Baxter equation (C.1). If we for example add the relation $\tau_i = \tau_i^{-1}$, we restrict ourselves to a subset of the braid group which is the *permutation group* on n objects S_n ; for the permutation group the direction of exchange is not relevant. But S_n is a finite group. Such groups (subsets, factor groups), which are generated by the generators of the braid group subjected to extra relations, have been called *truncated braid groups*. Truncated braid groups can be either of finite or infinite order. The particles in the spectrum of the quantum double $D(H)$ of a finite group H , from representations of a truncated braid group, because $\tau_i^m = e$ for some finite m and all i . Since truncated braid groups of this form, with generators τ_i of finite order, occur often, they have notation of their own: the associated ordinary braid group has been called $B(n, m)$ and the colored counterpart $P(n, m)$.

APPENDIX D

GRAPHICAL NOTATION FOR THE U -MATRIX

In this small appendix, we create some feeling for what the matrix U , as defined in chapter 3, ‘does’ by representing it graphically, as shown in figures D.1 and D.2. In these figures, traces are performed by closing loose ends into loops, which obviously preserves the cyclic property of the trace: $\text{Tr}(ABC) = \text{Tr}(CAB) = \text{Tr}(BCA)$.

This way of notation resembles illustrations used in both quantum computing and braid group theory (or even knot theory). As for now it is only useful to represent two, already known, identities: $\langle U \rangle = \langle \mathcal{R}^2 \rangle$ (if we assume that $\rho_{AB} = \rho_A \otimes \rho_B$) and $U^\dagger U = UU^\dagger$ (the proof given in 3 needed that \mathcal{R}^2 be unitary; here only braiding is used, so perhaps it is complete nonsense to picture it like this).

It is useful to recall that $\rho^\dagger = \rho$ and $\mathcal{R}^{2\dagger} = \mathcal{R}^{-2}$. Arrows are added to make it easier to ‘see 3D’, but are somehow also needed to distinguish U from U^\dagger .

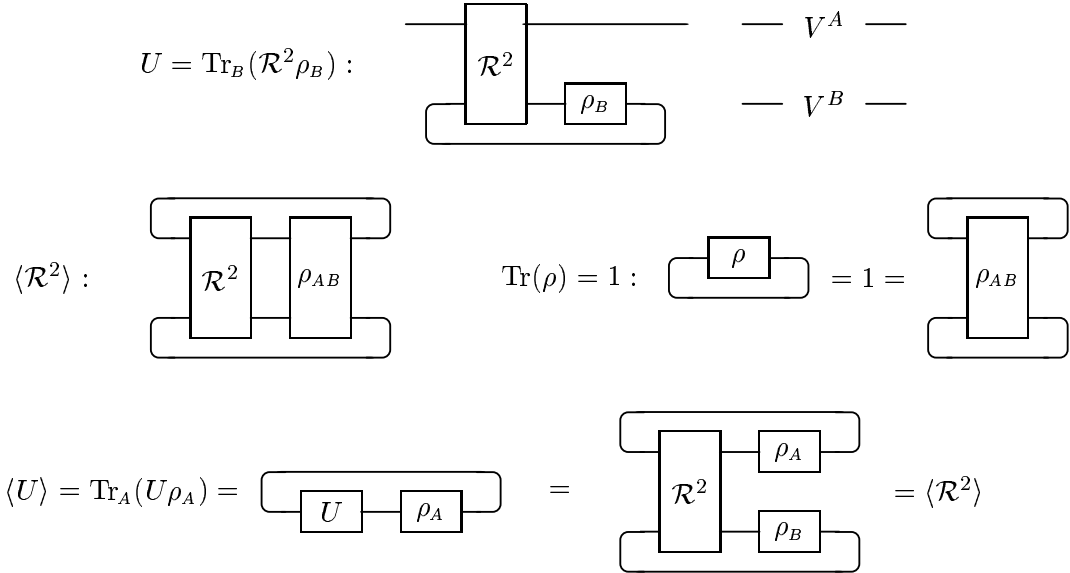


Figure D.1: Every line represents a vector space. Multiple lines denote the tensor product of the associated one-line vector spaces. The trace is performed by closing a line to a loop.

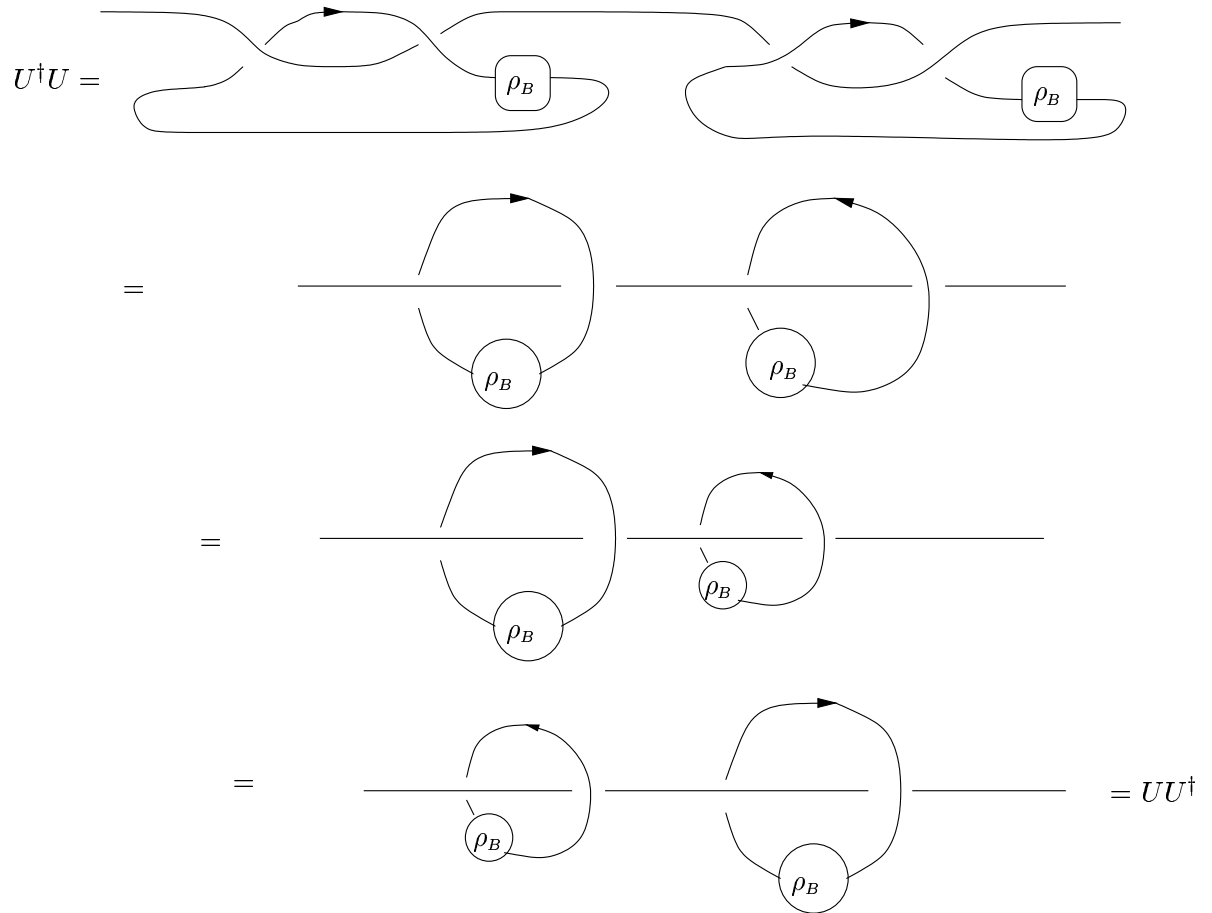


Figure D.2: 'Proof' of the fact that U is normal, i.e. $UU^\dagger = U^\dagger U$.

BIBLIOGRAPHY

- [1] John Preskill. Online lecture notes of quantum computation course. <http://www.theory.caltech.edu/people/preskill/ph229/>. This is more than just a tutorial on quantum computation. It treats various aspects of quantum information theory. Tip: section 2.3 on density matrices.
- [2] Quantum computation e-print archive, , `quant-ph`. <http://arXiv.org/>. Perform a search on the archive, with ‘year=all years’, ‘title=quantum and compu*’ and ‘abstract=review’.
- [3] Centre for quantum computation on the web, . <http://www.qubit.org>. Both tutorials and links on quantum computation can be found here.
- [4] Links on quantum computation on the web, . <http://squint.stanford.edu/qc/links.html>.
- [5] Peter W. Shor. Polynomial time algorithms for prime factorization and discrete logarithms on a quantum computer. *SIAM J. Computing*, 26:1484, 1997, `quant-ph/9508027`.
- [6] Peter W. Shor. Fault-tolerant quantum computation. 1996, `quant-ph/9605011`.
- [7] Adriano Barenco et al. Elementary gates for quantum computation. 1995, `quant-ph/9503016`.
- [8] John Preskill. Reliable quantum computers. 1997, `quant-ph/9705031`.
- [9] A. Yu. Kitaev. Fault-tolerant quantum computation by anyons. 1997, `quant-ph/9707021`.
- [10] John Preskill. Fault-tolerant quantum computation. pages 41–52, 1997, `quant-ph/9712048`.
- [11] M. De Wild Propitius and F. A. Bais. Discrete gauge theories. In G.W. Semenoff and L. Vinet, editors, *Particles and fields*, CRM series in Mathematical Physics, pages 353–440. Springer-Verlag, 1998, `hep-th/9511201`. This is a review of discrete gauge theories, which were developed in [17–19].
- [12] Bransden and Joachain. *Quantum Mechanics, 2nd edition*. Prentice Hall, 2000.
- [13] Stephen Gasiorowicz. *Quantum Physics*. Wiley, 1974.
- [14] Y. Aharonov and D. Bohm. Significance of electromagnetic potentials in the quantum theory. *Phys. Rev.*, 115:485, 1959.
- [15] R.P. Feynman, R.B. Leighton, and M. Sands. *The Feynman Lectures on Physics*, volume 2. Addison-Wesley, 1963. pp. 15.12–15.14.
- [16] Mark P. Silverman. *More than One Mystery: Explorations in Quantum Interference*. Springer-Verlag, 1995.
- [17] F. A. Bais. Flux metamorphosis. *Nucl. Phys.*, B170:32, 1980.

- [18] F. Alexander Bais, Peter van Driel, and Mark de Wild Propitius. Anyons in discrete gauge theories with chern-simons terms. *Nucl. Phys.*, B393:547–570, 1993, hep-th/9203047.
- [19] F. Alexander Bais, Peter van Driel, and Mark de Wild Propitius. Quantum symmetries in discrete gauge theories. *Phys. Lett.*, B280:63–70, 1992, hep-th/9203046.
- [20] P. Roche, V. Pasquier, and R. Dijkgraaf. Quasihopf algebras, group cohomology and orbifold models. *Nucl. Phys. Proc. Suppl.*, 18B:60, 1990.
- [21] S. Majid. *Foundations of quantum group theory*. Cambridge, UK: Univ. Pr., 1995.
- [22] T. H. Koornwinder, F. A. Bais, and N. M. Muller. Tensor product representations of the quantum double of a compact group. *Commun. Math. Phys.*, 198:157, 1998, q-alg/9712042.